# OPTIMISING AND STANDARDISING NEONATAL CHEST AND ABDOMEN IMAGING PROTOCOLS

**ANÉ NEL**

Dissertation submitted in fulfilment of the requirements for the degree

**MASTER OF RADIOGRAPHY**

**DIAGNOSTIC**

in the

Department of Clinical Sciences (Radiography Programme)

Faculty of Health and Environmental Sciences

at the

CENTRAL UNIVERSITY OF TECHNOLOGY, FREE STATE

Supervisor: Dr. Belinda van der Merwe

Co-supervisor: Dr. Bea van der Linde

BLOEMFONTEIN

July 2024

© Central University of Technology, Free State

# DECLARATION OF INDEPENDENT WORK

I, Ané Nel, declare that the dissertation, titled *Optimising and standardising neonatal chest and abdomen imaging protocols*, is my work, that it has not been submitted before for any degree or examination at any other university, and that all the sources I have used or quoted have been indicated and acknowledged as references.

This dissertation was verified for originality by submitting the electronic version to "SafeAssign" on the Blackboard server of the Central University of Technology, Free State. A similarity index of 9% was achieved (Appendix S).

1 September 2024

**Signature** **Date**

© Central University of Technology, Free State

# TABLE OF CONTENTS

**Page**


Acknowledgements ..... i
Summary ..... ii
List of acronyms and abbreviations ..... iv
List of definitions ..... vi

**CHAPTER1: OVERVIEW OF THE STUDY**

1.1 Introduction and background ..... 1
1.2 Problem statement ..... 2
1.3 Research question ..... 3
1.4 Research goal ..... 3
1.5 Research aim ..... 3
1.6 Objectives of the study ..... 3
1.7 Study population and sample size ..... 4
1.8 Demarcation of the field and scope of the study ..... 5
1.9 Research setting ..... 5
1.10 Study design ..... 5
1.11 Methodology ..... 6
1.11.1 Method of investigation ..... 6
1.11.2 Research tools ..... 8
1.12 Statistical analysis ..... 9
1.13 Significance and value of the study ..... 9
1.14 Ethical considerations ..... 10
1.14.1 Informed consent ..... 11
1.15 Quality assurance of the results ..... 12
1.15.1 Trustworthiness ..... 12
1.15.2 Validity ..... 12
1.15.3 Reliability ..... 13
1.16 Arrangement of the dissertation ..... 13
1.17 Conclusion ..... 14


© Central University of Technology, Free State

# TABLE OF CONTENTS

**Page**

**CHAPTER 2: LITERATURE REVIEW**


2.1 Introduction ..... 15
2.2 Neonatal patient ..... 18
2.3 Ionising radiation ..... 18
2.3.1 Air kerma ..... 19
2.3.2 Entrance skin dose ..... 19
2.3.3 Dosimeter ..... 19
2.4 Radiation dose to neonates ..... 21
2.5 Radiation protection principles ..... 21
2.5.1 Justification for X-ray examinations ..... 22
2.5.2 Optimisation of radiation protection ..... 22
2.5.3 Limitations of ionising radiation ..... 23
2.5.4 Radiographic equipment ..... 24
2.5.5 Protection of neonatal patients with shielding ..... 25
2.6 Technical factors ..... 25
2.6.1 Exposure and deviation index ..... 26
2.7 Chest X-ray examination of neonates ..... 27
2.7.1 Positioning technique for chest X-rays ..... 28
2.7.2 Criteria for chest X-rays ..... 29
2.7.3 Evaluation of chest X-rays ..... 32
2.8 Abdominal X-ray examination of neonates ..... 34
2.8.1 Positioning technique for the abdomen ..... 35
2.8.2 Criteria for abdominal X-rays ..... 36
2.8.3 Evaluation of abdominal X-rays ..... 37
2.9 Combined chest and abdominal X-ray examination of neonates ..... 39
2.9.1 Positioning technique for the combined chest and abdomen ..... 39
2.9.2 Criteria for the combined chest and abdomen ..... 39
2.9.3 Evaluation of the combined chest and abdomen ..... 39
2.10 Imaging protocols found in the literature ..... 40
2.10.1 Data synthesis for the literature-based imaging protocol ..... 40
2.10.2 Literature-based imaging protocol ..... 41
2.11 Conclusion ..... 51


© Central University of Technology, Free State

# TABLE OF CONTENTS

**Page**


**CHAPTER 3: METHODOLOGY**

3.1 Introduction ..... 52
3.2 Study population ..... 52
3.3 Sample size ..... 53
3.3.1 Inclusion and exclusion criteria ..... 55
3.4 Methods per phase ..... 56
3.4.1 Phase 2: Observational checklist ..... 57
3.4.1.1 Pilot study of the observational checklist ..... 63
3.4.1.2 Data collection method of the observational checklist ..... 63
3.4.1.3 Data analysis of the observational checklist ..... 64
3.4.2 Phase 3: Experimental checklist ..... 64
3.4.2.1 Pilot study of the experimental checklist ..... 66
3.4.2.2 Data collection method of the experimental checklist ..... 70
3.4.2.3 Data analysis of the experimental checklist ..... 83
3.4.3 Phase 4: Implementation checklist ..... 83
3.4.3.1 Pilot study of the implementation checklist ..... 84
3.4.3.2 Data collection method of the implementation checklist ..... 84
3.4.3.3 Data analysis of the implementation checklist ..... 89
3.4.4 Phase 5: Reflection post-implementation ..... 88
3.4.4.1 Data analysis of reflection ..... 89
3.5 Conclusion ..... 89

**CHAPTER 4: RESULTS AND DISCUSSION**

4.1 Introduction ..... 90
4.2 Data analysis definition ..... 90
4.3 Phase 2: Observational checklist ..... 91
4.4 Phase 3: Experiment ..... 113
4.4.1 Experimental chest X-ray results ..... 113
4.4.2 Experimental abdominal X-ray results ..... 127
4.4.3 Experimental combined chest and abdominal X-ray results ..... 128
4.5 The ideal protocols for implementation ..... 132


© Central University of Technology, Free State

# TABLE OF CONTENTS

**Page**

4.6 Phase 4: Implementation ..... 135
4.6.1 Implementation results ..... 135
4.7 Phase 5: Reflection ..... 148
4.8 Conclusion ..... 154

**CHAPTER 5: CONCLUSION, RECOMMENDATIONS, LIMITATIONS AND SIGNIFICANCE OF THE STUDY**

5.1 Introduction ..... 156
5.2 Overview of the study ..... 156
5.3 Recommendations for the application of a standardised protocol ..... 159
5.4 Recommendations for infection control ..... 163
5.5 Validity and reliability ..... 164
5.6 Contribution of the study ..... 165
5.7 Limitations of the study ..... 166
5.8 Recommendations to address the limitations of the study ..... 167
5.9 Feedback to the radiology department regarding in-service training ..... 168
5.10 Final remarks ..... 169

BIBLIOGRAPHY ..... 170

© Central University of Technology, Free State

# LIST OF TABLES

**Page**


**Table 2.1.** Literature search summary for chest X-ray (phase 1). ..... 46
**Table 2.2.** Literature-based imaging protocol for chest X-rays (phase 1). ..... 47
**Table 2.3.** Literature-based imaging protocol for abdominal X-rays (phase 1). ..... 48
**Table 2.4.** Literature-based imaging protocol for combined chest and abdominal X-rays (phase 1) ..... 49

**Table 3.1.** Inclusion and exclusion criteria for the observational phase (phase 2). ..... 55
**Table 3.2.** Inclusion and exclusion criteria for the experimental phase (phase 3). ..... 56
**Table 3.3.** Inclusion and exclusion criteria for the implementation phase (phase 4). ..... 56
**Table 3.4.** Part 1 of the observational checklist ..... 58
**Table 3.5.** Part 1, criterion 1 of the observational checklist. ..... 58
**Table 3.6.** Part 1, criterion 2 of the observational checklist. ..... 59
**Table 3.7.** Part 1, criterion 3 of the observational checklist ..... 59
**Table 3.8.** Part 1, criterion 4 of the observational checklist. ..... 60
**Table 3.9.** Part 2 of the observational checklist ..... 61
**Table 3.10.** Part 3, criteria 1 and 2 of the observational checklist. ..... 62
**Table 3.11.** Part 3, criteria 3 and 4 of the observational checklist. ..... 62
**Table 3.12.** Part 4 of the observational checklist. ..... 63
**Table 3.13.** Part 1 of the implementation checklist. ..... 85
**Table 3.14.** Part 2, criteria 1 and 2 of the implementation checklist. ..... 86
**Table 3.15.** Part 3, criteria 3 and 4 of the implementation checklist. ..... 86
**Table 3.16.** Part 4 of the implementation checklist. ..... 87

**Table 4.1.** Source-to-image distance (SID) (phase 2). ..... 101
**Table 4.2.** Observational checklist for machine specifications. ..... 104
**Table 4.3.** Exposure factors observed during phase 2. ..... 105
**Table 4.4.** Infection control section of the observational checklist. ..... 107
**Table 4.5.** Infection control measures followed by radiographers. ..... 108
**Table 4.6.** Part 2 of the observational checklist based on the nursing staff. ..... 109
**Table 4.7.** Radiographer and nurse interaction. ..... 110
**Table 4.8.** Part 3, criteria 1 to 4 of the observational checklist. ..... 111
**Table 4.9.** Part 4 of the observational checklist. ..... 112
**Table 4.10.** Object-to-image distance (OID) for optimal exposure index (EI) (phase 3 – CXR). ..... 115


© Central University of Technology, Free State

# LIST OF TABLES

**Page**


**Table 4.11.** Object-to-image distances (OID) for optimal deviation index (DI) (phase 3 – CXR) ..... 120

**Table 4.12.** Object-to-image distance (OID) for optimal entrance skin dose (ESD) (phase 3 – CXR). ..... 124

**Table 4.13.** Standardised imaging protocol for neonatal chest X-rays..... 126

**Table 4.14.** Standardised imaging protocol for neonatal abdominal X-rays. ..... 128

**Table 4.15.** Object-to-image distance (OID) for optimal entrance skin dose (ESD) (phase 3 – Combo) ..... 129

**Table 4.16.** Standardised imaging protocol for neonatal combined chest and abdominal X-rays (phase 3)..... 131

**Table 4.17.** Summary of optimal factors for chest X-rays. ..... 132

**Table 4.18.** Summary of optimal factors for combined chest and abdominal X-rays..... 132

**Table 4.19.** Part 2 (technical factors) of the implementation checklist. ..... 137

**Table 4.20.** Part 3 (exposure factors) of the implementation checklist. ..... 139

**Table 4.21.** Results of implementation of the one-pager protocol..... 144

**Table 4.22.** Part 2 and 3, criteria 1 to 4 of the implementation checklist for combined chest and abdominal X-rays. ..... 145

**Table 4.23.** Part 4 of the implementation checklist..... 146

**Table 4.24.** Optimal positioning technique for imaging protocols..... 148

**Table 4.25.** Statistical comparison of the exposure index for chest X-rays performed during phases 2 and 4. ..... 150

**Table 2.26.** Comparison of image evaluation of phase 2 versus phase 4. ..... 153

**Table 4.27.** Comparison of post-processing required in phase 2 versus phase 4..... 154


© Central University of Technology, Free State

# LIST OF FIGURES

**Page**


**Figure 1.1.** Research process and description of the different phases of the study. ..... 7

**Figure 2.1.** Literature search process. ..... 16
**Figure 2.2.** Literature review diagram. ..... 17
**Figure 2.3.** Dosimeter equipment. ..... 20
**Figure 2.4.** Chest X-ray positioning. ..... 28
**Figure 2.5.** Chest X-ray criteria. ..... 30
**Figure 2.6.** Chest X-ray evaluation. ..... 34
**Figure 2.7.** Abdominal X-ray positioning. ..... 36
**Figure 2.8.** Abdominal X-ray criteria. ..... 36
**Figure 2.9.** Abdominal X-ray evaluation. ..... 37
**Figure 2.10.** Combined chest and abdomen criteria. ..... 39
**Figure 2.11.** Collimation parameters for chest, abdominal and combined X-rays. ..... 50

**Figure 3.1.** Part 1 of the experimental checklist. ..... 65
**Figure 3.2.** Part 2 of the experimental checklist. ..... 65
**Figure 3.3.** Part 3 of the experimental checklist. ..... 66
**Figure 3.4.** Part 4 of the experimental checklist to record the inclusion and visibility of anatomical structures. ..... 66
**Figure 3.5.** Pilot study done for the experimental phase. ..... 68
**Figure 3.6.** Mobile machine used during phase 3. ..... 68
**Figure 3.7.** Marking of the collimator knob. ..... 69
**Figure 3.8.** Imaging protocols to be tested in experiment for chest X-rays. ..... 71
**Figure 3.9.** Data sheet for chest X-ray experimental results. ..... 72
**Figure 3.10.** Abdominal protocols (phase 3). ..... 74
**Figure 3.11.** Imaging protocols tested in the experimental phase for abdominal X-rays. ..... 75
**Figure 3.12.** Data sheet for abdominal X-ray experimental results. ..... 76
**Figure 3.13.** Imaging protocols tested in the experimental phase for combined chest and abdominal X-rays. ..... 77
**Figure 3.14.** Data sheet for experimental combined chest and abdominal X-ray results. ..... 78
**Figure 3.15.** Markings on the CosyCot™ mattress for consistent detector placement. ..... 78
**Figure 3.16.** Markings inside the incubator tray for consistent detector placement. ..... 79


© Central University of Technology, Free State

# LIST OF FIGURES

**Page**


**Figure 3.17.** Demonstration of the dosimeter placement. A: Dosimeter on the phantom. B: Dosimeter underneath the phantom. ..... 80
**Figure 3.18**. Placement of the dosimeter on top of the phantom. ..... 81
**Figure 3.19.** Centring points. ..... 81
**Figure 3.20.** Source-to-image distance (SID) measurement. ..... 82
**Figure 3.21.** Example of an image during phase 3. ..... 82
**Figure 3.22.** Technical factors displayed on the mobile unit. ..... 83
**Figure 3.23.** One-pager imaging protocol. ..... 88

**Figure 4.1.** Arm immobilisation technique observed (phase 2 – CXR). ..... 92
**Figure 4.2.** Arm immobilisation technique observed (phase 2 – AXR). ..... 92
**Figure 4.3.** Arm immobilisation technique observed (phase 2 – Combo). ..... 93
**Figure 4.4.** Head and chin position (phase 2 – CXR and Combo). ..... 94
**Figure 4.5.** Head position immobilisation techniques (phase 2 – CXR). ..... 95
**Figure 4.6.** Head position immobilisation techniques (phase 2 – Combo). ..... 95
**Figure 4.7.** Chin lifted immobilisation techniques (phase 2 – CXR). ..... 96
**Figure 4.8.** Chin lifted immobilisation techniques (phase 2 – Combo). ..... 98
**Figure 4.9.** Rotation of the thorax and pelvis during imaging (phase 2). ..... 98
**Figure 4.10.** Technical factors observed (phase 2). ..... 99
**Figure 4.11.** Detector placement (phase 2). ..... 100
**Figure 4.12.** Centring points (phase 2 – CXR). ..... 101
**Figure 4.13.** Centring points (phase 2 – AXR). ..... 102
**Figure 4.14.** Centring points (phase 2 – Combo). ..... 102
**Figure 4.15.** Angulation of the main radiation beam (phase 2) ..... 103
**Figure 4.16.** Physical lead protection used (phase 2). ..... 104
**Figure 4.17.** Box plot of kilovoltage peak (kVp) values (phase 2). ..... 106
**Figure 4.18.** Box plot of milliampere second (mAs) values (phase 2). ..... 106
**Figure 4.19.** Box plot of exposure index (EI) (phase 2). ..... 107
**Figure 4.20.** Imaging protocols producing optimal exposure index (EI) (phase 3 – CXR). ..... 114
**Figure 4.21.** Source-to-subject distance (SSD) for optimal exposure index (EI) (phase 3 – CXR) ..... 115
**Figure 4.22.** Kilovoltage peak (kVp) for optimal exposure index (EI) (phase 3 – CXR). ..... 116


© Central University of Technology, Free State

# LIST OF FIGURES

**Page**


**Figure 4.23.** Milliampere second (mAs) for optimal exposure index (EI) (phase 3 – CXR). 116

**Figure 4.24.** Source-to-image distance (SID) for optimal exposure index (EI) (phase 3 – CXR). 117

**Figure 4.25.** Angulation for optimal exposure index (EI) (phase 3 – CXR). 118

**Figure 4.26.** Imaging protocols producing optimal deviation index (DI) (phase 3 – CXR). 119

**Figure 4.27.** Source-to-subject distance (SSD) producing optimal deviation index (DI) (phase 3 – CXR). 119

**Figure 4.28.** Kilovoltage peak (kVp) for optimal deviation index (DI) (phase 3 – CXR). 120

**Figure 4.29.** Milliampere second (mAs) for optimal deviation index (DI) (phase 3 – CXR). 121

**Figure 4.30.** Source-to-image distance (SID) for optimal deviation index (DI) (phase 3 – CXR) 121

**Figure 4.31.** Angulation for optimal deviation index (DI) (phase 3 – CXR). 122

**Figure 4.32.** Imaging protocols producing optimal entrance skin dose (ESD) <80 µGy (phase 3 – CXR) 123

**Figure 4.33.** Source-to-subject distance (SSD) for optimal entrance skin dose (ESD) (phase – CXR). 123

**Figure 4.34.** Kilovoltage peak (kVp) for optimal entrance skin dose (ESD) (phase 3 – CXR). 124

**Figure 4.35.** Milliampere second (mAs) for optimal entrance skin dose (ESD) (phase – CXR). 125

**Figure 4.36.** Source-to-image distance (SID) for optimal entrance skin dose (ESD) (phase 3 – CXR). 125

**Figure 4.37.** Angulation for optimal entrance skin dose (ESD) (phase 3 – CXR). 126

**Figure 4.38.** Combined chest and abdominal X-rays yielding optimal exposure index (EI), deviation index (DI) and entrance skin dose (ESD) (phase 3) 128

**Figure 4.39.** Source-to-subject distance (SSD) for optimal entrance skin dose (ESD) (phase 3 – Combo). 129

**Figure 4.40.** Kilovoltage peak (kVp) for optimal entrance skin dose (ESD) (phase 3 – Combo). 130

**Figure 4.41.** Milliampere second (mAs) for optimal entrance skin dose (ESD) (phase 3 – Combo). 130


© Central University of Technology, Free State

# LIST OF FIGURES

**Page**


**Figure 4.42.** Source-to-image distance (SID) for optimal entrance skin dose (ESD) (phase 3 – Combo). ..... 131

**Figure 4.43.** Title slide of the educational training PowerPoint presentation. ..... 135

**Figure 4.44.** Arm immobilisation technique during the implementation phase (phase 4). ..... 136

**Figure 4.45.** Immobilisation of the head and chin: head and chin position (phase 4). ..... 136

**Figure 4.46.** Rotation of the pelvis and thorax (phase 4). ..... 137

**Figure 4.47.** Lead marker placement (phase 4). ..... 138

**Figure 4.48.** Detector placement (phase 4). ..... 138

**Figure 4.49.** Angulation of the main beam (phase 4). ..... 139

**Figure 4.50.** Kilovoltage peak (kVp) selection (phase 4). ..... 140

**Figure 4.51.** Milliampere second (mAs) selection (phase 4). ..... 141

**Figure 4.52.** Deviation index (phase 4). ..... 142

**Figure 4.53.** Reasons for repetition of X-rays (phase 4). ..... 147

**Figure 4.54.** Comparison of the exposure index for chest X-rays in phase 2 versus phase 4. ..... 150

**Figure 4.55.** Comparison of the exposure index for abdominal X-rays in phase 2 versus phase 4. ..... 151

**Figure 4.56.** Comparison of the exposure index for combined chest and abdominal X-rays in phase 2 versus phase 4. ..... 151

**Figure 4.57.** Centring points X-rays in phase 4. ..... 152


© Central University of Technology, Free State

# LIST OF APPENDICES


**Page**

**Appendix A** Observational checklist ..... 180
**Appendix B** Experimental checklist ..... 183
**Appendix C** Implementation checklist ..... 185
**Appendix D** Permission from hospital manager ..... 187
**Appendix E** Permission from radiology department ..... 189
**Appendix F** Permission from the unit manager: neonatal intensive care unit of the hospital ..... 191
**Appendix G** Approval from the Health Sciences Research Ethics Committee of the University of the Free State ..... 193
**Appendix H** Informed consent for participating radiographers ..... 194
**Appendix I** Informed consent for participating nurses ..... 196
**Appendix J** Informed consent from parents or guardians of neonatal patients ..... 198
**Appendix K** Calibration certificate ..... 205
**Appendix L** Quality control of mobile X-ray machine (phase 3) ..... 208
**Appendix M** Literature imaging protocols ..... 212
**Appendix N** Permission from the head radiographer to implement the imaging protocol ..... 215
**Appendix O** Permission from a Bloemfontein hospital for the implementation pilot study ..... 216
**Appendix P** PowerPoint presentation for pre-implementation training ..... 217
**Appendix Q** Standardised imaging protocol ..... 223
**Appendix R** SafeAssign similarity index summary ..... 224
**Appendix S** Letter from the statistician ..... 225
**Appendix T** Letter from the language editor ..... 226


© Central University of Technology, Free State

# ACKNOWLEDGEMENTS


- I would like to thank my supervisor; Dr. Belinda van der Merwe. Thank you for your consistent encouragement and motivation. I was often lost throughout my journey, but your motivational words and phrases kept me sane. I am privileged to work with someone with your level of expertise and I am honoured to be your final Master's student. You have been with me since my first day as radiography student and I salute you for the mentor that you are.
- My co-supervisor, Dr. Bea van der Linde, thank you for all the hours you put into my work even though you had a ton of your own. It was an honour to be your student and a privilege to work alongside you. You taught me a lot throughout this journey and always helped me find my way when I was stuck. You always answered my questions and uncertainties with such patience, I am in awe of you.
- Thank you to Mrs. Maryn Viljoen, you truly are the best statistician. Thank you for always explaining everything to me more than once. Someday I will get the hang of it.
- Thank you to all staff members who participated in the study. Without your help this would not have been possible.
- Thank you to my family for your continuous encouragement and motivation. You always spoke so highly of me and hopefully I made you proud.
- Thank you to my husband for your support throughout this journey. For all the late nights on the computer and the countless weekends behind the books. You were always ready to google a term for me or help me with synonyms. Thank you for your patience and your constant encouragement.
- Thank you to the CUT research centre for my bursary allowing me to pursue this dream. Without the necessary funding this research would not have been possible.




© Central University of Technology, Free State

# SUMMARY

Radiographers perform neonatal radiographic X-ray examinations daily for several diagnostic purposes. The South African radiographer's scope of practice is to provide radiographic X-ray images of optimal quality, while limiting repeats and keeping radiation dose to a minimum. The study aimed to determine which image acquisition techniques and radiation protection measures would contribute to a standardised neonatal chest and abdominal imaging protocol aligned with dose optimisation principles.

This aim was addressed by a five-phase research study. In the first phase, a literature-based imaging protocol was determined by means of a literature search. Six articles and four textbooks were used to design the literature-based imaging protocol. This literature-based imaging protocol included imaging aspects such as patient position, main beam direction and recommended exposure factors.

The study's second phase was based on neonatal intensive care unit radiographic X-ray examination observations. The observation checklist recorded the technique used by the radiographers and nursing staff during routine radiographic X-ray examinations. The observation checklist was derived from published literature. The researcher observed 158 radiographic X-ray examinations consisting of 109 chest, 16 abdominal, and 33 combined chest and abdominal X-rays. The data from this second phase were used during the third experimental phase of the study.

The third experimental phase of the study was to test the protocols observed in phase 2 with consideration of dose optimisation. From the experimental phase, an optimal chest X-ray imaging protocol was designed based on optimal recorded exposure index and deviation index, as well as calculated entrance skin dose (ESD) values. No optimal abdominal imaging protocol was created because there was no optimal recorded exposure index, deviation index, or calculated ESD values for any of the protocols assessed. For the combined chest and abdominal imaging protocol, only an optimal ESD protocol could be created. The experimental phase allowed the design of a one-pager imaging protocol stating the preferred positioning techniques, technical factors, and exposure factors for chest X-rays, abdominal X-rays, and combined chest and abdominal X-rays. The one-pager imaging protocol was used during the fourth implementation phase of the study.



© Central University of Technology, Free State

The fourth phase included a short training session created for and presented to the participating radiographers. The radiographers completed implementation checklists during the fourth phase when they performed routine radiographic X-ray examinations in the neonatal intensive care unit. Three chest X-rays, two abdominal and 45 combined chest and abdominal X-rays were performed during the fourth phase.

The fifth and final stage of the study compared the data accumulated in the second and fourth phases. This comparison was done to determine the effect on exposure index for dose optimisation after the one-pager imaging protocol had been implemented. The comparison indicated that the radiographers did not entirely abide by the imaging protocol. For chest X-rays, the maximum exposure index was reduced from 642 to 163, which was within the recommended range between 50 and 200 for the machine used in the study. For abdominal X-rays, the maximum exposure index was reduced from 583 to 382, within the range of 125–500. The exposure index for the combined chest and abdominal X-rays increased from 724 to 849, which exceeded the recommended range of 125–500. This phase showed that the standardised imaging protocol made a significant difference in neonatal imaging with alignment to dose optimisation techniques.

The study's overall goal was achieved to standardise a protocol for the department for radiographic X-ray imaging of the neonatal chest and abdomen, in an attempt to optimise the radiation dose and to guide uniform radiographic evaluation of images of diagnostic value.



© Central University of Technology, Free State

# LIST OF ACRONYMS AND ABBREVIATIONS

| | |
|---|---|
| µGy | microGray |
| Al | aluminium |
| ALARA | as low as reasonably achievable |
| AP | anterior-posterior |
| AXR | abdominal X-ray |
| BSF | backscatter factor |
| C1 | 1st cervical vertebra |
| C3 | 3rd cervical vertebra |
| C7 | 7th cervical vertebra |
| CF | calibration factor |
| cm | centimetres |
| CR | computed radiography |
| Cu | copper |
| CUT | Central University of Technology |
| CXR | chest X-ray |
| CXR-AXR | combined chest and abdominal X-rays |
| DAP | dose-area product |
| DI | deviation index |
| DNA | deoxyribonucleic acid |
| DR | digital radiography |
| EAK | entrance air kerma |
| EI | exposure index |
| ESD | entrance skin dose |
| EU | European Commission |
| FOV | field of view |
| Gy | Gray |
| HSREC | Health Sciences Research Ethics Committee |
| IAEA | Internation Atomic Energy Agency |
| IAK | incident air kerma |
| IC | iliac crest |
| ICRP | International Commission on Radiological Protection |
| ICU | intensive care unit |
| ID | identification |
| J/kg | joules per kilogram |



© Central University of Technology, Free State

| | |
|---|---|
| kVp | kilovoltage peak |
| LCM | left costal margin |
| mAs | milliampere seconds |
| mGy | milliGray |
| MSP | midsagittal plane |
| N/A | not applicable |
| Neg | negative |
| NICU | neonatal intensive care unit |
| OID | object-to-image distance |
| PA | posterior-anterior |
| PACS | Picture Archiving and Communication System |
| Pb Eq | lead equivalence |
| POPI | Protection of Personal Information |
| POPIA | Protection of Personal Information Act |
| Pt | patient |
| SAHPRA | South African Health Products Regulatory Authority |
| SD | standard deviation |
| SDD | source-to-detector distance |
| SID | source-to-image receptor distance |
| SOD | source-to-object distance |
| SP | symphysis pubis |
| SSD | source-to-subject distance |
| T7 | 7$^{th}$ thoracic vertebra |
| UFS | University of the Free State |
| URE | unnecessary radiation exposure |
| WHO | World Health Organization |



© Central University of Technology, Free State

# LIST OF DEFINITIONS

**Air kerma** – The kinetic energy released per unit mass when an X-ray beam travels through air, which is how the intensity of the beam is characterised (Huba, 2014).

**Deviation index** – An indication providing details on the appropriateness of radiation exposure on digital radiography equipment that could potentially aid in reducing the radiation exposure (Sutoro, Irsal & Cahya, 2023).

**Entrance skin dose** – A parameter in evaluating the dose received by a patient. The purpose of this unit is for dose optimisation purposes (Shamsi, Monafred, Deevband, Mohsenzadeh, Ghorbani, Gorji & Niksirat, 2020). Entrance surface dose is an alternative term used for this parameter.

**Evaluation criteria** – Each radiographer should use a specific format when reviewing and comparing radiographs to determine how close to an optimal image was achieved. It consists of four parts: anatomy demonstrated, position, rotation, tilt, exposure factors, collimation, and image markers (Bontrager & Lampignano, 2014; Lampignano & Kendrick, 2021).

**Exposure index** – A method by which manufacturers provide feedback to radiographers regarding the estimated exposure received by the detector and an indirect indicator of image quality (Seibert & Morin, 2011).

**Image acquisition** – Digital radiography (DR) uses a cassette-less imaging capturing system. The detector consists of a matrix of pixel-size detector elements that each include a thin film transistor (TFT) collecting the electric charges produced in the detector elements when the remaining radiation strikes it. The subject contrast in the remnant radiation is represented by the TFTs collecting varying intensities. These signals are then sent to the computer for processing and manipulation (McQuillen Martensen, 2011).

**Detector** (DDR detector)– A digital imaging system composed of amorphous selenium or amorphous silicon. Exposure of amorphous selenium to the X-ray photons result in the movement of electrons through the material into the electron collection portion of the thin film transistor (Bontrager & Lampignano, 2014; Lampignano & Kendrick, 2021).

**Main radiation beam (X-ray beam)** – The centre of the X-ray beam, which is without any divergence as it projects to the object at a 90° angle (Bontrager & Lampignano, 2014; Lampignano & Kendrick, 2021).

**Neonate** – The first 28 days of a newborn infant's life (WHO, 2024).

**Technical factors** – Technical factors refer to the placement and orientation of the detector, grid use and relevant exposure factors (kilovoltage peak [kVp] and milliampere second [mAs]) (Bontrager & Lampignano, 2014; Lampignano & Kendrick, 2021).



© Central University of Technology, Free State

# CHAPTER 1
## OVERVIEW OF THE STUDY

### 1.1 INTRODUCTION AND BACKGROUND

Radiography forms part of a neonatal patient's daily diagnostic cycle and recovery process. As radiographers, we expose this specific patient group to a potentially harmful medical imaging tool to assist in their recovery process. The different radiographs that are predominantly requested are X-ray images of the chest and abdomen. Concern has been raised, as the small size of the neonate is placed in the X-ray field, increasing the effective dose to the neonate compared to that of an adult (Aramesh, Zanganeh, Dehdashtian, Malekian & Fatahiasl, 2017: 124).

Normal routine radiographic X-ray imaging in the intensive care units is performed with a portable X-ray machine to ensure accurate diagnosis, correct treatment, and improved patient status (Aramesh *et al*., 2017: 124). Chest X-rays are performed on neonatal patients to evaluate chest pathologies and chronic lung diseases as well as cardiac conditions, and anatomical structures such as the lungs, heart, stomach and thymus. During evaluation of these X-rays, the placement of certain tubes, lines and catheters are also assessed (Yoon, 2016: 279–281).

There is an increase in the number of diagnostic radiation examinations received by the neonate when hospitalised due to chest pathologies such as pleural effusion, atelectasis, meconium aspiration, and acute respiratory distress syndrome. Neonatal patients are sensitive to ionising radiation and radiation exposure to this patient group should be justified and limited (Gunn, O'Brien, Fossa, Tonkopi, Lanca, Martins, Muller, Friedrich-Nel, Abdolell & Johansen, 2019: e66–e68).

While radiography is seen as a crucial diagnostic tool in identifying different neonatal pathologies, it is considered to have a high potential to cause cell damage and have harmful effects on neonates. Thus, the use of ionising radiation resulting from X-rays should be justified for each examination. It is also important to limit radiation exposure to neonatal patients and should not be used to monitor the patient's health status (Gunn *et al*., 2019: e66–e68).


© Central University of Technology, Free State

The benefit outweighs the risk when considering X-rays. Nevertheless, one must keep in mind the probability of stochastic effects (Gunn *et al*., 2019: e67). The risk of stochastic effects increases with increased radiation exposure during the lifetime of the patient (Aramesh *et al*., 2017: 124). The biological effects of ionising radiation are related to the direct absorption of radiation-associated energy. Ionising radiation may cause different biological changes such as cell damage, cell death and genetic mutations (World Health Organisation, 2023: online).

According to a survey conducted by the Image Gently campaign over three years, 40% of paediatric and neonatal patients underwent at least one radiographic examination (Don, MacDougall, Strauss, Moore, Goske, Cohen, Herrmann, John, Noble, Morrison, Lehman & Whiting, 2013: 431). In 2008, The Society for Pediatric Radiology initiated the Image Gently campaign (Applegate, 2015: 2) to create awareness of paediatric and neonatal protection against ionising radiation. Due to the lack of a precise and comprehensive protocol for the imaging of neonatal patients, radiographers do not uniformly apply dose optimisation principles and radiation protection (Armpilia, Fife & Croasdale, 2001: 539).

The researcher observed the lack of a standardised neonatal imaging protocol at a private radiology practice in Bloemfontein. Every qualified radiographer proceeds with imaging of neonatal patients in their own manner and in the way they were taught. Because of this lack of a standardised technique and insufficient knowledge by radiographers on this matter, neonates are often exposed repeatedly for unacceptable reasons, such as positioning errors, motion, or over-penetration (Gunn *et al*., 2019: e67).

The researcher observed that community service and junior radiographers learn through trial and error under the guidance of senior radiographers. All radiographers and newly appointed staff must be confident about the anatomical structures that must be included in the primary beam to diagnose certain pathologies. Irrelevant anatomical structures, however, can be excluded by using excessive collimation to apply basic radiation protection. This is only one example in support of the need for a scientifically proven neonatal chest and abdominal imaging protocol to ensure optimal exposure to radiation, while adhering to the as low as reasonably achievable (ALARA) principle (Gunn *et al*., 2019: e67–e69).

## 1.2 PROBLEM STATEMENT

The research problem identified was that no optimised and standardised protocol was available for chest and abdominal imaging of neonatal patients in a private hospital. This leads to the overexposure of neonatal patients due to a lack of a precise protocol or baseline.


© Central University of Technology, Free State

## 1.3 RESEARCH QUESTION

Which image acquisition techniques and radiation protection measures will contribute to standardised neonatal chest and abdominal imaging protocols for alignment with dose optimisation principles?

## 1.4 RESEARCH GOAL

The study's overall goal was to standardise a protocol for the radiographic X-ray imaging of the neonatal chest and abdomen, thus optimising the radiation dose.

## 1.5 RESEARCH AIM

The study aimed to develop a standardised imaging protocol to assist radiographers in producing diagnostic radiographic X-ray images of the neonatal chest and abdomen, while keeping the radiation dose as low as possible.

## 1.6 OBJECTIVES OF THE STUDY

To achieve the aim of the study, the following objectives were pursued:

**Objective 1** (Phase 1: Literature search)
To obtain previously published imaging protocols to benchmark the proposed baseline imaging protocol for neonatal mobile chest (CXR), abdominal (AXR) and combined chest-abdominal images (CXR-AXR).

**Objective 2** (Phase 2: Observations)
To observe radiographers and nursing staff in their workspace while performing neonatal mobile CXR, AXR and combined images, to record all imaging protocols used in the workspace.

**Objective 3** (Phase 3: Experiment)
To compare the estimated entrance skin dose for the different imaging protocols (recorded from the literature search and observed in the workspace within the recommended exposure range) to optimise the baseline imaging protocol.


© Central University of Technology, Free State

**Objective 4** (Phase 4: Implementation)

To implement the (standardised and optimised) baseline imaging protocol.

**Objective 5** (Phase 5: Reflection)

To determine the effect that the implemented baseline imaging protocol had on exposure index (for dose optimisation) and image critique.

## 1.7 STUDY POPULATION AND SAMPLE SIZE

**Phase 1:** Articles and published literature related to the research topic were used to create the literature-based imaging protocol. In total, six articles and four textbooks were consulted to create this protocol as discussed in Chapter 2.

**Phase 2:** Of the 16 radiographers currently employed for general X-rays at the particular radiology department, 12 participated in the study. The routine X-rays observed during the second phase of the study were performed daily at 06h00, and only the 12 participating radiographers working night shift performed the routine X-rays. Fourteen registered nurses were eligible for participation in the observational phase, but only eight participated in the study due to rostering and night-shift staff. All neonates receiving chest and abdominal X-rays, for whom permission was obtained from their parents or legal guardians, participated in the study for the observational phase. Throughout the observational phase, 158 images were observed by the researcher.

**Phase 3:** All data collected that met the set requirements formed part of the research. The inclusion parameters are discussed in Chapter 3. Sixty-eight CXR, 43 AXR and 43 combined CXR-AXR examinations were included.

**Phase 4:** Four of the 12 radiographers participated in the implementation phase of the research. The fourth phase ran over two weeks, and only four radiographers rostered over that time implemented the standardised imaging protocol (one-pager) in the imaging department.


© Central University of Technology, Free State

## 1.8 DEMARCATION OF THE FIELD AND SCOPE OF THE STUDY

This study dealt with the profession of Radiography regarding neonatal patients and a standardised protocol for the imaging procedures of neonates (in collaboration with nursing staff), adhering to certain dose optimisation principles in a private hospital in the Free State Province.

## 1.9 RESEARCH SETTING

The study was completed in a private hospital with 14 neonatal intensive care unit beds and four paediatricians. The neonatal intensive care unit (NICU) is equipped with 24-hour nursing staff, a paediatrician and a paediatric surgeon on call. The radiology department, emergency department and operating theatres are available to the NICU 24 hours a day. The hospital is equipped to perform complex general surgeries, cardiac surgeries and urological surgeries. The NICU can accommodate 14 neonates for as long as necessary while recovering and completing treatment. The units provide specialised treatment for premature neonates and disorders such as hyaline membrane disease, atresia, hernias, or bowel obstructions, among others.

The radiology department is privately owned; thus, the radiographers are not employed by the hospital but by the private practice itself. The radiology department provides 24-hour service to the hospital, including the NICU. The department provides several services including general X-rays, mammography, dual energy X-ray absorptiometry (DEXA), fluoroscopy, ultrasound, computed tomography (CT) and magnetic resonance imaging (MRI) scans. Six radiologists are reporting on the images and performing some minor procedures in the department using fluoroscopy and ultrasound.

The researcher performed the study at one private hospital to limit the study size. Every hospital and imaging department performs their X-rays uniquely and imaging equipment differs between practices. Thus, the variables observed at the one hospital were adequate to conclude the five phases of the research.

## 1.10 STUDY DESIGN

A case study research design was applied, which is an in-depth study of a complex research problem. It is mainly used to narrow down a very broad research field into easier research


© Central University of Technology, Free State

examples. A case study design is useful when a specific theory or method is to be tested on phenomena in the real world. A variety of sources and methodologies can be used to execute a study of this design (Crowe, Cresswell, Robertson, Huby, Avery & Sheikh, 2011: 1). The research had an undisguised naturalistic observational approach (Angrosino, 2007: 4). The participants were aware of the researcher's presence but unaware of what specifically was observed.

Quantitative research usually starts with a specific theory, leading to a specific hypothesis. Quantitative research makes use of study designs where the focus of the research is to describe, explain and predict a phenomenon (Khalid, Hilman & Kumar, 2012: 16). It is the numerical representation and manipulation of several observations to describe and explain the phenomena that those observations represent (Sukamolson, 2007: 2). In this study, quantitative data were collected throughout phases 2 to 4 where the data were statistically analysed to proceed with the following phase. The results of the study were based on the statistical significance of the data.

Descriptive research describes individuals, events or conditions as they occur in nature. Variables are not manipulated by the researcher. Descriptive studies observe the characteristics of a population, identify problems within a population or look at variations in characteristics or practices between institutions (Siedlecki, 2020: 8). This type of research was applied during the observational phase (phase 2) where the researcher observed the radiographers and the nursing staff in their natural work environment. The researcher made no changes to the factors observed and included all data on the checklist as it happened. This provided the researcher with true data collected and increased the validity and credibility of the study.

## 1.11 METHODOLOGY

Research methodology is regarded as the pathway followed by researchers to formulate research problems and objectives, and to present results from the data acquired during the specific study period (Sileyew, 2020: 27). In the following sections, the research methodology for the different phases of the study is discussed to provide background on data acquisition by introducing the research tools and the method of investigation.


© Central University of Technology, Free State

### 1.11.1 Method of investigation

The research was executed at a private hospital in the Free State Province of South Africa. The study was conducted in the NICU of the hospital and a privately owned radiological department in the same hospital. The phases of the study are demonstrated in Figure 1.1, showing the phases followed by the objective achieved in the relevant phases and the dates that each phase commenced and concluded.

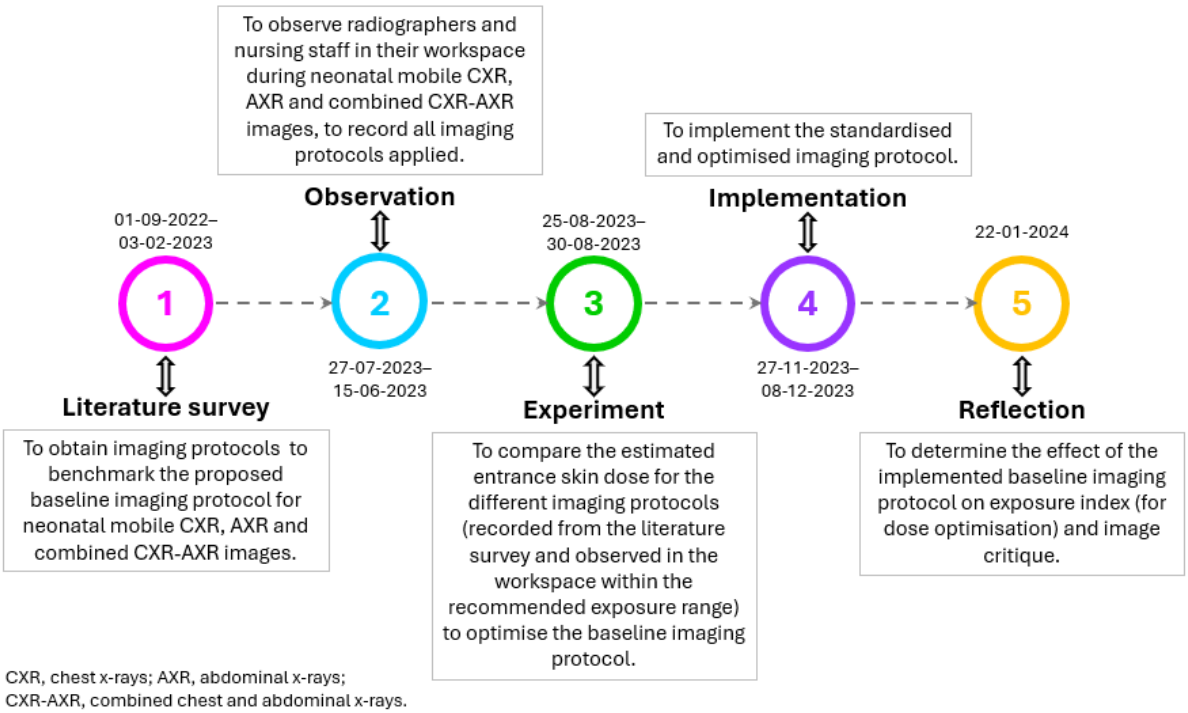



**Figure 1.1.** Research process and description of the different phases of the study.

In the first phase of the study, the researcher did a literature search to determine a baseline imaging protocol based on previously published information. Phase 1 started on 1 September 2022 after ethical approval for the study was obtained and concluded on 3 February 2023. This literature search included textbooks and research articles including any of the keywords or aspects to be investigated and tested during the experimental phase of the study. The literature-based imaging protocol benchmarked the observational checklist used in phase 2, which confirmed that all the parameters were included in the observational checklist of phase 2. A summary of the literature imaging protocol tested during the experimental phase (phase 3) is included in Chapter 3, Figures 3.7, 3.10 and 3.12.

Phase 2 of the study started on 27 March 2023 and finished on 15 June 2023. The researcher observed the radiographers and the NICU nursing personnel during routine radiographic


© Central University of Technology, Free State

mobile examinations. The second phase reflects the second objective by collecting checklist data through observations (Appendix A).

During the third phase of the study, undertaken from 25 to 30 August 2023, the researcher practically investigated various combinations of imaging protocols. The experiments measured the radiation doses of different imaging protocol combinations and the effect thereof on image quality, exposure index and deviation index. This phase addressed the third objective and was achieved by completing a set data sheet based on the literature search (phase 1) and the observation performed in phase 2.

The fourth phase of the study was done from 27 November 2023 to 8 December 2023. In this phase, the researcher provided the radiographers with an optimised and standardised imaging protocol to implement in the department. The research tool for this phase linked to objective four, which was an implementation checklist completed by the radiographers (Appendix B).

The fifth and final phase, indicated as reflection in Figure 1.1, was completed on 22 January 2024. The statistician compared the second and fourth phases' data. This comparison addressed objective five and finally concluded the aim of the research study.

### 1.11.2 Research tools

Data collection is the process of accumulating information to gain insight based on a specific research topic (Taherdoost, 2021: 10). Various research tools were used throughout the study for data collection. Three research tools were used during phases 2 to 4 of the study; a brief description of each is provided below.

➡ Phase 2: The observational checklist (Appendix A) was used. This phase involved an observation method performed by the researcher. The observational checklist was compiled by the researcher based on the literature identified during phase 1 of the study. The observational checklist was piloted on 28 February 2023 and 9 March 2023 at a different hospital than the main study.

➡ Phase 3: An experimental checklist (Appendix B) was used by the researcher while performing the experimental imaging protocols on a neonatal phantom. The checklist was compiled by the researcher based on the preceding two phases. The experimental checklist was tested during the pilot study that commenced on 24 August 2023.


© Central University of Technology, Free State

➡ Phase 4: The implementation checklist (Appendix C) compiled by the researcher was based on the previous phases 2 to 3. This implementation checklist was piloted on 21 November 2023, whereafter it was given to four radiographers who were not part of the main study, for completion during phase 4. The data collection with this checklist was done after a short training session had been provided.

## 1.12 STATISTICAL ANALYSIS

Data from the observational phase (phase 2) were captured by the researcher on printed checklists, whereafter the data were transferred from the hard copy to a Microsoft (Microsoft Corporation; Redmond, WA, USA) Excel (Office 16) spreadsheet before submitting it to the statistician. Data from the experimental phase (phase 3) were captured on Excel spreadsheets and presented to the statistician for further analysis. The reflection phase was completed by the radiographers on the printed implementation checklists during phase 4. The data were transferred to an Excel spreadsheet before submission to the statistician.

All further analyses were done by a statistician using SAS Version 9.4 (SAS Institute Inc.; Cary, NC, USA). Descriptive statistics, namely frequencies and percentages, were calculated for categorical data. Means and standard deviations, or medians and percentiles, were calculated for numerical data. The Shapiro-Wilk test was used to determine if numerical data followed a normal distribution.

Observational checklists from phase 2 were compared to implementation checklists from phase 4 by using analytical statistics, namely the independent T-test (or Mann-Whitney U-test) to compare mean (or median) values. The chi-square test was used to compare percentages. A significance level ($\alpha$) of 0.05 was used. Statistical analytic results are presented and discussed in Chapter 4.

## 1.13 SIGNIFICANCE AND VALUE OF THE STUDY

According to Gunn *et al*. (2019: e67), a lack of reference protocols causes an increase in radiation exposure to neonatal patients. These authors stated that the optimisation process should be initiated by reviewing the existing technique and positioning protocol for neonatal imaging and relating it to the dose received by the neonate. From this current technique, a protocol would be developed to be implemented in the hospital.


© Central University of Technology, Free State

The outcome of the study described could aid in the protection against radiation for these special patients, as a standardised protocol could prevent confusion among radiographers and raise awareness regarding methods and techniques to lower or limit radiation exposure to neonates. The specific study by Gunn *et al*. (2019) was selected to find an accurate measure to reduce radiation exposure or to limit the harmful aspects of the radiation field as much as possible. Neonatal patients are highly susceptible to the effects of ionising radiation and the amount of radiation given to these patients should be justified, limited and optimised. Because the implementation of crucial radiographic tools and techniques is non-existent, the radiation dose to the neonate might be increased, resulting in overexposure to the patient (Gunn *et al*., 2019: e67).

It remains the responsibility of the radiographer to protect a neonate from any potential harm. Therefore, being trained and educated in methods of radiation protection and radiation safety, it is expected of radiographers to not only protect the neonate but also the babies in the surrounding area, staff and family members and/or visitors who are present in the intensive care unit.

## 1.14 ETHICAL CONSIDERATIONS

The proposed study met the ethical considerations before commencement. Permission was obtained from the hospital manager and the head of the radiology department to observe their respective staff members in practice. Permission was granted for the study by the hospital (Appendix D), the radiology department (Appendix E) and the unit manager of the NICU (Appendix F). Ethical approval was obtained from the Health Sciences Research Ethical Committee (HSREC) of the University of the Free State in Bloemfontein, South Africa, with approval number UFS-HSD2022/1583/2803 (Appendix G).

The principles of ethics in medical research are based on the four principles of Beauchamp and Childress known as autonomy, non-maleficence, beneficence and justice (Avasthi, Ghosh, Sarkar & Grover, 2013: 86). During the study, compliance with all four of these principles were observed to ensure an ethical study and no harm to or exploitation of participants.

The first principle, autonomy, was exercised by allowing all the participants (members of staff) and the parents or the legal guardians of minor participants to voluntarily become involved in the study after allowing them time to understand their participation, as well as the benefits and risks of participation. Al-Bar and Chamsi-Pasha (2015: 119) stated that non-maleficence is a


© Central University of Technology, Free State

crucial obligation in morality and medical ethics and means to do no harm. During this study, the researcher assured participants that no harm would occur to any participating individual, as no invasive procedures would be performed, and no personal information would be recorded. Furthermore, the researcher assured anonymity when identifying staff members or images obtained.

Al-Bar and Chamsi-Pasha (2015: 129) described beneficence as all forms of action intended to promote or benefit the good of other people. Types of beneficence also include preventing harm and removing any harmful elements. Although the researcher stated that the participating neonates and medical staff might not benefit directly from this study, there will be future beneficial outcomes resulting from this research. No harm was intended by this study; thus, it was also made clear to all participants that withdrawal and refusal of participation would no negative implications concerning their medical care or work responsibilities, and they were allowed to withdraw from the study at any stage.

The fourth principle is justice, which refers to a person being treated to what is fair, due, or owed (Beauchamp, 2007: 6). All participants in this study were treated fairly and equally, and no participant received more benefits or experienced more harm than the next. By following these four ethical principles, the researcher ensured that proper ethical values were applied while conducting the research to prevent any harm towards participants.

### 1.14.1 Informed consent

Written informed consent was obtained from all participating radiographers and nurses and all parents or legal guardians of the patients. The radiographer's consent (Appendix H) was received before data collection in the second phase. All steps to be taken by the researcher during the observation were explained. The consent form did not elaborate on the specifics of the parameters to be observed to ensure the validity and reliability of the results. Twelve radiographers granted permission to participate in the observation phase and consent was also granted at the same time for the fourth phase of the study in which four of the 12 radiographers participated.

The researcher also obtained written informed consent from the nursing staff working in the neonatal intensive care unit. The consent form (Appendix I) was provided to the nurses before the observation phase commenced. Eight NICU nurses granted permission to participate in the observation phase of the study.


© Central University of Technology, Free State

The consent form for the parents and legal guardians was provided in English, Afrikaans and Sesotho for the convenience and understanding of the family (Appendix J). Consent from the parents and legal guardians was obtained only once, even when a patient was X-rayed on several occasions.

## 1.15 QUALITY ASSURANCE OF THE RESULTS

To ensure high quality research, two parameters – generalisation and the degree of certainty – were taken into consideration. A quantitative research method was implemented, employing a five-step research process (Swanson & Holton, 2005: 31).

### 1.15.1 Trustworthiness

According to Peels and Bouter (2023: 78), trustworthiness is the ability of something to be worthy of trust. Trustworthiness in research implies that the published research and findings are justified, genuine and rational. The indicators of trustworthiness in qualitative research are known as "credibility", "transferability", "dependability" and "confirmability". However, in quantitative research, the terms "internal validity", "external validity or generalisability", "reliability" and "objectivity" are used to define trustworthiness of research results (Chowdhury, 2015: 148).

### 1.15.2 Validity

Chowdhury (2015: 148) stated that validity in quantitative research is used to determine the quality assurance of the study. Validity is also divided into several subcategories, although beyond these subcategories, internal validity and external validity assess the trustworthiness of research.

Internal validity refers to the commonly used term "credibility" implying "the accuracy of research findings where investigators attempt to demonstrate that a true picture of the phenomenon under scrutiny is being presented", as stated by Shenton (2004: 63). Persistent observation, prolonged engagement at the research site, triangulation and peer debriefing are several procedures that can be followed to ensure credibility of a research study (Guba, 1981: 84–86).

As stated above, the internal validity or credibility of this study was important, especially during the second phase (observational phase). It was imperative for the researcher to remain


© Central University of Technology, Free State

impartial and invisible during the observations, and to capture exactly what happened and what was executed when performing these mobile X-rays. It was crucial not to make any changes regardless of any inconsistencies. The credibility of the study was improved as everything captured was exactly as it occurred. The researcher performed persistent observations for twelve weeks and spent each morning at the hospital. At that stage, the focus was exclusively on the observations.

### 1.15.3 Reliability

Reliability is the ability of the research tools to consistently produce the same results when it is used in the same manner on repeated occasions. In other words, reliability refers to the consistency of a measure (Heale & Twycross, 2015: 66).

The observational (Appendix A) and implementation (Appendix B) checklists were reliable because all factors included were based on literature and benchmarked to previous studies and academic articles. Both checklists were piloted by the researcher in a similar but smaller population group as that involved in the main study. The experimental checklist (Appendix C) used during the second phase of the study, was piloted by the researcher using the same equipment as used during the main study to assure accuracy and improve the validity of the study.

## 1.16 ARRANGEMENT OF THE DISSERTATION

The chapters are set out as follows

*Chapter 1: Introduction*
This chapter provides the reader with an overview and background of the study. It discusses several important factors, such as the research problem statement, the aim and objectives, and the background to the study.

*Chapter 2: Literature review*
The chapter reviewing the literature builds a foundation for the reader to understand the research topic. Chapter 2 elaborates on the important components forming part of the research. It elaborates on the importance of radiation protection and the vulnerability of neonatal patients when exposed to ionising radiation. The first objective was addressed by discussing the baseline literature imaging protocol, which is provided towards the end of this chapter.


© Central University of Technology, Free State

*Chapter 3: Methodology*

This chapter presents a descriptive elaboration of the research approach and several research tools used throughout the several phases of the study. Data collection methods and the several pilot studies are explained in Chapter 3.

*Chapter 4: Results and Discussion*

Results obtained from phases two to five of the study are discussed in this chapter, with the impact of the results on each of the subsequent phases.

*Chapter 5: Conclusion, recommendations, limitations and significance of the study*

The limitations and recommendations of the study are presented in this chapter. Taking these into account, measures to improve similar future research are proposed. Final remarks and observations are provided, leading to a conclusion of the study and dissertation.

## 1.17 CONCLUSION

In Chapter 1 the background to the study as well as the research problem, aim and objectives of the study are described. This chapter offered a brief description of the steps followed throughout the study for data collection. The different research tools used for data collection were introduced. The chapter briefly outlined the statistical analysis, ethical considerations, quality assurance and reliability of the results.

In the next chapter is an elaboration on the key components describing the literature-based foundation of the study. The content of the next chapter will provide a basic understanding of the research topic to the reader. The literature imaging protocol is discussed at length in Chapter 2.


© Central University of Technology, Free State

# CHAPTER 2
# LITERATURE REVIEW

## 2.1 INTRODUCTION

In this chapter the literature review conducted during the first phase with the intention to develop a literature-based imaging protocol for neonatal chest and abdominal X-rays is presented. An imaging protocol providing an accurate method of image acquisition when performing mobile neonatal chest and abdominal X-rays was the goal of this research. This final imaging protocol aimed to ensure uniform radiographic X-ray images with acceptable image quality and a low radiation dose to the patient.

Journal articles explaining the preferred imaging methods for neonatal patients were searched, which included articles explaining the positioning methods, exposure factors, or radiation protection techniques used for neonatal X-rays. Any articles discussing other radiographic examinations were excluded as well as articles performed in the radiology department. Articles discussing mobile radiographic procedures on pediatric patients were also excluded as the study solely focused on neonates. All articles using computed radiography (CR) were also excluded as the research site used digital radiography (DR). The literature search formed part of the first objective and first phase of the study. The literature search commenced on 1 September 2022 and concluded on 3 February 2023, before the start of the second phase.

Databases that were consulted to identify relevant research articles included Google Scholar, EBSCOhost, Science Direct, AJR Online, Scopus and PubMed. A combined of keywords was used to find articles related to the research topic, such as "neonatal chest", "neonate", "chest X-ray", "neonatal mobile", "neonatal abdomen", "abdomen X-ray", "neonatal imaging". Twenty-eight articles correlated with the research topic to some extent. Not one article was found that provided a precise imaging protocol for either of the examinations. After the exclusion criteria were applied, twenty-two articles were excluded from the literature search. Therefore, a combination of six articles was used to establish a baseline theoretical imaging protocol. The inclusion and exclusion criteria were based on relevant information as decided by the researcher and comprised any articles on positioning criteria, technical factors or exposure factors for neonatal chest and abdominal X-rays. The articles included for neonatal chest X-rays are listed in Table 2.1, section 2.10.2.


© Central University of Technology, Free State

Four textbooks were used to create the literature imaging protocol along with the published journal articles. The four textbooks used were the *Textbook of Radiographic Positioning and Related Anatomy* (Bontrager & Lampignano, 2014; Lampignano & Kendrick, 2021), *Radiographic Image Analysis* (McQuillen Martensen, 2011; 2015), *Clark's Positioning in Radiography* (Whitley, Jefferson, Holmes, Sloane, Anderson & Hoadley, 2015) and *Merrill's Atlas of Radiographic Positioning and Procedures* (Long, Rollins & Smith, 2019). The first two textbooks referred to were used, as they currently are the prescribed textbooks for Radiography students at the university in the vicinity of the hospital. No imaging protocols were found on online platforms as presented in the figure below. Figure 2.1 below illustrates the process to develop the literature-based theoretical imaging protocol.

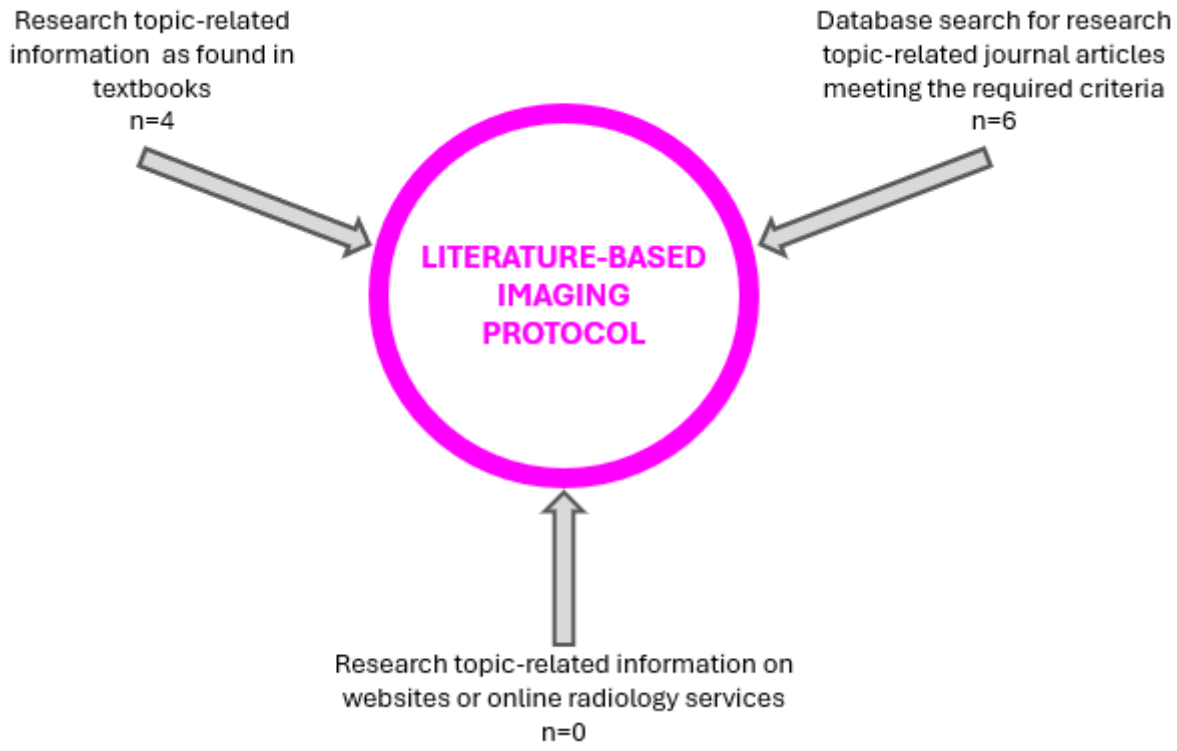



**Figure 2.1.** Literature search process (phase 1).

A summary of the literature-based imaging protocol is presented in Tables 2.2 to 2.4. This literature-based imaging protocol was used to create the observation checklist used during phase 2 of the study, and it also assisted with the design of the experimental protocols used in phase 3 of the study. The literature-based imaging protocol also contributed to the final standardised imaging protocol implemented by radiographers during the implementation phase (phase 4).


© Central University of Technology, Free State

The flow diagram in Figure 2.2 illustrates the literature search process. The important factors included in the review are discussed in sequence as shown in the figure. The first section describes all the important factors contributing to the purpose and aim of this study. It presents background information on the research topic, providing important intel on the research problem and question.

Neonatal patients are described and identified, as well as their susceptibility to ionising radiation and its associated biological effects and risks. The radiation dose absorbed by a neonatal patient is discussed, which was measured during the experimental phase (phase 3), and also the effects of the radiation dose on neonates. The radiation protection principles are discussed in depth regarding the ALARA principle. The chest and abdominal examinations are discussed in length with special attention to the positioning techniques, evaluation criteria and the critique technique of these procedures, as presented in published research.

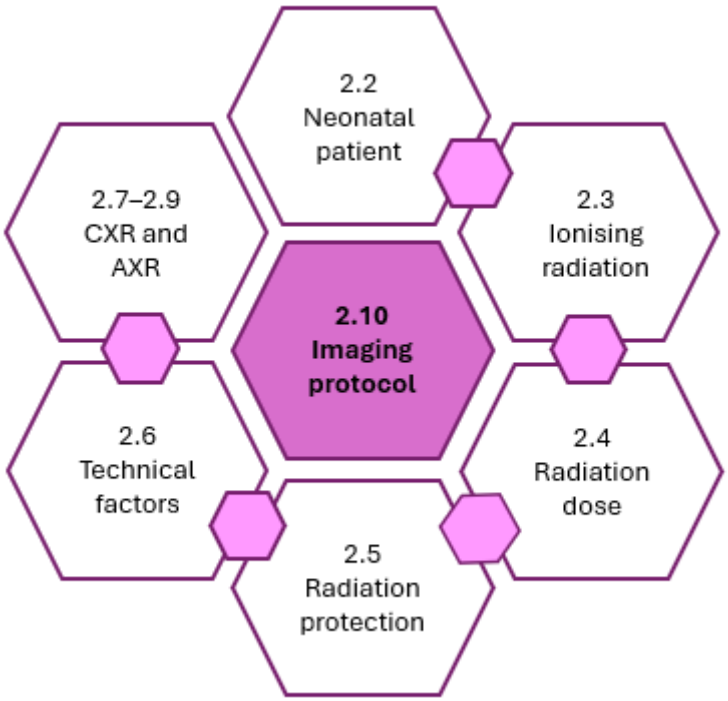



**Figure 2.2.** Literature review diagram.


© Central University of Technology, Free State

## 2.2 NEONATAL PATIENT

Newborn babies who may need special care or intensive medical care are admitted to the NICU, which offers advanced technology and specialised staff to provide care to these small patients (Stanford Children's Health, 2020: online).

Atherton, Gennery & Cant (2004: 14.1) described the neonatal period as the first four weeks after birth. A premature baby is regarded as a baby being born alive before the completion of 37 weeks of pregnancy. A baby born with a total birth weight lower than 2500 g is considered a low-birth-weight infant. According to the World Health Organization (WHO, 2024), the most critical time for neonatal patients is during labor and the immediate postnatal period. Postnatal intensive care is critical when the baby is born prematurely or with a low birth weight. Babies born with infections or abnormalities, or those that experienced oxygen deficiency during birth, need critical care directly after birth (WHO, 2024: online).

According to Martire, Polito, Ciucci, Solfaroli Camilocci, Longo, Genovese, Cirillo, Toma, Magistrelli and Cannata (2023: 6), the benefit outweighs the risk when it comes to chest X-rays, but it has to be taken into account that neonatal patients may receive a large number of X-rays throughout their hospital stay. The radiation risk is minimised when tight collimation is applied, correct patient positioning is applied and artefacts are removed prior to image acquisition. Aramesh et al. (2017: 124) stated that neonatal patients with a low birth weight may require more X-ray examinations over a short period of time. Due to their small size, a bigger area of their body is placed in the radiation field. This causes the neonates to have a higher effective dose compared to that of adults.

## 2.3 IONISING RADIATION

When a person is exposed to ionising radiation, cell changes occur. The cells can either be damaged and they can repair themselves, or the DNA can mutate, causing cells to become cancerous. Every cell reacts differently when exposed to ionising radiation and some cells are more sensitive than others. The cells that are mostly affected by ionising radiation are the cell types that reproduce the most, for example, the cells in a growing foetus or neonate (Ball, Moore & Turner, 2008: 341). Thus, adherence to the ALARA principle aims to minimise the radiation dose (Bontrager & Lampignano, 2014; Lampignano & Kendrick, 2021).


© Central University of Technology, Free State

The ionising radiation received for radiographic X-ray examinations is small and the benefit thereof outweighs the risk. However, for neonates admitted to the NICU for an extended period, regular exposure to ionising radiation is required to monitor their health, thus increasing the total dose of ionising radiation received (Kartikeswar, Parikh, Pandya & Pandit, 2019: 158). This is an important consideration since neonates have higher mitotic activity, increased radiosensitivity and longer lifetime to manifest consequences from the ionising radiation, rendering preterm neonates more vulnerable to radiation damage (Kartikeswar et al., 2019:160; Govender, Ntholeng, Vawda & Larson, 2013: 31). Radiation dose qualities such as air kerma and entrance surface dose (ESD) are discussed below to provide a better understanding of the medical physics terms.

### 2.3.1 Air kerma

Air kerma is a radiation quantity used to express the concentration of the X-ray beam delivered to a specific point. Kerma (kinetic energy released per unit mass of air) is a measurement of the amount of radiation energy (joules; J) deposited in or absorbed by a unit mass (kilogram) of air. Kerma is expressed as J/kg, which is the same radiation unit as Gray (Gy) (Sprawls, 1995: 46).

Incident air kerma (IAK) expresses the radiation concentration delivered to a certain point, such as the entrance surface to the human body. The air kerma calculated or measured at a certain point will be approximately equal to the absorbed dose at the same point (Sprawls, 1995: 46).

### 2.3.2 Entrance skin dose

The entrance skin dose (ESD) is the radiation that is absorbed by the skin of the patient. The ESD can be measured by placing a dosimeter on the surface of a phantom or baby where the X-ray beam enters. It is measured in milligray (mGy) and is used to determine the diagnostic reference levels used for radiation protection purposes (Murphy & Bell, 2017: online).

### 2.3.3 Dosimeter

The ESD in this study was calculated from incident air kerma (IAK) measurements obtained with a dosimeter during the experimental phase. ESD measurements were calculated to ensure that the lowest possible dose was achieved with increased image quality for diagnostic purposes. The incident air kerma was measured on top of the neonate phantom to determine the radiation dose (without backscatter factor included) entering the phantom. The exit air


© Central University of Technology, Free State

kerma was measured with a dosimeter placed underneath the neonatal phantom to determine the radiation dose exiting the phantom after absorption of the X-rays. These values were included in the experimental checklist (Appendix C) of phase 3. The imaging protocols not meeting the exposure index requirements were excluded from the study, as discussed in section 3.3.1.

The dosimeter used for the third phase of the study at the hospital was the Unfors U dosimeter consisting of the Mult-O-Meter (model 587L) with an attached probe (Unfors RaySafe AB; Hovås, Sweden). The dosimeter is the property of the Department of Clinical Sciences at the Central University of Technology, Free State (CUT). Figure 2.3 represents an image of the dosimeter used during phase 3. The neonatal radiographic X-ray examination was simulated with a neonate phantom and the incident air kerma was measured by placing a dosimeter directly in the X-ray beam on the surface of the phantom.




**Figure 2.3.** Dosimeter equipment (Unfors Raysafe AB, 2003: online).

The Mult-O-Meter makes use of a fast automatic range technique THAT eliminates the need to manually find an optimum measuring range. It also has a trigger function installed in the detector. The trigger limit is up to two times higher than that of the lower limit of the dose rate range for the irradiated dose sensor (Unfors Raysafe AB, 2003: online).

The dosimeter used during phase 3 was calibrated by the National Metrology Institute of South Africa (NMISA). The dosimeter was calibrated for the correct measurements and units used. The calibration certificate is attached as Appendix K.

The IAK value obtained from the Unfors U solid-state dosimeter was multiplied by a pre-determined calibration factor (CF). The calibration factor was determined by NMISA as 0.998. The solid-state dosimeter used does not include backscatter which had to be accounted for


© Central University of Technology, Free State

by means of a backscatter factor (BSF). The dosimeter used in phase 3 of the study has a backscatter dependency of less than 1% because of its lead lining. The backscatter factor of 1.4 was used in this study. The International Atomic Energy Agency (IAEA) (2007: online) indicated that the ESD can be calculated from the reordered IAK value. The equation used to determine the ESD during the experimental phase (phase 3) is (Al-Murshedi, Hogg & England, 2018: 3; International Atomic Energy Agency, 2007: online):

**ESD = IAK x CF x BSF**.

## 2.4 RADIATION DOSE TO NEONATES

Neonatal patients are highly susceptible to ionising radiation. Due to the neonate's small size, their organs are relatively closer or within the X-ray beam, which increases the overall radiation dose. Thus, radiation exposure to neonatal patients should be justified and minimised (Armpilia *et al.*, 2001: 539). According to Bahreyni Toossi & Malekzadeh (2012: 146), neonatal patients are more susceptible to low levels of ionising radiation because they possess many rapidly dividing cells and the radiation received can cause irreparable damage to the DNA. The authors stated that the risk of cancer induction per unit dose for this specific patient group is supposedly 2–3 times higher than that of the average population.

According to Kartikeswar, Parikh, Pandya and Pandit (2019: 160), concern is raised based on the ionising radiation received by neonates in the NICU as the effects of the radiation exposure of each patient are not known. The author suggests monitoring radiation exposure in the NICU and minimising the number of X-rays performed on each neonate while maximizing the radiation protection.

## 2.5 RADIATION PROTECTION PRINCIPLES

The WHO (2020: online) proposed that the possible reasons for inappropriate exposure to ionising radiation may be due to the following: being unaware of the radiation doses involved and the associated risks, pressure from other specialists or physicians, patient demand, concerns of malpractice (defensive medicine), lack of confidence in the clinical diagnosis, or the pressure to perform.

The aim of radiation protection is to prevent deterministic effects and reduce the risk of stochastic effects for a patient. Radiation dose should be kept ALARA by encouraging optimal


© Central University of Technology, Free State

patient radiation protection. The three basic radiation protection principles are discussed in the following section. The principles are justification, optimisation and limitation (Gupta & Chawla, 2023: 519).

### 2.5.1 Justification for X-ray examinations

Justification means that there should be a justified reason for performing X-rays on a neonate, and that the same result could not possibly be achieved with an alternative non-radiation imaging modality (Gupta & Chawla, 2023: 519). Justification implies that the radiographic X-ray examination should be more beneficial than harmful. The benefit of radiographic X-ray examinations should outweigh the possible risks associated with the examination (International Commission on Radiological Protection [ICRP], 2007: 127).

Ebdon-Jackson & Friya (2021: 1) argued that justification is the most effective measure to be taken to reduce radiation dose in paediatric and neonatal radiographic imaging. The three As were introduced to enhance justification of medical X-rays. The three As are awareness, appropriateness and audit. To understand justification, one must be aware of the risk involved. Appropriateness refers to the usefulness of X-rays in each patient's situation; thus, linking it with ensuring that the benefit outweighs the risk. Regular audit contributes to good practice. The authors indicated that clinical audit should be integrated into the framework of the imaging department. It should also assess compliance with referral guidelines and relevant patient communications (Malone, Guleria, Craven, Horton, Jarvinen, Mayo, O'Reilly, Picano, Remedios, Le Heron, Rehani, Holmberg & Czarwinski, 2012: 535).

Justification of a procedure is a measure to avoid unnecessary radiation exposure to any patient. Every ionising radiation examination must be justified to ensure that the X-rays obtained will make a difference and contribute to the diagnosis and/or treatment of the patient. The justification process includes the referral of the patient. This means that it should be established whether the patient already had X-rays that were documented in the file. Another measure is to determine whether the information can be obtained by another nonionising radiation modality, such as ultrasound or magnetic resonance imaging (MRI) (Ebdon-Jackson & Friya, 2021: 2).

### 2.5.2 Optimisation of radiation protection

The ICRP (2007: 89) stated that optimisation of radiation protection applies to examinations that have been deemed justified. Optimisation is defined by the Commission as a source-


© Central University of Technology, Free State

related process to keep (i) the likelihood of incurring exposures; (ii) the number of people exposed to ionising radiation; and (iii) the magnitude of individual exposures as low as reasonably achievable (ALARA). Optimisation considers economic and social factors. Optimisation of protection does not mean dose reduction, but rather the evaluation based on the balance between the harm of radiation exposure and the resources available for radiation protection (ICRP, 2007: 92).

Another method of optimisation is to optimise radiographic examinations of questionable image critique, as they do not possess the needed diagnostic information to ensure accurate and reliable diagnosis (International Atomic Energy Agency, 2012: 24).

### 2.5.3 Limitations of ionising radiation

The exposure of a patient to ionising radiation has certain limits and should not exceed these limits. The public dose limit is different from the occupational radiation workers' dose limit. These limits determine the amount of ionising radiation a patient may absorb per ionising radiation examination (Yu, 2010: 314). The dose limits for neonatal patients are recommended to be kept below 80 µGy (Armpilia *et al.*, 2001: 539).

Several technical measures are available that a radiographer can take to reduce the radiation dose to patients. These technical measures or factors include collimation, the use of filters (cf. section 2.5.5), lead protection (cf. section 2.5.6), proper positioning techniques (cf. sections 2.7.1, 2.8.1 and 2.9.1), immobilisation measures and exposure parameters (cf. section 2.6) (Alzen & Benz-Bohm**,** 2011: 407).

The South African Health Products Regulatory Authority (SAHPRA) (2022: online) stated that each projection should be examined before obtaining an additional projection. This approach presents another method of reducing unnecessary exposure of neonatal patients. As most of these neonatal patients are X-rayed daily for routine monitoring and line and tube placement, it is important to remember the effects of radiation on this sensitive patient group and the role that radiographers play in protecting them. Radiographers should educate the supporting staff on radiation effects and the application of possible radiation protection measures (SAHPRA, 2022: online).

The Health Professions Council of South Africa (HPCSA) indicate that a scope of practice defines the procedures, processes and actions for which a professional has the relevant knowledge, skills and expertise to practice effectively and safely without posing any danger to


© Central University of Technology, Free State

the public or said practitioner. The HPCSA provided the scope of practice for Diagnostic Radiography to protect healthcare personnel and patients from radiation while performing mobile radiographic examinations. Their scope of practice also includes performing a range of radiographic examinations while producing high quality diagnostic images and also evaluating these images for technical quality as well as medico-legal requirements (HPCSA, 2020: online).

### 2.5.4 Radiographic equipment

Radiographic equipment and technical factors can also contribute to successfully optimising protection for neonatal patients. Consideration must be given to specific dose reduction measures when purchasing and installing new equipment in practice. Specific measurements include the option of removable grids, adding copper or aluminium filters when not provided, and collimation (Del Rosario Pérez, 2015: 24).

Paediatric and neonatal patients can successfully be X-rayed without the use of a grid. Therefore, a grid should be avoided when working with this specific patient group (European Commission, 1996: 62). Jain *et al.* (2021: 483) indicated that the use of a grid is not justified as the tissue thickness is not meeting the requirements to warrant grid use and the use of grid also increases the radiation dose to the patient. Tugwell-Allsup, Morris, Thomas & England (2020: 7) reported that additional copper (Cu) filtration could reduce the patient radiation dose.

Collimation is a crucial measure in reducing radiation to patients. It reduces both the primary and scattered radiation emitted to the patient. The field of view (FOV) should be reduced as much as possible to ensure proper four-sided collimation (Alzen & Benz-Bohm, 2011: 410). External anatomical landmarks of the neonate may assist in the correct beam collimation to the size of the patient. Basic knowledge of neonatal anatomy and patient history can assist the radiographer in ensuring proper collimation. It is important not to collimate too tight as that may lead to repetition of images, which will also contribute to increased radiation dose to the patient (Del Rosario Pérez, 2015: 30).

The mobile X-ray machine used for the study was a Siemens Mobilett Mira Max(Siemens Healthineers; Erlangen, Germany). The machine has a digital detector, the MAX mini, which is 28.4 cm x 22.8 cm in active size, with a weight of 1.6 kg. The detector contains amorphous silicon crystals with a caesium iodide scintillator. The machine has a maximum arm height of 225 cm, but the maximum source-to-detector distance (SDD) is 213.5 cm. The collimator can be rotated 90°, is manually adjustable and has a multi-leaf collimator with 1.6 mm Al inherent


© Central University of Technology, Free State

filtration at 70 kilovoltage peak [kVp]. It has a 30-kilowatt (kW) output at 96 kV 10 ms (millisecond) (Siemens Healthineers, 2014: 20). The summary of the daily, quarterly and yearly quality control tests performed on the mobile machine and detector before the experimental phase is attached as Appendix L (phase 3).

### 2.5.5 Protection of neonatal patients with shielding

Neonatal patients should always be protected from ionising radiation as they are susceptible to radiation. Neonatal cells have a high rate of mitotic division. Due to the small size of the neonatal patients, their organs are located relatively close to one another, thus increasing the radiation dose received and hence a higher effective dose. Neonatal patients can be protected by adhering to the ALARA principle and applying several radiation protection measures. Babies can be protected from ionising radiation by increasing the source-to-image distance (SID), making use of high tube voltage (kilovoltage peak [kVp]) and mainly by utilising lead protection (Karami, Zabihzadeh, Isavand-Faraji & Karampour, 2019: 2–4).

Although the more recent different perspectives to shield or not to shield is outside the scope of this study, the researcher is aware that gonadal shields should only be applied during image acquisition when it does not interfere with the diagnostic process of the image (SAHPRA, 2022).

## 2.6 TECHNICAL FACTORS

Certain acquisition parameters do directly affect the radiation dose to the patient. Seibert and Morin (2011: 575) investigated the technical factors selected to contribute to the patient radiation dose. These authors indicated additional parameters that should also be considered when selecting the technique factors. According to Seibert and Morin (2011), factors also affecting the radiation dose to the patient include the use of a grid, SID, filtration methods and beam collimation.

Even though the technical radiation factors are lower than those of adults, it is still important to monitor the amount of ionising radiation dose to neonates. The argument is that neonates receive a high patient dose associated with the large number of X-rays taken when admitted to the intensive care unit (Faulkner, Barry & Smalley, 1989: 230–231).

The radiosensitivity of organs is inversely related to the age of the neonate. Therefore, neonatal patients are more sensitive to ionising radiation than children or adults. Furthermore,


© Central University of Technology, Free State

the relationship between the gestational age and birth weight of neonates is also inversely related to the cumulative dose rate (Aramesh *et al.*, 2017: 128).

Seibert and Morin (2011: 575) explained that the size and body part of the neonate being X-rayed directly affect the technical factors (kVp and milliampere second [mAs]) used when imaging a patient using digital radiography (DR). When the technical factors are set too low for the patient size or relative body part, the image appears underexposed. An underexposed image has high noise content and clinical information will be lost. An overexposed image has low noise content and is not easily recognised as such, but it has an indirect relationship to the patient dose. Thus, an overexposed radiographic X-ray image will contribute greatly to the overall degree of radiation exposure.

### 2.6.1 Exposure and deviation index

The exposure index (EI) provides feedback on the precise technical factors selected for a specific projection. This aids in reducing the patient radiation dose and providing a radiographic X-ray image with optimal quality for accurate diagnostic purposes. Each manufacturer sets their EI according to the functioning of their machine (Seibert & Morin, 2011: 573–574).

The deviation index (DI) was proposed to standardise the EI between manufacturers, as no two machines have the same EI value. It is important to note that neither EI nor DI indicates the patient radiation dose. The EI and DI provide feedback on the image quality obtained with specific technical factors (Seibert & Morin, 2011: 573–574). The DI indicator could also potentially reduce the patient radiation dose when used correctly (Sutoro, Irsal & Cahya, 2023: 58).

The DI indicates a null value when an appropriate amount of exposure is received by the detector. A positive one value indicates the image was overexposed by 25% more than the target value. Thus, a negative one value suggests the image was underexposed 20% less than desired. A positive three and a negative three DI suggests exposures that are two times more (overexposed) and less (underexposed) than the target exposure to be achieved. The purpose of the DI is to indicate whether the presentation of the anatomy for diagnostic purposes is of optimal quality (Seibert & Morin, 2011: 579). The DI compares the actual EI value to the target EI value (Sutoro *et al*., 2023: 60).


© Central University of Technology, Free State

In the department where the study was executed, an EI is used to determine the image quality of the radiographic X-ray image. Thus, the mobile machine has an EI value for each examination performed and the value will determine whether the image was overexposed or underexposed, and if the image requires repetition.

The recommended EI range for CXR is 50–200, while the recommended EI range for AXR and CXR-AXR is 125–500 (Siemens Healthineers, 2014: 73). For this system, when the EI indicator is above the mentioned recommended range, the image is overexposed while when the EI indicator is below the recommended range, the image is underexposed (Mothiram, Brennan, Lewis, Moran & Robinson, 2014: 113).

## 2.7 CHEST X-RAY EXAMINATION OF NEONATES

Chest X-rays consist of two projections, the posterior-anterior (PA) and lateral projections. During neonatal imaging, an anterior-posterior (AP) projection is obtained instead of the PA (Bontrager & Lampignano, 2014; Lampignano & Kendrick, 2021: 631). During a mobile radiographic X-ray examination in the NICU, only one projection will be obtained, which will be the AP projection of the chest (Whitley *et al*., 2015: 390) and this projection was the focus of this study.

The detector used for chest imaging in the NICU included one detector of 24 x 30 cm size. This size will include all relevant anatomy. The radiographic X-ray image must include and clearly indicate the patient identification such as the patient's name, surname, date of birth, gender, identification number or hospital number, and date of examination (Bontrager & Lampignano, 2014: 631–633; Lampignano & Kendrick, 2021). According to Titley and Cosson (2014: 43), a radiologist reporting on the images produced may refuse an image without an appropriate anatomical side marker and they may request another radiograph to be performed to include the marker. The authors also stated that the image may require repetition if the anatomical lead marker is not visible on the image due to medico-legal requirements.

The indications for a mobile unit chest X-ray in the NICU include cystic fibrosis, hyaline membrane disease, meconium aspiration, asthma, croup and aspiration (Bontrager & Lampignano, 2014: 627; Lampignano & Kendrick, 2021). Armpilia *et al*. (2001: 539), added possible indications to include a low gestational age and low birth weight.


© Central University of Technology, Free State

### 2.7.1 Positioning technique for chest X-rays

The positioning technique in radiography carries great importance. With a good positioning technique, accurate diagnostic information can be obtained and a decrease in the radiation dose to the patient will be achieved (Maruyama & Yamamoto, 2008: 25).

In Figure 2.4, the suggested positioning for a neonatal mobile chest X-ray is displayed, while the positioning techniques are discussed below. The centring is not optimal in the provided example.



**Figure 2.4.** Chest X-ray positioning (Long *et al*., 2019: 27).

The neonate will be in a supine position on the detector. The main radiation beam will therefore enter the neonate anterior and exit posterior (Bontrager & Lampignano, 2014: 631–633; Lampignano & Kendrick, 2021). The midsagittal plane should be perpendicular to the centre of the detector and X-ray field, while ensuring that the neonates' head is straight and the hips are level (Whitley *et al*., 2015: 390). It is important to move the arms away from the body (abduction) to prevent the scapulae from superimposing the lung fields. Should infection prevention require limited skin contact with the neonate, the nursing professional can be asked to move the arms away from the body (Bontrager & Lampignano, 2014: 631–633; Lampignano & Kendrick, 2021). Whitley *et al*. (2015: 390) stated that the arms should be flexed next to the head to prevent mimicking a pneumothorax, while the chin is lifted to prevent obscuring the lung apices.

Neonatal chest images are taken on suspended inspiration. It is important to observe the neonate for breathing. If the neonate is on a ventilator, the machine will indicate inspiration. If


© Central University of Technology, Free State

the neonate is not connected to a ventilator, the radiographers observe the thorax of the neonate to see expansion of the ribcage, which will indicate inspiration. One can also listen to the crying of the neonate for the breathing pause (Bontrager & Lampignano, 2014: 631–633; Lampignano & Kendrick, 2021). However, Whitley *et al*. (2015: 391) warned not to expose while the neonate is crying, as it can cause overexpansion of the lungs.

Figure 2.4 is only for reference purposes and shows the positioning technique, but the textbook (Long et al., 2019: 28) made use of a different centring point. The main radiation beam is centred towards thoracic vertebrae number 7 (T7) or on the nipple line of the neonate. Four-sided collimation should be evident (Bontrager & Lampignano, 2014: 631; Lampignano & Kendrick, 2021). The top border of the collimator should be 2.5 cm above the shoulders and the bottom collimator should be on the lower costal margin to prevent irradiation of unnecessary anatomical structures (Long *et al*., 2019: 28). The X-ray tube should be raised as high as possible to provide the largest distance possible and may vary between 125 cm and 150 cm. No grid is used for the imaging of neonatal CXR, due to the low body part thickness and low kVp setting (Bontrager & Lampignano, 2014: 631; Lampignano & Kendrick, 2021).

According to Pedersen, Hardy and Blankholm (2018: 262), the position of the neonate's head during a CXR can influence the rotation of the chest, while the arm position does not influence the rotation of the chest. These authors also indicated that the rotation of the lower thorax can occur independently of that of the upper thorax, thus they are indirectly related regarding rotation.

### 2.7.2 Criteria for chest X-rays

Displayed in the image below is an example of the criteria for CXR for neonates. The labels on the right (written in red text) indicate the suggested anatomy to be included for a CXR, while the text on the left (written in black) is the suggested criteria to check for neonatal CXR before passing an image. The anatomical structures included in the image below are stated as important criteria according to Bontrager and Lampignano (2021: 632) and Lampignano & Kendrick (2021).


© Central University of Technology, Free State

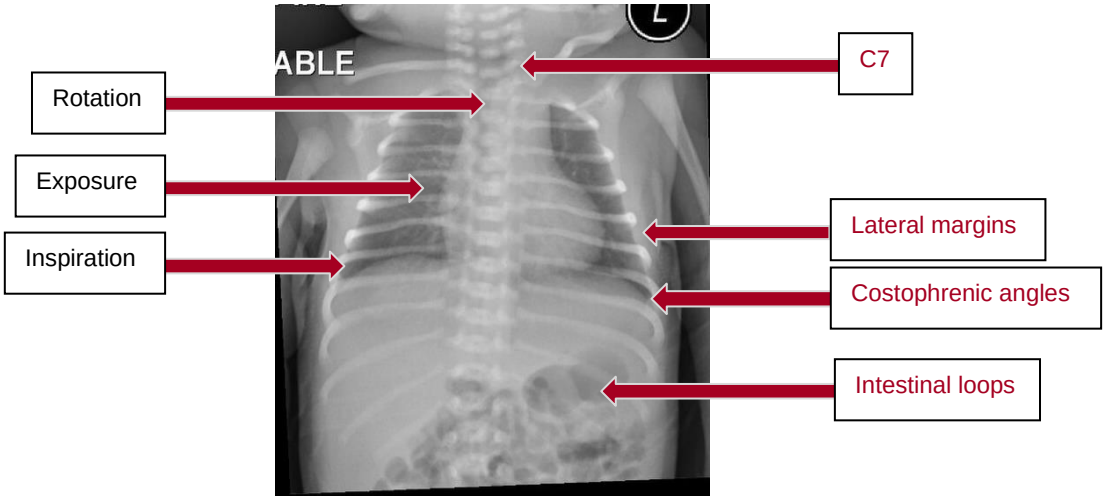



**Figure 2.5.** Chest X-ray criteria (Wikimedia, 2023: online).

The AP chest image must include a part of the abdomen to allow visualisation of the intestinal loops. The author noted that routine inclusion of the abdomen should not be allowed to limit radiation dose to the neonatal patient (Yoon, 2016: 280).

McQuillen Martensen (2015: 118) proposed criteria for a CXR that should include the entire lung fields. Cervical vertebra number seven must be included up to thoracic vertebra number 12 (T12). The clavicles must be on the same horizontal plane, and the scapulae must be located outside of the lung fields. The distances from the vertebral column to the sternoclavicular ends must be equidistant to indicate no rotation visible for the chest.

Pedersen *et al*. (2018: 260) argued that the popular method of determining rotation by assessing the distance from the medial ends of the clavicle to the vertebral bodies is not a reliable method for establishing rotation of the lower thorax. Whitley *et al*. (2019: 391) indicated that the anterior rib ends should be equidistant from the spine to indicate no rotation of the chest, while the medial ends of the clavicles should overlap the lung apices to indicate no tilting of the chest and no lordotic chest image.

Arthur (2001: 312) stated that during a supine chest image of a neonatal patient, cardiomegaly will be visible on the image as the distance is increased from the heart to the detector when performing the CXR in an AP projection. The correct size of the heart is also difficult to establish due to the supine position of the neonate and the presence of the thymus shadow. Rotation of the neonatal chest may also indicate cardiomegaly, mediastinal shift in the chest or an increase in the translucency of the lungs.


© Central University of Technology, Free State

Doctors Lewis Potter and Daniel Ward created a website named Geeky Medics to assist health professionals in medical education (Potter & Ward, 2024: online). The authors created checklists to ensure all important aspects are evaluated when reviewing a CXR. The mnemonic "**RIPE**" is used to assess image quality and stands for:

R – Rotation
I – Inspiration
P – Projection
E – Exposure

**Rotation** refers to the appearance of the chest cavity. To ensure no rotation is evident in the image, the medial aspects of the clavicles should appear equidistant from the spinous processes, while the spinous processes should appear in the middle of the vertebral bodies (Potter & Ward, 2024: online). The spine should lie in the centre of the chest cavity with symmetric appearance of the lung fields. The symmetric appearance and the length of the ribs will also aid in determining rotation (Trotter & Carey, 2000: 42).

**Inspiration** refers to the number of ribs seen above the diaphragm. According to Potter and Ward (2024, online), five to six posterior ribs should be seen above the diaphragm to represent full inspiration. The lung apices and the costophrenic angles should be clearly visible. Bontrager and Lampignano (2014: 631) and Lampignano & Kendrick (2021) stated that full inspiration is evident when nine posterior ribs are visible above the diaphragm (McQuillen Martensen 2015: 118). McQuillen Martensen (2015: 113) and Whitley *et al*. (2015: 391) specified that for a neonate, eight posterior ribs should be visible above the diaphragm.

**Projection** refers to the direction of the main X-ray beam as it passes through the infant (Bontrager & Lampignano, 2014: 18; Lampignano & Kendrick, 2021). Both the projection and the position of the baby should be indicated. Projection further refers to the CXR being an AP or PA projection where the position of the neonate would be supine, prone or erect.

**Exposure** involves the impact that the exposure factors or techniques (kVp and mAs settings) have on the image and how it is evaluated when evaluating at the image (Bontrager & Lampignano, 2014: 30; Lampignano & Kendrick, 2021). When evaluating the exposure of the radiographic image, there should be no motion evident, which is signified by the sharp outlines of the diaphragm, heart shadow and rib margins. Lung markings are visible and the faint outline of the ribs and vertebrae through the heart shadow is an effective method to determine optimal exposure (Bontrager & Lampignano, 2014: 632; Lampignano & Kendrick, 2021).


© Central University of Technology, Free State

According to Whitley *et al*. (2015: 391), proper exposure will allow the visualisation of the trachea and main bronchi, as well as the reproduction of the vascular pattern in the central two-thirds of the lungs.

### 2.7.3 Evaluation of chest X-rays

The lungs of a newborn will appear relatively hyperlucent with small hila and a rounded appearance of the heart. The thymus is described as draped around the heart and is relatively prominent in the thoracic cavity. The thymus presents as a sail sign as it causes a triangular projection laterally (Yoon, 2016: 279–280).

Trotter and Carey (2000: 36) listed important aspects to evaluate on a CXR. These anatomical structures and pathological landmarks include the following:

i. Check the surrounding soft tissue for any oedema.
ii. Study all the bony structures such as the bell-shaped ribcage, the vertebrae, humeri and clavicles. Look for bone density when possible.
iii. Evaluate the air-filled trachea to determine narrowing or deviation of any kind.
iv. Examine the hila to determine increased or decreased pulmonary blood flow.
v. Evaluate the mediastinum and all mediastinal structures including the heart, large blood vessels and the thymus. When evaluating these components of the mediastinum, it is crucial to evaluate their size, shape and location.
vi. The diaphragm and both costophrenic angles must be examined to determine the sharpness of the structures and eliminate any related pathologies.
vii. When visible, the gastric bubble must be evaluated, as well as the size and location of the liver.
viii. The general aeration of the lung fields must be examined, and also the width of the numerous intercostal spaces.
ix. When any medicinal lines or tubes are present in the thoracic cavity, their location and position must be established and reported.

Potter and Ward (2024: online) proposed the ABCDE approach that is used to evaluate a CXR image. It is a checklist containing all the relevant and important anatomical structures to be evaluated. The **ABCDE approach** contains the following:


© Central University of Technology, Free State

A – Airway: trachea, carina, bronchi and hilar structures
B – Breathing: lungs and pleura
C – Cardiac: heart size and borders
D – Diaphragm: including the costophrenic angles
E – Everything else: mediastinum, bones, soft tissue, tubes and lines

These anatomical structures were included in the observational checklist (phase 2) (Appendix A) as part of the image evaluation criteria.

For **airways**, the trachea must be inspected and evaluated for any evidence of a narrowing or deviated trachea. The trachea is normally centrally located or slightly deviated to the right. Thus, normal must be distinguished from abnormal appearance. The carina is the portion of the trachea where it bifurcates into the left and right primary bronchi. The carina must be visible and plays an important role when checking the placement of the nasogastric tube. The left and right main bronchus should be visible, and their sizes and shapes must be inspected. The hila usually represent symmetrical; thus, any asymmetric appearance should raise suspicion. These structures are an important landmark for the transition of the pulmonary arteries into the pulmonary veins (Potter & Ward, 2024: online).

To assess **breathing,** the lungs as well as the pleura are inspected. The lungs are divided into three zones. Lung markings must be present throughout the lung. On a healthy neonatal patient, the pleura should not be visible; when the pleura is visible when evaluating the image, some pathologic changes are present (Potter & Ward, 2024: online).

For **cardiac** assessment, the heart size must be evaluated to rule out any cardiac abnormalities or pathologies. The heart borders should be well-defined on an optimal image (Potter & Ward, 2024: online).

The **diaphragm** should be evaluated with sharp borders and no free air present. The costophrenic angles should appear sharp and free from any fluid (Potter & Ward, 2024: online).

**Everything else** refers to the mediastinal structures such as the aortic knuckle, the bones forming part of the chest cavity, and any other soft tissue structures. It also refers to the presence of medical lines and tubes (Potter & Ward, 2024: online).


© Central University of Technology, Free State

Potter and Ward (2024: online) included review areas that do not form part of the ABCDE approach but remain important areas. These areas to review on the CXR include:

- Lung apices
- Retrocardiac region
- Peripheral regions of the lung
- Area behind the diaphragm

To evaluate the placement of lines, two-thirds of the upper abdomen must be included on a chest radiograph (Potter & Ward, 2024: online). In Figure 2.6, the evaluation criteria of the neonatal chest X-ray are displayed with reference to the extensive elaboration above.

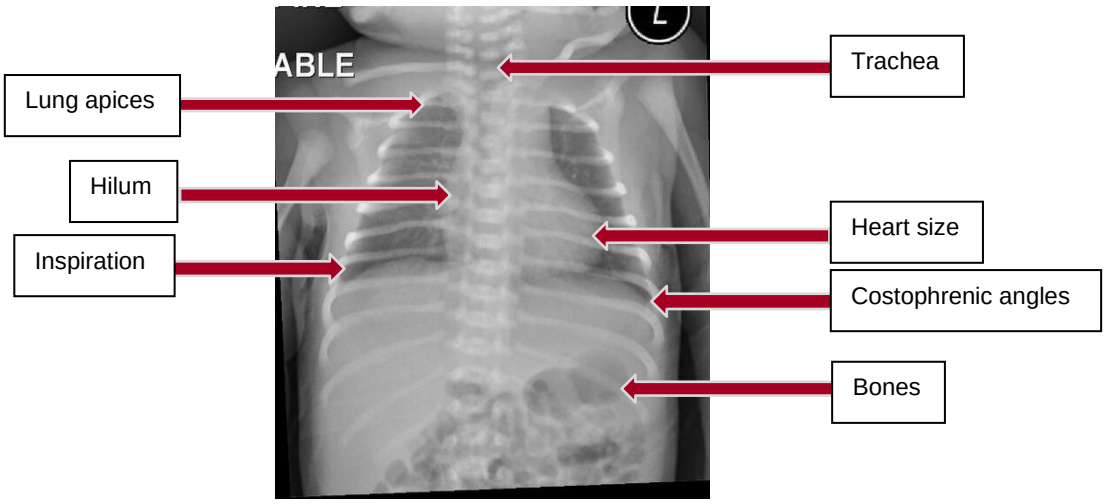



**Figure 2.6.** Chest X-ray evaluation (Wikimedia, 2023: online).

## 2.8 ABDOMINAL X-RAY EXAMINATION OF NEONATES

Routinely, both a supine and dorsal decubitus view of the abdomen will be obtained when imaging the abdomen of neonatal patients (Menashe, Iyer, Parisi, Otto, Weinberger & Stanescu, 2017: 418). Additional radiographic projections will be performed when a pneumothorax or pneumomediastinum is suspected (Del Vecchio, Salerno, Barbagallo, Chirico, Campoleoni, Cannata, Genovese, Granata, Magistrelli & Toma, 2020: 162). This practice has changed due to the biological effects of ionising radiation. For the abdomen, the routine X-rays have been reduced to a single supine X-ray to enhance radiation protection in this radiation-sensitive patient group. The dorsal decubitus as an additional projection should be obtained when suspecting perforation or obstruction. On the supine abdominal X-ray, the diaphragm superiorly and the pubic rami inferiorly should be included (Menashe *et al*., 2017: 418).


© Central University of Technology, Free State

An AXR consists of an AP image of the abdomen. It is preferred that the image be taken in an erect position, but with neonates, the X-rays are routinely performed in a supine position. A dorsal decubitus will be done, if necessary, to evaluate the presence of air-fluid levels and free air in the abdomen (Bontrager & Lampignano, 2014: 646; Lampignano & Kendrick, 2021).

An AP AXR will be obtained when a portable X-ray procedure is performed. A detector, 24 x 30 cm in size, is used for the abdomen without using a grid. The detector is placed underneath the neonate and a vertical straight X-ray beam will enter the neonate on the anterior side and exit on the posterior side. Four-sided collimation and the correct anatomical lead marker must be visible on the image. The image must be labelled to indicate that the neonate was in a supine position. Patient information such as the name, surname, biological sex, date of birth, date of the examination and hospital number or identification number must be visible on the radiographic X-ray image (Bontrager & Lampignano, 2014: 644; Lampignano & Kendrick, 2021).

The clinical indications for abdominal imaging in neonatal patients include intestinal obstruction, urinary tract infection, Hirschsprung's disease, polycystic kidney disease, atresia, neoplasms and pyloric stenosis (Bontrager & Lampignano, 2014: 630; Lampignano & Kendrick, 2021). According to Del Vecchio *et al*. (2020: 161), other indications for abdominal X-rays include positioning of several lines and tubes such as umbilical lines and central catheters.

### 2.8.1 Positioning technique for the abdomen

With a mobile X-ray unit, an AP projection of the abdomen is obtained with the neonate in a supine position. The neonate will lie on the back, with arms immobilised next to the head. The neonates' midsagittal plane should be perpendicular to the detector and the spine should be straight for alignment purposes (Whitley *et al*., 2015: 398). Immobilisation is crucial during this examination. Their hands must be kept above the head to prevent any overlapping of anatomy and their legs must be kept still to prevent any motion blur (Bontrager & Lampignano, 2014: 644; Lampignano & Kendrick, 2021). To ensure no rotation, the anterosuperior iliac spines should be equidistant from the detector (Whitley *et al*., 2015: 398).

The main radiation beam must enter the neonate anteriorly and exit posteriorly. During this examination, radiation protection is of utmost importance by implementing collimation to exclude the chest, thyroid, and eyes. Radiosensitive organs such as gonads are included in


© Central University of Technology, Free State

the region of interest, consequently receiving high radiation dose. To obtain an optimal abdominal X-ray, the radiographer must observe the respiration of the neonate. The chest must be observed for respiratory movement, or when a neonate is intubated, the machine can be observed for adequate expiration. Abdominal X-rays are taken on suspended expiration (Bontrager & Lampignano, 2014: 644; Lampignano & Kendrick, 2021).

The image in Figure 2.7 is an example of the positioning technique for a neonatal AXR to represent the positioning techniques discussed above.



**Figure 2.7.** Abdominal X-ray positioning (Lim, 2017: online).

### 2.8.2 Criteria for abdominal X-rays

Figure 2.8 represents an abdominal image of a neonate for reference purposes in this section. The labels on the right (in blue text) reflect the inclusion criteria for AXR. The labels on the left (in black text) display the evaluation criteria for abdominal structures on an X-ray.

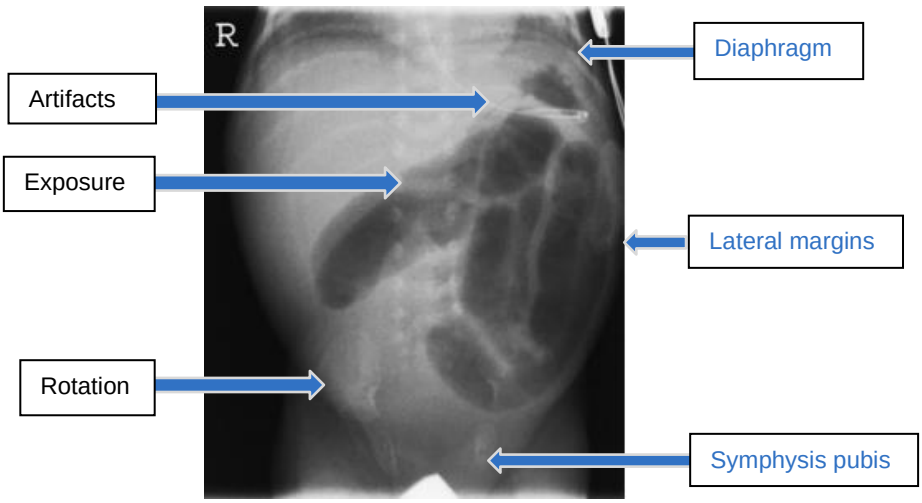



**Figure 2.8.** Abdominal X-ray criteria (Whitley *et al*., 2015: 399).


© Central University of Technology, Free State

On a neonatal AXR, soft tissue, air or gas and bone are distinguishable. The borders of different soft tissue structures such as the liver, stomach and spleen can be seen. The liver is in the upper right quadrant and the stomach and spleen are in the left upper quadrant. On a normal abdominal X-ray, gas is observed in the stomach and large intestine. This air serves as a type of contrast medium to evaluate the radiographic X-ray image and aids in the diagnostic process (Lee, 2011: 131).

The spine should be straight for proper alignment (Whitley *et al*., 2015: 399). The imaging criteria for the abdomen include that rotation should be limited, which is achieved when the iliac wings of the pelvis appear identical in size and shape. The distance from the lateral portion of the vertebral body to the lateral margin of the abdominal wall should be equal on both sides to ensure no rotation has occurred. Regarding the inclusion of anatomical structures, superiorly the domes of the diaphragm and the symphysis pubis inferiorly should be included in the images. The lateral borders of the abdomen with the preperitoneal fat lines (flank fat stripes) should be included to ensure optimal imaging (Lee, 2011: 133–136; Whitley *et al*., 2015: 399). Whitley *et al*. (2015: 399) also suggested inclusion of the ischial tuberosities inferiorly.

### 2.8.3 Evaluation of abdominal X-rays

The radiographic X-ray image shown in Figure 2.9 displays an example of the evaluation of abdominal X-rays for neonates.

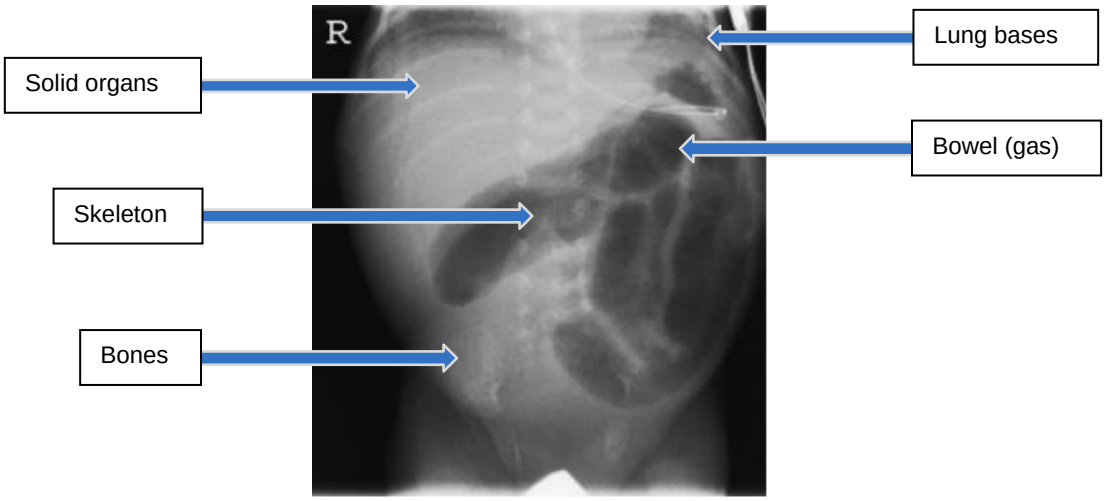



**Figure 2.9.** Abdominal X-ray evaluation (Whitley *et al*., 2015: 399).


© Central University of Technology, Free State

Potter and Ward (2024: online) created another mnemonic for the interpretation of abdominal X-rays; BBC. **BBC** was created for the easy evaluation of the abdominal structures and includes:

B – Bowel and other organs: small bowel, large bowel, liver, gallbladder, lungs, stomach, spleen, kidneys, bladder and psoas major muscles.
B – Bones: ribs, thoracic-lumbar vertebrae, sacrum, coccyx, pelvis and proximal femurs.
C – Calcification and artifact: renal stones, foreign body, and medicinal lines and tubes.

For the **bowel**, it is important to differentiate between the small and large intestines. There are a few ways to distinguish between the two as the small bowel is located more centrally and the large bowel is located around the periphery. The bowel diameter must be studied to exclude pathologies such as bowel obstruction. The lungs should be evaluated for pneumoperitoneum, pleural effusion or pneumonia. The size and location of the liver should be evaluated to exclude pathologies of the biliary system. The location of the stomach may indicate situs inversus or hiatal hernias. Thus, the stomach must be located and evaluated (Potter & Ward, 2024: online).

All **bones** should be evaluated to visualise clear cortical outlines. This will indicate any fractures or dislocations. The bones should be checked for loss of bone density or a mottled appearance (Potter & Ward, 2024: online).

Concerning **calcifications** and **artifacts**, several foreign bodies can appear on an abdominal radiographic X-ray image. These may include stitches, surgical clips, medicinal tubes and lines or contrast media (Potter & Ward, 2024: online).

James and Kelly (2013: 179) explained how to accurately interpret a radiograph. A step-by-step approach should be used to ensure no information is lost or no pathology is missed or overlooked. Firstly, the bowel gas pattern should be evaluated, searching for free air in the abdomen. Secondly, each solid intra-abdominal organ should be inspected and evaluated for enlargements and perforations. The third step is to identify any calcifications and the origin thereof. The skeleton should be analysed for any abnormalities or loss of density. The final step is to evaluate the lung bases for any pathological changes, metastases or pneumonia (James & Kelly, 2013: 179).


© Central University of Technology, Free State

## 2.9 COMBINED CHEST AND ABDOMINAL X-RAY EXAMINATION OF NEONATES

### 2.9.1 Positioning technique for the combined chest and abdomen

According to Del Vecchio *et al*. (2020: 162), obtaining a combined CXR-AXR image could be useful, especially when determining the position of some lines and catheters. However, the centring of the main radiation beam should be altered. When obtaining this type of image with the same centring point as for an abdominal X-ray, the chest may appear lordotic, which could cause a difficult diagnosis.

### 2.9.2 Criteria for the combined chest and abdomen

Figure 2.10 shows the inclusion criteria for anatomical structures for a combined chest and abdominal X-ray.

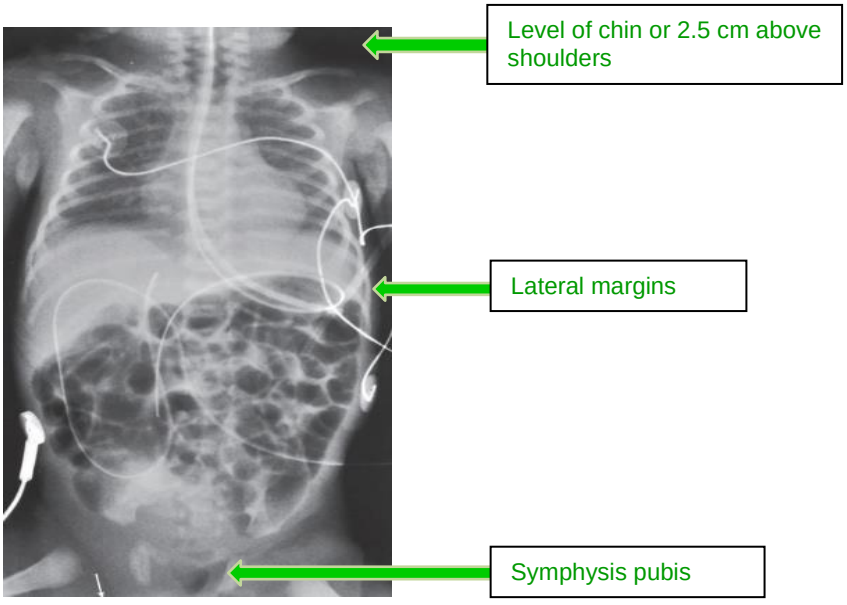



**Figure 2.10.** Combined chest and abdomen criteria (Long *et al*., 2019: 28).

### 2.9.3 Evaluation of the combined chest and abdomen

Long *et al*. (2019: 28) explained that the evaluation for the combined image remains the same as for the chest and abdominal X-rays. Therefore, these two imaging protocols described in the literature were integrated to compose an imaging protocol for the CXR-AXR image. These evaluation criteria for the chest and abdominal protocols are discussed in sections 2.7.3 (CXR) and 2.8.3 (AXR), respectively.


© Central University of Technology, Free State

## 2.10 IMAGING PROTOCOLS FOUND IN LITERATURE

The first objective of the study (as presented in Figure 1.1, Chapter 1) was to compile literature-based imaging protocols (Tables 2.2, 2.3 and 2.4, Chapter 1). The literature-based imaging protocol discussed in this section was used to benchmark the proposed baseline imaging protocol for neonatal mobile chest (CXR), abdomen (AXR) and combined CXR-AXR images with the literature. The literature-based imaging protocol was also used to benchmark the observational checklist of phase 2 (Appendix A).

### 2.10.1 Data synthesis for the literature-based imaging protocol

Twenty-eight articles were located to collect data associated with the study topic. The specific factors contributing to an optimal radiographic X-ray image were used to inform literature searches. Search engines consulted for relevant articles included Google Scholar, EBSCOhost, Science Direct, AJR Online, Scopus and PubMed.

A combination of keywords was used, such as "neonatal chest", "neonate", "chest X-ray", "neonatal mobile", "neonatal abdomen". Six articles and four books were found that provided evidence on specific techniques applied when imaging neonatal patients in the NICU. None of the articles or books provided a precise or complete neonatal imaging protocol. Therefore, a combination of articles was used to create a literature-based imaging protocol.

Articles were excluded for reasons such as reporting on studies that included closed incubators (n=3) and studies that used computed radiography (CR) (n=5). Closed incubators were excluded from this study as it changes the radiation dose received by the neonate. Because this study's focus was dose optimisation, the results would deflect the outcomes of the study. The hospital where the primary study was conducted also very rarely made use of closed incubators. Thus, the data captured would cause lopsided results. Articles discussing CR were also excluded as the hospital does not make use of CR systems, but only DR systems. Therefore, the literature data would not reflect in the practical application of phases 2 and 4 of this study.

The literature-based imaging protocol was the first step towards creating a standardised imaging protocol for the specific X-ray department where the study was undertaken. The researcher endeavoured to locate any articles and textbook chapters providing insight into the current practice of performing neonatal mobile examinations. Articles included contained any


© Central University of Technology, Free State

one of the criteria covered in the observational checklist. These criteria are related to exposure factors, positioning skills, or technical factors. The literature-based imaging protocol created from the published articles and books is discussed below.

### 2.10.2 Literature-based imaging protocol

Martire et al. (2023: 5) and Gunn et al. (2019: e2) found that the standardisation of procedures and techniques is crucial when working with neonates, as training and work experience of the radiographers have a direct influence on dose optimisation and positioning technique. These authors suggest that an optimised technique resulting in a lower radiation dose without compromising the image quality should be recommended for patients with prolonged hospital stays. It was found that most images were acceptable if good diagnostic quality was produced, even in those cases where the image quality criteria were not met (Martire *et al*., 2023: 5).

Table 2.1 provides a summary of the most distinctive aspects of the imaging protocol found in the literature. The table reflects the relevant articles and four books. Not all articles were included in the table as some of them only discussed one or two features already mentioned by other authors. Therefore, only the articles and books contributing the most information were included in this summary. All articles and textbooks have different publication dates ranging from 2014 to 2021, thus all information discussed below is still relevant and up to date with modern technology and imaging techniques. The different imaging factors are presented in Table 2.1 in no specific order.

Del Vecchio *et al*. (2020: 162) listed several factors that should be avoided to prevent repeating X-rays. These factors include incorrect patient positioning, unmaintained quality assurance programmes, poor quality of radiographic equipment (detectors that might have been dropped, artifacts on detectors), and poor execution of procedural protocol. According to these authors, the size of the collimation should be appropriate to the size of the patient.

All authors included in Table 2.1 indicated that a supine AP position is preferred during neonatal mobile chest examinations (Bontrager & Lampignano, 2014: 632; Del Vecchio *et al*., 2020: 162; Lampignano & Kendrick, 2021; Long *et al*., 2019: 28; McQuillen Martensen, 2015: 113; Tugwell-Allsup *et al*., 2020: 258; Whitley *et al*., 2015: 365).

Table 2.1 described the positioning of the neonate while performing CXR in the NICU. The arm position of the neonate does not influence the rotation of the thorax, and therefore, the arms may remain in a neutral position, placed outside of the region of interest. The lower


© Central University of Technology, Free State

thorax rotation or rotation of the pelvis occurs independently of the rotation of the thorax and does not have a direct influence on rotation of the chest. However, the head position of the neonate during chest radiography has a direct impact on the rotation of the upper thorax, and therefore, the head should remain in a straight position, facing upwards (Pedersen *et al*., 2018: 262).

Bontrager and Lampignano (2014: 390) and Lampignano & Kendrick (2021) suggested extending the arms of the neonate above the head to remove the scapulae from the lung fields, while the head should be lifted upwards to prevent superimposition over the superior lung fields. The authors also suggest extending the neonates' legs to prevent rotation on the pelvis. Another article indicated that the neonate's arms should be flexed next to the head, as extended arms could contribute to a lordotic image while the head is kept straight. The chin should be raised to prevent obscuring the lung apices (Whitley *et al*., 2015: 365). Long *et al*. (2019: 27) suggested that the arms of the neonate should be held next to the head, while the head could remain rotated.

McQuillen Martensen (2015: 118) suggested a perpendicular main radiation beam, with the midcoronal plane parallel to the sides of the detector. *Clark's Positioning in Radiography* indicated that the main radiation beam could either be straight or five to ten degrees caudally when performing mobile neonatal chest X-rays (Whitley *et al*., 2015: 365). *Merrill's Atlas of Radiographic Positioning and Procedures* proposed a perpendicular main radiation beam for chest X-rays (Long *et al*., 2019: 30).

Regarding the centring points for CXR, Bontrager and Lampignano (2014: 632) and Lampignano and Kendrick (2021) indicated the correct centring point to be on thoracic vertebra number seven (T7), while Tugwell-Allsup *et al*. (2020: 261) recommended that the correct centring point should be on the sternal angle. McQuillen Martensen (2015: 118) indicated the centring point should be on the nipple line, and Jain, Modi and Varma (2021: 483) advised to centre midway between cervical vertebra number 3 (C3) and the lower costal margin. Del Vecchio *et al*. (2020: 163) instructed to centre in the middle of the collimation rather than focusing on a specific centring point. This initiative inspired the researcher to follow a similar approach with the one-pager. The focus was placed on specific topographic landmarks for the collimation borders rather than identifying a specific centring point.

In chest X-rays, superiorly, the upper collimator line should be on the level of the chin, laterally collimation should be set to include lateral chest walls, and inferiorly, the bottom collimator line should be on the level just below the nipples (Del Vecchio *et al*. 2020: 162). For abdominal


© Central University of Technology, Free State

images, the collimation should include the top of the diaphragm superiorly, the symphysis pubis inferiorly, and the lateral abdominal walls laterally. During the combined CXR-AXR image, the collimation should be set at the level of the chin superiorly, the symphysis pubis inferiorly and the lateral chest and abdominal walls on the sides (Del Vecchio *et al*. 2020: 162).

Long *et al.* (2019: 28) agreed that for CXR of neonates, the top collimator should be placed 2.5 cm above the shoulders, while the bottom collimator is placed on the lower costal margin. The lateral collimators should be placed 2.5 cm from the lateral soft tissue. During a combined CXR-AXR, the top border of the collimation should be placed 2.5 cm above the shoulders, and the bottom collimator should be placed on the symphysis pubis. The lateral collimators should be placed 2.5 cm from the lateral soft tissue margins. Another author indicated that the top border of the collimation should be above the shoulders and the bottom border should be on the lower costal margin, while the transverse collimation should include 2.5 cm of the lateral skin line (McQuillen Martensen, 2015: 118). It is important to note that the detector size is much bigger than a neonatal chest and the placement thereof does not have to change only the collimation as it directly influences the radiation dose.

Del Vecchio *et al*. (2020: 163) suggested that apart from collimation, other parameters could reduce the radiation dose to neonates. Correct patient positioning can aid in decreasing the radiation dose as it reduces the repetition rate of X-rays taken. The X-ray field should not be larger than necessary, but still include all relevant anatomical structures to prevent repeat X-rays. They concluded that a combined CXR-AXR image should be kept to a minimum as the presentation of the chest may not appear anatomically correct and may result in a second exposure being required (Del Vecchio *et al*., 2020).

In four different publications, it was indicated that no grid should be used during neonatal mobile imaging. Bontrager and Lampignano (2014: 626) and Lampignano and Kendrick (2021) argued that a grid is not necessary as it reduces the radiation dose, and the patient part is smaller than 10 cm. The European Commission (EC) (1996: 29) suggested that grids should not be applied when working with neonatal patients as it increases the patient radiation dose. Jain *et al*. (2021: 483) indicated that grids are not necessary for neonatal imaging as the soft tissue thickness does not justify its use, which will increase the radiation dose to the patient. Whitley *et al*., 2015: 387 stated that a grid is not necessary when working with neonatal patients due to their smaller size and emphasised that using a grid should always be justified as it increased the radiation dose to the patient by 100%.


© Central University of Technology, Free State

According to Tugwell-Allsup *et al*. (2020: 258), one of the leading controversial aspects of neonatal mobile imaging is the placement of the detector. While placing the detector inside the incubator imaging tray aligns with infection control measures, leaving the neonate in a stable and still position without the possibility of disrupting any lines or tubes, this placement contributes to increased beam attenuation, increased effective dose and decreased image quality. Tugwell-Allsup *et al*. (2020: 258) found that placing the detector directly below the neonate is the best practice to optimise image quality while reducing radiation dose. Other authors stated that the detector should be placed directly under the neonate, and if the detector is placed inside the detector tray, the entire bed should be tilted five to ten degrees caudally to avoid a lordotic appearance (Whitley *et al*., 2015: 365). Furthermore, the detector should be placed in the detector tray where possible to reduce the possibility of cross infection. When the detector tray is not available, the detector should be placed directly underneath the neonate (Del Vecchio *et al*., 2020: 162). In *Merrill's Atlas of Radiographic Positioning and Procedures*, Long et al. (2019: 26) proposed placing the detector inside the detector tray attached to the incubator where possible.

Tugwell-Allsup *et al.* (2020: 261) found that for optimising image quality and radiation dose to neonatal patients, a SID of 100 cm, 60 kVp and 0.5 mAs, and the detector placed directly beneath the neonate, is best. Gunn *et al*. (2019: e5) stated that when applying lower kVp, the image will consist of high contrast and higher image quality due to increased signal-to-noise ratio. Another author suggested a higher kVp setting 70–80 kVp and a lower mAs setting of 1 mAs, while a longer SID of 125–150 cm should be applied (McQuillen Martensen, 2015: 78). Bontrager and Lampignano (2014: 631) and Lampignano and Kendrick (2021) recommended that a kVp range of 75–85 kVp and a short exposure time to reduce the possibility of movement should be used. A maximum SID should be applied, otherwise a minimum height of 128–153 cm should be achieved. However, applying higher kVp will result in decreased mAs, resulting in reduced patient dose (Jain *et al*., 2021: 483). According to Del Vecchio *et al.* (2020: 163), the voltage may range from 50–65 kVp and 0.5–3 mAs, with a SID of 100 cm.

Gunn *et al*. (2019: e70) stated that according to EC guidelines, additional filtration of up to 1 mm Al or 0.1–0.2 mm Cu should be applied to reduce the effective dose. By applying this extra filtration method, the image quality of the radiography was not affected (Del Vecchio *et al*., 2020: 162). Normal X-ray tube has inherent filtration of 2.5 mm Al, but an additional 0.1 mm Cu filtration to reduce the entrance dose by approximately 20% has been suggested (Whitley *et al*., 2015: 387).


© Central University of Technology, Free State

Del Vecchio *et al*. (2020: 162) indicated that when performing chest and abdominal X-rays, using proper positioning technique, the correct size of collimation and the added filtration required, the dose to the gonads is very little and would not necessarily need radiation protection, as there is a possibility it may obscure relevant anatomy. Efficient technical factors produce a good quality image and can reduce the patient dose considerably.


© Central University of Technology, Free State

Central University of Technology, Free State

**Table 2.1.** Literatu st X-ray (phase 1).

| Reference | Position of neonate | Arms position | Head position | Angulation | Centring point | Collimation | Grid use | Detector placement | Exposure | SID | Filtration |
|---|---|---|---|---|---|---|---|---|---|---|---|
| Tugwell-Allsup *et al*. (2020) | Supine AP | – | – | – | Sternal angle | – | – | Under neonate | 60 kVp 0.5 mAs | 100 cm | – |
| Gunn *et al*. (2019) | – | – | – | – | – | – | – | – | High kVp Low mAs | – | 1 mm Al 0.1–0.2 mm CU |
| Pedersen *et al*. (2018) | – | Arms to the side or above the head | Head straight | – | Middle of C3–L1 | 1 cm from external rib | – | – | | – | – |
| McQuillen-Martensen (2015) | Supine AP | – | – | Straight | Nipple line | Sup: above shoulders Inf: LCM | – | – | 70–80 kVp 1 mAs | 125–150 cm | – |
| Bontrager & Lampignano, (2014); Lampignano & Kendrick (2021) | Supine AP | Arms next to head | – | – | T7 | – | No grid | – | Low kVp | Maximum SID | – |
| European Commission (1996) | – | – | – | – | – | – | No grid | – | | 100 cm | 0.1 mm Cu or 3 mm Al |
| Jain *et al*. (2021) | – | – | – | – | Halfway C3 and LCM | | No grid | – | High kVp Low mAs | – | – |
| Whitley *et al*. (2015) | Supine AP | Arms next to the head | Head and chin up | 5°–10° caudal | – | – | No grid | Under baby | High kVp | Maximum SID | 3 mm Al 0.1 mm Cu |
| Del Vecchio *et al*. (2015) | Supine AP | – | – | – | Centre with collimation | Sup: chin Inf: below nipples | – | In tray | 50–65 kVp 0.5–3 mAs | 100 cm | 1.5–2 mm Al 0.1 mm Cu |
| Long *et al*. (2019) | Supine AP | Arms abducted | Leave head rotated | Straight | Midpoint of chest and MSP | Sup: 1 cm above shoulders Inf: LCM | – | In tray | – | – | – |

Al, aluminium; AP, anterior-posterior; C3, 3rd cervical vertebra; C3–L1, 3rd cervical to 1st lumbar vertebra; Cu, copper; Inf, inferior; kVp, kilovolt peak; LCM, lower costal margin; mAs, milliampere second; MSP, midsagittal plane; SID, source-to-image receptor distance; Sup, superior; T7, 7th thoracic vertebra.


© Central University of Technology, Free State

These literature sources were combined and synthesised into three literature-based imaging protocols. These imaging protocols are presented in Tables 2.2 to 2.4. The tables that follow show the literature-based imaging protocols for CXR, AXR, and combined CXR-AXR for neonatal patients imaged in the NICU. The literature sources that inform each aspect of the specific protocol are provided in the tables. Table 2.2 proposes the CXR literature-based imaging protocol derived from Table 2.1.

**Table 2.2.** Literature-based imaging protocol for chest X-rays (phase 1).

| Variable | Protocol | Reference |
|---|---|---|
| kVp | 50–65 kVp | Bontrager & Lampignano (2014); Del Vecchio *et al*. (2020); Gunn *et al*. (2020); Lampignano & Kendrick (2021) |
| mAs | 0.5–3 mAs | Bontrager & Lampignano (2014); Del Vecchio *et al*. (2020); Gunn *et al*. (2020); Lampignano & Kendrick (2021) |
| SID | 100 cm | Del Vecchio *et al*. (2020); Pedersen *et al*. (2018); Tugwell-Allsup *et al*. (2020) |
| Collimation upper margin | Mentum | Del Vecchio *et al*. (2020) |
| Collimation lower margin | Below nipples | Del Vecchio *et al*. (2020) |
| Collimation on side | Lateral chest walls | Del Vecchio *et al*. (2020); Long *et al*. (2019) |
| Centring point | Nipple line | Bontrager & Lampignano (2014); Lampignano & Kendrick (2021) |
| Main radiation beam | Straight | Long *et al*. (2019); McQuillen Martensen (2015); Whitley *et al*. (2015) |
| Detector placement | Directly under patient | Tugwell-Allsup *et al*. (2020); Whitley *et al*. (2015) |

kVp, kilovoltage peak; mAs, milliampere second; SID, source-to-image distance.

As shown in Table 2.2, the upper collimator margin should be placed on the mentum according to literature, but the researcher indicated that it should be placed on the lip line. The lip line is more inclusive if the chin of the patient is not lifted during image acquisition, to ensure inclusion of all relevant anatomy.

Table 2.3 reflects the literature-based imaging protocol for abdominal X-rays. Of note is the lack of information found for the specific exposure factors such as the kVp and mAs settings for abdominal X-rays. Del Vecchio *et al*. (2020: 164) indicated a sufficient SID is set at 100 cm, while exposing on expiration. Bontrager and Lampignano (2014: 644) and Lampignano and Kendrick (2021) suggested that the SID should be at a minimum of 102 cm, and the exposure should be made at suspended breathing.



© Central University of Technology, Free State

Del Vecchio *et al.* (2020: 163) indicated that the collimation should include the diaphragm superiorly, the symphysis pubis inferiorly and the lateral abdominal margins. Menashe *et al.* (2017: 418) suggested that abdominal collimation should include the lung bases and diaphragm superiorly, the inferior pubic rami inferiorly and the lateral abdominal walls.

Bontrager and Lampignano (2014: 644) and Lampignano and Kendrick (2021) indicated that the centring point for abdominal X-rays on neonates is 2.5 cm superior to the umbilicus (navel). The authors also suggested a straight main radiation beam (Bontrager & Lampignano, 2014: 644; Lampignano & Kendrick, 2021; Long *et al.* 2019: 28).

According to Tugwell-Allsup *et al.* (2020: 263), the image quality decreased while the radiation dose to the neonate increased when placing the detector in the incubator tray, rather than directly underneath the patient.

**Table 2.3.** Literature-based imaging protocol for abdominal X-rays (phase 1).

| Variable | Protocol | Reference |
|---|---|---|
| kVp | None found | |
| mAs | None found | |
| SID | 100 cm | Bontrager & Lampignano (2014); Del Vecchio *et al*. (2020); Lampignano & Kendrick (2021) |
| Collimation upper margin | Top of diaphragm | Del Vecchio *et al*. (2020); Menashe *et al*. (2017) |
| Collimation lower margin | Symphysis pubis | Del Vecchio *et al*. (2020); Menashe *et al*. (2017) |
| Collimation on side | Soft tissue margin | Del Vecchio *et al*. (2020) |
| Centring point | 2.5 cm above the navel | Bontrager & Lampignano (2014); Lampignano & Kendrick (2021) |
| Main radiation beam | Straight | Bontrager & Lampignano (2014); Lampignano & Kendrick (2021); Long *et al.* (2019) |
| Detector placement | Under patient | Tugwell-Allsup *et al*. (2020) |

kVp, kilovoltage peak; mAs, milliampere second; SID, source-to-image distance.

Table 2.4 represents the literature-based imaging protocol for combined CXR-AXR. Of note is the lack of information regarding the exposure factors and collimation margins. A specific centring point for combined images has also not been found in the literature. Del Vecchio *et al.* (2020: 163) suggested that a SID of 100 cm should be used and the centring point should be adjusted for the combined image.



© Central University of Technology, Free State

For collimation, the top collimator should be placed 2.5 cm above the shoulders, the bottom collimator should be placed on the symphysis pubis, and the lateral chest and abdominal margins should be included (Long *et al.,* 2019: 28). Long *et al.* (2019: 28) also suggested that the main radiation beam should be centred to the midpoint of the chest and abdomen.

A straight main radiation beam should be applied (Bontrager & Lampignano, 2014: 644; Lampignano & Kendrick, 2021). According to Tugwell-Allsup *et al.* (2020: 263), by placing the detector directly underneath the patient, the image quality is increased while the radiation dose to the patient is decreased.

**Table 2.4.** Literature-based imaging protocol for combined chest and abdominal X-rays (phase 1).

| Variable | Protocol | Reference |
|---|---|---|
| kVp | None found | |
| mAs | None found | |
| SID | 100 cm | Del Vecchio *et al*. (2020) |
| Collimation upper margin | 2.5 cm above shoulders | Long *et al*. (2019) |
| Collimation lower margin | Symphysis pubis | Long *et al*. (2019) |
| Collimation on side | Lateral chest and abdominal walls | Del Vecchio *et al*. (2020); Long *et al*. (2019) |
| Centring point | Midpoint of chest and abdomen | Long *et al.* (2019) |
| Main radiation beam | Straight | Bontrager & Lampignano (2014); Lampignano & Kendrick, (2021) |
| Detector Placement | Under patient | Tugwell-Allsup *et al*. (2020) |

kVp, kilovoltage peak; mAs, milliampere second; SID, source-to-image distance.

The literature-based imaging protocols were used to benchmark the criteria included in the observational checklist of phase 2 (Appendix A). These imaging protocols (Tables 2.2, 2.3 and 2.4) also formed part of the baseline imaging protocols tested during the third phase (experimental phase) of the study. It is clear from Tables 2.2–2.4 limited published information is available on abdominal and combined images.

The criteria from the literature-based imaging protocols, in addition to the data obtained from the observational phase by means of the observational checklist, provided the imaging protocol used during the implementation phase (Appendix B).

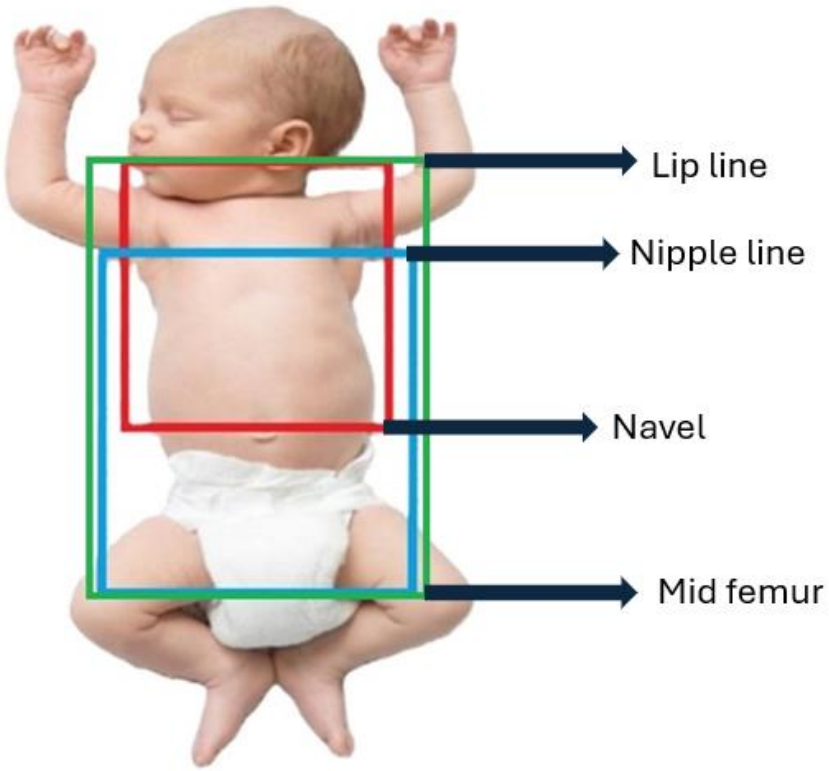
The implementation phase protocol, according to the literature cited up to this point, included a high kVp setting of 50–65 kVp with a low mAs of 0.5–3 mAs. The patient should remain in a supine position with the head kept straight and the arms next to the head. The detector



© Central University of Technology, Free State

placement should be directly under the patient without a grid, and maximum SID should be applied. Several centring points were suggested by the literature. Consequently, the researcher experimented with collimation sizes rather than specific centring points. This decision was based on experience in the field. Each neonate differs in size, and therefore, a specific size (given in centimetres) could cause cut-off in some cases, whereas in others, it could include irrelevant anatomical structures causing an increased radiation dose to the neonate. By explaining collimation size by topographic landmarks, each image will anatomically be the same size, but it will accommodate each individual neonate's size.

The collimation proposed for the implementation phase was derived from Tables 2.2–2.4. In Figure 2.11, the collimation is demonstrated. The collimation sizes were allocated to specific topographic landmarks for easy application to ensure the inclusion of relevant anatomy. The line of the top collimators, bottom collimators and transverse collimators are marked on the image. The red block demonstrates the collimation for the chest, the blue block demonstrates the collimation for the abdomen and the green block demonstrates the collimation parameters for the combined image as described by literature.




Red, chest X-ray; blue, abdominal X-ray; green, combined chest and abdominal X-ray.

**Figure 2.11.** Collimation parameters for chest, abdominal and combined X-rays.



© Central University of Technology, Free State

## 2.11 CONCLUSION

In Chapter 2 the specific importance of a standardised imaging protocol when performing X-rays on neonates, by highlighting the vulnerability of this patient group to ionising radiation are described. The chapter explained the positioning and evaluation criteria for specific radiographic X-ray examinations and different protection principles for neonatal patients. A summary of the literature-based imaging protocol regarding the several sources used, and the criteria to be included in the observational checklist in phase 2 and the experimental checklist during the experimental phase are also provided in this chapter.

In Chapter 3 the methodology used during the study for phases 2 to 5 are described. This chapter elaborates on the research tools and specific data collection methods. The statistical data analysis is also explained.



© Central University of Technology, Free State

# CHAPTER 3
# METHODOLOGY

## 3.1 INTRODUCTION

As stated by Snyder (2019: 334), strategic steps should be followed for a literature review to become research methodology, and action should be taken to ensure accurate, reliable, and trustworthy results. A series of steps were followed to create the literature-based imaging protocol by performing a literature review. This literature search formed part of the methodology for the primary research study as the first of five steps and objectives by creating the literature-based imaging protocol and the baseline checklist for the observational phase (phase 2).

Materials and methods describe the methodology used to conduct the study. The materials and methods chapter enables the reader to determine the appropriateness of the research methodology. This chapter aids in proving the reliability and validity of the study results. If written appropriately, the methodology chapter enables other researchers to replicate the study similarly (Kumar, 2011: 139). Figure 1.1 in Chapter 1 represents the phases of the study. The first literature search phase, which addressed objective one, was described in Chapter 2. The methodological approaches for the observation (phase 2), experimental (phase 3), implementation (phase 4) and reflection (phase 5) phases will receive attention in this chapter.

The study followed a case study design, collecting quantitative data throughout the study. Phase 2 (observational phase) of the study was based on an undisguised naturalistic observational approach with descriptive research. The primary research took place at a private hospital in the Free State Province, while observing staff members in the neonatal intensive care unit (NICU) as well as radiographers employed by the privately owned radiology department.

## 3.2 STUDY POPULATION

The research population comprised qualified radiographers (n=16), the nursing staff (n=14) working in the NICU, and neonates admitted to the NICU. A total neonatal population was difficult to establish, as the researcher did not have any access to this information and the Protection of Personal Information Act (POPIA) prevented the researcher from obtaining information, as it does not directly contribute to the primary study.



© Central University of Technology, Free State

Qualified radiographers were chosen for this study as they have the most experience when dealing with neonatal patients when compared to student radiographers. As the observational phase (phase 2) was mainly based on trial and error throughout their career, qualified radiographers were an obvious fit. Also, in this specific department, student radiographers are not allowed to X-ray neonatal and paediatric patients while unsupervised or without the assistance of a qualified radiographer, due to their lack of experience. The nursing staff are present during radiographic X-ray examinations in the NICU. They are responsible for the neonatal patients, and the radiographers work very closely with them. They also have an influence on the X-rays acquired as they have the authority to make decisions regarding the management of the neonate. Neonatal patients are a very special and sensitive patient group to X-ray. Therefore, some uncertainties and confusion could occur regarding the imaging of this patient group, especially when new or inexperienced staff is involved. An imaging protocol will hopefully provide the radiographers with a basic framework on where to start when approaching the NICU, and it will also guide them with several techniques and the criteria required for these specific X-rays.

The (i) production of and (ii) actually produced radiographic X-ray images of mobile CXR, AXR and combined CXR-AXR neonatal examinations were investigated in this study. Therefore, the radiographic X-ray images of the neonates were part of the study population as they were the patient group when the protocol of the radiographer and nurse were observed during their imaging in phases 2 and 4 of the study. During a quick statistical survey conducted by the researcher at the study site before the commencement of the study, neonatal patient examination statistics performed over eight months (February 2020 – September 2020) were obtained. In total, 309 CXR, 39 AXR and 241 CXR-AXR were performed over the eight-month period surveyed.

### 3.3 SAMPLE SIZE

**Phase 1:** A literature search included six articles and four textbooks that provided insight into the factors involved in obtaining an optimal chest and abdominal radiographic X-ray image in neonates. These factors were included in the establishment of the literature-based imaging protocol and answers to these factors were included where applicable. A minimum of three similar imaging protocols were sourced from the literature (a CXR, AXR and combined CXR-AXR imaging protocol). The three literature-based protocols were completed



© Central University of Technology, Free State

with information found in published literature. As a result, several factors were missing from these protocols as presented in the tables attached (Appendix M).

**Phase 2:** Twelve qualified radiographers and eight qualified registered nurses were sampled to be observed during the observational phase. Therefore, the phase 2 sample included all qualified radiographers performing routine X-rays in the NICU and all qualified registered nurses rostered weekly for the night shift. Night shift staff were specifically chosen as the routine radiographic X-ray examinations are performed at 06h00 daily, hence the night shift staff is present during the routine X-rays. Each radiographer was observed over one week with the relevant nurse accompanying. The researcher observed all routine mobile X-rays taken daily at 06h00.

All the radiographic X-ray images for CXR, AXR and CXR-AXR examinations performed by the radiographers during the twelve-week observation phase were included in the study. During the second observational phase of the study, the researcher observed 109 CXR, 16 AXR and 33 combined CXR-AXR examinations performed by the radiographers. No images were excluded as the researcher wanted as much data as possible to compile an accurate, valid, and user-friendly checklist for the standardised imaging protocol. The data collected during the second phase (observational phase) were used to construct the imaging protocols tested during the third phase (experimental phase), which contributed to providing the final standardised imaging protocol.

**Phase 3:** No sampling of the study population was required for this phase. An experiment was performed by the researcher to establish optimal centring points, exposure factors and entrance skin dose factors. The experiment was performed by the researcher with a neonate phantom and a dosimeter for dose measurement. Sixty-eight CXR protocols, 45 AXR protocols, and 45 CXR-AXR protocols were performed during phase 3 (experimental) of the study. After applying the exclusion criteria, 56 CXR, 43 AXR and 41 combined CXR-AXR images were included in the statistical analysis.

**Phase 4:** The baseline imaging protocol was implemented by four radiographers during phase 4 of the study. These four radiographers also participated in phase 2 (observational phase). The baseline imaging protocol was implemented by the four radiographers for a two-week period. There were no restrictions on the number of images taken of neonatal patients with the baseline imaging protocol.



© Central University of Technology, Free State

A total of 50 reflection checklists were completed by the four radiographers during phase 4 (implementation) throughout the two-week period. Permission to implement the imaging protocol was obtained from the head radiographer of the radiology department where the study was conducted (Appendix N). CXR were performed three times during the two weeks, while two AXR and 45 CXR-AXR were performed by these four radiographers over two weeks.

**Phase 5:** For the final reflection phase, the statistician compared observational checklists completed during observational phase 2 (n=158) with reflection checklists completed during implementation phase 4 (n=50). The comparison was made to reflect upon the usefulness of the imaging protocol after implementation. The exposure indices of the second and fourth phases were compared to determine if there were significant changes in these values. The statistician further compared the change in collimation for inclusion of relevant anatomy, the selection of exposure factors (kVp and mAs), the change in the SID, the object-to-image distance (OID) used and the centring points.

### 3.3.1 Inclusion and exclusion criteria

The study followed several phases and for each phase a different study population, sample size, and inclusion and exclusion criteria were applied. The inclusion and exclusion criteria of the observational, experimental and implementation phases are explained in Tables 3.1–3.3, respectively.

**Table 3.1.** Inclusion and exclusion criteria for the observational phase (phase 2).

| Inclusion criteria | Exclusion criteria |
|---|---|
| **Radiographer observation** | |
| • Radiographers registered with the HPCSA<br>• Radiographers appointed full-time by the radiology department | • Radiographers not registered with the HPCSA<br>• Locum and student radiographers |
| **Mobile examinations observed** | |
| • CXR, AXR and combined chest and abdominal mobile X-rays of neonates<br>• Open incubator mobiles of neonates | • Other X-ray examinations (skull, pelvis) of neonates<br>• Closed incubator mobiles of neonates |
| **Nursing observation** | |
| • Nurses registered with SANC<br>• Nurses working in NICU | • Nurses not registered with SANC<br>• Nursing students |

AXR, abdominal X-ray; CXR, chest X-ray; HPCSA, Health Professions Council of South Africa; NICU, neonatal intensive care unit; SANC, South African Nursing Council.



© Central University of Technology, Free State

Table 3.2 provides the inclusion and exclusion criteria for images included in the statistical analysis for phase 3 (experimental phase). Images not meeting the criteria were not analysed during statistical analyses as it did not contribute to the compilation of an optimal imaging protocol.

**Table 3.2.** Inclusion and exclusion criteria for the experimental phase (phase 3).

| Inclusion criteria | Exclusion criteria |
|---|---|
| • Any X-ray images meeting the inclusion and visibility of anatomical structures | • Any X-ray image excluding any necessary anatomical structures or any anatomical structure not visible |
| • CXR images with an EI inside the recommended EI range (50–200) | • CXR image with an EI above or below the recommended EI range (<50 or >200) |
| • AXR and combined images with an EI inside the recommended EI range (125–500) | • AXR and combined images with an EI above or below the recommended EI range (<125 or >500) |

AXR, abdominal X-ray; CXR, chest X-ray; EI, exposure index.

In Table 3.3, the inclusion and exclusion criteria are presented for the fourth phase (implementation phase) of the study. The inclusion and exclusion criteria for the radiographers (n=4) participating in the implementation phase as well as the mobile radiographic X-ray examinations (n=50) included in this phase are summarised.

**Table 3.3.** Inclusion and exclusion criteria for the implementation phase (phase 4).

| Inclusion criteria | Exclusion criteria |
|---|---|
| **Radiographer implementation** | |
| • Radiographer involved during the observation phase (phase 2) | • Radiographers not involved during the observation phase (phase 2) |
| **Mobile examinations included** | |
| • CXR, AXR and combined chest and abdominal mobile X-rays of neonates | • Other X-ray examinations (skull, pelvis) of neonates |

AXR, abdominal X-ray; CXR, chest X-ray.

## 3.4 METHODS PER PHASE

The specific research tools employed in phases 2 to 5 are presented in this section. The pilot study for each phase is described with the relevant dates performed. The data collection methods used in each phase and the data analysis methods per phase are provided. Figure 1.1 (Chapter 1) reflects how these phases followed each other and should be referred to as needed.



© Central University of Technology, Free State

### 3.4.1 Phase 2: Observational checklist

The research tool included a radiographic observational checklist (Appendix A). The checklist was benchmarked, compiled and completed by the researcher, and was used during the observation of radiographer while performing mobile radiographic X-ray examinations in the neonatal intensive care unit. The checklist was constructed using literature, the literature-based imaging protocol, and after consultation with a radiologist at the practice to determine the factors ensuring an optimal radiographic X-ray image with diagnostic value.

Different evaluation criteria for neonatal chest and abdominal imaging were applied to compile the checklist. Works published by several authors, such as Bontrager and Lampignano (2014), Lampignano and Kendrick (2021), McQuillen Martensen (2015), Long et al. (2019) and Whitley et al. (2015) were consulted to construct the observational checklist used during the observation in the NICU.

Friedrich-Nel, van der Merwe and Kotze (2018: 2) described a design for an imaging checklist. In the checklist, the authors included seven aspects to observe. These aspects were (i) correct centring of the main beam; (ii) rotation of the thorax of the neonate; (iii) main beam angulation; (iv) artefacts observed on the image; (v) anatomical lead marker placement; (vi) lead shielding used; and (vii) four-sided collimation visible on the image.

The checklist used by Gunn *et al*. (2019: e67) included the gestational age and weight of the neonate. The technical factors they observed included the kVp, mAs and SID. The field of view (FOV) was also part of the checklist with the dose-area product (DAP). The FOV measurements were calculated on the Picture Archiving and Communication System (PACS) and the DAP reading was calculated by means of a formula. The placement of a correct lead marker formed part of the checklist as it is crucial in the imaging of neonatal patients.

A review from a different study (Pedersen, Hardy & Blankholm, 2018: 258) was used to determine the existing working practice. Three main categories were set up, which included general information, exposure factors and techniques, and the design of the incubator. The first step was to determine whether the system used was computed radiography (CR) or digital radiography (DR). The exposure factors and techniques included SID, tube angulation, positioning sponges used, and the radiation protection applied.

The final segment of the review determined the design of the incubator. It included questions establishing whether the radiographer placed the detector inside the incubator tray or directly



© Central University of Technology, Free State

underneath the neonate. Another pitfall in neonatal imaging is whether the radiographer opens the canopy of the closed incubator or whether they keep it shut for the health of the neonate. This was asked in the review to determine accurate working practice. The last question of the review was to identify any artefacts present in the image since it may impact EI values. This was an elaborative question and could include any relevant artefact such as electrocardiogram (ECG) lines, the canopy of a closed incubator or the mattress of the neonate (Tugwell-Allsup & England, 2020: 19–20).

The first heading was to state the examination type and gestational age of the neonate, as well as the intubation status of the neonate. The type of examination was also marked by the researcher.

**Table 3.4.** Part 1 of the observational checklist.

| NEONATAL PATIENT INFORMATION | | | |
|---|---|---|---|
| Gestational age | | | |
| Is the neonate intubated? | Yes | No | |
| Type of examination | CXR | AXR | CXR + AXR |

AXR, abdominal X-ray; CXR, chest X-ray.

Part one, criterion one of the checklist was aimed at the radiographers and the criterion included positioning factors, such as the positioning of the head and arms, possible rotation seen, and immobilisation techniques implemented.

**Table 3.5.** Part 1, criterion 1 of the observational checklist.

| CRITERION 1: POSITIONING FACTORS | | | |
|---|---|---|---|
| Arms abducted from body | | | |
| Immobilisation technique | | | |
| Head facing up | | | |
| Immobilisation technique | | | |
| Chin lifted | | | |
| Immobilisation technique | | | |
| Rotation of pelvis | | | |
| Rotation of thorax | | | |

Part one, criterion two included the technical factors, namely initial placement of the lead marker, removal of possible artefacts, SID selection, centring point, main beam direction and angulation degrees, and radiation protection measures applied. The radiographers were



© Central University of Technology, Free State

asked whether the initial lead marker was present and observed on the image, and whether it was placed in the correct orientation.

**Table 3.6.** Part 1, criterion 2 of the observational checklist.

| CRITERION 2: TECHNICAL FACTORS | | | |
|---|---|---|---|
| Lead marker placed? | | | |
| Lead marker placement | On Pt | | On detector |
| Placement of detector | Inside tray | | Directly under pt |
| Collimation | None | | Size |
| Artefacts removed? (e.g., teddy bears, sandbag, dummy clips) | | | |
| SID (cm) in cm | | | |
| OID (cm) (distance from neonate to detector) | | | |
| Centring point | | | |
| Main beam direction (degrees of angulation) | | | |
| Physical lead protection used (pt): (elaborate) | | | |
| Lead equivalence (Pb Eq) | 0.25 Pb Eq | | 0.35 Pb Eq |
| Detector | CR | | DR |
| Detector speed (focus) | | | |
| X-ray mobile machine make | Siemens Mobilett 1 | | Siemens Mobilett 2 |
| Generator | 3 phase | | 3 phase |
| Filtration | Al | | Cu |
| Incubator brand | Dräger | | |
| Mattress thickness (when applicable) | | | |

Al, aluminium; CR, computed radiography; Cu, copper; DR, digital radiography; OID, object-to-image distance.; Pt, patient; SID, source-to-image distance.

Part one, criterion three focused on the exposure factors including the selection of kVp, mAs and the exposure index. The exposure index (EI) value was obtained from the image.

**Table 3.7.** Part 1, criterion 3 of the observational checklist.

| CRITERION 3: EXPOSURE FACTORS | |
|---|---|
| kVp value | |
| mAs value | |
| Exposure index | |

kVp, kilovoltage peak; mAs, milliampere second.



© Central University of Technology, Free State

Part one, criterion four was for infection control measures applied. This might include disinfecting the detector and lead markers, wearing gloves, or washing hands before touching the neonate.

**Table 3.8.** Part 1, criterion 4 of the observational checklist.

| **CRITERION 4: INFECTION CONTROL** |
| --- |
| • What infection control measures were followed? Elaborate below: |
| • Example: *Detector was sanitised pre- and post-X-ray acquisition. Lead marker was sanitised and was not placed on the neonate.* |

Part two of the checklist was aimed at the nursing staff in the NICU. They were observed by the researcher while the mobile examinations were performed to determine what was allowed and what might not be done by the radiographer. Factors included in their checklist were whether the neonate's position might be altered from prone to supine when applicable.

Another important factor to include in the checklist that would ensure no overlapping of anatomical structures, was to abduct the arms from the body and to lift the chin of the neonate. The researcher also observed whether the neonate's head might be turned when intubated with an endotracheal tube. The final factor was to ensure whether the neonate might be lifted to place the detector directly under the neonate, under the mattress or in the detector tray underneath.



© Central University of Technology, Free State

**Table 3.9.** Part 2 of the observational checklist.

| PART 2: NURSING STAFF | | | |
|---|---|---|---|
| | **YES** | **NO** | **COMMENT** |
| **Is it preferred that the radiographer** | | | |
| • Touch the neonate | | | |
| • Place Pb protection directly on the Pt | | | |
| • Abduct the arms of the neonate | | | |
| • Turn the head of the neonate | | | |
| • Lift the chin of the neonate | | | |
| • Move lines out of the FOV | | | |
| • Place the detector directly under the Pt | | | |
| • Place the detector under the mattress | | | |
| • Place the detector in the detector tray | | | |
| **Comments radiographer/nurse interaction** | | | |
| • Warned before exposure (exit room) | | | |
| • Provided nurse shielding (in room) | | | |
| Extra | | | |

FOV, field of view; Pb, lead; Pt, patient.

Part three of the checklist was dedicated to image evaluation of CXR, which is presented in Table 3.10.

Criterion 1 evaluated the important anatomical structures to be included in the image of the CXR. Structures included cervical vertebra seven (C7) up to an including thoracic vertebra twelve (T12), soft tissue on the lateral margins of the chest, bilateral costophrenic angles, lung apices and the lateral rib margins.

Criterion 2 evaluated the visibility of the anatomical structures for the CXR. This included the visibility of the air-filled trachea, the carina, lung markings, the hilar regions, cortical margins of the bones (ribs, vertebra, clavicles and humeri) and the sharp border of the heart shadow.



© Central University of Technology, Free State

**Table 3.10.** Part 3, criteria 1 and 2 of the observational checklist.

| CHEST X-RAY | | | |
|---|---|---|---|
| | **YES** | **NO** | **COMMENT** |
| **CRITERION 1: ANATOMICAL STRUCTURES INCLUDED** | | | |
| C7 superiorly | | | |
| Bilateral costophrenic angles | | | |
| Soft tissue laterally | | | |
| ⅓ of the upper abdomen | | | |
| Only up to level of gastric bubble | | | |
| Mid-abdomen to IC | | | |
| Entire abdomen including SP | | | |
| **CRITERION 2: ANATOMICAL STRUCTURES VISIBLE** | | | |
| Air-filled trachea | | | |
| Carina | | | |
| Lung markings | | | |
| Hilar regions | | | |
| Sharp heart border | | | |
| Sharp costophrenic angles | | | |
| Stomach bubble | | | |

C7, 7$^{th}$ cervical vertebra; IC, iliac crest; SP, symphysis pubis.

Criterion 3 referred to the anatomical structures included in the abdominal X-ray. Inclusion of bilateral costophrenic angles and symphysis pubis was covered in this part of the checklist. Criterion 4 referred to the visibility of anatomical structures for the abdominal X-ray, including the gas-bowel pattern and the stomach bubble.

**Table 3.11.** Part 3, criteria 3 and 4 of the observational checklist.

| ABDOMINAL X-RAY | | | |
|---|---|---|---|
| | **YES** | **NO** | **COMMENT** |
| **CRITERION 3: ANATOMICAL STRUCTURES INCLUDED** | | | |
| Costophrenic angled superiorly | | | |
| Symphysis pubis inferiorly | | | |
| Soft tissue laterally | | | |
| **CRITERION 4: ANATOMICAL STRUCTURES VISIBLE** | | | |
| Stomach bubble | | | |
| Gas-bowel pattern | | | |



© Central University of Technology, Free State

Part four of the checklist dealt with the post-processing methods required, such as the collimation applied afterwards, adapting the window width and level for the darkness or brightness of the image, and the placement of an electronic marker.

**Table 3.12.** Part 4 of the observational checklist.

| PART 4: POST-PROCESSING REQUIRED | |
|---|---|
| Collimation too big | |
| Collimation too small (cut-off) | |
| Overexposed (image too dark) | |
| Underexposed (image to white) | |
| Image requires small rotation (malalignment) | |
| Electronic marker placement | |

The complete observational checklist used during the second phase of the study is presented as Appendix A.

#### *3.4.1.1 Pilot study of the observational checklist*

The pilot study was conducted at a different hospital from where the primary study was performed. Permission for the pilot study was obtained from this hospital (Appendix O). The literature-based imaging checklist was used during the pilot study and the head radiographer of the imaging department, together with the researcher, completed the observational checklists during the pilot study to record the data acquired. The data collected were not used as part of the main data analysis for the primary study. The pilot study included a sample size of six images (n=6), which comprised two CXR, two AXR and two combined CXR-AXR observed on two separate occasions.

The pilot study allowed for corrections to be made to unresolved questions or inconsistencies, while grammatical errors were addressed and additions to the checklist were made. The layout was changed after the pilot to allow for a smoother approach during observation.

#### *3.4.1.2 Data collection method of the observational checklist*

Data collection was done by the researcher during the second phase of the study by completing an observational imaging checklist in the neonatal intensive care unit (NICU) at the research site. CXR, AXR and a combined CXR-AXR were observed during the 12 weeks of data collection for the second phase of the study. The checklist was completed by the



© Central University of Technology, Free State

researcher while observing the performance of the radiographic X-ray procedures in the NICU at 06h00 daily during routine radiography. Informed consent from the radiographers and nursing staff was acquired before the observational phase started. Consent from the parents or legal guardians for each neonate was obtained only once.

The observational image checklist focused on two aspects of the NICU relating to the radiographer and the nurse. The checklist included several positioning methods such as arm placement, head position and rotation of the patient, while it also included technical factors such as exposure factors, exposure index, placement of the detector and several radiation protection measures applied. Each radiographer was observed for one week of the 12 weeks comprising phase 2, while performing routine mobile radiographic X-ray examinations in the ICU on neonatal patients. This phase of the study commenced on 27 March 2023 and continued for 12 weeks until 15 June 2023.

The validity and accuracy of the radiographer and nurse performance were assured by eliminating the d effect. The Hawthorne effect is the tendency by individuals to adapt and alter their behavior when they are aware of being observed (Fox, Brennan & Chasen, 2008: 111). This was achieved by keeping the data recorded on the checklist confidential without elaborating on what was observed to ensure optimal and reliable data collection.

#### *3.4.1.3 Data analysis of the observational checklist*

Data from the observational checklist were captured electronically in Microsoft Excel (Office 16) spreadsheet (Microsoft Corporation; Redmond, WA, USA). All further analysis was done by an appointed statistician. A summary of the data was provided to the researcher and supervisors by the statistician on 10 August 2023. Twelve radiographers formed part of the observation during these 12 weeks and a total of 158 radiographic X-ray images were performed by them and observed by the researcher. During this observation, 109 CXR were performed, 16 AXR and 33 CXR-AXR images.

### 3.4.2 Phase 3: Experimental checklist

The checklist used in the experimental phase of the study (Appendix C) included factors determined during the literature evaluation and observational phases. X-rays were performed on a phantom. Information obtained by means of the checklist included the type of examination, selected kVp and mAs, and SID (cm). The placement and position of the



© Central University of Technology, Free State

dosimeter, the exposure index of the image and the dose as read from the dosimeter were also recorded on the checklist.

Figure 3.1 shows the experimental checklist used by the researcher during the third phase of the study. This was completed throughout the experiment on an Excel spreadsheet presented to the statistician afterwards.

The first and second columns of the checklist were the collimation size set, which was the length and the width of the collimators as presented on the screen after image acquisition. The third column represented the total field of view (FOV) measured in $cm^2$, which is collimation length multiplied by collimation width. The fourth column was the source-to-subject distance (SSD), which is the distance measured from the X-ray tube to the specific centring point on the phantom, measured in centimetres. The part thickness (column 5) was measured in centimetres with a calliper on the specific centring point, and the sixth column was the OID, which is the measurement from the phantom to the detector, measured in centimetres.

| 1 | 2 | 3 | 4 | 5 | 6 |
|---|---|---|---|---|---|
| **Colimation length** (cm) | **Collimation width** (cm) | **FOV** $(cm)^2$ | **SSD** (cm) | **Part thickness** (cm) | **OID** (cm) |

**Figure 3.1.** Part 1 of the experimental checklist.

Columns 7–9 were the EI captured, which is presented on the screen after image acquisition, and columns 10–12 represented the deviation index (DI) of the image. Both the EI and DI were measured three times as presented in Figure 3.2, because each imaging protocol was repeated three times to ensure accuracy with regards to dose optimisation.

| 7 | 8 | 9 | 10 | 11 | 12 |
|---|---|---|---|---|---|
| **EI rep 1** | **EI rep 2** | **EI rep 3** | **DI rep 1** | **DI rep 2** | **DI rep 3** |

**Figure 3.2.** Part 2 of the experimental checklist (EI and DI).

Columns 13–18 (Figure 3.3) captured the radiation dose. Incident air kerma (IAK) (columns 13–15) was the radiation dose entering the phantom and was measured in µGy with a



© Central University of Technology, Free State

dosimeter placed on top of the phantom on the specific centring point. Columns 16–18 represented the radiation dose exiting the phantom on the bottom, measured with a dosimeter placed beneath the phantom on the specific centring point. The entrance air kerma (EAK) was also measured in µGy. Similar to the EI and DI, both the IAK and EAK were measured three times to promote accuracy and validity with regard to dose optimisation.

| 13 | 14 | 15 | 16 | 17 | 18 |
|---|---|---|---|---|---|
| IAK rep 1 (µGy) | IAK rep 2 (µGy) | IAK rep 3 (µGy) | EAK rep 1 (µGy) | EAK rep 2 (µGy) | EAK rep 3 (µGy) |

**Figure 3.3.** Part 3 of the experimental checklist (IAK and EAK).

The subsequent part of the experimental checklist (Figure 3.4) was based on the inclusion of anatomical structures and the visibility thereof based on the exposure factors set.

| | | | | |
|---|---|---|---|---|
| T7 in centre of images | Include cervical vertebrae nr 7 | Include thoracic vertebra nr 12 | Include diaphragm and costophrenic angles | Include gastric bubble |

| | | | | |
|---|---|---|---|---|
| Air-filled trachea visible | Include bilateral chest wall | Well defined and sharp heart borders | Visible lung markings | Retrocardiac lung visible |

**Figure 3.4.** Part 4 of the experimental checklist to record the inclusion and visibility of anatomical structures.

### *3.4.2.1 Pilot study of the experimental checklist*

The pilot study for the experimental checklist was conducted at the research site. The reason was that the same mobile X-ray machine was used to ensure and promote the accuracy and trustworthiness of the checklist. A neonate phantom and two exactly similar dosimeters from the CUT were used to test the several exposures and determine the dose measurement as produced. Data obtained during the pilot study were not included in the main data collection process and did not contribute statistically to the primary study. The pilot study allowed for an opportunity to address uncertainties, correct grammatical errors and ensure proper functioning of the dose measurement equipment. It also assisted the researcher in ensuring that all the relevant desired data were included in the checklist.



© Central University of Technology, Free State

A pilot study for the third phase of the study was done on 24 August 2023 at the research site. The Siemens Mobilett Mira Max 2 was used during the pilot study with the Fischer & Paykel CosyCot™ (Fischer & Paykel Healthcare; Auckland, New Zealand), as used in the neonatal intensive care unit. The pilot study was conducted by the researcher and co-supervisor to ensure that the checklist for the experimental phase was accurate and valid before performing the primary data collection for the study. The pilot study also allowed the researcher to ensure that all variables were in working order, such as the mobile machine, relevant measurements and the dosimeter used. Figures 3.5 and 3.6, respectively, represent the pilot study of the experimental phase, and the mobile X-ray machine used in this study.

The phantom used during the experimental phase is the Newborn Whole Body Phantom PBU-80 (Imaging Solutions; Kyoto, Japan). The phantom is 53 cm in length and weighs 3.5 kg. It is made of a urethane-based resin with synthetic bone made of epoxy resin. The phantom was designed for applications of computed tomography (CT), plain x-ray and dosimetry. It contains a Hounsfield unit (HU) of an average newborn and is made of Kyoto Kagaku original human tissue substitute (Kyoto Kagaku, 2020: online).



© Central University of Technology, Free State



**Figure 3.5.** Pilot study done for experimental phase.




**Figure 3.6.** Mobile machine used during phase 3.



© Central University of Technology, Free State

During the pilot study, the researcher marked all variables forming part of the study and named them accordingly, as presented in Figure 3.7. The collimator lever was marked to ensure that the collimation remained the same throughout. It was labelled "1" representing the first protocol, "2" for the second protocol, and "3" for the third protocol. The mark on the collimator knob warranted specific collimator size each time. Each set of anatomical structures included was allocated a specific number to maintain consistent collimation size.

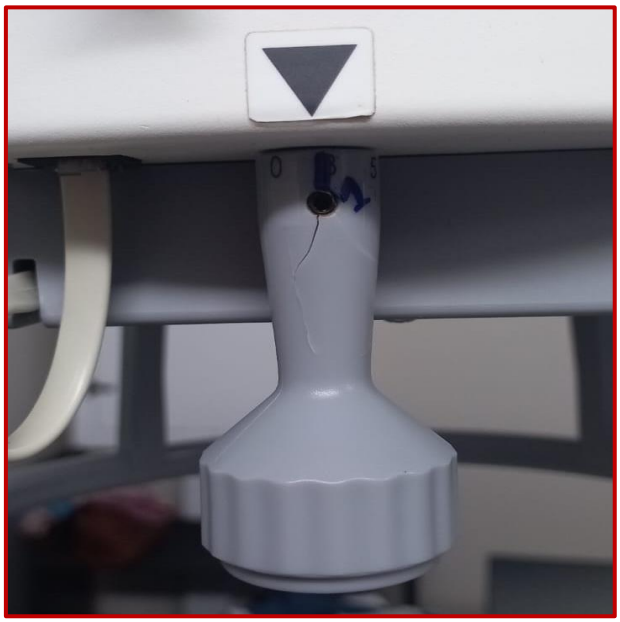


**Figure 3.7.** Marking on the collimator knob.

The angulation of the bed was marked to ensure that the angulation would remain constant when the protocol required angulation or tilting of the bed. On the mattress, bed and in the incubator tray, the placement of the detector was marked with tape to ensure constant placement of the detector in the same position. Centring points or topographic landmarks such as the nipple line, lower costal margin, clavicle level and sternal angle were marked on the phantom using stickers to ensure centring was on the same point for each protocol to increase accuracy and validity.

Five image combinations for the CXR were performed to ensure that all relevant parts of the mobile X-ray machine were working, such as the collimation, distance measuring tape, exposure index reader, as well as the deviation index reader and collimation light. With these exposures, the dosimeter placed on the phantom was also tested to guarantee working order and calibration accuracy.



© Central University of Technology, Free State

While the different combinations were performed, the researcher captured these data on an Excel spreadsheet to test the practicality of the spreadsheet. In this manner, the researcher established whether the data collection would be a rapidly performed process, or whether the format of the sheet should be adapted for the primary data collection.

#### *3.4.2.2 Data collection method of the experimental checklist*

During phase 3, the data of the experimental checklist were recorded by the researcher in Microsoft Excel on a predesigned checklist. The exposure combinations were made with the Mobilett Mira Max 2 (provided by the imaging department) on the neonate phantom (property of the CUT) in the CosyCot™ bed provided by the NICU. The IAK and EAK were measured with the dosimeter from the CUT.

Data collection for phase 3 started on 25 August 2023 and concluded on 30 August 2023. Data collection was done by the researcher at the same research site as phase 2.

On the datasheet, several items of information were captured for data analysis. The data sheet included the collimation size, part thickness of the phantom, source-to-subject distance (SSD), SID, EI for all three exposures, DI for all three exposures, IAK for all three exposures as measured on top of the phantom and EAK for all three exposures as measured below the phantom, after the X-ray beam passed through.

The experimental checklist (Appendix C) was used by the researcher to complete all set imaging protocols for dose measurement purposes and optimal image quality. As seen in the example image presented in Figure 3.8, the researcher performed these imaging protocols on the phantom three consecutive times for accurate dose measurement and captured the results in the Excel data sheet (Figure 3.8).

The **chest imaging protocols** tested during phase 3 are presented in the figure as an example. The different colours indicate different imaging protocols. In Figure 3.8, the green indicates one imaging protocol and the text in red shows the variable tested during that exposure. For example, line 1 is the baseline image while in lines 2–4, everything is kept consistent with the baseline imaging protocol except for the kVp, which changed three times. For line 2, the variable tested was the kVp which was lowered to 52 kVp, while the rest remained constant to the baseline imaging. Thus, 52 kVp was the variable tested. The blue shading indicates the second imaging protocol, and the red text represents the variable tested.



© Central University of Technology, Free State

As illustrated in Figure 3.8, the first imaging protocol tested the application of 55 kVp, 2 mAs with a 100 cm SID. The upper collimation margin was above the shoulders, while the lower margin of the collimators was on the lower costal margin and the centring point was on the nipple line. No angulation was used; thus, a straight beam was assured, and the detector was placed inside the tray of the Cosycot™. One factor was changed with each exposure as determined by phases 1 and 2, and the data were captured on the data sheet as presented in Figure 3.8.

| Exp nr | kVp | mAs | SID | Collimation U | Collimation L | Centering | Angulation | IR Placement |
|---|---|---|---|---|---|---|---|---|
| 1 | 55 | 2 | 100 | Above shoulders | Lower costal margin | Nipple line | Straight | In tray |
| 2 | 52 | 2 | 100 | Above shoulders | Lower costal margin | Nipple line | Straight | In tray |
| 3 | 57 | 2 | 100 | Above shoulders | Lower costal margin | Nipple line | Straight | In tray |
| 4 | 60 | 2 | 100 | Above shoulders | Lower costal margin | Nipple line | Straight | In tray |
| 5 | 55 | 2.2 | 100 | Above shoulders | Lower costal margin | Nipple line | Straight | In tray |
| 6 | 55 | 1.8 | 100 | Above shoulders | Lower costal margin | Nipple line | Straight | In tray |
| 7 | 55 | 0.8 | 100 | Above shoulders | Lower costal margin | Nipple line | Straight | In tray |
| 8 | 55 | 2 | 90 | Above shoulders | Lower costal margin | Nipple line | Straight | In tray |
| 9 | 55 | 2 | 80 | Above shoulders | Lower costal margin | Nipple line | Straight | In tray |
| 10 | 55 | 2 | 100 | Thyroid cartilage | Xiphoid process | Nipple line | Straight | In tray |
| 11 | 55 | 2 | 100 | Lip line | Navel | Nipple line | Straight | In tray |
| 12 | 55 | 2 | 100 | Mentum | Below nipples | Nipple line | Straight | In tray |
| 13 | 55 | 2 | 100 | Above shoulders | Lower costal margin | Sternal angle | Straight | In tray |
| 14 | 55 | 2 | 100 | Above shoulders | Lower costal margin | Lower costal margin | Straight | In tray |
| 15 | 55 | 2 | 100 | Above shoulders | Lower costal margin | Nipple line | Sternum parallel | In tray |
| 16 | 55 | 2 | 100 | Above shoulders | Lower costal margin | Nipple line | Straight | Under pt |
| 17 | 55 | 2 | 100 | Above shoulders | Lower costal margin | Nipple line | Straight | Under mattress |
| 18 | 57 | 2.2 | 90 | Thyroid cartilage | Xiphoid process | Sternal angle | Sternum parallel | Under pt |
| 19 | 55 | 2.2 | 90 | Thyroid cartilage | Xiphoid process | Sternal angle | Sternum parallel | Under pt |
| 20 | 52 | 2.2 | 90 | Thyroid cartilage | Xiphoid process | Sternal angle | Sternum parallel | Under pt |
| 21 | 60 | 2.2 | 90 | Thyroid cartilage | Xiphoid process | Sternal angle | Sternum parallel | Under pt |
| 22 | 57 | 2 | 90 | Thyroid cartilage | Xiphoid process | Sternal angle | Sternum parallel | Under pt |
| 23 | 57 | 1.8 | 90 | Thyroid cartilage | Xiphoid process | Sternal angle | Sternum parallel | Under pt |
| 24 | 57 | 0.8 | 90 | Thyroid cartilage | Xiphoid process | Sternal angle | Sternum parallel | Under pt |
| 25 | 57 | 2.2 | 100 | Thyroid cartilage | Xiphoid process | Sternal angle | Sternum parallel | Under pt |
| 26 | 57 | 2.2 | 80 | Thyroid cartilage | Xiphoid process | Sternal angle | Sternum parallel | Under pt |
| 27 | 57 | 2.2 | 90 | Above shoulders | Lower costal margin | Sternal angle | Sternum parallel | Under pt |
| 28 | 57 | 2.2 | 90 | Lip line | Navel | Sternal angle | Sternum parallel | Under pt |
| 29 | 57 | 2.2 | 90 | Mentum | Below nipples | Sternal angle | Sternum parallel | Under pt |
| 30 | 57 | 2.2 | 90 | Thyroid cartilage | Xiphoid process | Nipple line | Sternum parallel | Under pt |
| 31 | 57 | 2.2 | 90 | Thyroid cartilage | Xiphoid process | Lower costal margin | Sternum parallel | Under pt |
| 32 | 57 | 2.2 | 90 | Thyroid cartilage | Xiphoid process | Sternal angle | Sternum parallel | Under pt |
| 33 | 57 | 2.2 | 90 | Thyroid cartilage | Xiphoid process | Sternal angle | Straight | Under pt |
| 34 | 57 | 2.2 | 90 | Thyroid cartilage | Xiphoid process | Sternal angle | Sternum parallel | In tray |
| 35 | 57 | 2.2 | 90 | Thyroid cartilage | Xiphoid process | Sternal angle | Sternum parallel | Under mattress |

**Figure 3.8.** Imaging protocols tested in experiment for chest X-rays.

The data collected during the third phase of the study were captured in an Excel spreadsheet as presented in Figure 3.9. The factors captured in the spreadsheet included the collimation size measured by the mobile unit, the SSD, the part thickness measured with a calliper, and the OID. The EI and the DI were recorded for all three exposures. The IAK and EAK were



© Central University of Technology, Free State

measured with the dosimeter placed either on top of or underneath the phantom, respectively. A separate data sheet was used for the three types of examinations to limit confusion and promote trustworthiness.

| Colimation length (cm) | Collimation width (cm) | FOV $(cm)^2$ | SSD (cm) | Part thickness (cm) | OID (cm) | EI rep 1 | EI rep 2 | EI rep 3 | DI rep 1 | DI rep 2 | DI rep 3 | IAK rep 1 (µGy) | IAK rep 2 (µGy) | IAK rep 3 (µGy) | EAK rep 1 (µGy) | EAK rep 2 (µGy) | EAK rep 3 (µGy) |
|---|---|---|---|---|---|---|---|---|---|---|---|---|---|---|---|---|---|
| 11 | 17 | 187 | 85,5 | 5,5 | 9 | 609 | 611 | 611 | 4 | 4 | 4 | 79,32 | 79,78 | 78,96 | 2,995 | 3,02 | 3,051 |
| 11 | 17 | 187 | 85,5 | 5,5 | 9 | 835 | 838 | 837 | 5 | 5,5 | 5 | 94,36 | 93,97 | 94,35 | 3,997 | 4,008 | 4,013 |
| 11 | 17 | 187 | 85,5 | 5,5 | 9 | 461 | 461 | 461 | 2,5 | 2,5 | 1,5 | 96,22 | 69,34 | 69,02 | 2,44 | 2,433 | 2,434 |
| 11 | 17 | 187 | 85,5 | 5,5 | 9 | 526 | 526 | 527 | 3 | 3 | 3 | 68,63 | 68,92 | 68,91 | 2,638 | 2,638 | 2,624 |
| 11 | 17 | 187 | 85,5 | 5,5 | 9 | 314 | 313 | 314 | 1 | 1 | 1 | 43,06 | 42,37 | 43,04 | 1,656 | 1,669 | 1,652 |
| 11 | 17 | 187 | 75,5 | 5,5 | 9 | 704 | 705 | 707 | 4,5 | 4,5 | 4,5 | 100,6 | 101,2 | 101,1 | 3,829 | 3,863 | 3,828 |
| 10 | 19 | 190 | 65,5 | 5,5 | 9 | 913 | 914 | 917 | 5,5 | 5,5 | 5,5 | 141,5 | 141,9 | 141,3 | 4,767 | 4,774 | 4,77 |
| 11 | 17 | 187 | 85,5 | 5,5 | 9 | 569 | 570 | 569 | 3,5 | 3,5 | 3,5 | 67,88 | 67,75 | 68,07 | 2,995 | 3,048 | 3,047 |
| 11 | 19 | 209 | 85,5 | 5,5 | 9 | 596 | 597 | 596 | 4 | 4 | 4 | 66,76 | 66,8 | 66,72 | 2,965 | 2,946 | 2,974 |
| 11 | 17 | 187 | 85,5 | 5,5 | 9 | 568 | 569 | 569 | 3,5 | 3,5 | 3,5 | 67,63 | 68,03 | 67,65 | 2,977 | 2,944 | 2,942 |
| 11 | 17 | 187 | 85,5 | 5,5 | 9 | 604 | 604 | 602 | 4 | 4 | 4 | 67,48 | 67,77 | 67,96 | 2,977 | 3,005 | 3,031 |
| 11 | 15 | 165 | 85,5 | 5,5 | 9 | 597 | 599 | 599 | 4 | 4 | 4 | 86,36 | 86,06 | 86,42 | 3,235 | 3,248 | 3,225 |
| 11 | 16 | 176 | 85,5 | 5,5 | 9 | 600 | 600 | 602 | 4 | 4 | 4 | 85,87 | 85,67 | 86,04 | 7,08 | 7,16 | 7,138 |
| 10 | 17 | 170 | 94,5 | 5,5 | 0 | 906 | 910 | 917 | 5,5 | 5,5 | 5,5 | 71,96 | 72,72 | 73,47 | 4,798 | 3,322 | 3,431 |
| 10 | 17 | 170 | 92,5 | 5,5 | 2 | 820 | 819 | 820 | 5 | 5 | 5 | 71,58 | 71,04 | 71,15 | 3,199 | 3,173 | 3,207 |
| 10 | 15 | 150 | 84,5 | 5,5 | 0 | 987 | 989 | 992 | 6 | 6 | 6 | 92,59 | 92,74 | 92,93 | 3,941 | 3,933 | 3,946 |
| 10 | 15 | 150 | 84,5 | 5,5 | 0 | 722 | 722 | 721 | 4,5 | 4,5 | 4,5 | 78,6 | 78,42 | 78,61 | 3,03 | 3,078 | 2,982 |
| 10 | 15 | 150 | 84,5 | 5,5 | 0 | 609 | 611 | 612 | 4 | 4 | 4 | 72,54 | 72,35 | 72,29 | 2,622 | 2,594 | 2,645 |
| 10 | 15 | 150 | 84,5 | 5,5 | 0 | 1157 | 1157 | 1157 | 6,5 | 6,5 | 6,5 | 107,2 | 108,1 | 108,4 | 4,573 | 4,557 | 4,59 |
| 10 | 15 | 150 | 84,5 | 5,5 | 0 | 580 | 584 | 583 | 3,5 | 3,5 | 3,5 | 57,31 | 57,52 | 57,15 | 2,431 | 2,454 | 2,41 |
| 11 | 15 | 165 | 94,5 | 5,5 | 0 | 845 | 847 | 847 | 5,5 | 5,5 | 5,5 | 71,31 | 71,16 | 71,14 | 3,115 | 3,155 | 3,15 |
| 10 | 16 | 160 | 74,5 | 5,5 | 0 | 1209 | 1210 | 1209 | 7 | 7 | 7 | 123 | 124 | 123,1 | 5,218 | 5,188 | 5,194 |
| 10 | 16 | 160 | 84,5 | 5,5 | 0 | 1009 | 1012 | 1008 | 6 | 6 | 6 | 90,19 | 90,38 | 89,8 | 7,798 | 7,796 | 7,836 |
| 10 | 19 | 190 | 84,5 | 5,5 | 0 | 1066 | 1065 | 1066 | 6,5 | 6,5 | 6,5 | 90,66 | 90,29 | 90,91 | 7,879 | 7,812 | 7,851 |
| 10 | 18 | 180 | 84,5 | 5,5 | 0 | 1010 | 1013 | 1013 | 6 | 6 | 6 | 90,02 | 90,16 | 90,49 | 7,725 | 7,865 | 7,833 |
| 10 | 19 | 190 | 84,5 | 5,5 | 0 | 1045 | 1047 | 1048 | 6 | 6 | 6 | 91,55 | 90,96 | 91,18 | 7,329 | 7,369 | 7,333 |
| 10 | 15 | 150 | 84,5 | 5,5 | 0 | 1003 | 1001 | 1003 | 6 | 6 | 6 | 85,88 | 85,62 | 85,81 | 4,683 | 4,674 | 4,676 |

**Figure 3.9.** Data sheet for chest X-ray experimental results.

The data analysis and configuration were performed for an optimal exposure index, deviation index and entrance skin dose. Thus, all factors were repeated three times for each exposure measurement factor.

During the image acquisition for the mobile CXR protocol, 68 different combinations were performed to measure the difference in dose, image quality and anatomical structures included. All combinations were performed three times to verify the trustworthiness of the dosimeter readings. The collimator setting, centring point and bed angulation were marked by the researcher to guarantee consistency and accuracy.

For the **abdominal X-ray protocol**, 45 different combinations were tested and recorded on the data sheet. For the CXR-AXR image protocol, 45 different combinations were tested and imaged and the data were recorded on the data sheet. With all these exposures performed for the several combinations, only one variable was changed during each exposure while the rest of the factors remained constant. This allowed accurate data capturing as the number of variables was limited and the change in patient dose could be traced back to the specific image acquisition factor.



© Central University of Technology, Free State

In Figure 3.10, the various factors tested during the experimental phase are indicated. Each colour represents a different protocol created through a literature search (orange protocol) and by performing the observational phase (green, blue and yellow protocols). For the literature protocol, the relevant references used were indicated if applicable, while for the observational protocols, the n-values (total number of individuals) were provided as configured through statistical analysis.

Each observational protocol also indicated a patient size (small, medium and large), which was done to ensure optimal image quality in relation to the exposure factors. The researcher collected the gestational age to determine the different sizes of the protocol (small, medium and large). The higher kVp and lower mAs were allocated to the larger neonate protocol even though the phantom is only one size. The higher kVp selection was paired with the lower mAs, while *vice versa*, the lower kVp was paired with the higher mAs value. The percentages included in the observational protocols indicate the selection by the radiographers, i.e., the study population was 16 (n=16), for the beam angulation remained straight for all 16 images (100%) performed by the radiographers.



© Central University of Technology, Free State

**Abdomen protocols (N=16)**

| Protocol (medium) | 1 | Observation statistic to support | |
|---|---|---|---|
| kVp | 57 | mean (p-value = 1,48183) | *SD = 3* |
| mAs | 2.6 | mean (p-value = 0,214445) | *SD = 0.4* |
| SID | 100 | 66% | *n-value = 105* |
| Collimation upper margin (edge of margin placed on) | Axilla (Diaphragm) | 100% | *n-value = 16* |
| Collimation lower margin (edge of margin placed on) | Symphysis pubis | 100% | *n-value = 16* |
| Collimation on sides (edge of margin placed next to) | Soft tissue margin | 100% | *n-value = 16* |
| Centring | Navel | 63% | *n-value = 10* |
| Main radiation beam angulation (angle the neonatal bed until) | Straight | 100% | *n-value = 16* |
| IR placement | Incubator IR tray | 56% | *n-value = 9* |

| Protocol (small) | 2 | Observation statistic to support | |
|---|---|---|---|
| kVp | 60 | 57kVp (mean) + SD of 3kVp | |
| mAs | 3 (or 3.2) | 2.6mAs (mean) + SD of 0.4mAs | |
| SID | 90 | 22% | *n-value = 34* |
| Collimation upper margin (edge of margin placed on) | Nipple line | Literature | |
| Collimation lower margin (edge of margin placed on) | Greater trochanter | Literature | |
| Collimation on sides (edge of margin placed next to) | Soft tissue margin | 100% | *n-value = 16* |
| Centring | Lower costal margin | 25% | *n-value = 4* |
| Main radiation beam angulation (angle the neonatal bed until) | Straight | 100% | *n-value = 16* |
| IR placement | Under patient | 44% | *n-value = 7* |

| Protocol (large) | 3 | Observation statistic to support | |
|---|---|---|---|
| kVp | 54 | 57kVp (mean) - SD of 3kVp | |
| mAs | 2.2 | 2.6mAs (mean) - SD of 0.4mAs | |
| SID | 80 | 12% | *n-value = 19* |
| Collimation upper margin (edge of margin placed on) | Clavicle | Literature | |
| Collimation lower margin (edge of margin placed on) | Diaper edge | Literature | |
| Collimation on sides (edge of margin placed next to) | Soft tissue margin | 100% | *n-value = 16* |
| Centring | 2.5cm superior to navel | 12% | *n-value = 2* |
| Main radiation beam angulation (angle the neonatal bed until) | Straight | 100% | *n-value = 16* |
| IR placement | Under mattress | 100% | *n-value = 8* |

| Protocol | 4 | Reference(s) to support |
|---|---|---|
| kVp | None found | |
| mAs | None found | |
| SID | 100cm | del Vecchio, Bontrager and Lampignano |
| Collimation upper margin (edge of margin placed on) | Top of diapraghm | del Vecchio, Menashe |
| Collimation lower margin (edge of margin placed on) | Symphysis pubis | del Vecchio, Menashe |
| Collimation on sides (edge of margin placed next to) | Lateral abdominal walls | del Vecchio |
| Centring | 2.5cm above navel | Bontrager and Lampignano |
| Main radiation beam angulation (angle the neonatal bed until) | Straight | Bontrager and Lampignano |
| IR placement | Under pt | Tugwell-Allsup, Bontrager and Lampignano |

**Figure 3.10.** Abdominal protocols (phase 3).

This approach provided 45 imaging protocols to test with several variables. The imaging protocols tested during phase 3 are presented in Figure 3.11 as an example. The different colours indicate different imaging protocols. In the figure, the blue indicates one imaging protocol and the red text shows which variable was tested during that exposure. For example, line one is the baseline image, while in lines two and three, everything is kept consistent with the baseline imaging protocol except for the kVp, which was changed twice. For line two, the variable tested was the kVp, which was lowered to 57 kVp while the rest remained constant in the baseline imaging. Thus, the 57 kVp was the variable tested. The yellow indicates the second imaging protocol, and the red text represents the variable tested.

In Figure 3.11, the first imaging protocol tested used a 60 kVp, 3.2 mAs and a 90 cm SID. The upper margin of the collimation was on the nipple line, while the lower margin was on the level of the greater trochanters. The centring point was on the level of the lower costal margin. No angulation was used; thus, a straight beam was assured, and the detector was placed directly



© Central University of Technology, Free State

under the patient. One factor was changed with each exposure as determined by phases 1 and 2, and the data were captured on the data sheet presented in Figure 3.11.

| | | | | | | | |
|---|---|---|---|---|---|---|---|
| 60 | 3.2 | 90 | Nipple line | Greater trochanter | Lower costal margin | Straight | Under pt |
| 57 | 3.2 | 90 | Nipple line | Greater trochanter | Lower costal margin | Straight | Under pt |
| 54 | 3.2 | 90 | Nipple line | Greater trochanter | Lower costal margin | Straight | Under pt |
| 60 | 2.5 | 90 | Nipple line | Greater trochanter | Lower costal margin | Straight | Under pt |
| 60 | 2.2 | 90 | Nipple line | Greater trochanter | Lower costal margin | Straight | Under pt |
| 60 | 3.2 | 100 | Nipple line | Greater trochanter | Lower costal margin | Straight | Under pt |
| 60 | 3.2 | 80 | Nipple line | Greater trochanter | Lower costal margin | Straight | Under pt |
| 60 | 3.2 | 90 | Axilla | Greater trochanter | Lower costal margin | Straight | Under pt |
| 60 | 3.2 | 90 | Clavicle | Greater trochanter | Lower costal margin | Straight | Under pt |
| 60 | 3.2 | 90 | Nipple line | Symphysis pubis | Lower costal margin | Straight | Under pt |
| 60 | 3.2 | 90 | Nipple line | Edge of diaper | Lower costal margin | Straight | Under pt |
| 60 | 3.2 | 90 | Nipple line | Greater trochanter | Navel | Straight | Under pt |
| 60 | 3.2 | 90 | Nipple line | Greater trochanter | 2.5cm above naval | Straight | Under pt |
| 60 | 3.2 | 90 | Nipple line | Greater trochanter | Lower costal margin | Straight | In tray |
| 60 | 3.2 | 90 | Nipple line | Greater trochanter | Lower costal margin | Straight | Under mattress |
| 54 | 2.2 | 80 | Clavicle | Edge of diaper | 2.5cm above naval | Straight | Under mattress |
| 57 | 2.2 | 80 | Clavicle | Edge of diaper | 2.5cm above naval | Straight | Under mattress |
| 60 | 2.2 | 80 | Clavicle | Edge of diaper | 2.5cm above naval | Straight | Under mattress |
| 54 | 2.5 | 80 | Clavicle | Edge of diaper | 2.5cm above naval | Straight | Under mattress |
| 54 | 3.2 | 80 | Clavicle | Edge of diaper | 2.5cm above naval | Straight | Under mattress |
| 54 | 2.2 | 100 | Clavicle | Edge of diaper | 2.5cm above naval | Straight | Under mattress |
| 54 | 2.2 | 90 | Clavicle | Edge of diaper | 2.5cm above naval | Straight | Under mattress |
| 54 | 2.2 | 80 | Axilla | Edge of diaper | 2.5cm above naval | Straight | Under mattress |
| 54 | 2.2 | 80 | Nipple line | Edge of diaper | 2.5cm above naval | Straight | Under mattress |
| 54 | 2.2 | 80 | Clavicle | Symphysis pubis | 2.5cm above naval | Straight | Under mattress |
| 54 | 2.2 | 80 | Clavicle | Greater trochanter | 2.5cm above naval | Straight | Under mattress |
| 54 | 2.2 | 80 | Clavicle | Edge of diaper | Navel | Straight | Under mattress |
| 54 | 2.2 | 80 | Clavicle | Edge of diaper | Lower costal margin | Straight | Under mattress |
| 54 | 2.2 | 80 | Clavicle | Edge of diaper | 2.5cm above naval | Straight | In tray |
| 54 | 2.2 | 80 | Clavicle | Edge of diaper | 2.5cm above naval | Straight | Under pt |

**Figure 3.11.** Imaging protocols tested in the experimental phase for abdominal X-rays.

The data collected during the third phase of the study were captured in an Excel spreadsheet (Figure 3.12). The factors captured in the spreadsheet included the collimation size measured by the mobile unit, the SSD, the part thickness measured with a calliper, and the OID. The EI and the DI were captured for all three exposures, as well as the IAK measured with the dosimeter on top of the phantom and the EAK measured with the dosimeter underneath the phantom. A separate data sheet was used for the three types of examinations (CXR, AXR and combined CXR-AXR) to limit confusion and promote trustworthiness.



© Central University of Technology, Free State

| Colimation length (cm) | Collimation width (cm) | FOV (cm)² | SSD (cm) | Part thickness (cm) | OID (cm) | EI rep 1 | EI rep 2 | EI rep 3 | DI rep 1 | DI rep 2 | DI rep 3 | IAK rep 1 (µGy) | IAK rep 2 (µGy) | IAK rep 3 (µGy) | EAK rep 1 (µGy) | EAK rep 2 (µGy) | EAK rep 3 (µGy) |
|---|---|---|---|---|---|---|---|---|---|---|---|---|---|---|---|---|---|
| 9 | 12 | 108 | 84,5 | 5,5 | 0 | 969 | 972 | 973 | 6.0 | 6.0 | 6.0 | 107,8 | 107,8 | 107,4 | 4,32 | 4,349 | 4,359 |
| 9 | 12 | 108 | 84,5 | 5,5 | 0 | 708 | 708 | 709 | 4.5 | 4.5 | 4.5 | 90,91 | 91,48 | 91,6 | 3,358 | 3,341 | 3,34 |
| 9 | 12 | 108 | 84,5 | 5,5 | 0 | 554 | 553 | 553 | 3.5 | 3.5 | 3.5 | 79,6 | 78,46 | 79,83 | 2,743 | 2,729 | 2,716 |
| 9 | 12 | 108 | 84,5 | 5,5 | 0 | 761 | 760 | 763 | 5.0 | 5.0 | 5.0 | 81,89 | 81,96 | 82,3 | 3,426 | 3,402 | 3,437 |
| 9 | 12 | 108 | 84,5 | 5,5 | 0 | 654 | 655 | 655 | 4.0 | 4.0 | 4.0 | 70,65 | 70,81 | 70,99 | 2,977 | 2,974 | 3,006 |
| 11 | 12 | 132 | 94,5 | 5,5 | 0 | 851 | 853 | 851 | 5.5 | 5.5 | 5.5 | 82,01 | 82,33 | 82,01 | 3,607 | 3,063 | 3,609 |
| 9 | 12 | 108 | 74,5 | 5,5 | 0 | 1146 | 1146 | 1150 | 6.5 | 6.5 | 6.5 | 142,6 | 142,6 | 142,5 | 5,547 | 5,547 | 5,569 |
| 10 | 13 | 130 | 84,5 | 5,5 | 0 | 1076 | 1076 | 1079 | 6.5 | 6.5 | 6.5 | 106,3 | 106,7 | 106,3 | 5,872 | 5,889 | 5,791 |
| 10 | 14 | 140 | 84,5 | 5,5 | 0 | 1122 | 1118 | 1120 | 6.5 | 6.5 | 6.5 | 106,9 | 106,6 | 106,6 | 6,095 | 6,117 | 6,186 |
| 10 | 12 | 120 | 84,5 | 5,5 | 0 | 1060 | 1060 | 1062 | 6.5 | 6.5 | 6.5 | 107,2 | 107,1 | 106,6 | 7,482 | 7,466 | 7,552 |
| 10 | 13 | 130 | 84,5 | 5,5 | 0 | 1106 | 1107 | 1110 | 6.5 | 6.5 | 6.5 | 105,7 | 105,4 | 105 | 8,992 | 8,922 | 9,013 |
| 10 | 12 | 120 | 84,5 | 5,5 | 0 | 1096 | 1097 | 1104 | 6.5 | 6.5 | 6.5 | 85,62 | 85,93 | 87,2 | 4,98 | 5,008 | 3,989 |
| 10 | 16 | 160 | 84,5 | 5,5 | 0 | 1187 | 1188 | 1192 | 7.0 | 7.0 | 7.0 | 103,2 | 104,2 | 104,3 | 9,365 | 9,347 | 9,371 |
| 9 | 11 | 99 | 75,5 | 5,5 | 9 | 853 | 859 | 857 | 5.5 | 5.5 | 5.5 | 128,7 | 127,9 | 127,9 | 4,851 | 4,832 | 4,843 |
| 9 | 11 | 99 | 82,5 | 5,5 | 2 | 927 | 929 | 933 | 5.5 | 5.5 | 5.5 | 112,8 | 113,2 | 112 | 4,531 | 4,5 | 4,485 |
| 11 | 17 | 187 | 72,5 | 5,5 | 2 | 523 | 525 | 524 | 3.0 | 3.0 | 3.0 | 73,08 | 72,89 | 73,17 | 2,317 | 2,335 | 2,306 |
| 11 | 17 | 187 | 72,5 | 5,5 | 2 | 662 | 662 | 664 | 4.0 | 4.0 | 4.0 | 81,88 | 81,69 | 81,57 | 2,9 | 2,867 | 2,887 |
| 11 | 17 | 187 | 72,5 | 5,5 | 2 | 966 | 971 | 967 | 6.0 | 6.0 | 6.0 | 99,26 | 99,73 | 99,47 | 3,863 | 3,795 | 3,844 |
| 11 | 17 | 187 | 72,5 | 5,5 | 2 | 615 | 613 | 614 | 4.0 | 4.0 | 4.0 | 83,87 | 84,25 | 84,58 | 2,679 | 2,68 | 2,683 |
| 11 | 17 | 187 | 72,5 | 5,5 | 2 | 815 | 816 | 808 | 5.0 | 5.0 | 5.0 | 110,5 | 110,5 | 111,9 | 3,522 | 3,559 | 3,427 |
| 10 | 16 | 160 | 92,5 | 5,5 | 2 | 334 | 333 | 334 | 1.5 | 1.0 | 1.5 | 42,09 | 42,19 | 41,97 | 1,432 | 1,446 | 1,401 |
| 9 | 17 | 153 | 82,5 | 5,5 | 2 | 413 | 414 | 417 | 2.0 | 2.0 | 2.0 | 52,48 | 52,37 | 53,03 | 1,702 | 1,705 | 1,705 |
| 11 | 16 | 176 | 72,5 | 5,5 | 2 | 498 | 501 | 502 | 3.0 | 3.0 | 3.0 | 72,17 | 72,86 | 73,01 | 2,375 | 2,39 | 2,386 |
| 11 | 15 | 165 | 72,5 | 5,5 | 2 | 468 | 476 | 479 | 2.5 | 3.0 | 3.0 | 71,84 | 72,76 | 72,57 | 2,288 | 2,318 | 2,384 |
| 11 | 16 | 176 | 72,5 | 5,5 | 2 | 507 | 507 | 508 | 3.0 | 3.0 | 3.0 | 73,04 | 72,3 | 72,01 | 2,363 | 2,41 | 2,337 |
| 11 | 15 | 165 | 72,5 | 5,5 | 2 | 486 | 490 | 490 | 3.0 | 3.0 | 3.0 | 72,17 | 72,43 | 72,54 | 2,298 | 2,359 | 2,321 |
| 10 | 16 | 160 | 72,5 | 5,5 | 2 | 523 | 523 | 524 | 3.0 | 3.0 | 3.0 | 64,36 | 64,34 | 64,37 | 2,282 | 2,272 | 2,29 |
| 12 | 16 | 192 | 72,5 | 5,5 | 2 | 451 | 451 | 452 | 2.5 | 2.5 | 2.5 | 73 | 72,68 | 73,17 | 2,454 | 2,479 | 2,49 |
| 9 | 19 | 171 | 65,5 | 5,5 | 9 | 478 | 481 | 480 | 3.0 | 3.0 | 3.0 | 57,97 | 57,86 | 57,76 | 2,283 | 2,282 | 2,288 |
| 10 | 15 | 150 | 74,5 | 5,5 | 0 | 442 | 441 | 441 | 2.5 | 2.5 | 2.5 | 70,38 | 70,16 | 69,79 | 2,305 | 2,321 | 2,312 |

**Figure 3.12.** Data sheet for abdominal X-ray experimental results.

The data analysis and configuration were performed for an optimal exposure index, optimal deviation index and an optimal entrance skin dose. Thus, all factors were analysed three times for each exposure measurement factor.

The **CXR-AXR imaging protocols** tested during phase 3 are presented in Figure 3.13 as an example. The different colours indicate different imaging protocols. In Figure 3.13, the green indicates one imaging protocol and the red text shows which variable was tested during that exposure. For example, line 1 is the baseline image, while in line 2, everything is kept consistent with the baseline imaging protocol except for the kVp, which changed twice. For line 2, the variable tested was the kVp which was increased to 60 kVp while the rest remained constant in the baseline imaging. Thus, the 60 kVp was the variable tested. The blue shading represents the second imaging protocol, and the red text indicates the variable tested.

As shown in Figure 3.13, the first imaging protocol tested used a 57 kVp, 3.2 mAs and a 100 cm SID. The upper margin of the collimation was above the shoulders and the lower margin on the level of the symphysis pubis. The centring point was on the navel. No angulation was used; thus, a straight beam was assured, and the detector was placed inside the tray of the Cosycot™. One factor was changed with each exposure as determined by phases 1 and 2, and the data were captured on the spreadsheet represented by Figure 3.13.



© Central University of Technology, Free State

| | | | | | | | |
|---|---|---|---|---|---|---|---|
| 57 | 3.2 | 100 | Above shoulders | Symphysis pubis | Navel | Straight | In tray |
| 60 | 3.2 | 100 | Above shoulders | Symphysis pubis | Navel | Straight | In tray |
| 54 | 3.2 | 100 | Above shoulders | Symphysis pubis | Navel | Straight | In tray |
| 57 | 2.8 | 100 | Above shoulders | Symphysis pubis | Navel | Straight | In tray |
| 57 | 1.8 | 100 | Above shoulders | Symphysis pubis | Navel | Straight | In tray |
| 57 | 3.2 | 90 | Above shoulders | Symphysis pubis | Navel | Straight | In tray |
| 57 | 3.2 | 80 | Above shoulders | Symphysis pubis | Navel | Straight | In tray |
| 57 | 3.2 | 100 | Thyroid cartilage | Symphysis pubis | Navel | Straight | In tray |
| 57 | 3.2 | 100 | Lip line | Symphysis pubis | Navel | Straight | In tray |
| 57 | 3.2 | 100 | Above shoulders | Greater trochanter | Navel | Straight | In tray |
| 57 | 3.2 | 100 | Above shoulders | Edge of diaper | Navel | Straight | In tray |
| 57 | 3.2 | 100 | Above shoulders | Symphysis pubis | Lower costal margin | Straight | In tray |
| 57 | 3.2 | 100 | Above shoulders | Symphysis pubis | 4cm above naval | Straight | In tray |
| 57 | 3.2 | 100 | Above shoulders | Symphysis pubis | Navel | Straight | Under pt |
| 57 | 3.2 | 100 | Above shoulders | Symphysis pubis | Navel | Straight | Under mattress |
| 60 | 2.8 | 90 | Thyroid cartilage | Greater trochanter | Lower costal margin | Straight | Under pt |
| 57 | 2.8 | 90 | Thyroid cartilage | Greater trochanter | Lower costal margin | Straight | Under pt |
| 54 | 2.8 | 90 | Thyroid cartilage | Greater trochanter | Lower costal margin | Straight | Under pt |
| 60 | 3.2 | 90 | Thyroid cartilage | Greater trochanter | Lower costal margin | Straight | Under pt |
| 60 | 1.8 | 90 | Thyroid cartilage | Greater trochanter | Lower costal margin | Straight | Under pt |
| 60 | 2.8 | 100 | Thyroid cartilage | Greater trochanter | Lower costal margin | Straight | Under pt |
| 60 | 2.8 | 80 | Thyroid cartilage | Greater trochanter | Lower costal margin | Straight | Under pt |
| 60 | 2.8 | 90 | Above shoulders | Greater trochanter | Lower costal margin | Straight | Under pt |
| 60 | 2.8 | 90 | Lip line | Greater trochanter | Lower costal margin | Straight | Under pt |
| 60 | 2.8 | 90 | Thyroid cartilage | Symphysis pubis | Lower costal margin | Straight | Under pt |
| 60 | 2.8 | 90 | Thyroid cartilage | Edge of diaper | Lower costal margin | Straight | Under pt |
| 60 | 2.8 | 90 | Thyroid cartilage | Greater trochanter | Navel | Straight | Under pt |
| 60 | 2.8 | 90 | Thyroid cartilage | Greater trochanter | 4cm above naval | Straight | Under pt |
| 60 | 2.8 | 90 | Thyroid cartilage | Greater trochanter | Lower costal margin | Straight | In tray |
| 60 | 2.8 | 90 | Thyroid cartilage | Greater trochanter | Lower costal margin | Straight | Under mattress |

**Figure 3.13.** Imaging protocols tested in the experimental phase for combined chest and abdominal X-rays.

The data collected during the third phase of the study were captured in an Excel spreadsheet (Figure 3.14). The factors captured in the spreadsheet included the collimation size measured by the mobile unit, the SSD, the part thickness measured with a calliper, and the OID. The EI and the DI were captured for all three exposures, as well as the IAK measured with the dosimeter on top of the phantom and the EAK measured with the dosimeter under the phantom. A separate data sheet was used for the three types of examinations to limit confusion and promote trustworthiness.



© Central University of Technology, Free State

| Collimation length (cm) | Collimation width (cm) | FOV (cm)² | SSD (cm) | thickness (cm) | OID (cm) | EI rep 1 | EI rep 2 | EI rep 3 | DI rep 1 | DI rep 2 | DI rep 3 | IAK rep 1 (µGy) | IAK rep 2 (µGy) | IAK rep 3 (µGy) | EAK rep 1 (µGy) | EAK rep 2 (µGy) | EAK rep 3 (µGy) |
|---|---|---|---|---|---|---|---|---|---|---|---|---|---|---|---|---|---|
| 11 | 17 | 187 | 85,5 | 5,5 | 9 | 609 | 611 | 611 | 4 | 4 | 4 | 79,32 | 79,78 | 78,96 | 2,995 | 3,02 | 3,051 |
| 11 | 17 | 187 | 85,5 | 5,5 | 9 | 835 | 838 | 837 | 5 | 5,5 | 5 | 94,36 | 93,97 | 94,35 | 3,997 | 4,008 | 4,013 |
| 11 | 17 | 187 | 85,5 | 5,5 | 9 | 461 | 461 | 461 | 2,5 | 2,5 | 1,5 | 96,22 | 69,34 | 69,02 | 2,44 | 2,433 | 2,434 |
| 11 | 17 | 187 | 85,5 | 5,5 | 9 | 526 | 526 | 527 | 3 | 3 | 3 | 68,63 | 68,92 | 68,91 | 2,638 | 2,638 | 2,624 |
| 11 | 17 | 187 | 85,5 | 5,5 | 9 | 314 | 313 | 314 | 1 | 1 | 1 | 43,06 | 42,37 | 43,04 | 1,656 | 1,669 | 1,652 |
| 11 | 17 | 187 | 75,5 | 5,5 | 9 | 704 | 705 | 707 | 4,5 | 4,5 | 4,5 | 100,6 | 101,2 | 101,1 | 3,829 | 3,863 | 3,828 |
| 10 | 19 | 190 | 65,5 | 5,5 | 9 | 913 | 914 | 917 | 5,5 | 5,5 | 5,5 | 141,5 | 141,9 | 141,3 | 4,767 | 4,774 | 4,77 |
| 11 | 17 | 187 | 85,5 | 5,5 | 9 | 569 | 570 | 569 | 3,5 | 3,5 | 3,5 | 67,88 | 67,75 | 68,07 | 2,995 | 3,048 | 3,047 |
| 11 | 19 | 209 | 85,5 | 5,5 | 9 | 596 | 597 | 596 | 4 | 4 | 4 | 66,76 | 66,8 | 66,72 | 2,965 | 2,946 | 2,974 |
| 11 | 17 | 187 | 85,5 | 5,5 | 9 | 568 | 569 | 569 | 3,5 | 3,5 | 3,5 | 67,63 | 68,03 | 67,65 | 2,977 | 2,944 | 2,942 |
| 11 | 17 | 187 | 85,5 | 5,5 | 9 | 604 | 604 | 602 | 4 | 4 | 4 | 67,48 | 67,77 | 67,96 | 2,977 | 3,005 | 3,031 |
| 11 | 15 | 165 | 85,5 | 5,5 | 9 | 597 | 599 | 599 | 4 | 4 | 4 | 86,36 | 86,06 | 86,42 | 3,235 | 3,248 | 3,225 |
| 11 | 16 | 176 | 85,5 | 5,5 | 9 | 600 | 600 | 602 | 4 | 4 | 4 | 85,87 | 85,67 | 86,04 | 7,08 | 7,16 | 7,138 |
| 10 | 17 | 170 | 94,5 | 5,5 | 0 | 906 | 910 | 917 | 5,5 | 5,5 | 5,5 | 71,96 | 72,72 | 73,47 | 4,798 | 3,322 | 3,431 |
| 10 | 17 | 170 | 92,5 | 5,5 | 2 | 820 | 819 | 820 | 5 | 5 | 5 | 71,58 | 71,04 | 71,15 | 3,199 | 3,173 | 3,207 |
| 10 | 15 | 150 | 84,5 | 5,5 | 0 | 987 | 989 | 992 | 6 | 6 | 6 | 92,59 | 92,74 | 92,93 | 3,941 | 3,933 | 3,946 |
| 10 | 15 | 150 | 84,5 | 5,5 | 0 | 722 | 722 | 721 | 4,5 | 4,5 | 4,5 | 78,6 | 78,42 | 78,61 | 3,03 | 3,078 | 2,982 |
| 10 | 15 | 150 | 84,5 | 5,5 | 0 | 609 | 611 | 612 | 4 | 4 | 4 | 72,54 | 72,35 | 72,29 | 2,622 | 2,594 | 2,645 |
| 10 | 15 | 150 | 84,5 | 5,5 | 0 | 1157 | 1157 | 1157 | 6,5 | 6,5 | 6,5 | 107,2 | 108,1 | 108,4 | 4,573 | 4,557 | 4,59 |
| 10 | 15 | 150 | 84,5 | 5,5 | 0 | 580 | 584 | 583 | 3,5 | 3,5 | 3,5 | 57,31 | 57,52 | 57,15 | 2,431 | 2,454 | 2,41 |
| 11 | 15 | 165 | 94,5 | 5,5 | 0 | 845 | 847 | 847 | 5,5 | 5,5 | 5,5 | 71,31 | 71,16 | 71,14 | 3,115 | 3,155 | 3,15 |
| 10 | 16 | 160 | 74,5 | 5,5 | 0 | 1209 | 1210 | 1209 | 7 | 7 | 7 | 123 | 124 | 123,1 | 5,218 | 5,188 | 5,194 |
| 10 | 16 | 160 | 84,5 | 5,5 | 0 | 1009 | 1012 | 1008 | 6 | 6 | 6 | 90,19 | 90,38 | 89,8 | 7,798 | 7,796 | 7,836 |
| 10 | 19 | 190 | 84,5 | 5,5 | 0 | 1066 | 1065 | 1066 | 6,5 | 6,5 | 6,5 | 90,66 | 90,29 | 90,91 | 7,879 | 7,812 | 7,851 |
| 10 | 18 | 180 | 84,5 | 5,5 | 0 | 1010 | 1013 | 1013 | 6 | 6 | 6 | 90,02 | 90,16 | 90,49 | 7,725 | 7,865 | 7,833 |
| 10 | 19 | 190 | 84,5 | 5,5 | 0 | 1045 | 1047 | 1048 | 6 | 6 | 6 | 91,55 | 90,96 | 91,18 | 7,329 | 7,369 | 7,333 |
| 10 | 15 | 150 | 84,5 | 5,5 | 0 | 1003 | 1001 | 1003 | 6 | 6 | 6 | 85,88 | 85,62 | 85,81 | 4,683 | 4,674 | 4,676 |
| 10 | 16 | 160 | 84,5 | 5,5 | 0 | 946 | 947 | 947 | 6 | 6 | 6 | 94,55 | 93,4 | 93,99 | 5,3 | 5,232 | 5,299 |
| 9 | 16 | 144 | 75,5 | 5,5 | 9 | 834 | 836 | 837 | 5 | 5 | 5 | 111,3 | 112 | 111,7 | 4,223 | 4,218 | 4,184 |
| 9 | 16 | 144 | 82,5 | 5,5 | 2 | 895 | 895 | 896 | 5,5 | 5,5 | 5,5 | 98,58 | 97,36 | 98,14 | 3,893 | 3,838 | 3,858 |

**Figure 3.14.** Data sheet for experimental combined chest and abdominal X-ray results.

The data analysis and configuration were performed for an optimal exposure index, deviation index and entrance skin dose. Thus, all factors were analysed three times for each exposure measurement factor.

As illustrated in Figures 3.15 and 3.16, markers were placed on the mattress and bed, and inside the incubator tray to ensure consistent placement of the detector throughout the experiment.




**Figure 3.15.** Markings on the CosyCot™ mattress for consistent detector placement.



© Central University of Technology, Free State

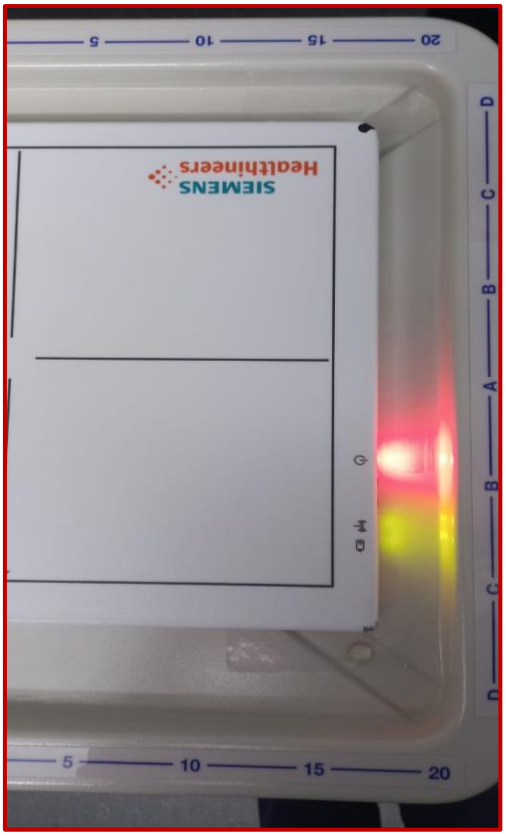



**Figure 3.16.** Markings inside the incubator tray for consistent detector placement.

Figures 3.17A and 3.17B demonstrate the placement of the dosimeter for the dose measurement. One dosimeter was placed on top of the phantom to measure the entrance skin dose (ESD) and another dosimeter was placed underneath the phantom to measure the exit skin dose.



© Central University of Technology, Free State




A



B

**Figures 3.17.** Demonstration of the dosimeter placement. **A:** Dosimeter on the phantom. **B:** Dosimeter underneath the phantom.

Transpore™ tape (3M; Johannesburg, South Africa) was used to ensure that no movement of the dosimeter occurred on or underneath the phantom on the detector during the setup change, and to safeguard that the dosimeter remained on the specific centring point each time (Figure 3.18). The blue cross on the dosimeter made it easier to place it on the exact centring point and by taping it to the phantom, consistent dosimeter placement was assured. This approach enhanced the accuracy and validity of the results during the experimental phase of the study.



© Central University of Technology, Free State




**Figure 3.18.** Placement of the dosimeter on top of the phantom.

The image in Figure 3.19 illustrates consistent centring with the main radiation beam. A cross was placed on the different centring points to ensure consistent centring for optimal dose measurements.

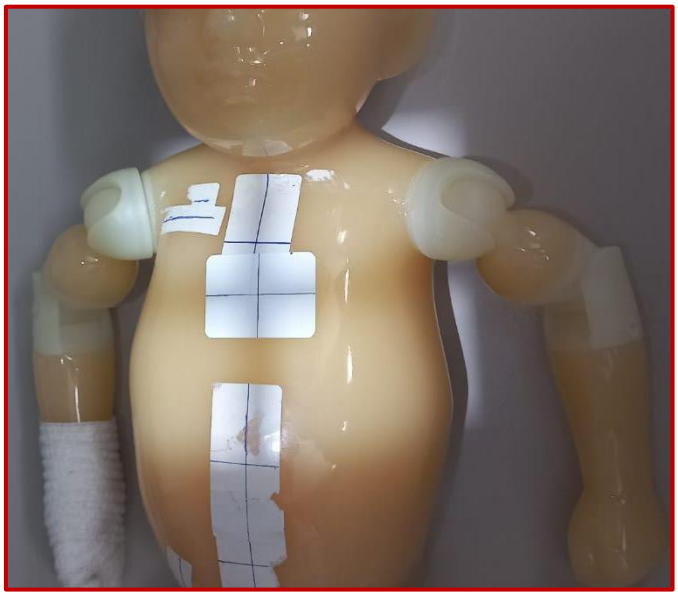


**Figure 3.19.** Centring points.



© Central University of Technology, Free State

Figure 3.19 shows how the SID was measured in each case to ensure the correct SID and consistent tube height. The tape measure was attached to the machine by the manufacturer and SID was measured in centimetres.



**Figure 3.20.** Source-to-image distance (SID) measurement.

Figure 3.21 shows one of the images acquired during the experimental phase. From the image, the researcher marked the anatomical inclusion criteria form, as well as the anatomical structures visible on the image (Figure 3.4).

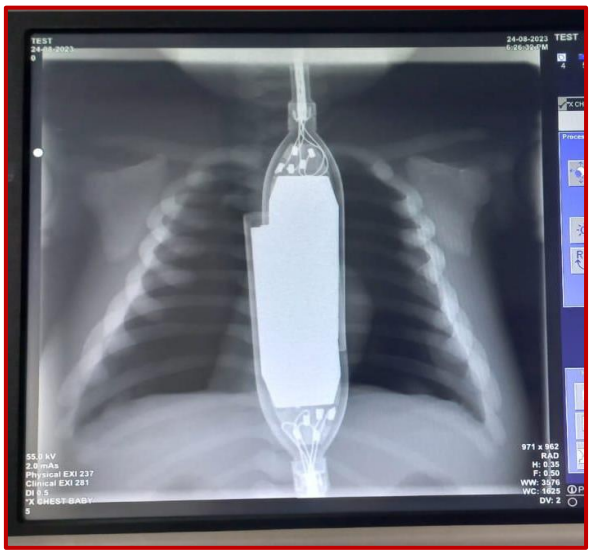


**Figure 3.21.** Example of an image during phase 3.



© Central University of Technology, Free State

Figure 3.22 illustrates technical factors displayed on the mobile X-ray unit. These factors include the exposure index and deviation index for each image. In the top right-hand corner of the image, the collimation size for each image is displayed.




**Figure 3.22.** Technical factors displayed on the mobile unit.

### *3.4.2.3 Data analysis of the experimental checklist*

All data recorded were analysed by an appointed statistician. The data acquired during the third phase of the study were captured on an Excel spreadsheet by the researcher and presented to the statistician. The statistician included all data meeting the requirements in the statistical analysis. The statistician determined which imaging protocols included the relevant anatomy and the visibility of anatomical structures. It was also determined which imaging protocols provided an optimal EI, DI and ESD. Before statistical analysis commenced, inadequate imaging protocols were removed to provide only optimal protocols of diagnostic value.

The data received from the statistical analysis allowed the researcher to compile the preliminary implementation checklist used during phase 4 of the study.

### 3.4.3 Phase 4: Implementation checklist

This phase started with a brief educational session presented by the researcher to the participating radiographers based on the checklist that they should complete. The training session consisted of a PowerPoint presentation attached as Appendix P, where the researcher



© Central University of Technology, Free State

explained the purpose of the study and specifically this phase of the study. The imaging protocol was presented as the one-pager that should be applied during their routine X-rays, whereafter they had to complete the implementation checklist. This implementation checklist (Appendix B) was completed by four radiographers after performing the mobile X-ray examination during the two-week implementation to determine the efficacy and usefulness of the imaging protocol. They were asked to evaluate the structures included, the visibility of lead markers and the collimation applied. Radiographers judged these images as part of their daily routine, and as stated in their scope of practice. No diagnostic conclusions were made from these images, nor were any pathologies or personal information included.

#### *3.4.3.1 Pilot study of the implementation checklist*

For the pilot study, the implementation checklist was completed by diagnostic radiography students (n=6) after attending the educational training session (Appendix P) to ensure the accuracy and validity of the checklist. The students did not perform any examinations on patients, they only attended the training session to ensure complete clarity and understanding of the implementation protocol and to correct any grammatical errors, address uncertainties and to add any missed information to the checklist. The secondary purpose of the pilot study was to ensure a comfortable flow of data collection and strategic placement of each heading. This allowed the researcher to promote understanding and interpretation of each subject. No changes were made to the checklist after the pilot study as everything was comprehensible and the order of information made sense from a practical perspective.

#### *3.4.3.2 Data collection method of the implementation checklist*

The data collection process was initiated with a training session for the completion of the checklist before the commencement of the implementation phase. This consisted of a brief slideshow presentation (Appendix P) to explain the purpose of this phase and the value of the participants' cooperation and honesty. The training programme allowed for a comprehensive summary of the entire phase and the importance of accurate completion of the checklists. All questions and concerns from the radiographers' side were addressed and resolved. A one-pager summary of the imaging protocol was given to the radiographers and placed on the mobile units as a reference and a guideline to ensure consistent imaging during routine mobile examinations. The fourth phase of the research study started on 27 November 2023 and concluded on 8 December 2023.



© Central University of Technology, Free State

The first part of the implementation checklist (Table 3.13) was based on positioning factors such as arm placement and head position with immobilisation techniques. The second part of the checklist was based on the technical factors that included the SID, the detector placement and the position and direction of the main radiation beam. The third part was the exposure factors including the kVp and mAs settings with the exposure index and the deviation index.

**Table 3.13.** Part 1 of the implementation checklist.

| **POSITIONING FACTORS** | |
|---|---|
| Arms abducted from body | |
| Immobilisation technique | |
| Head facing up | |
| Immobilisation technique | |
| Chin lifted | |
| Immobilisation technique | |
| Rotation on pelvis | |
| Rotation of thorax | |
| **TECHNICAL FACTORS** | |
| Lead marker placed | |
| Detector placement | |
| Source-to-object distance (SOD) | |
| Source-to-image distance (SID) | |
| Centring and Angulation | |
| **EXPOSURE FACTORS** | |
| Kilovoltage peak (kVp) value | |
| Milliampere second (mAs) value | |
| Exposure index | |
| Deviation index | |

Part two consisted of four criteria, with criteria one and two based on CXR referring to the anatomical structures included, and the visibility of the structures. Table 3.14 is an example of this part of the implementation checklist.



© Central University of Technology, Free State

**Table 3.14.** Part 2, criteria 1 and 2 of the implementation checklist.

| CHEST X-RAY | | |
|---|---|---|
| | **YES** | **NO** |
| **CRITERION 1: ANATOMICAL STRUCTURES INCLUDED** | | |
| C7 superiorly | | |
| Bilateral costophrenic angles | | |
| Soft tissue laterally | | |
| ⅓ of the upper abdomen | | |
| Only up to level of gastric bubble | | |
| Mid-abdomen to IC | | |
| Entire abdomen including SP | | |
| **CRITERION 2: ANATOMICAL STRUCTURES VISIBLE** | | |
| Air-filled trachea | | |
| Carina | | |
| Lung markings | | |
| Hilar regions | | |
| Sharp heart border | | |
| Sharp costophrenic angles | | |
| Stomach bubble | | |

C7, 7$^{th}$ cervical vertebra; IC, iliac crest; SP, symphysis pubis.

Criteria three and four were applicable to abdominal X-rays with regard to the anatomical structures included and the visibility of the anatomical structures (Table 3.15).

**Table 3.15.** Part 3, criteria 3 and 4 of the implementation checklist.

| ABDOMINAL X-RAY | | |
|---|---|---|
| | **YES** | **NO** |
| **CRITERION 3: ANATOMICAL STRUCTURES INCLUDED** | | |
| Costophrenic angled superiorly | | |
| Symphysis pubis inferiorly | | |
| Soft tissue laterally | | |
| **CRITERION 4: ANATOMICAL STRUCTURES VISIBLE** | | |
| Stomach bubble | | |
| Gas-bowel pattern | | |

The final part of the checklist was the post-processing of the images (Table 4.16). This included placement of lead markers, possible repetition, and rotation visible on the images.



© Central University of Technology, Free State

**Table 3.16.** Part 4 of the implementation checklist.

| PART 4: POST-PROCESSING REQUIRED | | |
|---|---|---|
| | **YES** | **NO** |
| Collimation too big | | |
| Collimation too small (cut-off) | | |
| Overexposed (image too dark) | | |
| Underexposed (image to white) | | |
| Image requires small rotation (malalignment) | | |
| Electronic marker placement | | |
| Any repeats | | |
| Reason for repetition: | | |

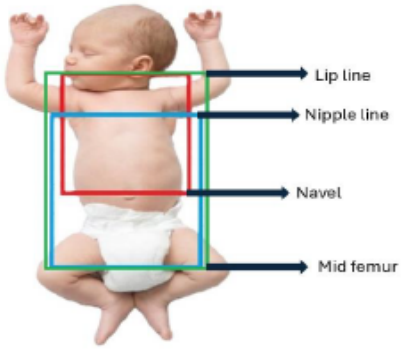
Figure 3.23 shows the one-pager attached to the mobile X-ray machine to serve as a reference for the radiographers, to ensure the application of the imaging protocol to their daily routine for consistent imaging. The one-pager presented the desired positioning method and technical factors such as the detector placement, the centring point and the angulation of the main radiation beam. The exposure factors, including the ideal exposure index range and the optimal deviation index, were also presented as proven during the experimental phase.



© Central University of Technology, Free State

# PICK THE ENDING

| POSITIONING FACTORS | | | |
|---|---|---|---|
| Arms abducted from body | | | |
| Head facing up | | | |
| Chin lifted | | | |
| No rotation on pelvis | | | |
| No rotation of thorax | | | |
| **TECHNICAL FACTORS** | | | |
| Lead marker placed | | | |
| Detector placement | Underneath patient if possible | | |
| Source-to-object distance (SOD)<br>*Tube to mattress* | 98 cm (depending on mattress thickness) | | |
| Source-to-image distance (SID)<br>*Tube to detector* | 100 cm | | |
| Centering point | Nipple line | Navel | Navel |
| Angulation of main beam | Straight beam | | |
| **EXPOSURE FACTORS** | | | |
| **Exam type:** | **CXR** | **AXR** | **Combo** |
| kVp value | 57 or 60 kVp | 54 kVp | 54 kVp |
| mAs value | 0.80 mAs | 1.80 mAs | 1.80 mAs |
| Exposure index | Optimal EI:<br>50 – 200 | Optimal EI: 125 – 500 | |
| Deviation index | Optimal DI: 0 | | |




RED – Chest x-ray
BLUE – Abdominal x-ray
GREEN – Combo x-ray

Compiled by: A Nel (2024)

AXR, abdominal X-ray; CXR, chest X-ray; kVp, kilovoltage peak; mAs, milliampere second; µGy, microGray.

**Figure 3.23.** One-pager imaging protocol.

The researcher provided checklists to the participating radiographers to complete after each routine mobile was performed, to critique their own images. They completed each criterion included in the checklist to be evaluated by the statistician afterwards to ensure the validity



© Central University of Technology, Free State

and helpfulness of the imaging protocol. The radiographers were assigned codes for anonymity, but each protocol was assigned an identification number for quality control purposes. The radiographers completed all the relevant criteria such as centring point, SID, exposure factors and positioning factors. After completion of the checklists, they placed them in a box for the researcher for safekeeping until the end of the two weeks. The researcher transferred all the data to an Excel spreadsheet for statistical analysis.

#### *3.4.3.3 Data analysis of the implementation checklist*

The data from the implementation checklists were captured on an Excel spreadsheet and analysed by the statistician to determine several factors. These factors included the most frequently used exposure factors and positioning techniques, as well as post-processing techniques applied. The results of the statistical analysis are presented and discussed in Chapter 4.

### 3.4.4 Phase 5: Reflection post-implementation

The researcher compared the exposure index, image critique factors and the post-processing techniques applied and captured on the completed observational checklists (cf. section 3.4.1) as observed during phase 2, with the implementation reflection checklists (cf. section 3.4.3) completed by the radiographers during phase 4, to determine success after implementing the baseline imaging protocol.

#### *3.4.4.1 Data analysis of reflection*

The data acquired from the checklists completed by the radiographers were documented on an Excel spreadsheet by the researcher and presented to the statistician for statistical analysis. The statistician compared imaging techniques observed during phase 2 with those applied during phase 4. The purpose of the comparison was to evaluate whether improvement occurred after the implementation of the imaging protocol.

## 3.5 CONCLUSION

Elaboration on the methodology used for phases 2 to 5 of the study was done in this chapter. In Chapter 3 a description of the research tools used, data collection methods and the data analysis procedures followed are included. In Chapter 4 the data and results of phases 2 to 5 are shared. Phase 1, which was the literature survey, was unpacked in Chapter 2. In Chapter 4 the final standardised imaging protocol is provided.



© Central University of Technology, Free State

# CHAPTER 4
# RESULTS AND DISCUSSION

## 4.1 INTRODUCTION

An imaging protocol set in a department should be followed by all radiographers for an opportunity to reduce the radiation dose to patients with increased sensitivity to ionising radiation (Gunn *et al*., 2020: e71). Radiographers should follow the set protocols and actively participate in developing and revising these protocols to ensure diagnostic quality images, minimised patient radiation dose and efficient workflow (DeMaio, Herrmann, Noble, Orth, Peterson, Young & Odle, 2019: 198).

The results are discussed per phase, starting with phase 2 (observational phase) and ending with phase 5 (reflection phase). Phase one (discussed in Chapter 2) contributed to the execution of both phase 2 and phase 3, as the literature imaging protocols assisted in the establishment of both the observational (Appendix A) and the experimental (Appendix C) checklists.

## 4.2 DATA ANALYSIS DEFINITION

Data from the observational, experimental and reflection checklists were captured on separate spreadsheets in Microsoft Excel. Analysis was performed by a statistician using SAS Version 9.4. Descriptive statistics, namely distribution frequencies and percentages were calculated for categorical data and means, and standard deviations or medians and percentiles were calculated for numerical data.

The Shapiro-Wilk test was used to determine if numerical data followed a normal distribution. Checklists from phase 2 were compared to checklists from phase 4 by using analytical statistics. The independent T-test (or Mann-Whitney U-test) was used to compare mean (or median) values, and the chi-square test was used to compare percentages. A significance level ($\alpha$) of 0.05 was used.



© Central University of Technology, Free State

## 4.3 PHASE 2: OBSERVATIONAL CHECKLIST

Quantitative data was collected during the observation phase. The aim was to compile a single protocol representing the technique used by each radiographer at the research site. Only the protocols within the acceptable EI range (50–200) were included.

The researcher captured data from the observational checklist (Appendix A) electronically in Microsoft Excel. Analysis was done by an appointed statistician. Twelve radiographers were observed while performing mobile examinations in the NICU. A total of 158 mobile examinations were performed over twelve weeks. The 158 radiographic X-ray images obtained included 109 CXR, 16 AXR, and 33 CXR-AXR images.

The gestational age of the neonates ranged from 26 weeks to 38 weeks, with 18% (n=29) of the neonates intubated. The results are presented according to the sequence of the observational checklist (Appendix A). For part 1, aimed at radiographers, the following criteria are described

- Criterion 1: Positioning factors
- Criterion 2: Technical factors

Table 3.5 (Chapter 3) summarised the positioning factors that were observed by the researcher during the observation phase of the study. The findings of these positioning criteria, pertaining to the arms abducted from the body, head position, chin, rotation of the pelvis and the thorax are presented by including the immobilisation techniques in the following pages.

The radiographers abducted the arms from the body in 73% (n=115) of cases. The arm immobilisation technique was divided into different aspects. The radiographers either held the neonate during exposure, placed sandbags on the arms or legs of the neonate, or immobilisation was achieved by placing the neonate in a nook. The nook refers to a sleeping "nest" created by the nurse by using a towel or blanket. The nook limits movement and allows the neonate to feel safe and secure; thus, limiting the need for specific immobilisation techniques (Rohmah, Saputri & Bahari, 2020: 119).

Figure 4.1 shows the different immobilisation techniques applied by the radiographers for the 109 CXR imaging procedures observed during phase 2. The radiographer positioned the arms to the side in 1% (n=2) of the examinations, 6% (n=7) of the neonates were in a nook, and in 12% (n=13), sandbags were used to immobilise the neonate. Lastly, 57% (n=62) of the



© Central University of Technology, Free State

immobilisation technique was recorded as the radiographer holding the patient. None (22%) refer to no immobilisation technique applied.

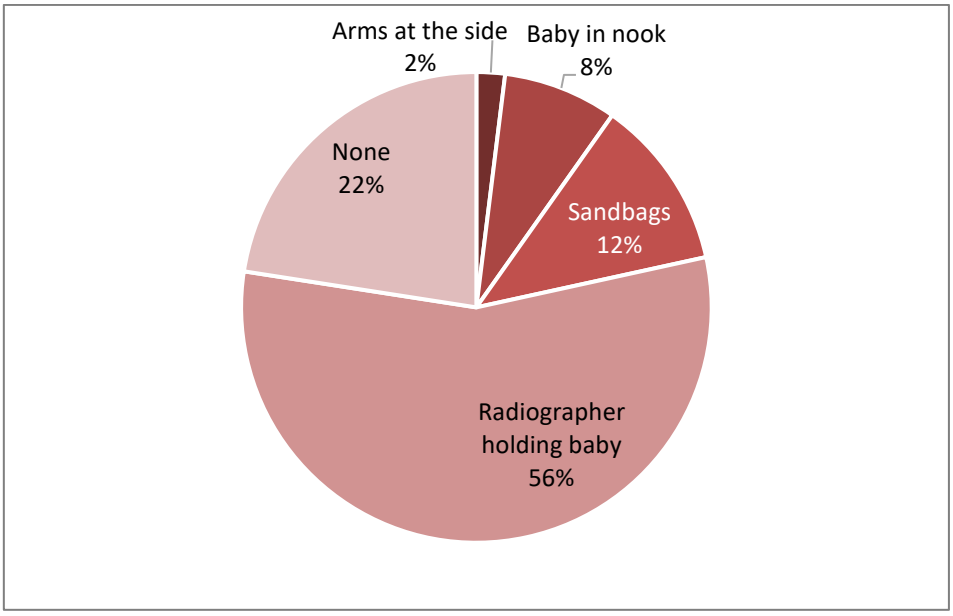



**Figure 4.1.** Arm immobilisation technique observed (phase 2 – CXR; n=109).

Figure 4.2 shows the arm immobilisation techniques for AXR. Of the 16 AXR performed during phase 2, the only immobilisation technique applied was the radiographer holding the baby 56% (n=9). For the remaining 44% (n=7), no immobilisation was applied. No immobilisation in this case referred to the radiographer not abducting the arms; thus, no immobilisation technique was needed.

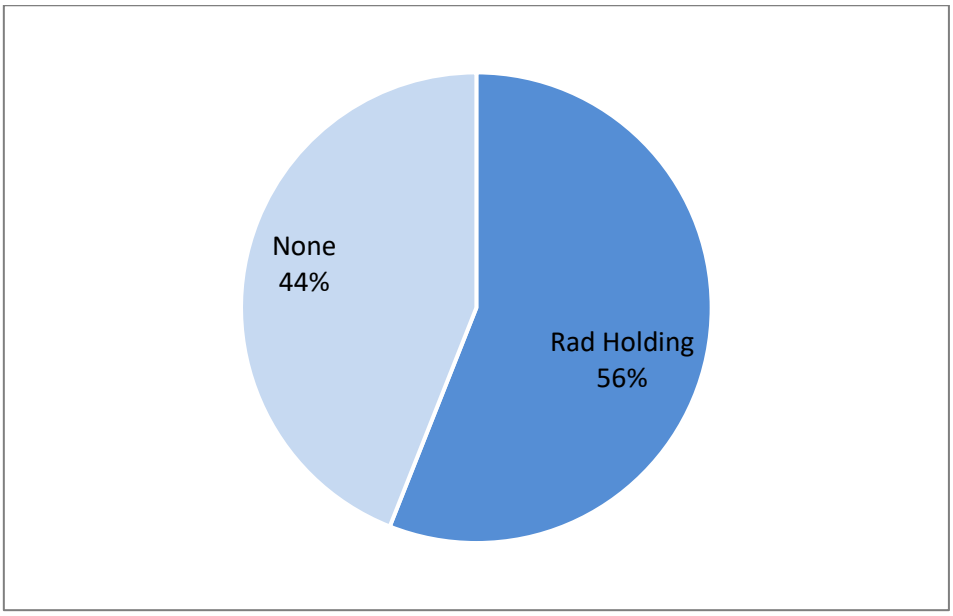



**Figure 4.2.** Arm immobilisation technique observed (phase 2 – AXR; n=16).



© Central University of Technology, Free State

In Figure 4.3, the arm abduction immobilisation techniques applied during the combined image for phase 2 are presented. The most common immobilisation technique applied was the radiographer holding the patient (n=16; 48%) while the second most common immobilisation technique was sandbag placement (n=4; 12%). Arms to the side and baby in a nook were equal (each n=1; 3%). For 11 (33%) neonates, no immobilisation was needed as the arms were not abducted.

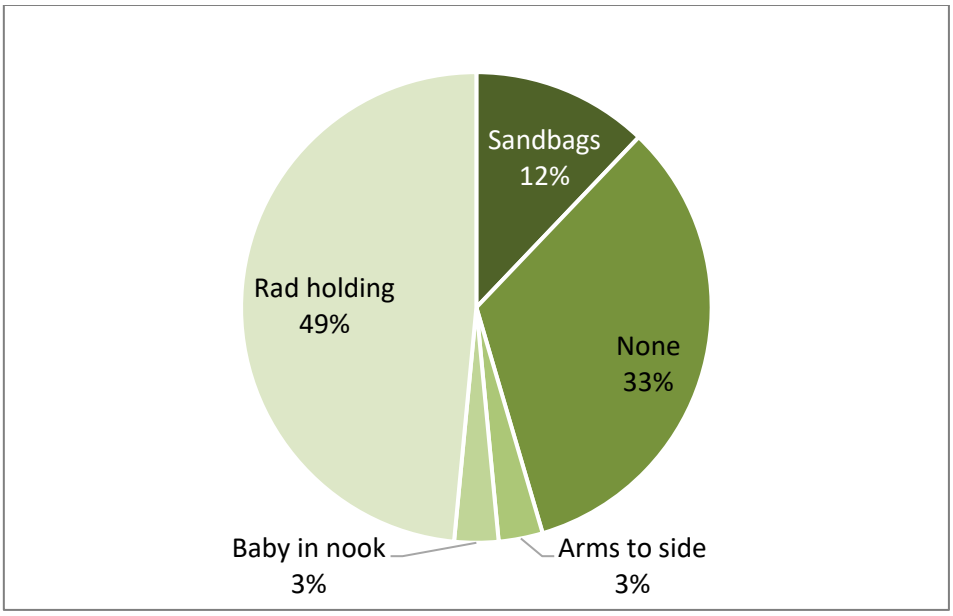
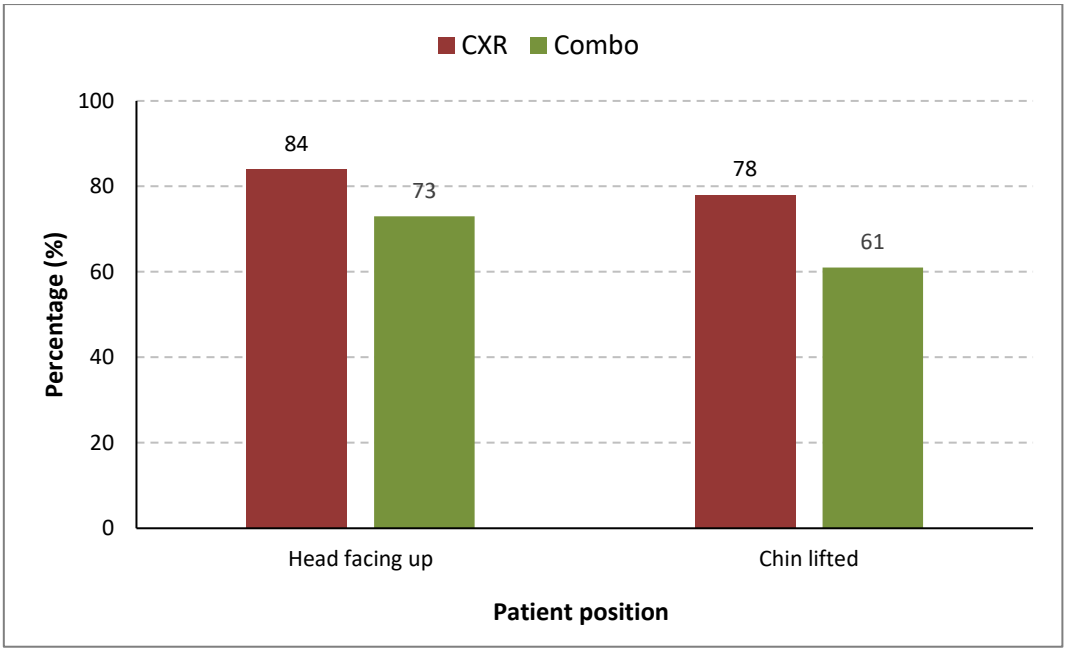



**Figure 4.3.** Arm immobilisation technique observed (phase 2 – Combo; n=33).

Several immobilisation techniques were applied for the head position, as seen in Figure 4.4. The radiographer held the neonate during X-ray exposure and ensured a straight head position, or the radiographer placed sandbags next to the head to assist with immobilisation. Some patients were in a natural position with their head facing straight up and others remained in that position due to intubation. As explained above, some of the patients were placed in a nook, which assured immobilisation of the head. For the CXR, 84% (n=92) of patients' heads were facing up and 73% (n=24) of patients' chins were lifted, whereas for the combo, the patients' heads were facing up in 78% (n=85) and the chin was lifted in 61% (n=20). Bontrager and Lampignano (2014: 631) and Lampignano and Kendrick (2021) suggested that the head and chin of the neonate be lifted to prevent superimposition of the chin over the apices of the lungs. According to the statistics, the radiographers mostly applied this positioning method to improve the diagnostic quality of the image.



© Central University of Technology, Free State



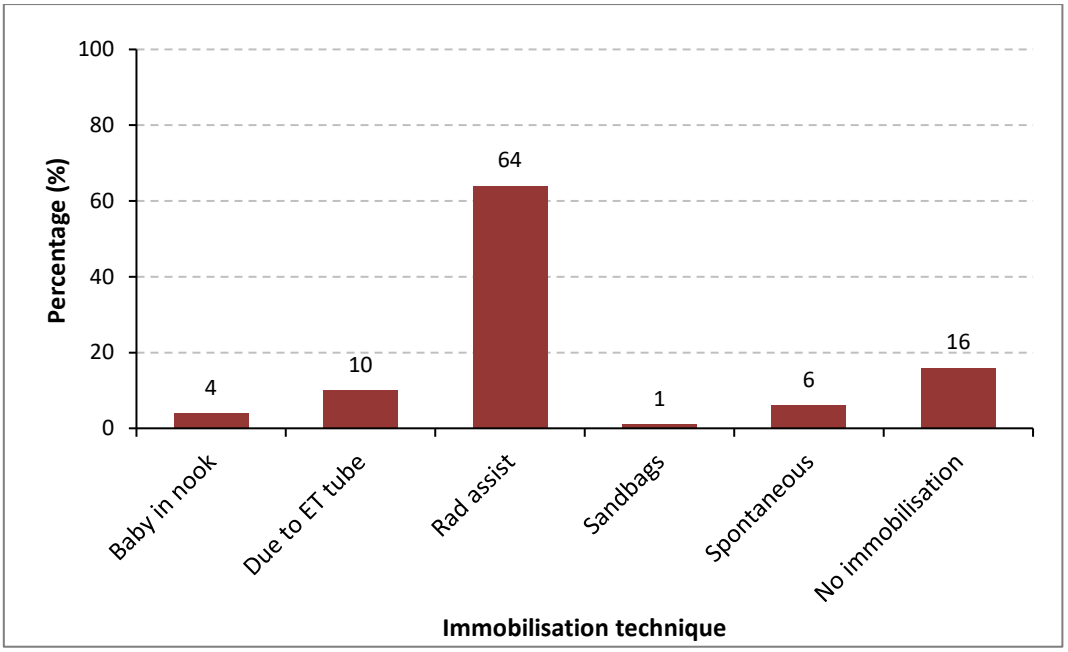

CXR, chest X-ray; Combo, combined chest and abdominal X-ray.

**Figure 4.4.** Head and chin position (phase 2 – CXR [n=109] and Combo [n=33]).

Figure 4.5 shows the head and chin position during the combined images for phase 2. For the CXR, the most common technique used to immobilise the head was the radiographer assisting (64%) (indicated as "rad assist"). SAHPRA stated that no person shall hold a patient or detector during image acquisition unless is it impossible to obtain a diagnostically useful image. They also stated that a family member accompanying the patient should hold them instead of a radiation worker (SAHPRA, 2022: 17). As seen above, the radiographers mainly held the patients instead of applying other immobilisation techniques.



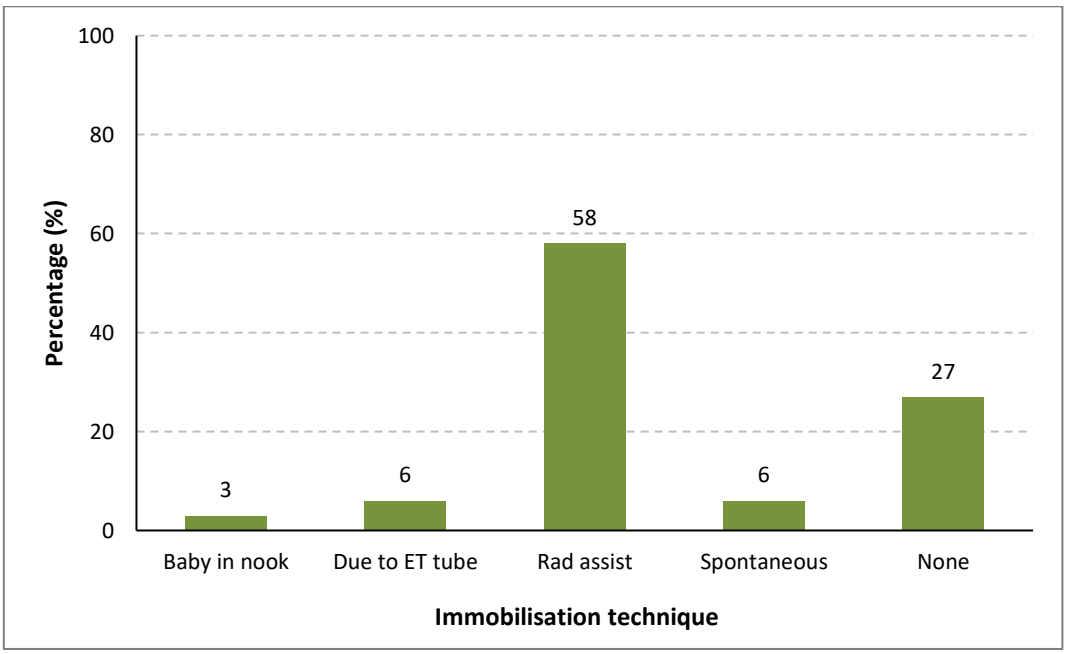
© Central University of Technology, Free State




ET, endotracheal tube; Rad, radiographer.

**Figure 4.5.** Head position immobilisation techniques (phase 2 – CXR; n=109).

For the head immobilisation techniques for the combined images, the results are presented in Figure 4.6 below. The most common immobilisation technique to keep the head facing up was the radiographer assisting (58%).



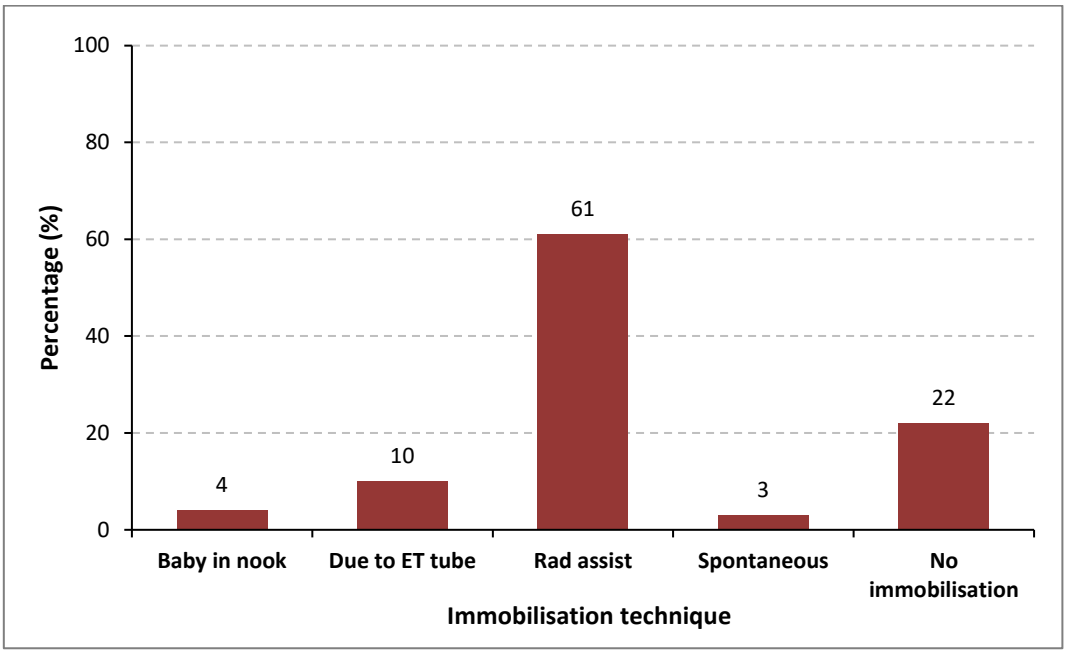

ET, endotracheal tube; Rad, radiographer.

**Figure 4.6.** Head position immobilisation techniques (phase 2 – Combo; n=33).



© Central University of Technology, Free State

The infants' chins were lifted by several immobilisation techniques such as immobilisation by intubation or even a spontaneous position of the head. Other immobilisation techniques included radiographers holding the patient, as shown in Figure 4.7, or the neonate lying in a nook or sleeping nest allowing them to keep their chin lifted. As seen in Figure 4.7, no immobilisation techniques were applied by the radiographers in 22% of the cases. By implication, in these cases the neonate's chin was not lifted for image acquisition. The most common immobilisation technique applied to keep the chin lifted was with radiographer assistance (61%).



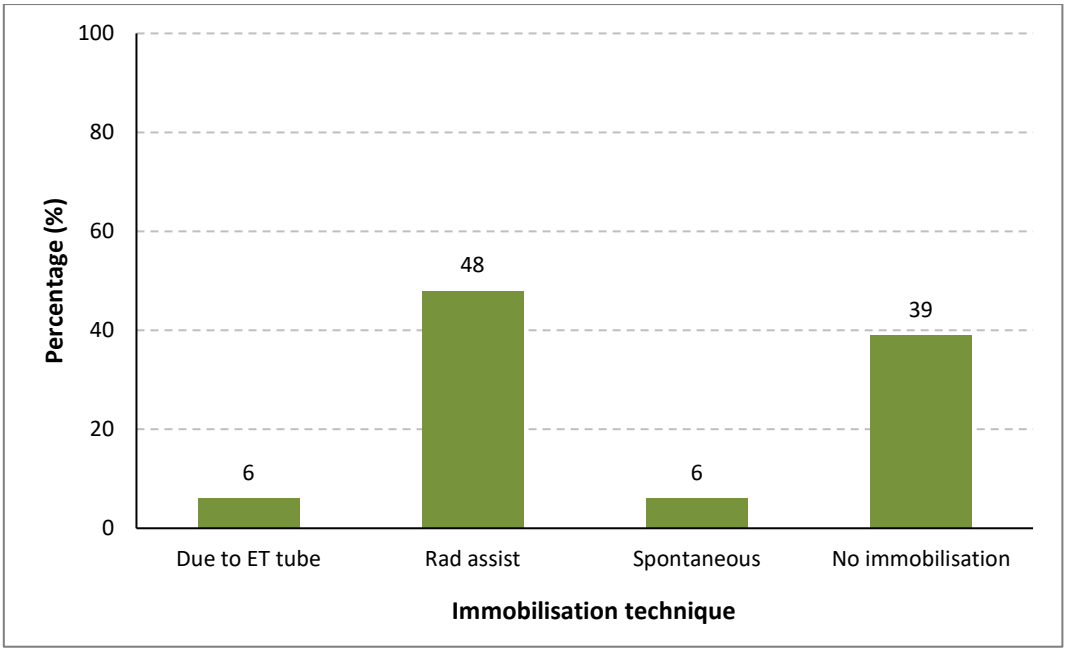

ET, endotracheal tube; Rad, radiographer.

**Figure 4.7.** Chin lifted immobilisation techniques (phase 2 – CXR; n=109).

Figure 4.8 below displays the immobilisation techniques to keep the chin lifted during radiographic X-ray acquisition for the combined images. The most common immobilisation technique applied was the radiographer assisting at 48% (n=16), while no immobilisation techniques were applied for 39% (n=13) of the neonates. No immobilisation implies that the chin had not been lifted during radiographic X-ray acquisition.



© Central University of Technology, Free State



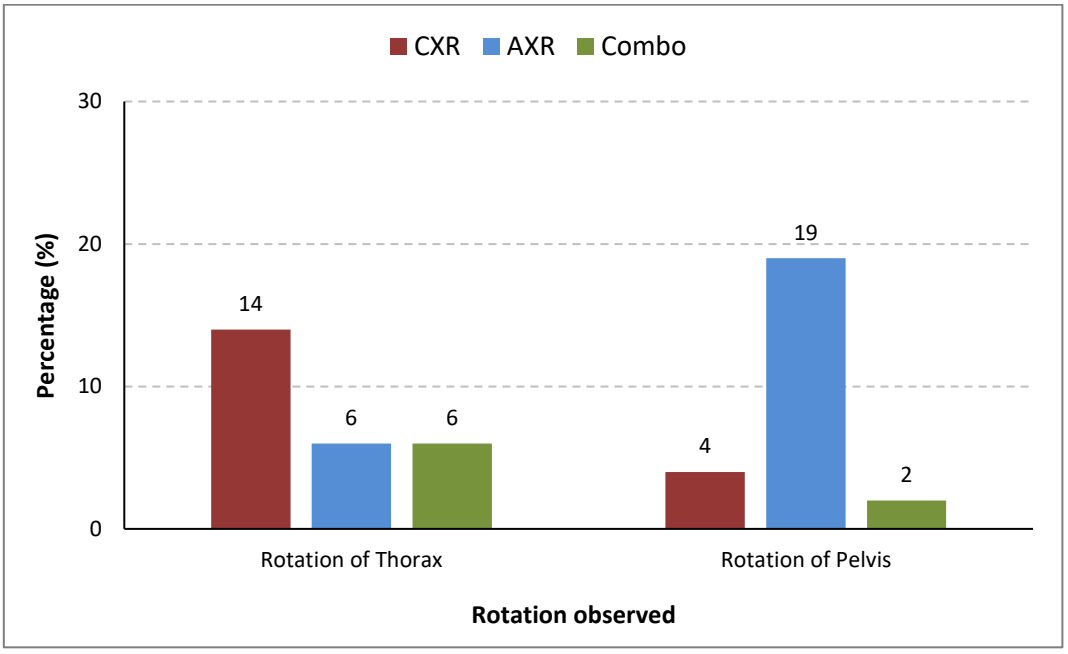

ET, endotracheal tube; Rad, radiographer.

**Figure 4.8.** Chin lifted immobilisation techniques (phase 2 – Combo; n=33).

Figure 4.9 shows the rotation of the thorax and pelvis for each examination type for phase 2 (observational phase). Rotation of the thorax was most common during CXR acquisition (14%) and rotation of the pelvis was more common during AXR (19%). This was only recorded by the researcher as there was no interaction between the researcher and the participating radiographer during the observation to ensure the accuracy of the results.



© Central University of Technology, Free State




CXR, chest X-ray, AXR, abdominal X-ray, Combo, combined chest and abdominal X-ray.

**Figure 4.9.** Rotation of the thorax and pelvis during imaging (phase 2; CXR n=109, AXR n=16, Combo n=33).

In Table 3.6 (Chapter 3), criterion 2 was based on the technical factors observed by the researcher. Results related to these factors are presented below pertaining to the lead marker, detector, collimation, artefacts, centring, distances of the tube, main beam direction, shielding and the specification of the equipment.

Titley and Cosson (2014: 43) indicated the importance of placing an anatomical lead marker in the primary radiation field as a medico-legal requirement. The HPCSA (2020: 5) stipulated that it is part of a radiographer's scope of practice to ensure that the radiographic images meet all medico-legal requirements, along with ensuring an image of optimal, diagnostic quality. Figure 4.10 below shows the technical factors observed for all examination types combined. In only 65% of the cases, a physical lead marker was included and it was placed on the patient (86%) in most of the examinations. Artefacts (sandbags, teddy bears, electrocardiogram monitor, or pacifier) visible were removed by the radiographers 96% of the time before exposure to prevent obscuring any relevant anatomy.



© Central University of Technology, Free State

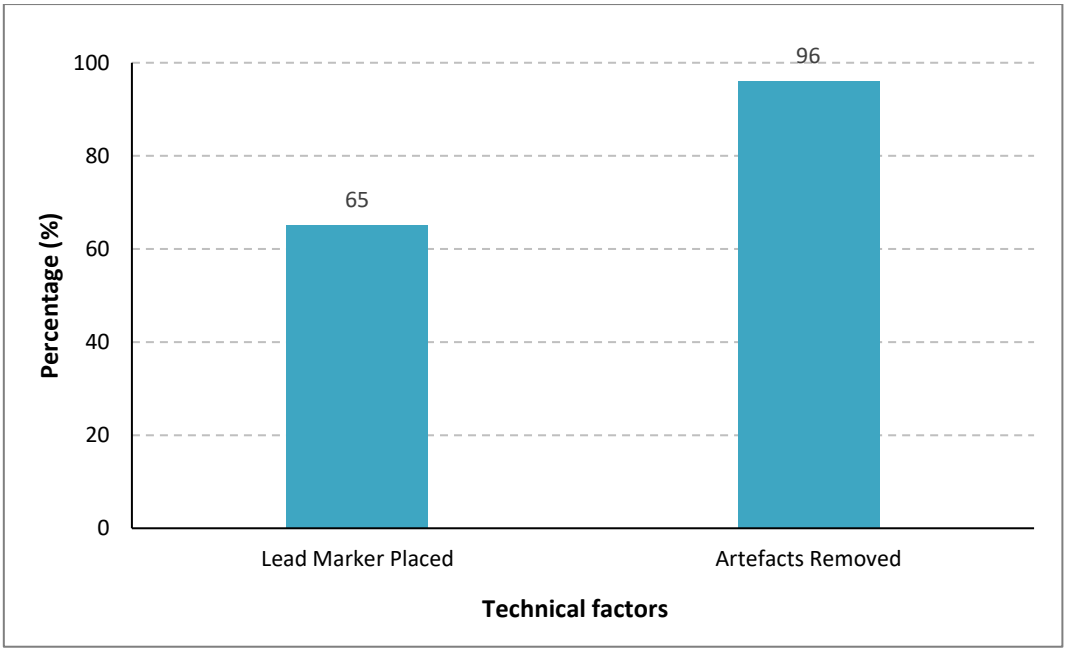
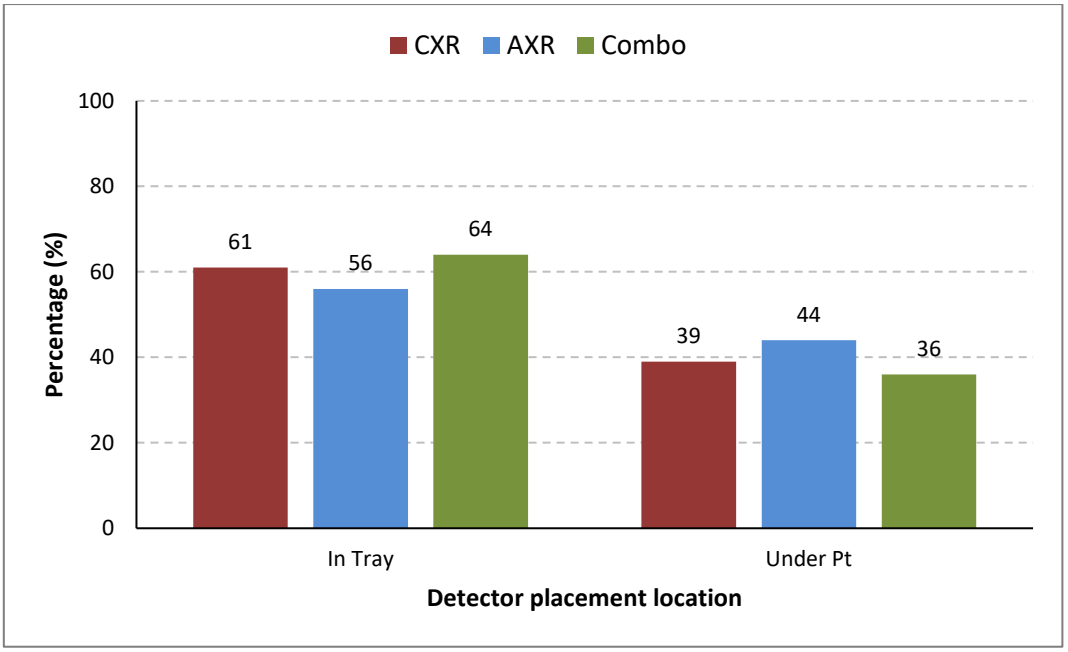



**Figure 4.10.** Technical factors observed (phase 2; n=158).

For CXR, the detector was placed inside the tray in 61% of the cases, and directly under the patient in 39% of the cases observed. For AXR, the most common placement was in the tray (56%), and for the CXR-AXR, the radiographers preferred placing the detector in the tray (64%). These observations are presented in Figure 4.11. Tugwell-Allsup *et al*. (2020: 263) found that placing the detector directly underneath the neonate favours higher image quality with a lower radiation dose. As seen, the radiographers preferred placing the detector directly under the neonate in 39% of the CXRs. The radiographers primarily preferred placing the detector in the tray in 61% (CXR), 56% (AXR) and 64% (CXR-AXR) of the cases. This method was suggested by del Vecchio *et al.* (2015: 164) to prevent cross-contamination between these vulnerable patients.



© Central University of Technology, Free State




CXR, chest X-ray, AXR, abdominal X-ray, Combo, combined chest and abdominal X-ray; Pt, patient.

**Figure 4.11.** Detector placement (phase 2; CXR n=109, AXR n=16, Combo n=33).

Table 4.1 shows the SID measurements set for each examination type during phase 2. Each colour represents an examination type. As presented in the table, the most common SID for each examination type was 100 cm (CXR = 66%; AXR = 63%; Combo = 70%). The shortest SID measurement during phase 2 was 80 cm, although it was not commonly set (CXR = 11%; AXR = 13%; Combo = 12%). Tugwell-Allsup and England (2020: 22) stated that the maximum achievable SID would ensure a lower radiation dose and would also reduce the magnification. The results of the implementation show that the radiographers mostly complied with the proposed imaging protocol in making use of a large SID.



© Central University of Technology, Free State

**Table 4.1.** Source-to-image distance (SID) (phase 2; CXR n=109, AXR n=16, Combo n=33).

| Exam Type | SID | Frequency (f) | Percentage (%) |
|---|---|---|---|
| CXR | 80 cm | 12 | 11% |
| CXR | 87 cm | 0 | 0% |
| CXR | 90 cm | 25 | 23% |
| CXR | 100 cm | 72 | 66% |
| AXR | 80 cm | 2 | 13% |
| AXR | 87 cm | 0 | 0% |
| AXR | 90 cm | 4 | 25% |
| AXR | 100 cm | 10 | 63% |
| Combo | 80 cm | 4 | 12% |
| Combo | 87 cm | 1 | 3% |
| Combo | 90 cm | 5 | 15% |
| Combo | 100 cm | 23 | 70% |

AXR, abdominal X-ray; CXR, chest X-ray; Combo, combined chest and abdominal X-ray.

The most frequently used centring point for mobile CXR was the nipple line, which was used in 46% of cases. Figure 4.12 summarises the centring points used by the radiographers for CXR during phase 2.

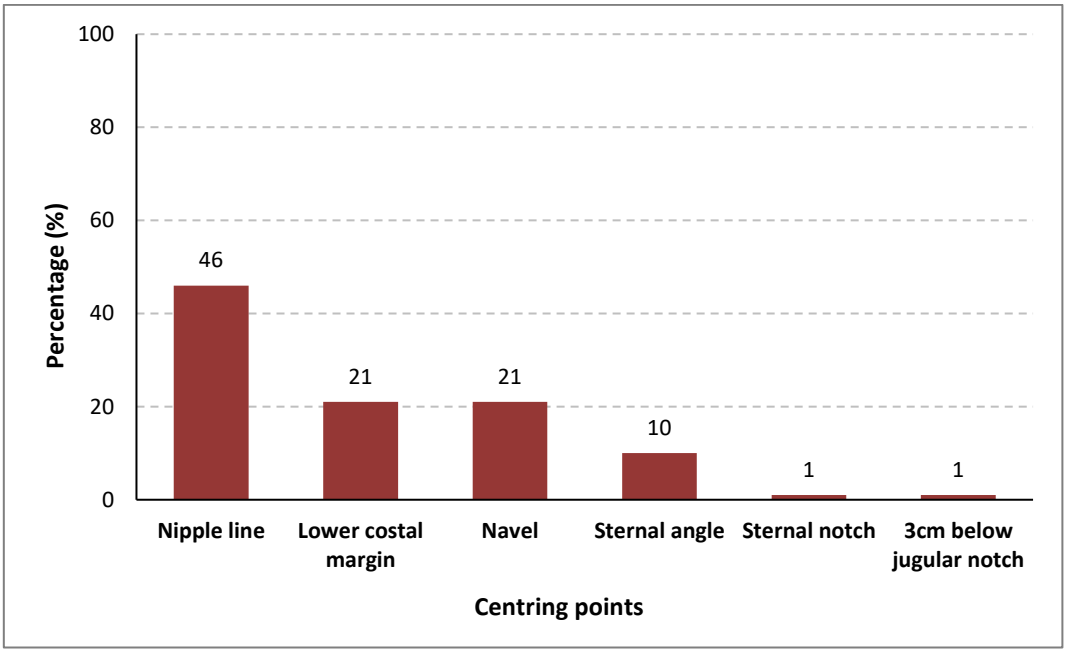



**Figure 4.12.** Centring points (phase 2 – CXR; n=109).



© Central University of Technology, Free State

Figure 4.13 shows the results for the centring points set for abdominal X-rays during phase 2. The most common centring point used for AXR was the navel (63%), while the second most common centring point was the lower costal margin (25%).

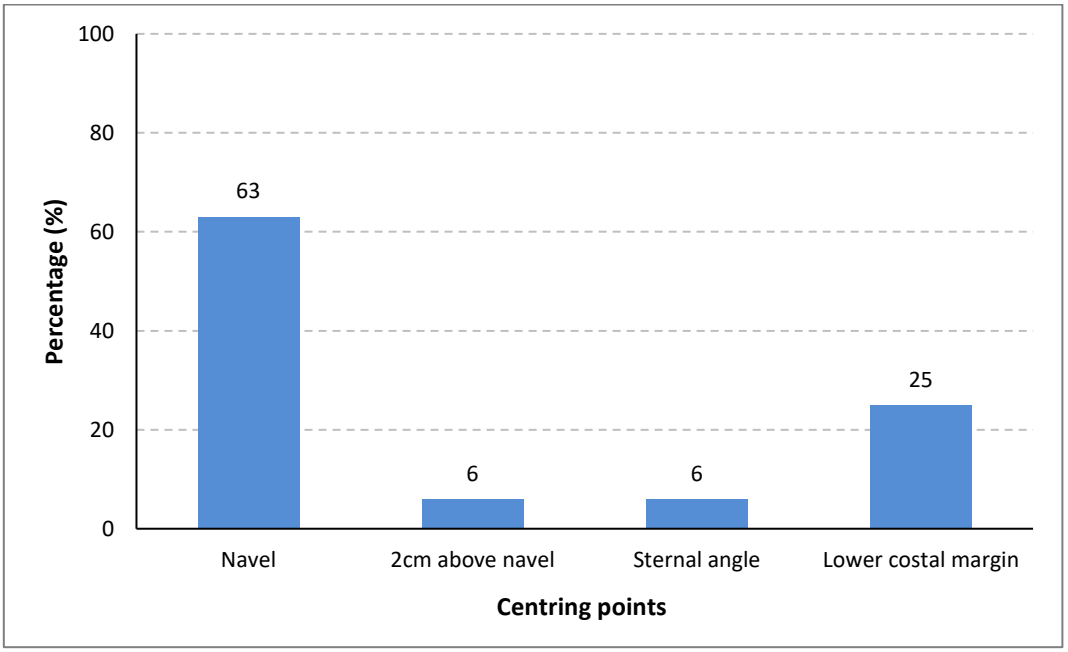



**Figure 4.13.** Centring points (phase 2 – AXR; n=16).

Figure 4.14 shows the centring points used for the CXR-AXR during phase 2. The most common centring point used by the radiographers was the navel (64%).

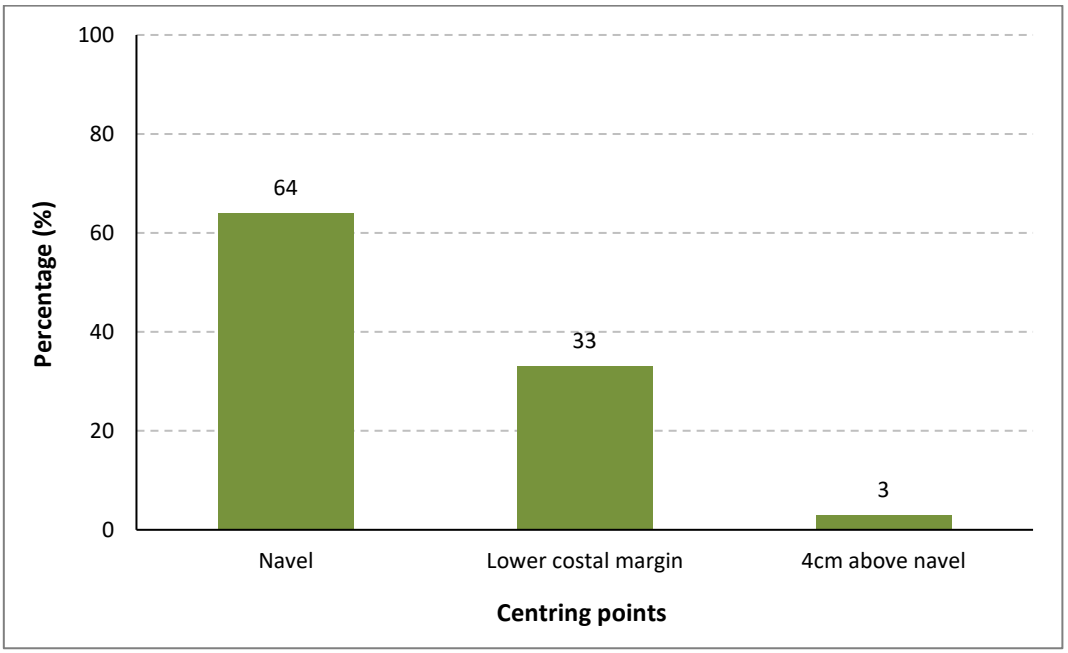
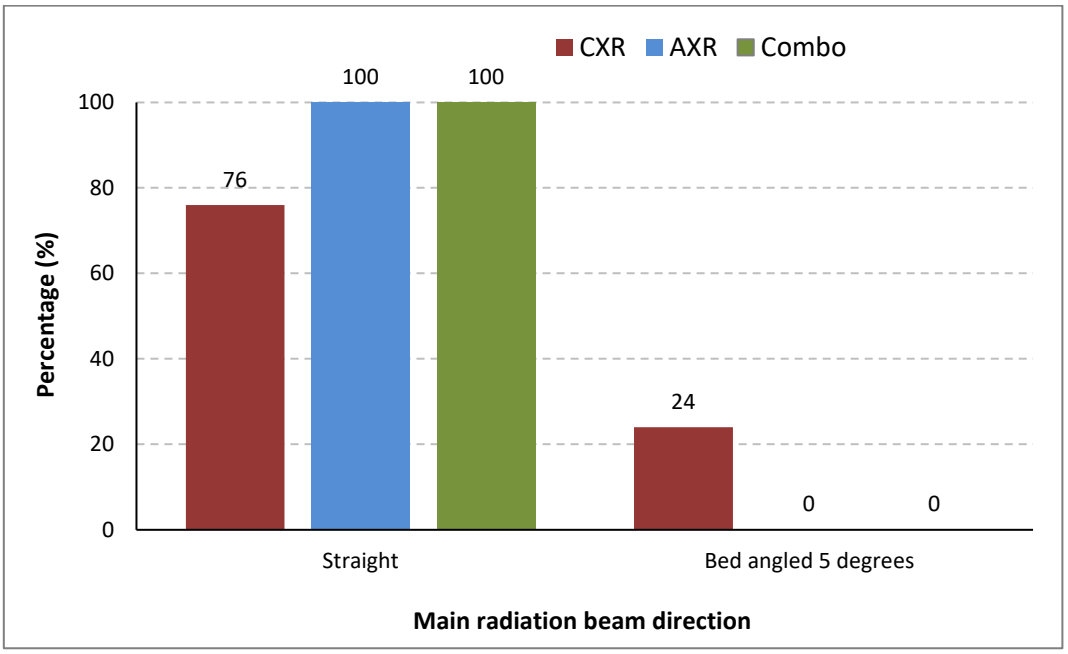



**Figure 4.14.** Centring points (phase 2 – Combo; n=33).



© Central University of Technology, Free State

Angulation of the main beam or tilting of the bed was observed, and the findings are presented in Figure 4.15. Only 24% of the radiographers angled the bed or the main radiation beam for CXR, while 74% preferred a straight beam. For both AXR and the combined CXR-AXR, the radiographers preferred a straight main radiation beam. A straight main radiation beam has been proposed by McQuillen Martensen (2015: 118) and Long *et al.* (2019: 30) and as seen by the results of the implementation phase (phase 4), the radiographers complied with the proposed imaging protocol and applied a straight beam.




CXR, chest X-ray, AXR, abdominal X-ray, Combo, combined chest and abdominal X-ray; Pt, patient.

**Figure 4.15.** Angulation of the main radiation beam (phase 2; CXR n=109, AXR n=16, Combo n=33).

The researcher observed the usage of gonadal shielding for neonates. SAHPRA (2022: 5) states that gonadal shielding should only be placed when it is not interfering with the diagnostic process. The results are shown in Figure 4.16. In 99% of the mobile examinations, the radiographers did not make use of any shielding. Only once a radiographer applied a thyroid shield for gonadal protection, as shown in Figure 4.16. The lead equivalence (Pb Eq) of the thyroid shield placed over the gonads during the observational phase was 0.5 Pb Eq.



© Central University of Technology, Free State

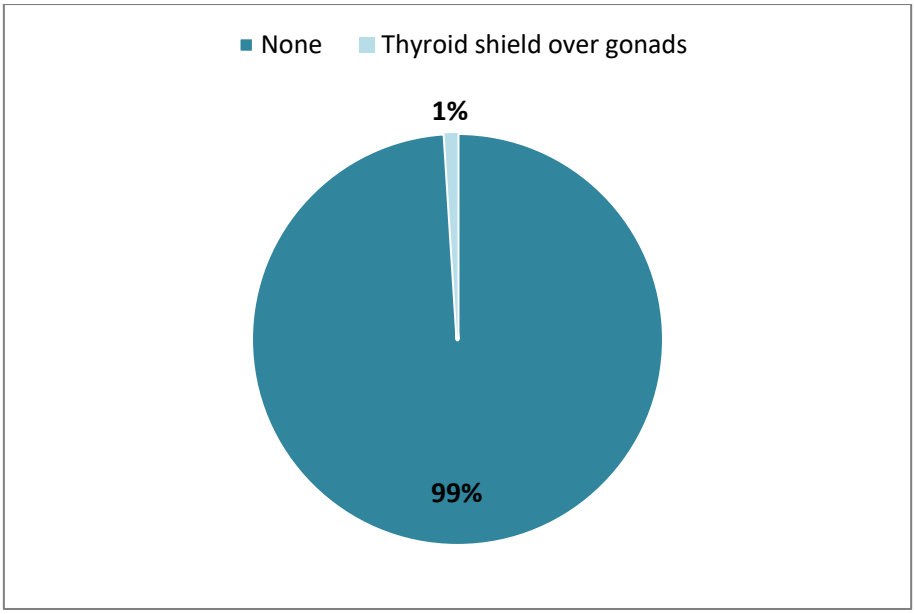



**Figure 4.16.** Physical lead protection used during mobile examinations (phase 2; n=158).

In Table 4.2, the rest of the observational checklist is presented and refers to the radiographic equipment used. In the department where the study was conducted, they have two mobile machines of the same brand with the same specifications, generator and filtration. It was included in the checklist to indicate that the radiographic equipment plays an important role in dose production and dose measurement. The incubator brand is also included in this part of the checklist to indicate the difference between incubators, because an open incubator might allow a different absorbed dose than a closed incubator, based on the researcher's experience.

**Table 4.2.** Observational checklist for machine specifications.

| **Variable** | **Specifications** | |
|---|---|---|
| Detector | CR | DR |
| Detector speed (focus) | | |
| X-ray mobile machine make | Siemens Mobilett 1 | Siemens Mobilett 2 |
| Generator | 3 phase | 3 phase |
| Filtration | Al | Cu |
| Incubator brand | Fischer & Paykel | |
| Mattress thickness (when applicable) | | |

Al, aluminium; CR, computed radiography; Cu, copper; DR, digital radiography.

The mobile unit used by the department was a Siemens Mobilex, which has aluminium (Al) filtration. The imaging department has two mobile machines of the same brand and model;



© Central University of Technology, Free State

thus, it has been indicated on the checklist as machine 1 and machine 2. The open incubator in the NICU was a Fischer & Paykel CosyCot™ each with a similar mattress. The NICU visited during this study used mainly open incubators, but they also have closed incubators to use when necessary. No closed incubators were used as part of the research study, as indicated in the exclusion criteria (cf. section 3.3.1.). Neonates are kept in a closed incubator to control the environmental heat they are placed in to ensure survival and growth for stable physiological functions (Décima, Stéphan-Blanchard, Pelletier, Ghyselen, Delanaud, Degrugilliers, Telliez, Bach & Libert, 2012: 2957).

**Criterion 3** was based on the exposure factors used during image acquisition of the observational phase. Table 4.3 shows that these factors observed included kVp, mAs and exposure index.

**Table 4.3.** Exposure factors observed during phase 2.

| **CRITERION 3: EXPOSURE FACTORS** | | |
|---|---|---|
| kVp value | | |
| mAs value | | |
| Exposure index | | |

kVp, kilovoltage peak; mAs, milliampere second.

According to the Shapiro-Wilk test, the distributions of all three exposure factors were skewed ($p<0.05$). Specifically, the distribution of kVp values ($W=0.877$, $p<0.0001$), mAs values ($W=0.779$, $p<0.0001$) and the exposure index ($W=0.955$, $p<0.0001$) did not follow a normal distribution, necessitating the use of medians and interquartile ranger (IQR).

The findings regarding kVp and mAs values are presented in Figures 4.17 and 4.18, respectively. The kVp IQR was 55 kVp to 58 kVp (Figure 4.17). This graph indicates the minimum kVp (48 kVp) and maximum kVp (65 kVp) values selected. The median for kVp was 55 kVp, which was also the value of the first quartile. Several authors suggested the use of a high kVp value with a lower mAs settings (del Vecchio *et al.,* 2015: 163; Gunn *et al.,* 2019: e5; Jain *et al.,* 2021: 483; McQuillen Martensen, 2015: 78; Tugwell-Allsup *et al.,* 2020: 261). The proposed imaging protocol suggested a kVp setting 57–60 kVp for CXR and 54 kVp for AXR and CXR-AXR. According to Figure 4.17, the radiographers implemented a kVp selection of 55–58 kVp, showing they complied with the standardised protocol.



© Central University of Technology, Free State

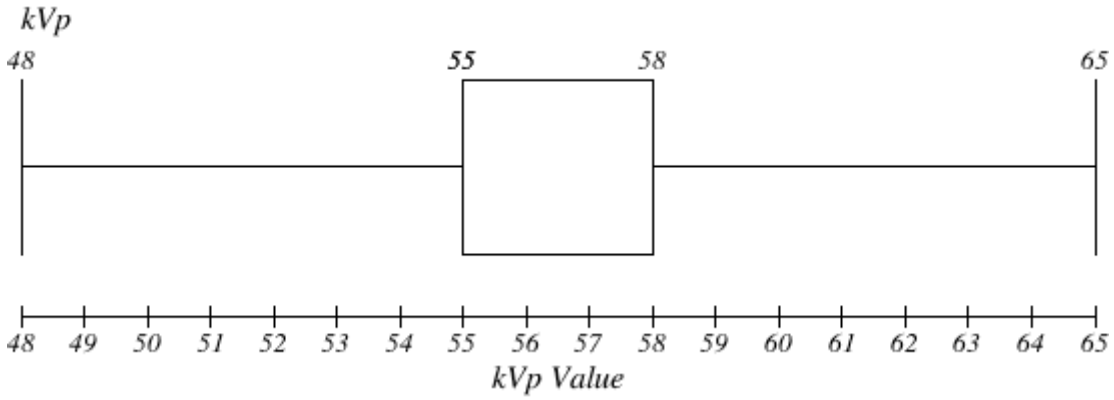



**Figure 4.17.** Box plot of kilovoltage peak (kVp) values (phase 2).

The mAs IQR was 1.80 mAs to 2.20 mAs, as shown in Figure 4.18. The minimum and maximum mAs values were 1.80 mAs and 3.20 mAs, respectively, with the median set on 2 mAs. Most authors suggested a lower mAs setting to reduce patient radiation dose (del Vecchio *et al.,* 2015: 163; Gunn *et al.,* 2019: e5; Jain *et al.,* 2021: 483; McQuillen Martensen, 2015: 78; Tugwell-Allsup *et al.,* 2020: 261). The standardised protocol also suggested a lower mAs setting of 0.8 mAs for CXR and 1.80 mAs for both AXR and CXR-AXR as suggested by the literature. As seen in Figure 4.18 below, the radiographers applied higher mAs values than proposed by the protocol during phase 2 (observational phase) with an average mAs setting of 2 mAs.

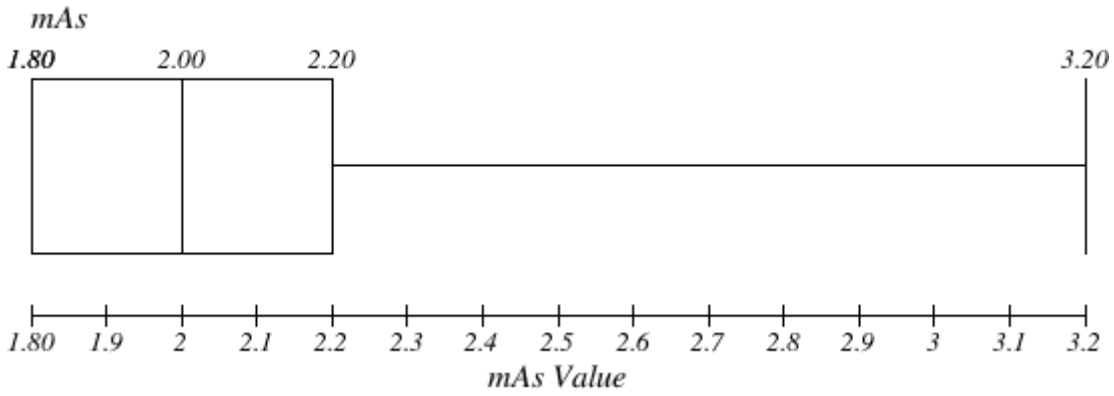



**Figure 4.18.** Box plot of milliampere second (mAs) values (phase 2).

The IQR of the exposure index ranged from 194 to 377, which is shown in Figure 4.19. The lowest exposure index (EI) of the images was 78 and the highest was 724. The optimal range for EI for CXR is 50–200. The median EI was 278.



© Central University of Technology, Free State

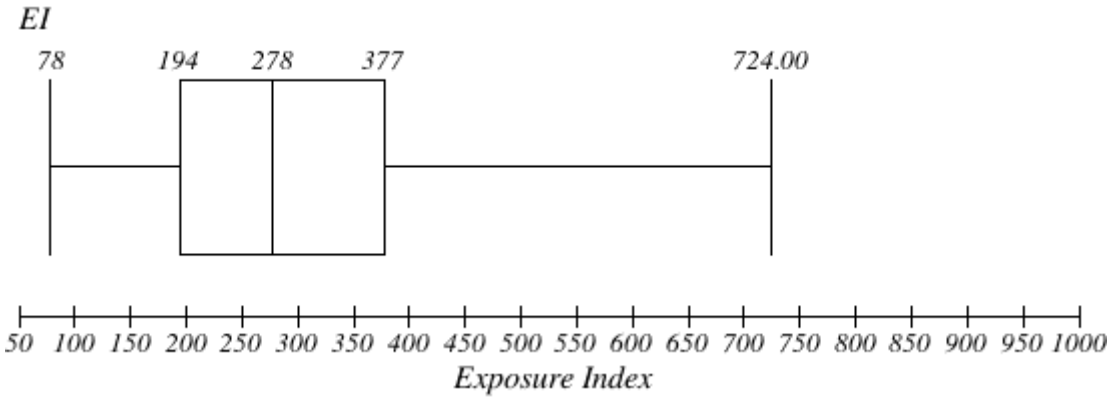



**Figure 4.19.** Box plot of exposure index (EI) (phase 2).

**Criterion 4** of the observational checklist was based on the infection control measures applied by the radiographers entering and working inside the NICU. In Table 4.4, an example of the infection control section of the observational checklist is presented.

**Table 4.4.** Infection control section of the observational checklist.

| **CRITERION 4: INFECTION CONTROL** |
|---|
| What infection control measures were followed? Elaborate below: |
| Example given: *detector was sanitised pre and post X-ray acquisition. Lead marker was sanitised and was not placed on the neonate.* |

Table 4.5 summarises the distribution frequencies and percentages of the type of infection control measures applied by radiographers before and after interaction with the neonates. As seen in Table 4.5, for 36% of the imaging procedures (n=158), the radiographers applied no infection control measures before or after interaction with the neonates. In 22% of the procedures, the radiographers washed their hands only before performing the imaging, while in 18% of cases, they washed their hands before and after interaction with the neonates. Finally, for 13% of the procedures, the radiographers only sanitised their hands instead of applying the recommended complete hand-wash technique.

According to Schlaeppi, Minotti and Bielicki (2024: 175), premature infants and critically ill neonatal patients are at greater risk for nosocomial infections. The authors also stated that sepsis is a leading cause of neonatal mortality worldwide. Some of the factors related to nosocomial infections in NICUs include prolonged hospital stay, too many persons providing care to the patient and failure to apply aseptic techniques (Pathak, Kharol, Kharol & Chaturvedi, 2022: 1042). As seen in Table 4.5 below, the radiographers did apply infection



© Central University of Technology, Free State

prevention measures but the table shows very low frequencies, which could be greatly improved.

**Table 4.5.** Infection control measures followed by radiographers (n=158 procedures).

| Infection control measures applied | Frequency (f) | Percentage (%) |
|---|---|---|
| None | 57 | 36 |
| Hands washed before | 35 | 22 |
| Hands washed before and after | 29 | 18 |
| Hands sanitised | 21 | 13 |
| Hands washed after | 13 | 8 |
| Detector sanitised, hands washed before and after | 2 | 1 |
| Hands sanitised after | 1 | 1 |

**Part 2** of the observational checklist was aimed at the nursing staff and is presented in Table 4.6, which includes all the factors the researcher observed during the routine X-rays in the NICU, specifically what the nurses allowed and what not. The statistical results are also presented for clarity on what the nursing professionals allowed when working with neonatal patients. Eight nurses were participated/included in the observation phase. In 91% of the 158 imaging procedures, the radiographer warned the nursing staff in the immediate vicinity of radiographic X-ray exposure, while in 9% of procedures, the beam was activated without warning. The findings in Table 4.6 indicate that in only 5% of procedures, lead protection was provided to the nursing staff near the patient.

According to Table 4.6, radiographers asked the nurse if physical lead protection could be placed directly on the patient in 107 (68%) of the imaging procedures. However, as shown in Figure 4.16, only one radiographer actually placed lead protection during one radiographic X-ray acquisition during phase 2. There were several reasons for the lack of lead protection including the nurse's refusing placement, isolation patients limiting direct contact and radiographers choosing not to make use of lead protection.

The preferred detector placement is also shown in Table 4.6. The radiographers asked the nursing staff prior to placement what the preferred location was, and in only 1% of procedures, it was indicated by the nurse that the detector should not be placed directly underneath the patient, while there were no objections to placing the detector in the tray or underneath the mattress. Overall, the nurses did not seem to have specific preferences for detector placements.



© Central University of Technology, Free State

In only 5% of the 158 procedures, the nurse was presented with lead protection, although in 91% of cases, the radiographers warned of radiographic X-ray exposure prior to beam activation. In this NICU, the nursing staff preferred to keep their distance rather than wearing lead protection, explaining the use of shielding for only 5% of the procedures.

**Table 4.6.** Part 2 of the observational checklist based on the nursing staff (n=158 procedures).

| **Is it preferred that the radiographer:** | **YES** | |
|---|---|---|
| | **Frequency** | **Percentage** |
| Touch the neonate | 158 | 100% |
| Asked nurse permission to place Pb protection | 107 | 68% |
| Abduct the arms of the neonate | 158 | 100% |
| Turn the head of the neonate | 139 | 88% |
| Lift the chin of the neonate | 141 | 89% |
| Move medical lines out of the FOV | 100 | 63% |
| Place the detector directly under the patient | 157 | 99% |
| Place the detector under the mattress | 158 | 100% |
| Place the detector in the detector tray | 158 | 100% |
| Warned before exposure (exit room) | 143 | 91% |
| Provided nurse shielding (in room) | 8 | 5% |

FOV, field of view; Pb, lead.

In Table 4.7 it is shown that in only 9% of the procedures, the radiographers asked for assistance from the nurses when handling the neonates. For only 15% of the procedures, the patient's identity (Pt ID) was confirmed (either Pt ID confirmation only, or confirmation of both X-rays and Pt ID) but in only 26%, it was confirmed that X-rays were requested (confirm X-rays + confirming both X-rays and pt ID).

During 30% of the routine mobile examinations, radiographers enquired whether the patient room they were entering was an isolation area or not. Isolation measures are recommended and commonly applied to prevent cross-infection in the NICU (Hanna, Shah, Marquez, Barzegar, Gordon & Pammi, 2023: 1).



© Central University of Technology, Free State

**Table 4.7.** Radiographer and nurse interaction (n=158 procedures).

| Radiographer and nurse interaction | Frequency (f) | Percentage (%) |
|---|---|---|
| None | 87 | 55 |
| Confirm X-rays only | 29 | 18 |
| Ask for assistance | 14 | 9 |
| Confirm both X-rays and Pt ID | 12 | 8 |
| Confirm Pt ID only | 11 | 7 |
| Ask if isolation is applicable | 4 | 3 |
| Request reason for X-rays | 1 | 1 |

Pt ID, patient's identity.

**Part 3** of the observational checklist was based on image evaluation after image acquisition, to determine optimal image quality regarding inclusion and visibility of anatomical structures. The European Commission (1996: 16) stated that proper knowledge of external anatomical (topographic) landmarks is crucial when applying collimation to any radiographic image. These landmarks may differ due to patient age and size depending on different body habitus. They also stated that a basic knowledge of pediatric pathology may enhance the application of collimation due to the size of the primary radiation field being dependent on a specific pathological disorder (European Commission, 1996: 16). An example of part 3 of the checklist is presented in Table 4.8, as well as the results of the image evaluation. The results for both CXR and AXR are presented and in the instance of a combined image, the results are presented with either the chest or abdomen statistics.

For the chest X-rays, all anatomical structures were visible (100%), but a lack of compliance regarding the inclusion of anatomical structures was observed. The anatomical inclusion criteria for chest and abdominal X-rays are discussed in depth in sections 2.7.2 and 2.8.2, respectively. C7 was included superiorly in all the images (100%), while the costophrenic angles were cut off in 1% of the chest images. Laterally, the required features were included in all the images (100%).

Inclusion to only up to the level of the gastric bubble occurred in 16% of the X-rays (both CXR, AXR and CXR-AXR combination), while 49% included a larger area than stipulated, namely the upper third of the abdomen. The abdomen up to the level of the iliac crest was included in 12% of the radiographic images, and 1% included the symphysis pubis for CXR acquisition as the centring point was set on the iliac crests. For abdominal X-rays, all the requirements for criteria 3 and 4 were met, as all relevant anatomical structures were included (100%) and visible (100%).



© Central University of Technology, Free State

**Table 4.8.** Part 3, criteria 1 to 4 of the observational checklist.

| PART 3: IMAGE EVALUATION | | |
|---|---|---|
| | **YES** | **NO** |
| **CHEST X-RAYS** | | |
| **CRITERION 1: ANATOMICAL STRUCTURES INCLUDED** | | |
| C7 superiorly | 100% | 0% |
| Bilateral costophrenic angles | 99% | 1% |
| Soft tissue laterally | 100% | 0% |
| ⅓ of the upper abdomen | 49% | 51% |
| Only up to the level of gastric bubble | 16% | 84% |
| Mid-abdomen to IC | 12% | 88% |
| Entire abdomen including SP | 24% | 76% |
| **CRITERION 2: ANATOMICAL STRUCTURES VISIBLE** | | |
| Air-filled trachea | 100% | |
| Carina | 100% | |
| Lung markings | 100% | |
| Hilar regions | 100% | |
| Sharp heart border | 100% | |
| Sharp costophrenic angles | 100% | |
| Stomach bubble | 100% | |
| **ABDOMINAL X-RAYS** | | |
| **CRITERION 3: ANATOMICAL STRUCTURES INCLUDED** | | |
| Costophrenic angled superiorly | 100% | |
| Symphysis pubis inferiorly | 100% | |
| Soft tissue laterally | 100% | |
| **CRITERION 4: ANATOMICAL STRUCTURES VISIBLE** | | |
| Stomach bubble | 100% | |
| Gas-bowel pattern | 100% | |

C7, 7$^{th}$ cervical vertebra; IC, iliac crest; SP, symphysis pubis.

Table 4.9 is an example of **part 4** of the observational checklist that was completed by the researcher after image acquisition. This part of the checklist was based on the post-processing actions applied to the image by the radiographer, to ensure proper diagnostic quality of the image along with lead marker placement.

As noted in Table 4.9, 41% of the images were collimated too big, while 2% of the images had important anatomical cut-off because of collimation being too small. Overexposure occurred in 9% of the images, while the underexposed images, meaning the image was too white with excessive noise (quantum mottle), constituted 8% of all the images. Overexposure and



© Central University of Technology, Free State

underexposure were identified by the EI values of each image. If the EI value was either above or below the recommended range, the image was considered overexposed or underexposed, respectively. In total, 14% of the images required repetition due to rotation of the neonate, while 34% of the images required an electronic marker placement due to a lack of placement of a physical lead marker, or the marker was placed outside the X-ray field.

**Table 4.9.** Part 4 of the observational checklist (n=158).

| PART 4: POST-PROCESSING REQUIRED | |
|---|---|
| Collimation too big | 41% |
| Collimation too small (cut-off) | 2% |
| Overexposed (image too dark) | 9% |
| Underexposed (image to white) | 8% |
| Image required repetition due to small rotation (malalignment) | 14% |
| Electronic marker placement | 34% |

After the conclusion of phase 2, the data were used in addition to the literature-based imaging protocols established during phase 1 (cf. Chapter 2, section 2.10) to compile the experimental protocols to be tested on the phantom. Phase 2 (observational phase) was an extended phase conducted over 12 weeks. The observational phase contributed significantly towards the outcome of the study. During this observational phase, it was interesting to study the execution of procedures and choices made by each radiographer. Furthermore, it was quite inspiring and even educational to see their preferences and thought patterns. The thought patterns are related to the application of theoretical criteria and the problem-solving skills of each radiographer. Phases 1 and 2 contributed toward the subsequent experimental phase where the baseline imaging protocols were tested on a phantom to scientifically ensure optimal image quality and assist with dose measurement.

Due to different training backgrounds and experience levels, the technical factors applied by each radiographer were diverse. Each radiographer applied different exposure factors, SID, centring points and collimation. These variations identified the need for a standardised imaging protocol to ensure uniform imaging techniques and consistent image quality. The differences observed finally resulted in the compilation of 68 CXR, 45 AXR and 45 CXR-AXR imaging protocols that were tested during the experimental phase 3 of the study.

When these combinations of technical factors recorded an EI in the 50–200 range for CXR and 125–500 for AXR and combined CXR-AXR, the particular protocols were simulated and tested on the neonatal phantom in the experimental phase (phase 3).



© Central University of Technology, Free State

## 4.4 PHASE 3: EXPERIMENT

The neonatal phantom was exposed for each protocol setup. The average dose to the phantom was calculated to record the dose per protocol. The average dose value (shown as ESD) and image quality values (shown as EI and DI values, respectively) were compared for different average protocol parameters/factors such as SSD, OID, kVp, mAs, SID and angulation of the radiation beam. These data comparisons were used to establish the final optimised protocol for the imaging of neonatal patients in the NICU.

From phase 1 and 2 data, 68 mobile CXR experimental protocol combinations were compiled and tested on the phantom, while 45 AXR examinations were performed, and 45 combined CXR-AXR protocols (cf. Chapter 3, section 3.4.2.2) were tested. Strict inclusion and exclusion criteria were applied for the imaging protocols during the experimental phase, as explained in section 3.3.1. During each protocol experiment test, only one variable was involved to determine the true impact of the change applied. This means that for each protocol, one of the factors was changed each time, while the remaining factors remained constant. In total, 158 imaging protocols were tested, each repeated three times for every change in a specific variable, ultimately amounting to 474 exposures, (204 CXR, 135 AXR and 135 combined CXR-AXR images). During data analysis, 56 CXR, 43 AXR and 41 combined CXR-AXR imaging protocols were included because of a lack of adherence to specific requirements that are elucidated in the sections that follow.

### 4.4.1 Experimental chest X-ray results

The purpose of the exposure index (EI) is to provide the radiographer with feedback on detector exposure. The EI provides information regarding the adequacy of each exposure, as the EI is proportional to the signal-to-noise ratio squared, and it can be related to image quality. The EI has also been defined as *"a measure of a digital detector's response to radiation in the relevant image region of an image acquired using DR"* (Mothiram *et al.*, 2014: 113).

Sixty-eight imaging protocols for CXR were performed during the third phase of the study but after exclusion of protocols due to lack of specific requirements, 56 CXR protocols were included for statistical analysis. Twelve imaging protocols were excluded because these protocols did not include the costophrenic angles on the CXR, which is an important requirement for a CXR image (Bontrager & Lampignano, 2014: 631; Lampignano & Kendrick, 2021). The centring points for these excluded protocols were on either the sternal angle or



© Central University of Technology, Free State

nipple line, but interestingly the lower collimator was set on either the xiphoid process or below nipples which caused the exclusion of relevant anatomy.

The results discussed below are based on imaging protocol factors producing an optimal EI for CXR images. Optimal EI for the chest is in the range 50–200 for this specific mobile machine. The EI was recorded on the data sheet as presented on the mobile unit. This was repeated three times for three separate exposures made to ensure the accuracy of measurement. Eleven of the 56 (20%) imaging protocols produced an optimal EI as intended for the third objective (Figure 4.20). The specific factors of CXR acquisition that contributed to an optimal EI value are discussed next.

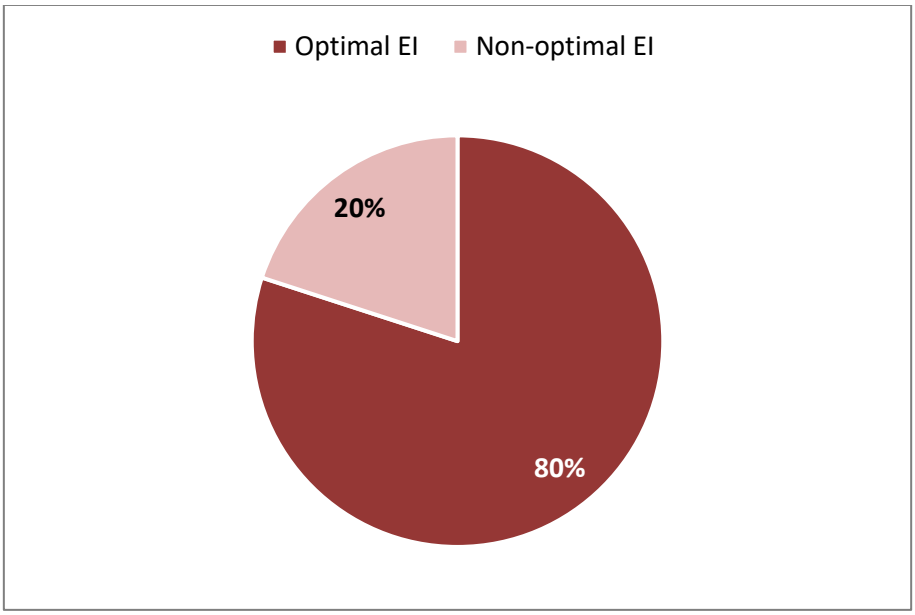



**Figure 4.20.** Imaging protocols producing optimal exposure index (EI) (phase 3 – CXR; n=56).

The source-to-subject distance (SSD) was measured from the tube to the specific centring point, which changed with each exposure as the centring point was also a variable tested. The SSD was measured with the measuring tape attached to the mobile unit tube. For the imaging protocol of the mobile CXR for neonatal patients, the optimal range for the SSD for optimal EI was proven by statistical analysis to be between 94 cm and 96 cm.

As seen in Figure 4.21, the dark red line indicates the optimal EI value relating to SSD. An elevation was observed at 86 cm to 87 cm and again from 94 cm to 96 cm. Those distances presented an optimal EI value; thus, the SSD should be kept as large as possible for optimal EI values during mobile CXR.



© Central University of Technology, Free State

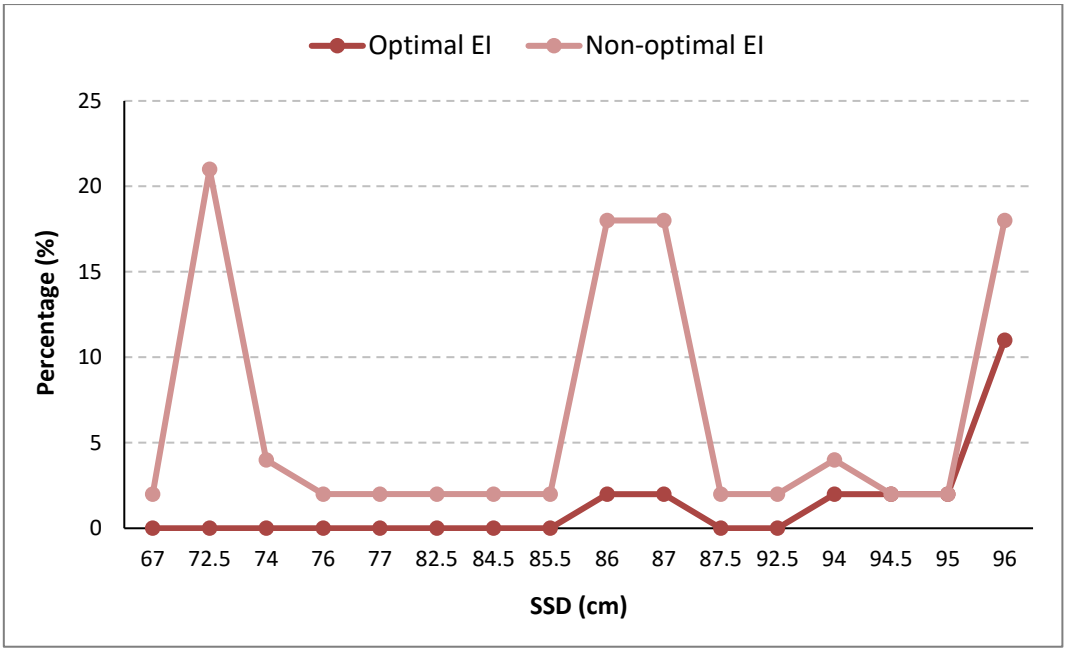



**Figure 4.21.** Source-to-subject distance (SSD) for optimal exposure index (EI) (phase 3 – CXR; n=56).

The object-to-image distance (OID) for optimal EI values is provided in Table 4.10. The three different OIDs are indicated in the table with their relevant percentages. A 0 cm OID refers to the radiographer placing the detector directly underneath the patient, providing the shortest distance. A 2 cm distance refers to the radiographer placing the detector underneath the mattress (as the mattress was measured at 2 cm thickness) and 9 cm was measured from the patient to the detector tray, creating the largest OID. The OID was proven optimal at the smallest possible distance, which during the experimental study was 0 cm.

**Table 4.10.** Object-to-image distance (OID) for optimal exposure index (EI) (phase 3 – CXR; n=56).

| | Optimal EI by OID (cm) for CXR | | |
|---|---|---|---|
| | **0 cm** | **2 cm** | **9 cm** |
| Non-optimal EI | 29% | 27% | 25% |
| Optimal EI | 16% | 2% | 2% |

Findings of the different kVp values applied to obtain optimal EI are provided in Figure 4.22. The dark red indicates the optimal EI relating to the kVp settings. These results showed that the 60 kVp setting was more suitable for optimal EI. The kVp was proven as optimal at a setting of 60 kVp or 57 kVp.



© Central University of Technology, Free State

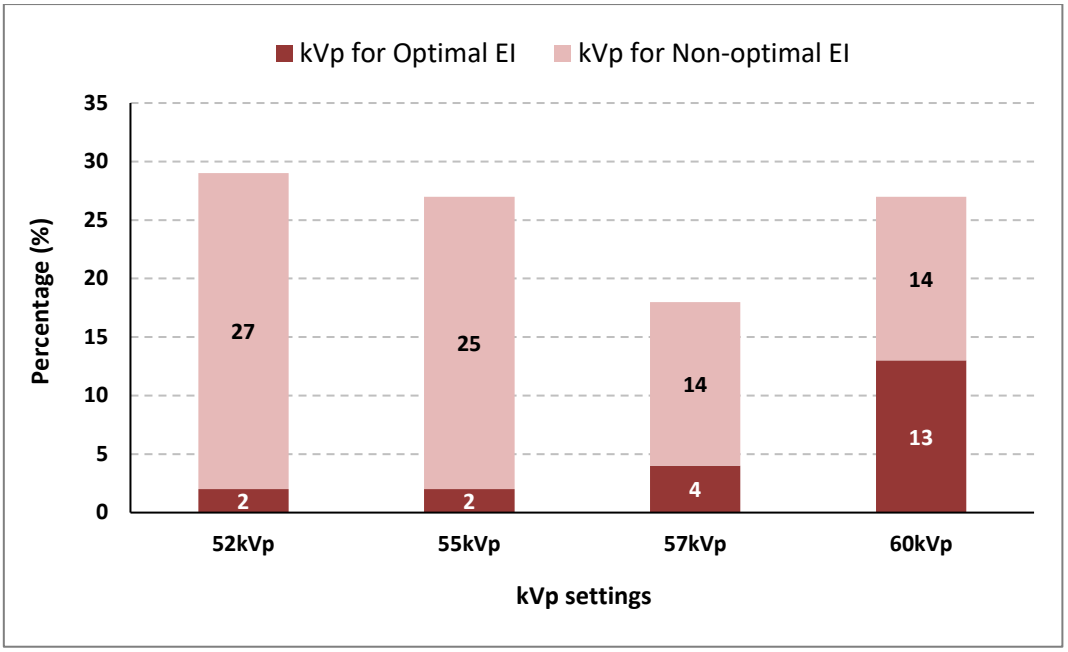



**Figure 4.22.** Kilovoltage peak (kVp) for optimal exposure index (EI) (phase 3 – CXR; n=56).

The optimal mAs within the EI range was 0.8 mAs. As seen in Figure 4.23, no other mAs selection provided an optimal EI value for chest X-rays. The only mAs setting providing an optimal EI value was the 0.8 mAs setting, which was observed in 20% of the procedures.

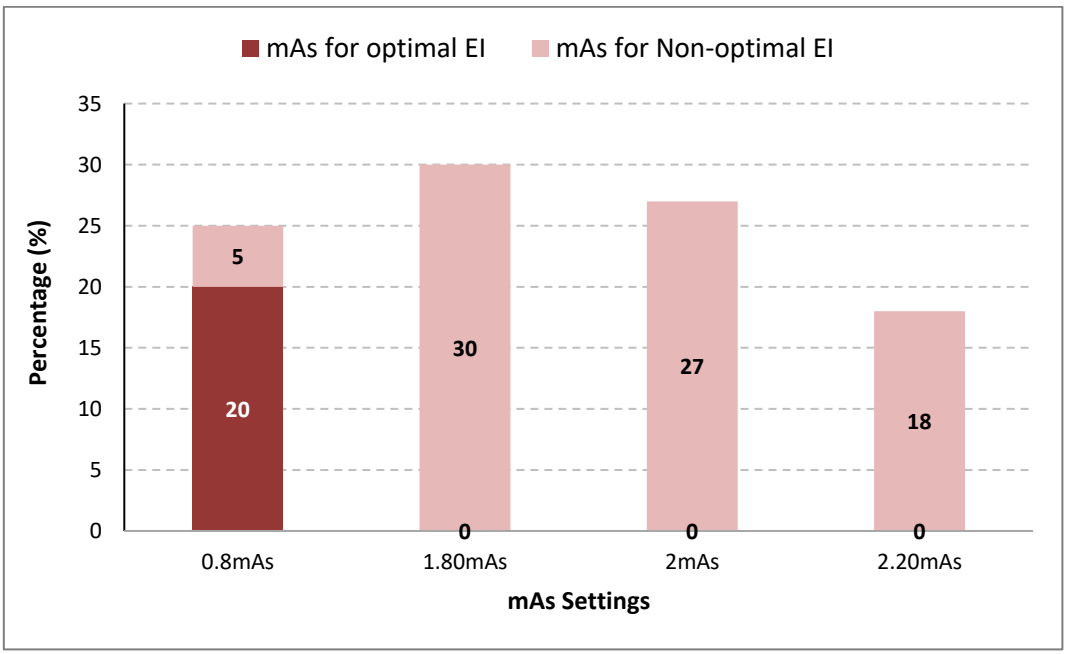



**Figure 4.23.** Milliampere second (mAs) for optimal exposure index (EI) (phase 3 – CXR; n=56).



© Central University of Technology, Free State

The experimental phase of the study showed with data analysis that the largest possible SID yielded the best results, which was 100 cm. Source-to-object distance (SOD) is the distance measured from the X-ray tube to the centring point on the phantom, while source-to-image distance (SID) is the distance measured from the X-ray tube to the detector, which is inversely related to magnification and distortion (Sy, Samboju & Mukhdomi, 2024: online). Figure 4.24 confirms that a SID of 100 cm provided an optimal EI in 18% of the CXR experiments.

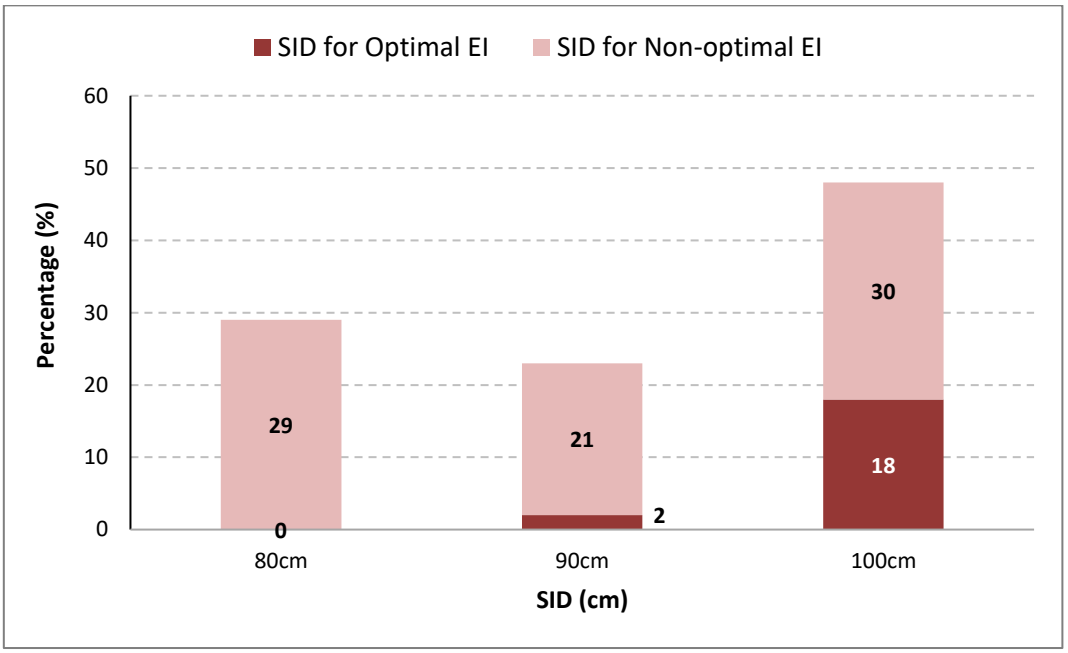



**Figure 4.24.** Source-to-image distance (SID) for optimal exposure index (EI) (phase 3 – CXR; n=56).

The experiment and statistical analysis proved that a straight beam contributed to an optimal exposure index, while an angulated beam or tilted bed (to align the sternum parallel to the detector) should be avoided (Figure 4.25). Figure 4.25 shows the effect of the main radiation beam angle on the exposure index. As presented by the dark red, a straight main radiation beam was found to provide an optimal EI value in 16% of the CXR procedures.



© Central University of Technology, Free State

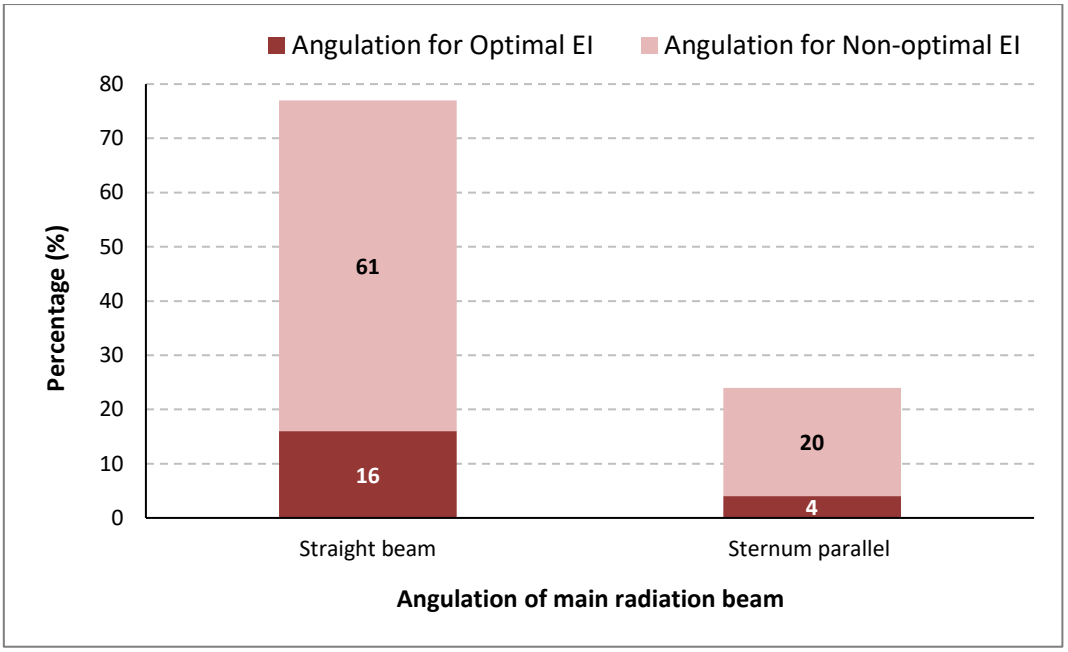



**Figure 4.25.** Angulation for optimal exposure index (EI) (phase 3 – CXR; n=56).

The deviation index reflects the difference between the target exposure and the actual exposure (Cohen, Cooper, Piersall & Apgar, 2011: 593). The results discussed below are for imaging protocols providing an optimal deviation index. The DI was also recorded three times for the three individual exposures performed for each protocol. The DI was displayed on the console of the mobile unit. The optimal DI value is 0, where an overexposed image resulted in a positive DI value and an underexposed image resulted in a negative DI value. Four (7%) of the 56 CXR imaging protocols provided an optimal DI (Figure 4.26). The key parts of these optimal imaging protocols are discussed below.



© Central University of Technology, Free State

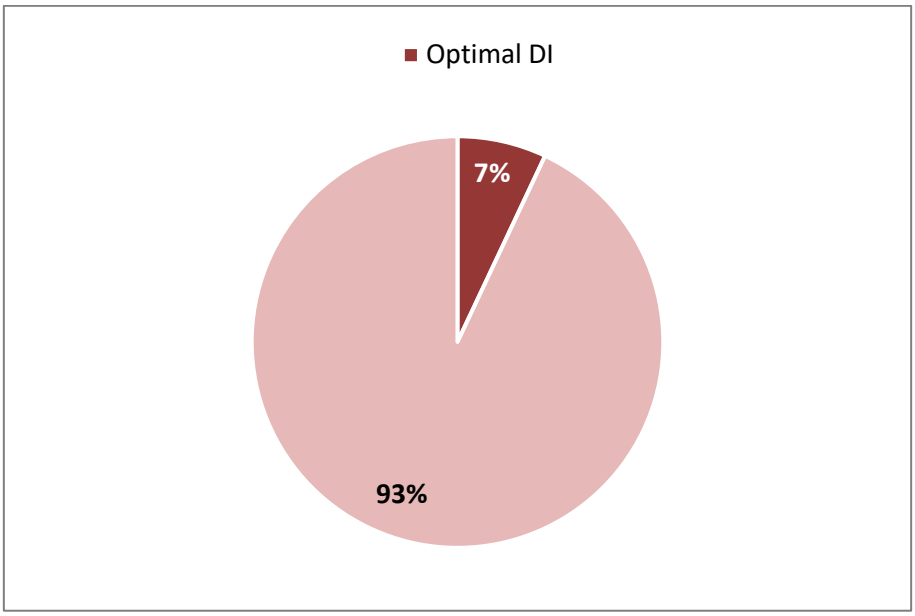



**Figure 4.26.** Imaging protocols producing optimal deviation index (DI) (phase 3 – CXR; n=56).

The dark red line in Figure 4.27 indicates the SSD measurements contributing to an optimal DI. The SSD yielded optimal results in a range of 86 cm to 87 cm.

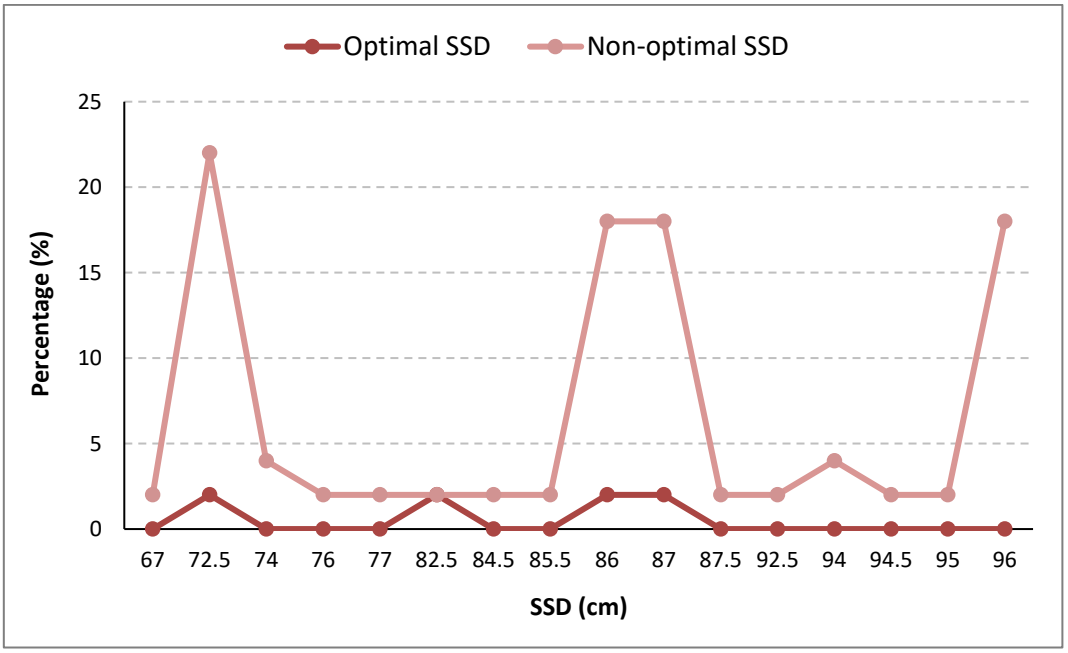



**Figure 4.27.** Source-to-subject distance (SSD) producing optimal deviation index (DI) (phase 3 – CXR; n=56).



© Central University of Technology, Free State

To achieve an optimal deviation index for CXR, it was found that the object-to-image distance, the distance from the patient to the detector, should be as large as possible. The OID was proven optimal at a distance of 9 cm, as indicated by the values in Table 4.11.

**Table 4.11.** Object-to-image distance (OID) for optimal deviation index (DI) (phase 3 – CXR; n=56).

| | Optimal DI by OID (cm) for CXR | | |
|---|---|---|---|
| | **0 cm** | **2 cm** | **9 cm** |
| Non-optimal DI | 34% | 27% | 23% |
| Optimal DI | 2% | 2% | 4% |

For exposure factors, an optimal deviation index was achieved with 52 kVp in 4% of the CXR procedures. These findings are provided in Figure 4.28, with the dark red representing the optimal DI.

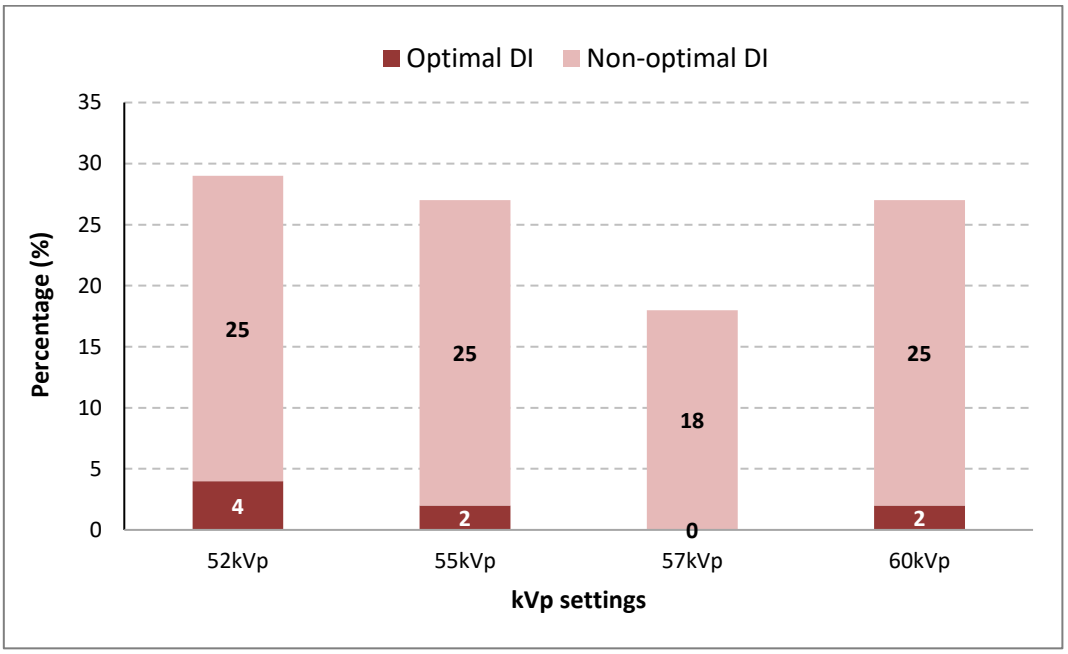



**Figure 4.28.** Kilovoltage peak (kVp) for optimal deviation index (DI) (phase 3 – CXR; n=56).

Figure 4.29 shows the mAs values that were applied for CXR imaging. The mAs settings contributing to an optimal DI are represented in dark red. Results showed that 1.80 mAs contributed to an optimal DI in 5% of procedures.



© Central University of Technology, Free State

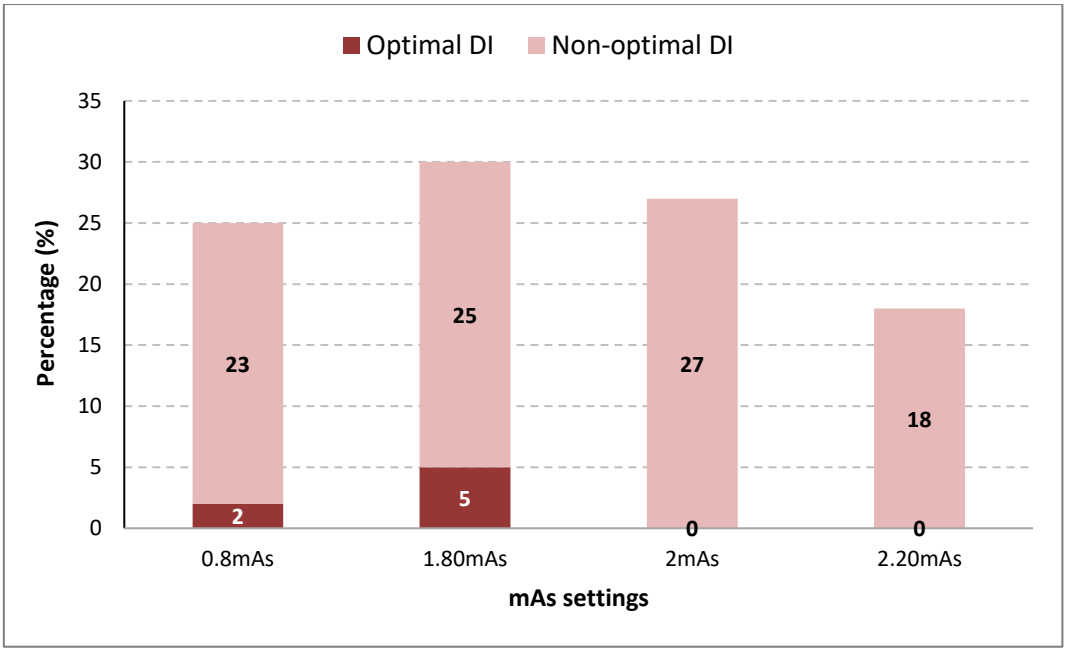



**Figure 4.29.** Milliampere second (mAs) for optimal deviation index (DI) (phase 3 – CXR; n=56).

To obtain an optimal DI, the SID was optimal at 90 cm, as represented by the dark red in Figure 4.30.

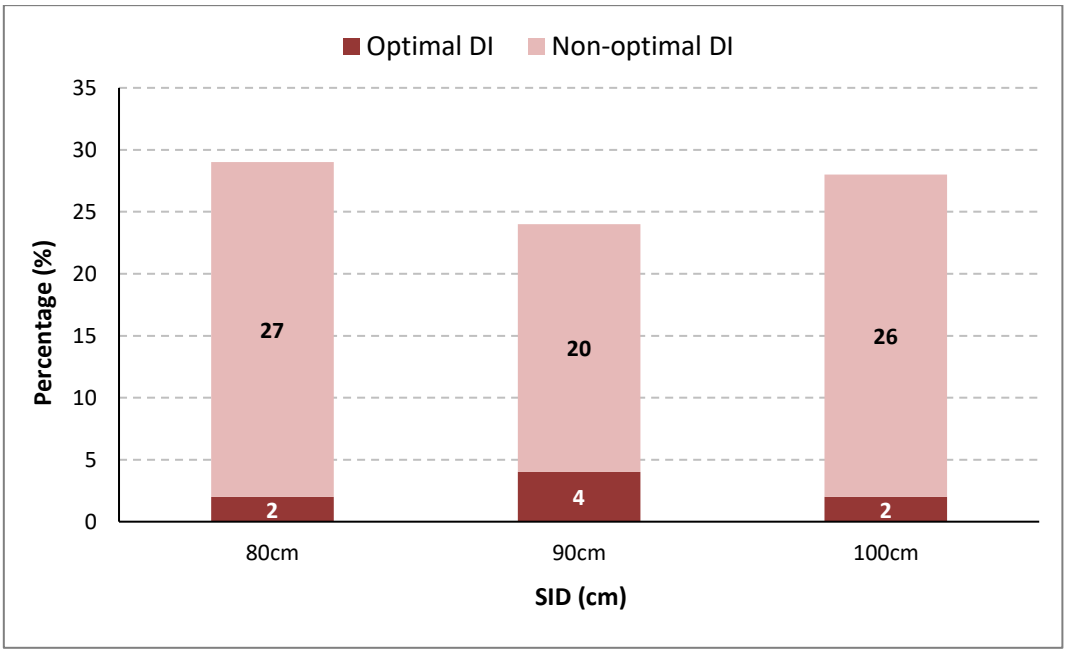



**Figure 4.30.** Source-to-image distance (SID) for optimal deviation index (DI) (phase 3 – CXR; n=56).

A straight beam proved to provide an optimal deviation index instead of angulating the main radiation beam or tilting the bed to align the sternum parallel to the detector. The dark red in



© Central University of Technology, Free State

Figure 4.31 represents the findings, showing that in 7% of CXR procedures, a straight beam produced an optimal DI.

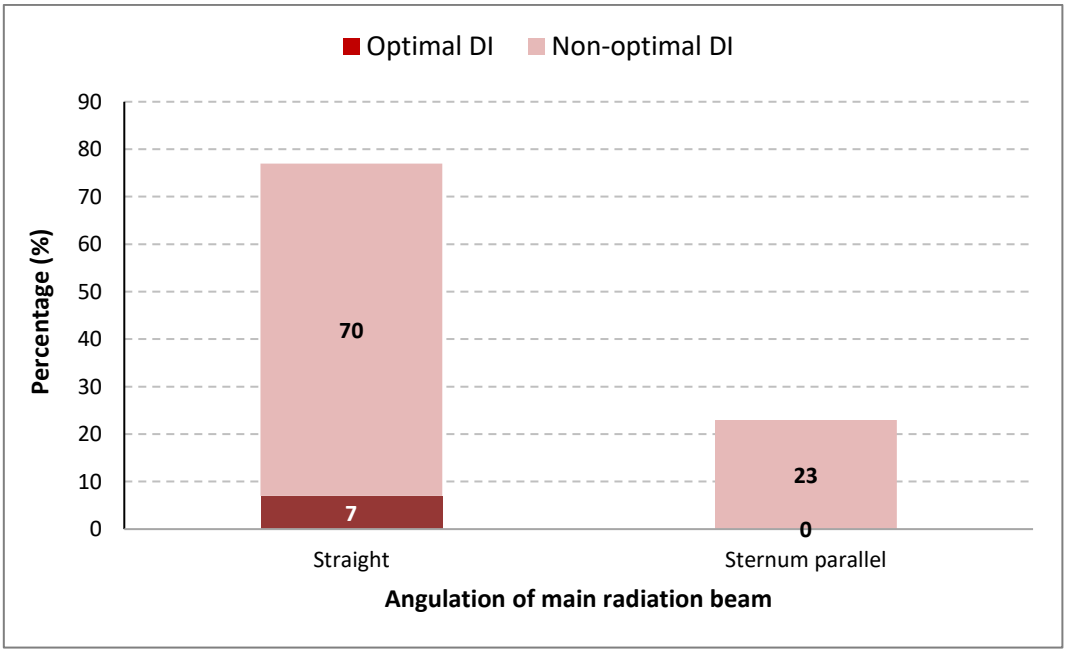



**Figure 4.31.** Angulation for optimal deviation index (DI) (phase 3 – CXR; n=56).

According to Compagnone, Pagan and Bergamini (2005: 101), entrance skin dose is regarded as a crucial parameter to determine the radiation dose received by a patient during a single radiographic exposure. The ESD was calculated by using a dosimeter placed on top of the phantom, measuring the IAK, multiplied by CF, multiplied by BSF, as indicated by the equation in section 2.3.3. Thirteen (23%) CXR exposure protocols produced an optimal ESD. Optimal ESD was defined as below 80 µGy for CXR (Armpilia *et al.*, 2001: 539; European Commission, 1996: 28). Findings are presented in Figure 4.32.



© Central University of Technology, Free State

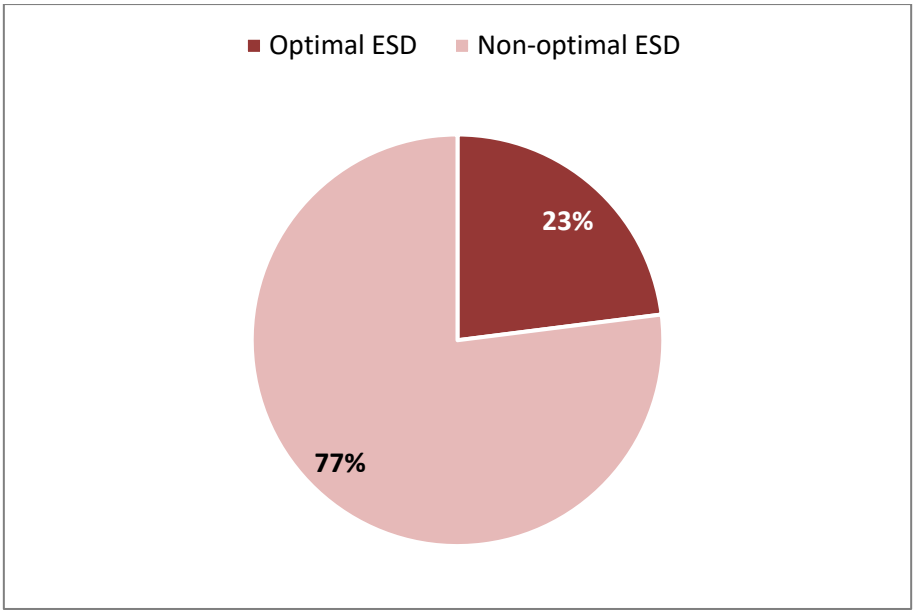



**Figure 4.32.** Imaging protocols producing optimal entrance skin dose (ESD) <80 µGy (phase 3 – CXR; n=56).

As seen in Figure 4.33, the ESD, represented by the dark red, showed a positive change when the SSD was set above 86 cm and again above 94 cm. Thus, the ESD was optimal at a distance larger than 94 cm.

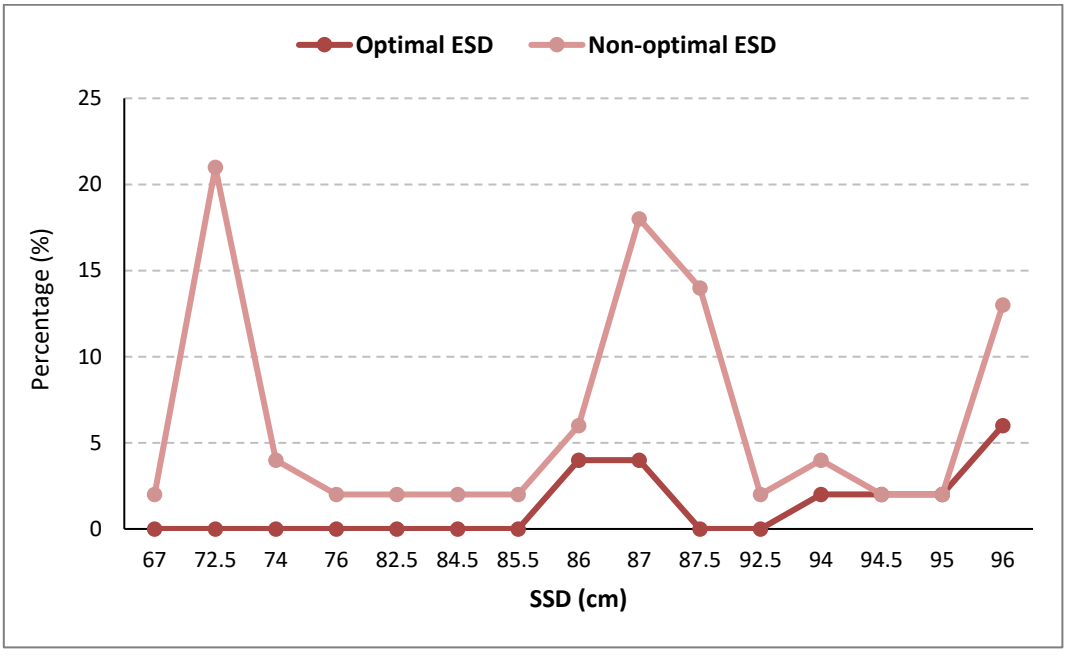



**Figure 4.33.** Source-to-subject distance (SSD) for optimal entrance skin dose (ESD) (phase 3 – CXR; n=56).



© Central University of Technology, Free State

An OID of 0 cm yielded an optimal ESD when the detector was placed directly underneath the patient, as indicated in Table 4.12.

**Table 4.12.** Object-to-image distance (OID) for optimal entrance skin dose (ESD) (phase 3 – CXR; n=56).

| | Optimal ESD by OID (cm) for CXR | | |
|---|---|---|---|
| | **0 cm** | **2 cm** | **9 cm** |
| Non-optimal ESD | 27% | 27% | 23% |
| Optimal ESD | 18% | 2% | 4% |

Figure 4.34 below represents the kVp selections during phase 3. The kVp setting providing an optimal ESD for CXR was 60 kVp, which was similar to that for an optimal EI.

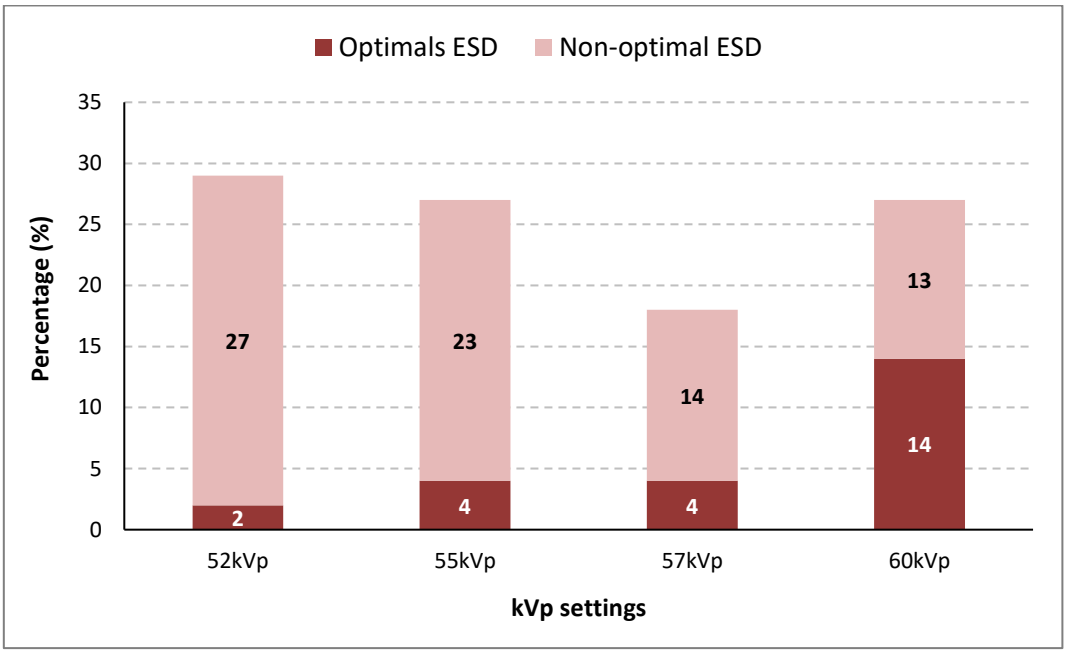



**Figure 4.34.** Kilovoltage peak (kVp) for optimal entrance skin dose (ESD) (phase 3 – CXR; n=56).

The mAs settings are illustrated in Figure 4.35. The mAs selection contributing to an optimal ESD during CXR was 0.80 mAs, similar to the mAs required for an optimal EI.



© Central University of Technology, Free State

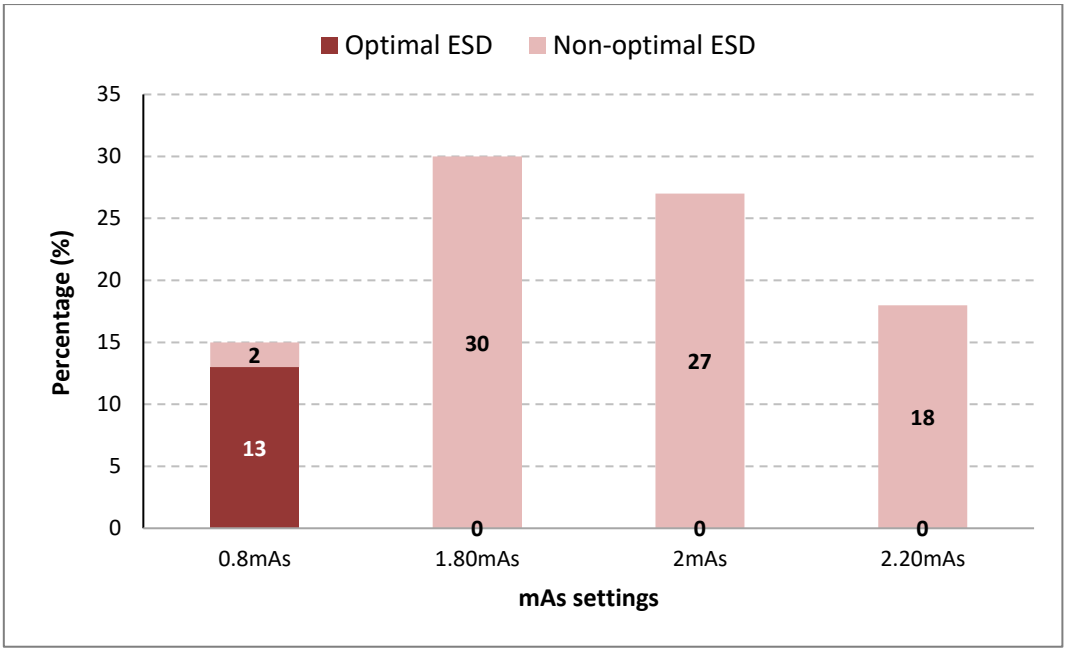



**Figure 4.35.** Milliampere second (mAs) for optimal entrance skin dose (ESD) (phase 3 – CXR; n=56).

An SID of 100 cm contributed to optimal ESD, which was found in 20% of the CXR procedures, as shown in Figure 4.36.

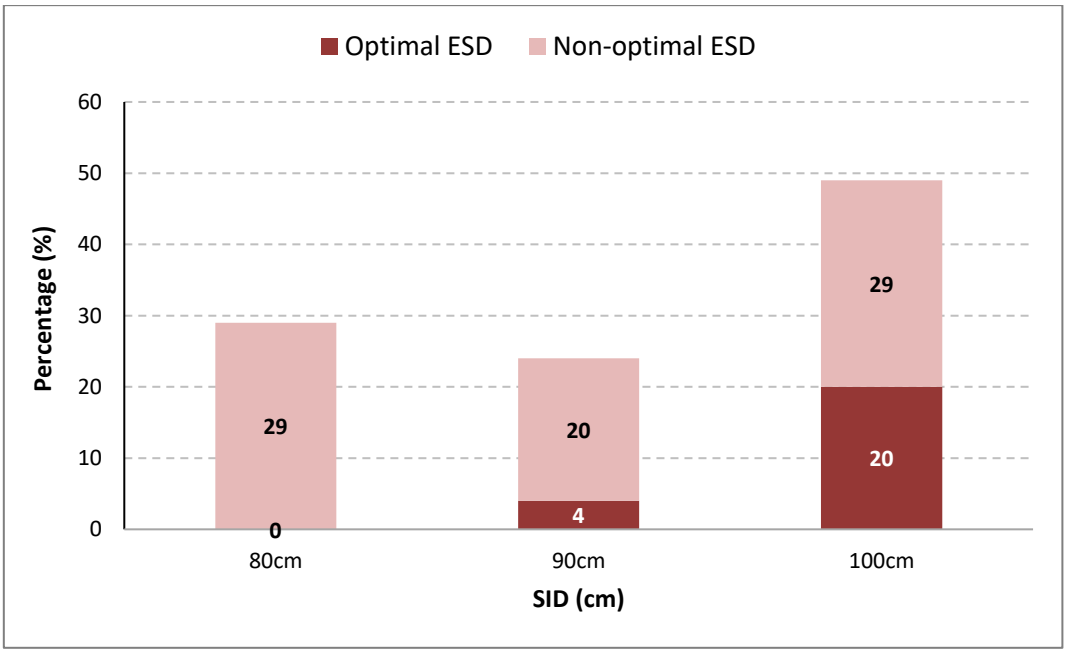



**Figure 4.36.** Source-to-image distance (SID) for optimal entrance skin dose (ESD) (phase 3 – CXR; n=56).



© Central University of Technology, Free State

The main radiation beam selections for optimal ESD are shown in Figure 4.37. Once again, a straight radiation beam was the more suitable option and contributed to an optimal ESD, which was similar to that of an optimal EI and DI.

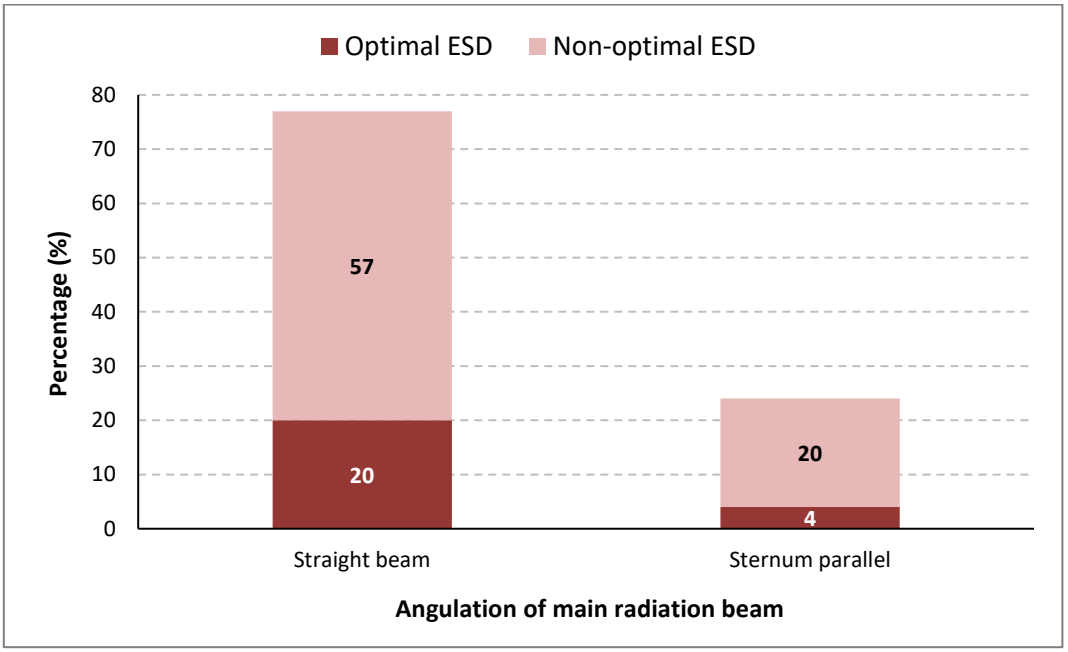



**Figure 4.37.** Angulation for optimal entrance skin dose (ESD) (phase 3 – CXR; n=56).

To summarise, in order to obtain an optimal neonatal CXR, the radiographic settings should be 60 kVp and 0.8 mAs, a large SID of 100 cm and a small OID at 0 cm, performed with a straight main radiation beam. These proposed parameters, presented in Table 4.13, provided the best possible image with an optimal EI, DI and ESD. The proposal of the standardised imaging protocol was based on the percentage of the 56 experimental CXR exposures that yielded optimal images, also shown in Table 4.13.

**Table 4.13.** Standardised imaging protocol for neonatal chest X-rays (n=56).

| Radiographic factor | Standardised imaging protocol for CXR | Percentage of optimal exposures obtained |
|---|---|---|
| Kilovoltage peak (kVp) | 60 kVp | 29% |
| Milliampere second (mAs) | 0.8 mAs | 35% |
| Source-to-image distance (SID) | 100 cm | 40% |
| Object-to-image distance (OID) | 0 cm | 36% |
| Main beam direction | Straight | 43% |



© Central University of Technology, Free State

### 4.4.2 Experimental abdominal X-ray results

Forty-five protocols for abdominal X-rays were tested during the experimental phase. Two abdominal imaging protocols were excluded from the statistical analysis due to non-adherence to specific requirements. These two protocols were excluded because they did not include the symphysis pubis inferiorly on the images. Consequently, the data of 43 AXR protocols were included in the statistical analysis.

The protocols tested were constructed from the literature search and the results of the observation performed during phase 2 of the study. The optimal exposure index for abdominal X-rays is 125–500 and the optimal DI is equal to zero. None of these protocols tested provided optimal settings, as mentioned previously. Even though no optimal imaging protocols were established after the statistical analysis for the observational phase, the abdominal protocol still formed part of the experimental phase.

The researcher used the analysed data from the literature search and the data collected from the observational phase to compile an imaging protocol with the prevalent factors selected by the radiographers to test during the experimental phase. Below is an illustration (Table 4.14) of the abdominal protocols created from the research performed. The researcher used the same protocol created for the combined CXR-AXR images, as the criteria for the inclusion of anatomical structures and partial thickness were similar. Consequently, the exposure factors were derived from the combined chest and abdominal X-ray protocol.

Mobile AXR were not requested often during this current study, as the doctors usually prefer a combined CXR-AXR image to visualise and evaluate line and tube placement (endotracheal [ET] and nasogastric [NG] tubes, and umbilical lines).

In Table 4.14, the proposed abdominal X-ray protocol is presented. The exposure factors (kVp and mAs values) were derived from the combined X-rays, as the part thickness was similar and also the visibility of the required anatomical structures included. This was done by the researcher as no protocols provided the desired optimal factors. The SID and main radiation beam direction were derived from the statistical analysis of phase 3 data and the literature (cf. section 2.10.2). The OID was derived from the phase 3 combined images' statistical analysis, as presented in Table 4.16.



© Central University of Technology, Free State

**Table 4.14.** Standardised imaging protocol for neonatal abdominal X-rays.

| Radiographic factor | Standardised imaging protocol for AXR |
|---|---|
| Kilovoltage peak (kVp) | 54 kVp |
| Milliampere second (mAs) | 1.8 mAs |
| Source-to-image distance (SID) | 100 cm |
| Object-to-image distance (OID) | 2 cm |
| Main beam direction | Straight |

### 4.4.3 Experimental combined chest and abdominal X-ray results

Forty-five imaging protocols were tested to find the optimal EI, DI and ESD for the combined CXR-AXR. Four imaging protocols were excluded from the study for non-adhere to the requirements initially set. These four imaging protocols did not include the symphysis pubis inferiorly on the images, which is an important anatomical structure for inclusion on an abdominal X-ray (Bontrager & Lampignano, 2014: 644; Lampignano & Kendrick, 2021). Therefore, 41 protocols were included for statistical analysis. Only one exposure provided an optimal ESD, while none of the exposures captured provided an optimal exposure index (125–500) or deviation index (DI = 0).

Figure 4.38 indicates that one imaging protocol provided an optimal entrance skin dose (ESD).

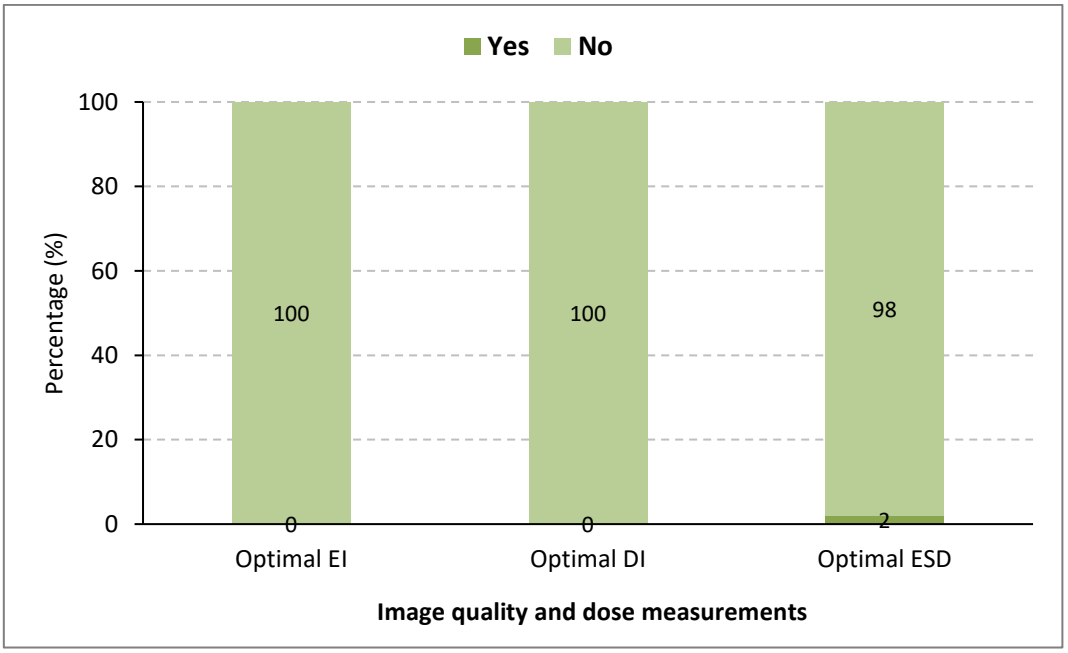



**Figure 4.38.** Combined chest and abdominal X-rays yielding optimal exposure index (EI), deviation index (DI) and entrance skin dose (ESD) (phase 3; n=41).



© Central University of Technology, Free State

In Figure 4.39, the dark green line represents the SSD settings for an optimal ESD with the combined images. The SSD was optimal at 92.5cm.

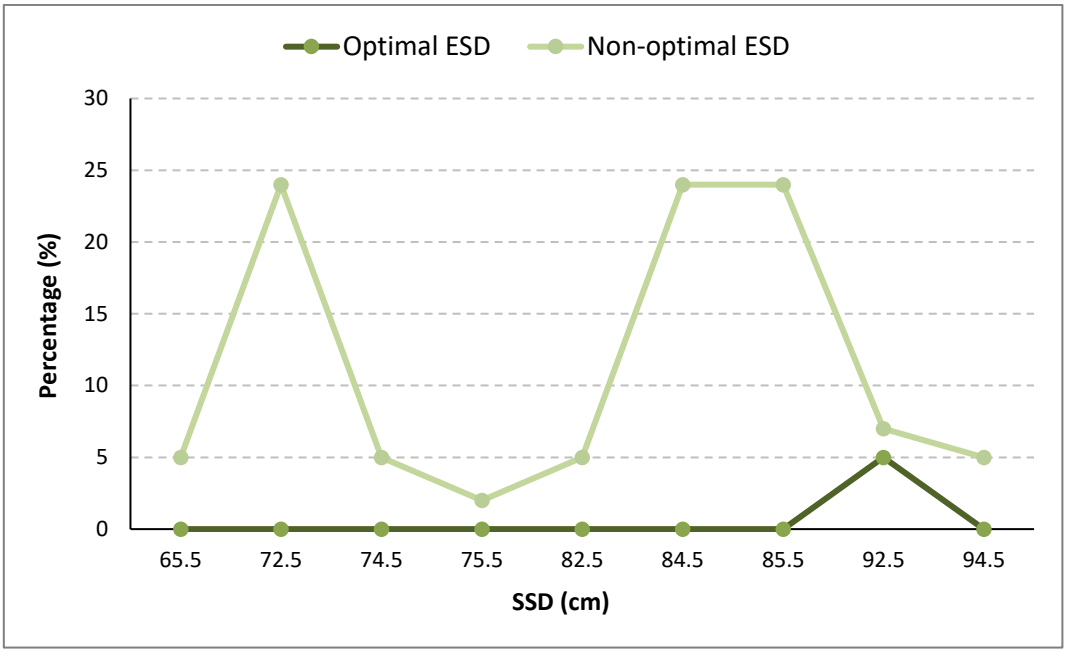



**Figure 4.39.** Source-to-subject distance (SSD) for optimal entrance skin dose (ESD) (phase 3 – Combo; n=41).

Only one exposure with an OID of 2 cm provided optimal ESD Table 4.15), meaning that it is advisable to place the detector at a smaller distance from the neonate and not in the detector tray.

**Table 4.15.** Object-to-image distance (OID) for optimal entrance skin dose (ESD) (phase 3 – Combo; n=41).

| | Optimal ESD by OID (cm) for Combo X-rays (n-value) | | |
|---|---|---|---|
| | **0 cm** | **2 cm** | **9 cm** |
| Non-optimal ESD | 14 | 13 | 13 |
| Optimal ESD | 0 | 1 | 0 |

Figure 4.40 shows that 54 kVp provided an optimal ESD during an exposure for a combined CXR-AXR.



© Central University of Technology, Free State

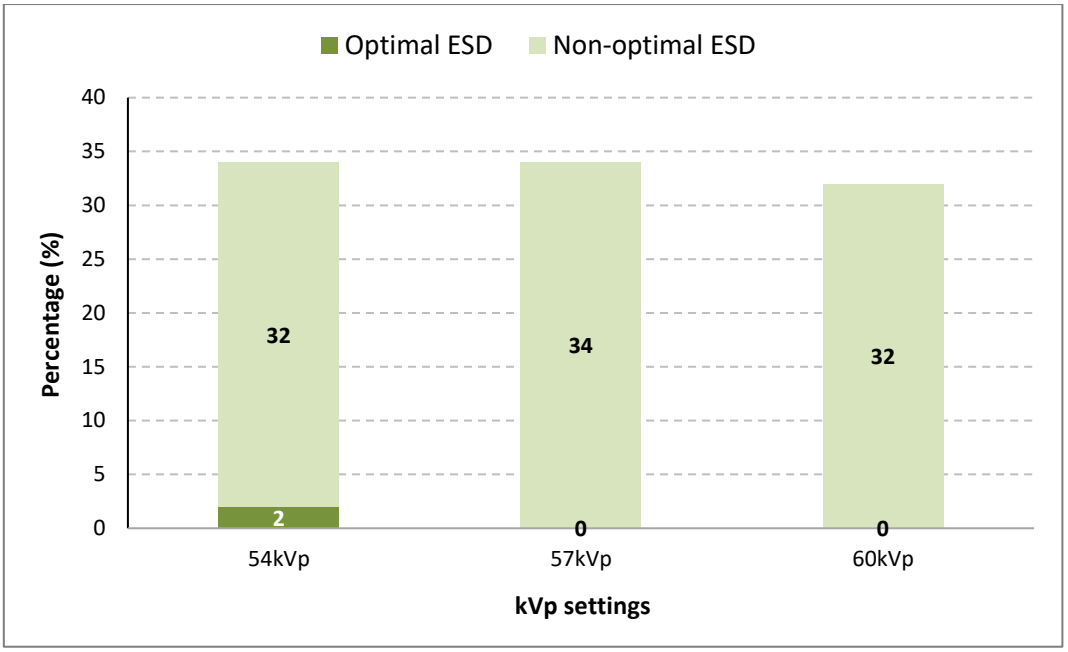



**Figure 4.40.** Kilovoltage peak (kVp) for optimal entrance skin dose (ESD) (phase 3 – Combo; n=41).

Only 2% of exposures with mAs at a setting of 1.80 mAs provided an optimal ESD, as illustrated in Figure 4.41.

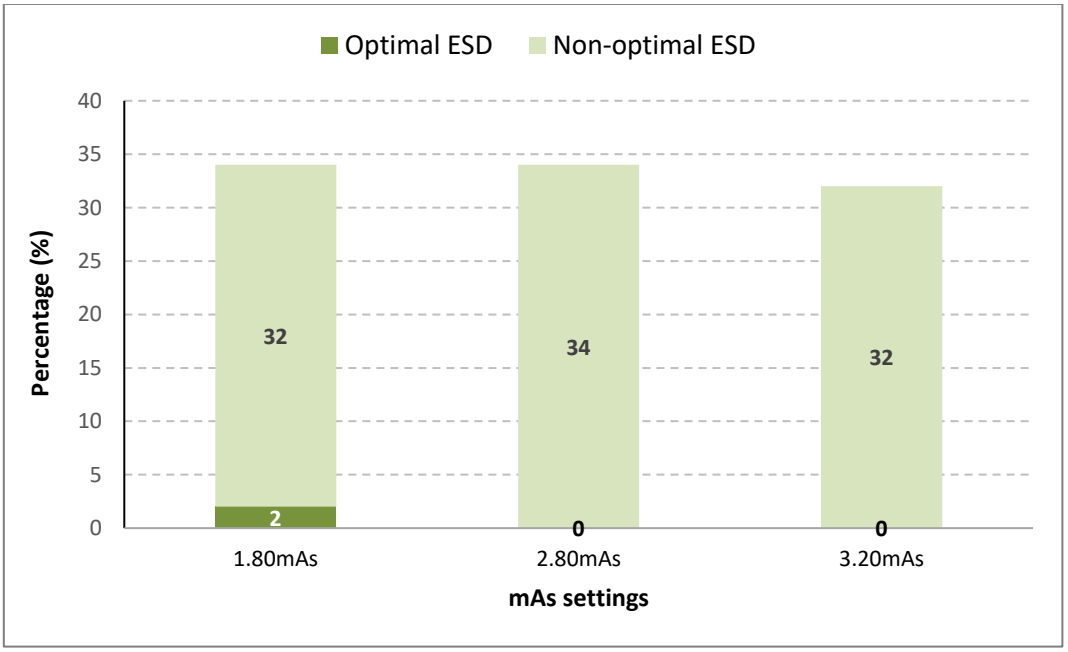



**Figure 4.41.** Milliampere second (mAs) for optimal entrance skin dose (ESD) (phase 3 – Combo; n=41).

The SID set at 100 cm for the combined X-rays presented an optimal ESD measured during the experimental phase, as presented in Figure 4.42.



© Central University of Technology, Free State

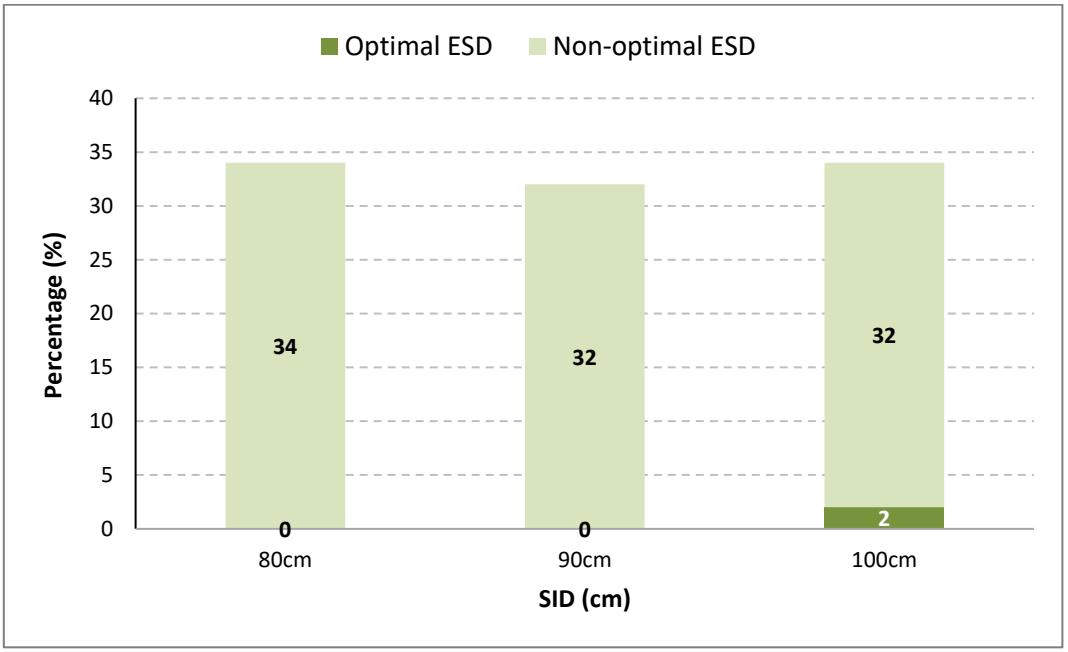



**Figure 4.42.** Source-to-image distance (SID) for optimal entrance skin dose (ESD) (phase 3 – Combo; n=41).

Settings at 54 kVp, 1.8 mAs and a large source-to-image receptor distance of 100 cm with a straight main radiation beam and an object-to-image receptor distance of 2 cm, will provide an image with an optimal exposure index, deviation index and entrance skin dose. These findings are presented in Table 4.16.

The standardised imaging protocol presented in Table 4.16 is derived from the statistical analysis done and discussed for phase 3. The percentages included are from the statistical analysis done for phase 3. The exposure factors are set at 54 kVp (2%) and 1.80 mAs (2%) while the SID should be measured at 100 cm (2%) and the OID at 2 cm (2%) with a straight main radiation beam (2%).

**Table 4.16.** Standardised imaging protocol for neonatal combined chest and abdominal X-rays (phase 3; n=41).

| Radiographic factor | Standardised imaging protocol for combined X-rays |
|---|---|
| Kilovoltage peak (kVp) | 54 kVp |
| Milliampere second (mAs) | 1.8 mAs |
| Source-to-image distance (SID) | 100 cm |
| Object-to-image distance (OID) | 2 cm |
| Main beam direction | Straight |



© Central University of Technology, Free State

## 4.5 THE IDEAL PROTOCOLS FOR IMPLEMENTATION

Table 4.17 provides a summary of the proposed CXR imaging protocol to achieve optimal EI, DI and ESD.

**Table 4.17.** Summary of optimal factors for chest X-rays.

| | SSD | OID | kVp | mAs | SID | Angulation |
|---|---|---|---|---|---|---|
| EI | 94–96 cm | 0 cm | 57–60 | 0.80 | 100 cm | Straight |
| DI | 94 cm | 9 cm | 52–55 | 1.80 | 90 cm | Straight |
| ESD | 94–96 cm | 0 cm | 57–60 | 0.80 | 100 cm | Straight |

DI, deviation index; EI, exposure index; ESD, entrance skin dose; kVp, kilovoltage peak; mAs, milliampere second; OID, object-to-image distance; SID, source-to-image distance; SSD, source-to-subject distance.

Table 4.18 summarises the settings required for an imaging protocol to achieve an optimal ESD for the combined CXR-AXR. Even though authors such as Quinn & Carroll (2023: 732) recommend that digital radiography should apply a higher kVp and a lower mAs to ensure optimal image quality at a lower patient radiation dose, these exposure factors provided an optimal ESD on the phantom. Thus, this could possibly change when imaging a neonatal patient.

**Table 4.18.** Summary of optimal factors for combined chest and abdominal X-rays.

| | SSD | OID | kVp | mAs | SID | Angulation |
|---|---|---|---|---|---|---|
| ESD | 92.5 cm | 2 cm | 54 | 1.80 | 100 cm | Straight |

ESD, entrance skin dose; kVp, kilovoltage peak; mAs, milliampere second; OID, object-to-image distance; SID, source-to-image distance; SSD, source-to-subject distance.

Due to the limited number of mobile abdominal X-rays requested during data collection, the researcher used the literature and the data collected during the observational phase (phase 2) to create the abdominal protocol. This is a specific limitation of the study, as abdominal X-rays are not commonly performed, but rather combined CXR-AXR imaging (cf. section 5.7).

The proposed imaging protocol for mobile AXR on neonates is similar to that of the combined CXR-AXR imaging protocol. The centring point and part thickness of the abdomen are the same as for the combined image. Consequently, the researcher suggested the same protocol for the implementation phase.



© Central University of Technology, Free State

Figure 3.23 illustrates the standardised imaging protocol (Pick The Ending) used during the implementation phase (phase 4) to ensure consistent imaging techniques. It was also used to determine whether the imaging protocol would make a difference in the EI after the protocols have been implemented.

After the observational (phase 2) and experimental phases (phase 3), a final standardised imaging protocol remained for implementation. The standardised imaging protocol was derived from all previous phases of the study and constructed from both the literature and physical findings after observation and experimental testing. During phase 5 of the study, the researcher determined whether a change in the exposure index and image critique occurred after the implementation of the imaging protocol during the fourth phase.

The standardised imaging protocol was named Pick The Ending as the letters refer to the three radiographic factors contributing to an optimal image: **P**ositioning, **T**echnical and **E**xposure factors. By allowing the radiographer to change these factors by assessing the situation and applying all three of these factors, they can essentially "pick the ending" and choose the outcome regarding image quality, image critique and radiation dose exerted.

Figure 3.23 (section 3.4.3.2.) shows the Pick The Ending one-pager standardised imaging protocol created by the researcher and provided to the participating radiographers during the implementation phase of the study. The one-pager indicates that the preferred position for the neonates during radiographic X-ray acquisition is with the arms abducted from the body, with the head and chin facing up. The radiographer should ensure that no rotation of the chest and pelvis occurs.

The lead marker should be placed on the detector and not directly on the patient to comply with infection control, while the detector should be placed directly underneath the neonate with a short object-to-image distance (OID). The source-to-subject distance (SSD) should be as large as possible, depending on the mattress thickness and the SID applied. The SID should be as large as possible or set at 100 cm. The centring point for the chest should be on the nipple line, while the centring point for the AXR and combined CXR-AXR should be on the navel.

The exposure factors for a CXR should be a high kVp setting of 57–60 kVp, with a low mAs setting of 0.80 mAs. The exposure factors for the AXR and combined CXR-AXR image should be set to 54 kVp and 1.80 mAs. The final part of the imaging protocol is the specifications of



© Central University of Technology, Free State

the machine regarding the exposure index (EI) and deviation index (DI), which should be 50–200 and zero, respectively.

The collimator guidelines are indicated in the one-pager and were explained during the neonatal imaging training presentation. The red block over the infant indicates the collimation for a CXR, showing that the top collimator should be on the lip line and the bottom collimator on the navel to ensure inclusion of all the relevant anatomical structures. The blue box refers to the abdominal X-ray, with the top collimator border on the nipple line, while the inferior border of the collimator shadow should be on the mid-femur. The green box represents the combined CXR-AXR, where the superior border of the collimator should be on the lip line, and the inferior border of the collimator on the level of the mid-femur.

Figure 4.43 shows the title slide of the neonatal imaging training PowerPoint session (cf. Appendix P for the complete set of slides) presented before the implementation phase. The purpose of the presentation was to ensure that all the participants understood the aim and objectives of the study, and specifically, the purpose of the implementation phase. They were also assured of the importance of their participation and honesty. The researcher provided the implementation checklist used when performing routine mobile examinations and explained to the participants how to complete the checklist. All criteria included on the checklist (positioning factors, technical factors, and exposure factors) for CXR, AXR and the combined CXR-AXR images were explained in depth and all questions were answered. They were also instructed on where to place the completed checklists to ensure anonymity and promote safekeeping of the completed checklists.



© Central University of Technology, Free State

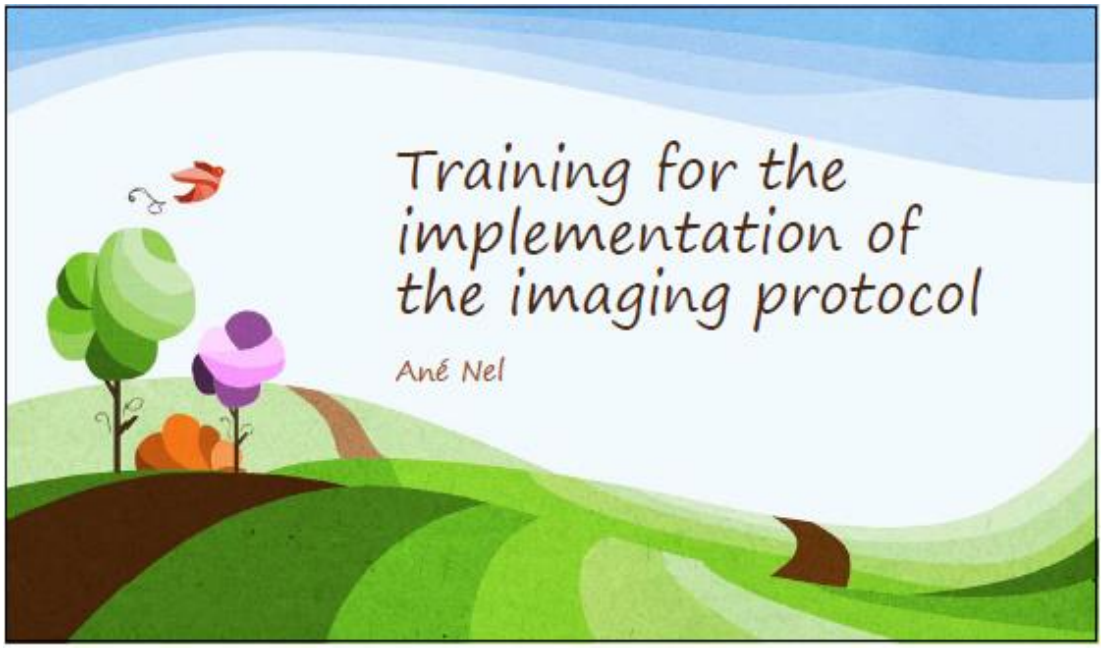



**Figure 4.43.** Title slide of the neonatal imaging training PowerPoint presentation (cf. Appendix P).

## 4.6 PHASE 4: IMPLEMENTATION

### 4.6.1. Implementation results

During the two-week implementation phase, a total of 50 neonatal X-rays were performed by the participating radiographers, which included three (6%) CXR, two (4%) AXR and 45 (90%) combined CXR-AXR.

The neonates' arms were abducted by the radiographers for 96% of the X-rays during the implementation of the imaging checklist. Abduction of the arms was proposed as part of the positioning factors on the one-pager checklist. The main immobilisation technique employed was the radiographers themselves assisting with immobilisation by holding the infant (46%). Sandbags were used for immobilisation in 40% and the bedding (to create a nook) in 10% of the procedures. The findings are presented in Figure 4.44.



© Central University of Technology, Free State

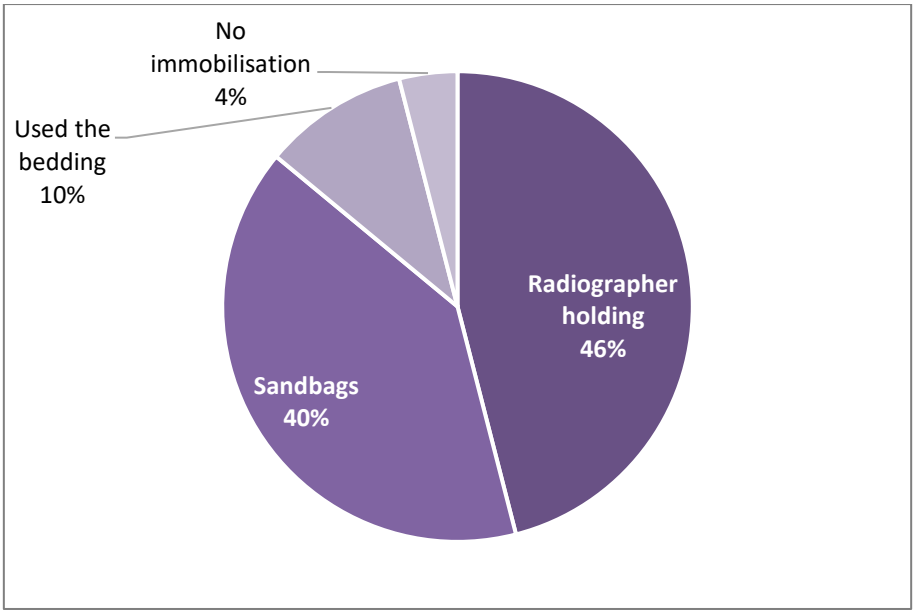



**Figure 4.44.** Arm immobilisation technique during the implementation phase (phase 4; n=50).

In 82% of the cases, the neonates' heads were facing up. Their chins were lifted (88%) to prevent superimposition over the fields, while the radiographers assisted with positioning and immobilisation (32%). These findings are presented in Figure 4.45.

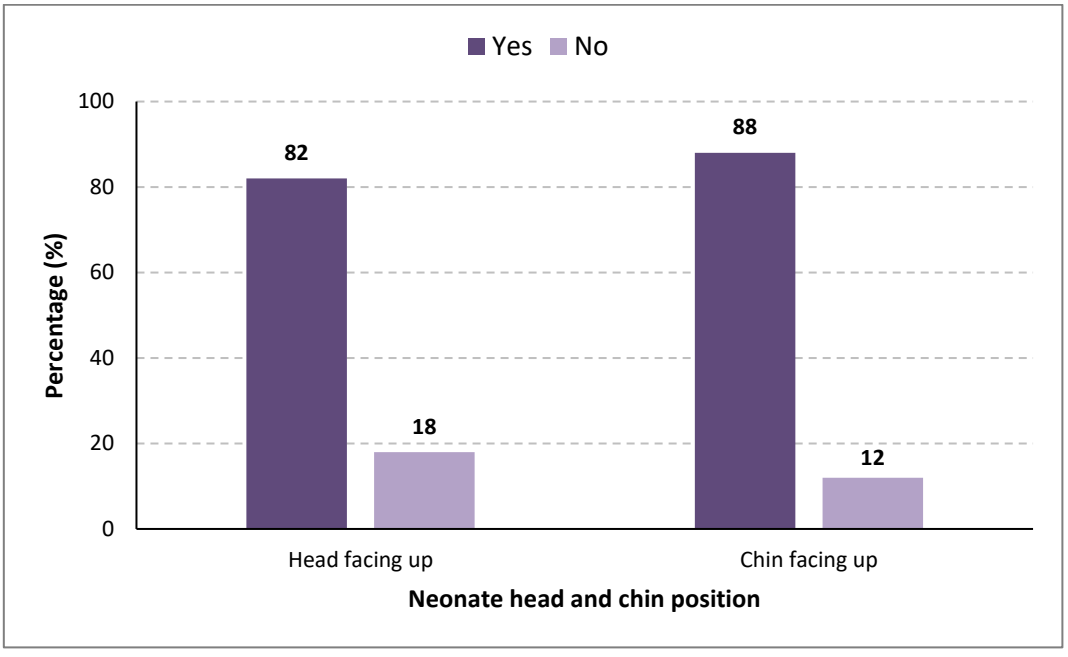



**Figure 4.45.** Immobilisation of the head and chin: head and chin position (phase 4; n=50).

The radiographers recorded rotation of the patient on the checklist using their own discretion. In 50% of the cases, there was no rotation visible prior to exposure. However, in 36% of cases,



© Central University of Technology, Free State

the radiographers identified moderate rotation of the pelvis. One radiographer selected not applicable (N/A) as a CXR was performed and pelvis rotation did not apply to the chest examination. Rotation of the thorax was also evaluated. Minimal thoracic rotation occurred in 30% of the procedures and in 12% of cases, moderate rotation was observed. These findings are presented in Figure 4.46.

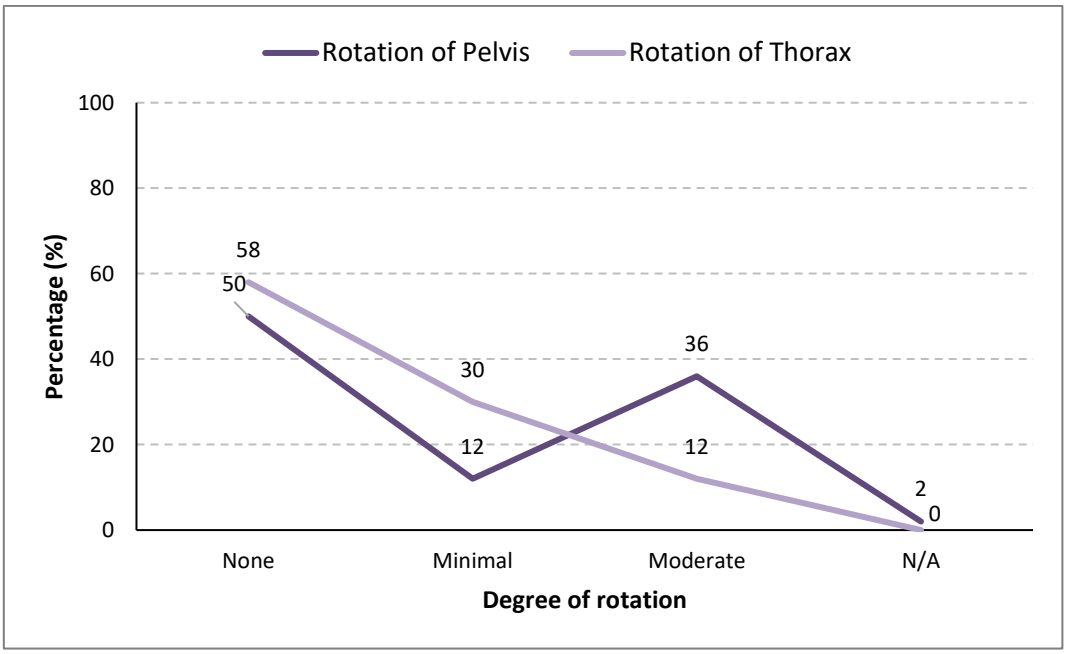



**Figure 4.46.** Rotation of the pelvis and thorax (phase 4; n=50).

The **second set of criteria** on the implementation checklist was based on the technical factors (presented in Table 4.19), including the lead marker and detector placement, SID and SOD, and the centring points and main radiation beam direction.

**Table 4.19.** Part 2 (technical factors) of the implementation checklist.

| TECHNICAL FACTORS | |
|---|---|
| Lead marker placed | |
| Detector placement | |
| Source-to-object distance (SOD) | |
| Source-to-image distance (SID) | |
| Centring and angulation | |

A lead marker was placed only twice (4%) when performing the X-rays during the implementation phase, as presented in Figure 4.47.



© Central University of Technology, Free State

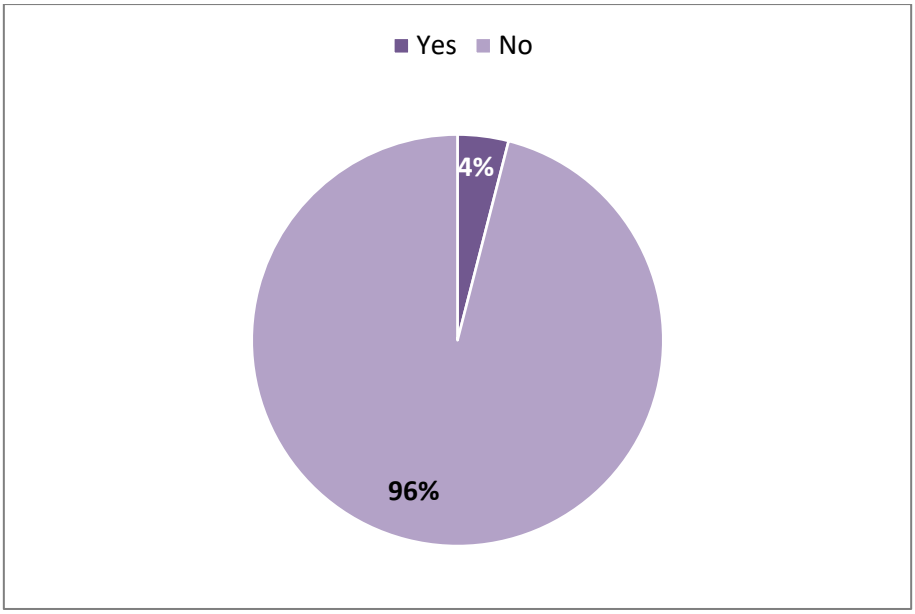



**Figure 4.47.** Lead marker placement (phase 4; n=50).

Most radiographers opted to place the detector underneath the mattress (56%) rather than in the detector tray (32%) as indicated by the imaging protocol (one-pager). The detector was also placed directly under the neonate for six patients (12%). These results are displayed in Figure 4.48.

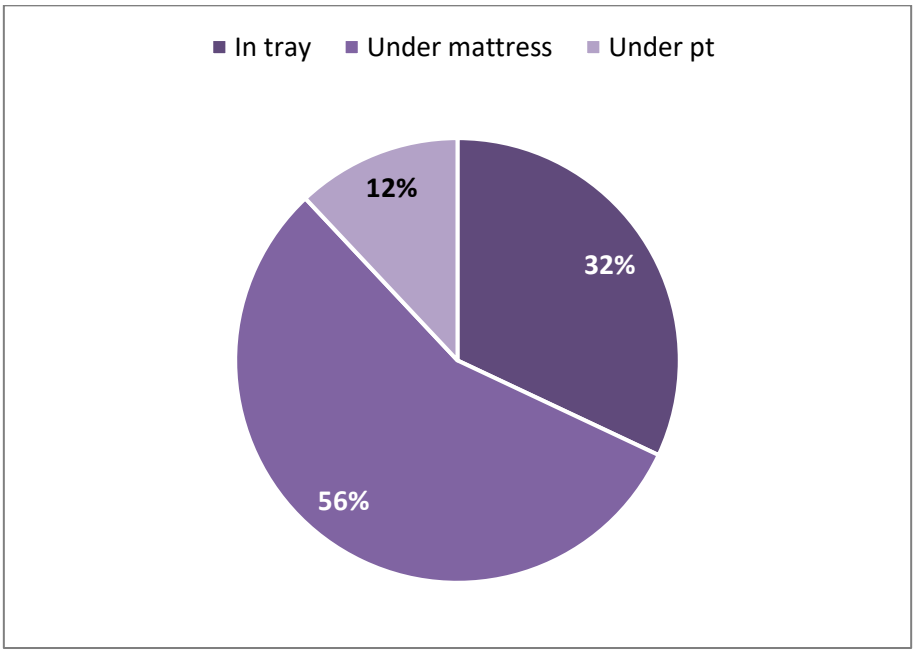



**Figure 4.48.** Detector placement (phase 4; n=50).

The main radiation beam was angulated only once during the implementation phase, implying that a straight beam was preferred by the participating radiographers in 98% of the



© Central University of Technology, Free State

procedures, as suggested on the one-pager. Findings on the angulation of the main radiation beam are presented in Figure 4.49.

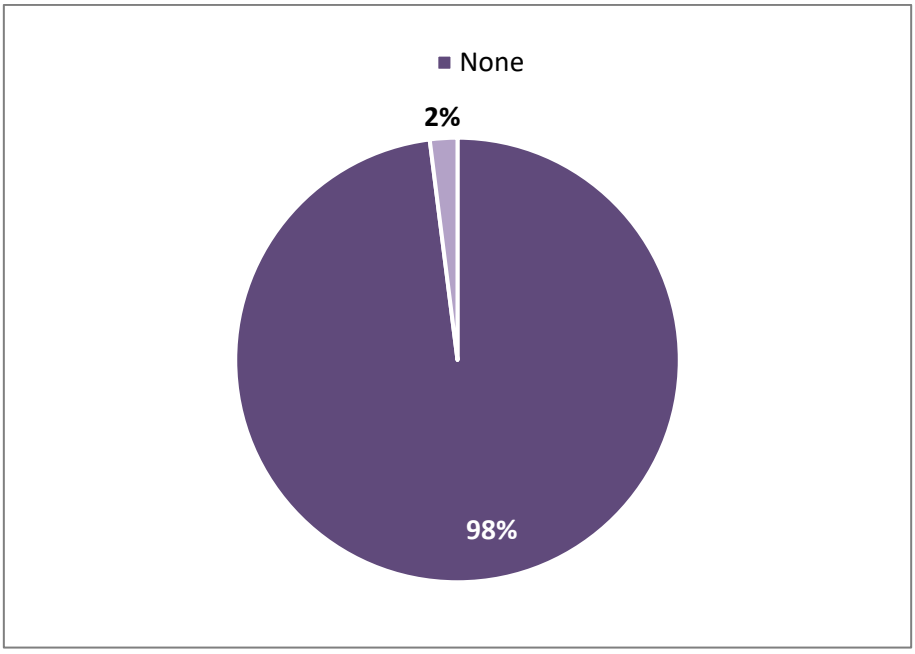



**Figure 4.49.** Angulation of the main beam (phase 4; n=50).

Table 4.20 represents the part of the implementation checklist pertaining to the exposure factors, such as the kVp and mAs selection, with the EI and DI presented on the mobile unit after image acquisition.

**Table 4.20.** Part 3 (exposure factors) of the implementation checklist.

| EXPOSURE FACTORS | |
|---|---|
| Kilovoltage peak (kVp) value | |
| Milliampere second (mAs) value | |
| Exposure index | |
| Deviation index | |

The exposure factors selected, as well with the preferred selection of 55 kVp (38%) and 1.6 mAs (50%) were documented, as presented in Figures 4.50 and 4.51, respectively. The recommended exposure settings for CXR were 57–60 kVp and 0.80 mAs, while the exposure setting, for the abdominal and combined X-rays were 54 kVp and 1.80 mAs. Some of the radiographers indicated that the settings were too low and proceeded with their own selection of exposure setting without trying the proposed exposures. Figure 4.50 shows that the most popular kVp selection for all three examination types was 52 kVp. The minimum kVp setting



© Central University of Technology, Free State

for CXR was 48 kVp and the maximum 52kVp, with a median of 52 kVp. The kVp setting for AXR ranged between a minimum of 52 kVp and a maximum of 55 kVp, with a median of 53.50 kVp (rounding up to 54 kVp). The minimum kVp setting for the combined CXR-AXR was 48 kVp, the maximum was 56 kVp and the median 52 kVp.

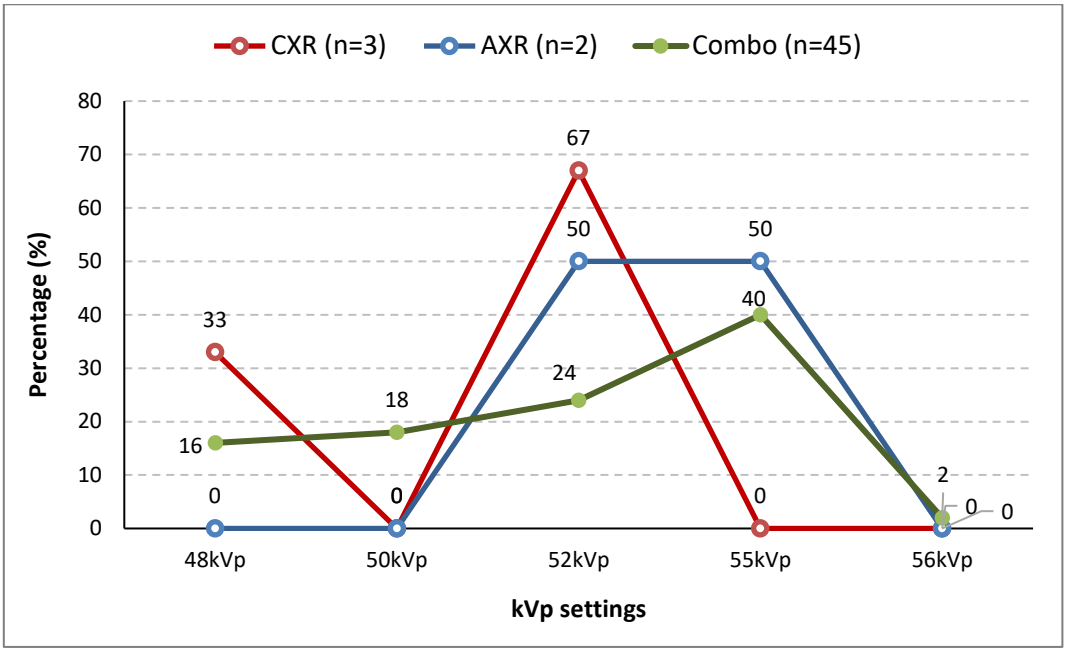



**Figure 4.50.** Kilovoltage peak (kVp) selection (phase 4; n=50).

Figure 4.51 shows that 1.6 mAs was the most common mAs selection for all three examination types, followed by 2.5 mAs for abdominal and combined images. The minimum setting for CXR was 1.30 mAs and the maximum 1.60 mAs; the median was 1.60 mAs and the standard deviation (SD) 0.17. The minimum setting for AXR was 1.60 mAs, the maximum 2.50 mAs and the median 2.05 mAs (SD 0.64). The minimum setting for the combined CXR-AXR was 1.60 mAs, the maximum 2.50 mAs, and the median 2 mAs (SD 0.41).



© Central University of Technology, Free State

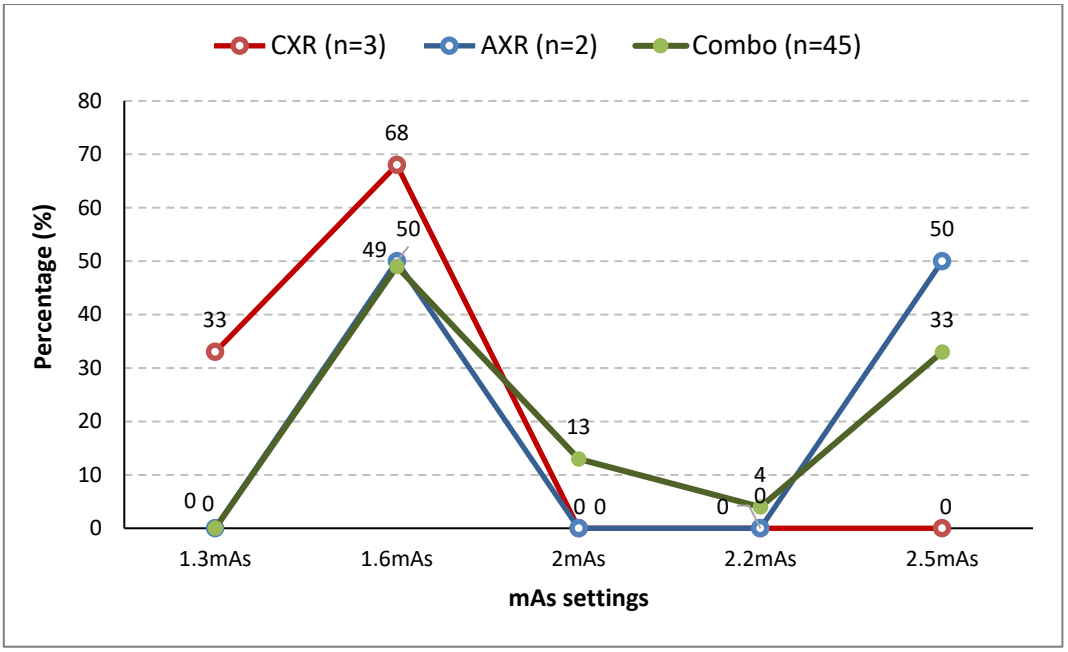



**Figure 4.51.** Milliampere second (mAs) selection (phase 4).

The optimal EI of 50–200 for CXR was achieved with all three CXR cases (100%). For AXR, both (100%) X-rays performed were in the recommended EI range. In 35 (78%) of the 45 combined CXR-AXR, the optimal EI of 125–500 was obtained. The EI was below the recommended range for 8 (18%) of CXR-AXR combination X-rays, above the recommended range for 2 (4%) X-rays. This shows that the radiographers favoured underexposure instead of overexposure of the detector. Only 6% of the X-rays performed reached the desired deviation index (DI=0) for the three different examination types. These findings are presented in Figure 4.52, which reflects the radiographers' tendency to favour underexposure instead of overexposure of the images when performing neonatal mobile X-rays.



© Central University of Technology, Free State

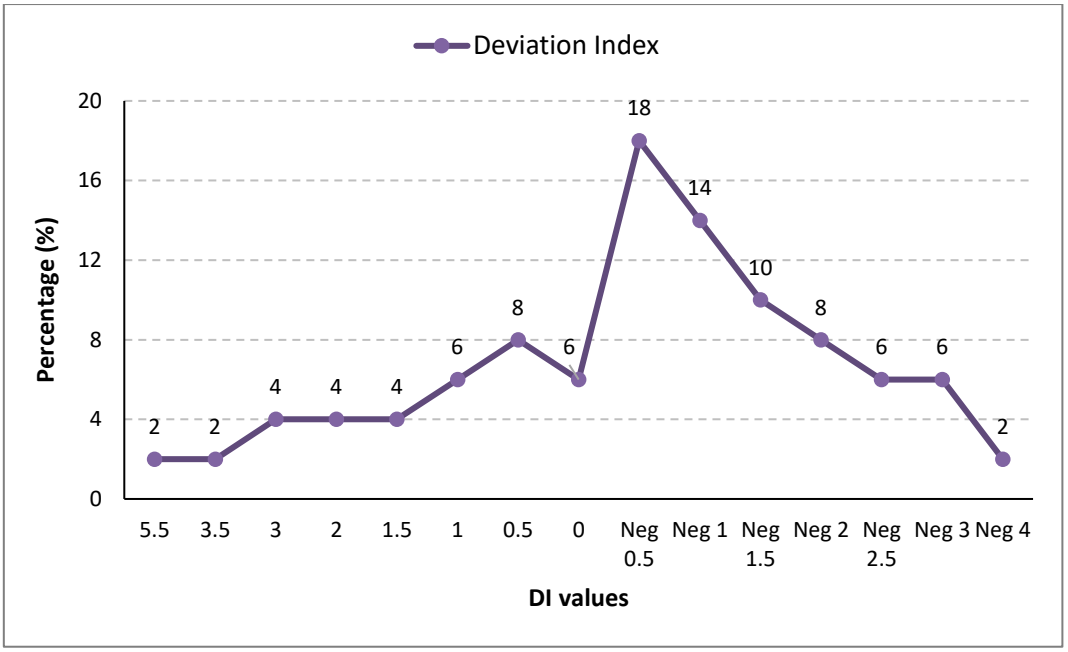



**Figure 4.52.** Deviation index (phase 4; n=50).

The statistician determined the percentages of each factor as performed by the radiographers (cf. Table 4.21). This indicated how the radiographers implemented the standardised protocol. The radiographers did not entirely adhere to the one-pager standardised imaging protocol and diverged from the protocol with the exposure factors and placement of the detector. They opted to place the detector underneath the mattress instead of directly under the patient, while 94% did not place a lead marker on and only 46% used the SID of 100 cm as indicated on the imaging protocol.

Although the ideal position for the detector placement is directly underneath the patient, only 12% radiographers complied. In 56% of cases, it was placed under the mattress, which could be related to infection control preferences of the nursing staff, and/or the presence of patient lines causing the placement directly underneath the patient to be unfeasible. In the 32% of cases where the detector placement was in the tray, it did NOT result in any harm to the patient. Therefore, it was apparent that not following the protocol, but rather applying the advocated method of placing the detector in the tray, was also acceptable. This method is also supported by Tugwell-Allsup *et al.* (2020: 258).

The preferred SID, proposed at 100 cm, was applied in only 46% of procedures, while some radiographers still opted for a shorter SID of 90 cm. Possible explanations for this occurrence might be the height of the radiographer or the restriction on the vertical movement of the mobile machine.



© Central University of Technology, Free State

Regarding the exposure factors, the desired kVp and mAs settings for combined CXR-AXR were 54 kVp and 1.80 mAs. Nevertheless, none of the radiographers selected these exposures, with the most common exposure settings being 55 kVp and 1.60 mAs. The suggested exposure factors for CXR on the imaging protocol were 57–60 kVp and 0.80m As. The protocol exposure factors were ignored and the habitual 52 kVp and 1.60m as were applied.

For the positioning criteria, the radiographers mostly complied and showed improvement from phase 2 to phase 4. Arm abduction increased from 73% to 96%, while the head position improved from 79% to 82% and the chin position from 71% to 88%.

The standardised imaging protocol suggested a straight main radiation beam. In 98% of X-rays, the radiographers complied with this technical feature. Table 4.21 summarises the results of the Pick The Ending standardised imaging protocol as performed by the participating radiographers during phase 4 of the study. For example, the standardised imaging protocol proposed arm abduction, and in 96% of the procedures, arm abduction was applied during X-ray acquisition. However, despite the imaging protocol suggesting detector placement directly underneath the neonate, this was adhered to in only 12% of the X-rays. All the aspects noted in the table, with their respective results, represent the factors proposed for a standardised imaging protocol.



© Central University of Technology, Free State

**Table 4.21.** Results of implementation of the one-pager protocol (n=50).

| | | |
|---|---|---|
| **POSITIONING FACTORS** | | |
| Arms abducted from the body | 96% | |
| Immobilisation technique for the arms: radiographer holding the patient | 46% | |
| Head facing up | 82% | |
| Immobilisation technique for the head: radiographer holding and sandbags | 30% | |
| Chin lifted | 88% | |
| Immobilisation technique for the chin: radiographer holding | 32% | |
| No rotation of the pelvis | 50% | |
| No rotation of the thorax | 58% | |
| **TECHNICAL FACTORS** | | |
| Lead marker placed | 4% | |
| Detector placement directly underneath the patient | 12% | |
| Detector placement under the mattress | 56% | |
| Source-to-object distance (SOD) 98 cm | 20% | |
| Source-to-image distance (SID) 100 cm | 46% | |
| No angulation of the radiation beam | 98% | |
| **EXPOSURE FACTORS** | | |
| | **CXR** | **Combo** |
| Kilovoltage peak (kVp) value | 38%; 55 kVp | 40%; 55 kVp |
| Milliampere second (mAs) value | 50%; 1.6 mAs | 49%; 1.6 mAs |
| Exposure index (chest 50–200; combo 125–500) | 100% | 76% |
| Deviation index (DI=0) | 0% | 7% |

Combo, combined chest and abdominal X-rays; CXR, chest X-rays.

The next part of the checklist pertained to the anatomical structures included and their visibility on the X-ray image. The statistical findings for this part of the checklist are summarised in Table 4.22. The results reflect the 45 (90%) combined CXR-AXR examinations, as this was the most performed examination type throughout phase 4. The entire abdomen including the symphysis pubis were included in 94% of the images.



© Central University of Technology, Free State

**Table 4.22.** Part 2 and 3, criteria 1 to 4 of the implementation checklist for combined chest and abdominal X-rays (n=45).

| | |
|---|---|
| **CHEST X-RAY** | |
| **CRITERION 1: ANATOMICAL STRUCTURES INCLUDED** | |
| C7 superiorly | 98% |
| Bilateral costophrenic angles | 100% |
| Soft tissue laterally | 100% |
| ⅓ of the upper abdomen | 6% |
| Only up to level of gastric bubble | 0% |
| Mid-abdomen to IC | 0% |
| Entire abdomen including SP | 94% |
| **CRITERION 2: ANATOMICAL STRUCTURES VISIBLE** | |
| Air-filled trachea | 100% |
| Carina | 98% |
| Lung markings | 100% |
| Hilar regions | 100% |
| Sharp heart border | 100% |
| Sharp costophrenic angles | 100% |
| Stomach bubble | 100% |
| **ABDOMINAL X-RAY** | |
| **CRITERION 3: ANATOMICAL STRUCTURES INCLUDED** | |
| Costophrenic angle superiorly | 100% |
| Symphysis pubis inferiorly | 100% |
| Soft tissue laterally | 100% |
| **CRITERION 4: ANATOMICAL STRUCTURES VISIBLE** | |
| Stomach bubble | 100% |
| Gas-bowel pattern | 100% |

Part 4 of the implementation checklist was based on the post-processing performed by the radiographer before finally signing off the image. These factors included collimation, rotation and image quality. Table 4.23 presents the statistical analysis of these variables. The results represent the combined CXR-AXR (n=45), which were performed more frequently than CXR (n=3) and AXR (n=2).



© Central University of Technology, Free State

**Table 4.23.** Part 4 of the implementation checklist.

| POST-PROCESSING REQUIRED | Percentage |
|---|---|
| Collimation too big | 48% |
| *Top border structures visible on the image* | |
| Chin (correct structure included) | 78% |
| Eye level | 20% |
| Top of skull | 0% |
| *Bottom border structures visible on the image* | |
| Iliac crest | 2% |
| Symphysis pubis (correct structure included) | 64% |
| Knees | 28% |
| Collimation too small (cut-off) | 2% |
| Overexposed (image too dark) | 4% |
| Underexposed (image to white) | 2% |
| Small rotation correction required | 28% |
| Electronic marker placement | 96% |
| Repetition of the procedure | 6% |

Table 4.23 indicates the collimation sizes for the respective examination types, with 78% of the X-rays collimating with the top border on the chin, while in 20% of procedures, the top border was placed on the eye level. The bottom border was placed on the iliac crest only 2% of the time and 64% on the symphysis pubis, while the collimation included the neonates' knees in 28% of cases.

The most common reason for repetition was anatomical cut-off (2%), and artefacts (2%) and rotation (2%) visible on the image. These findings are presented in Figure 4.53 below.



© Central University of Technology, Free State

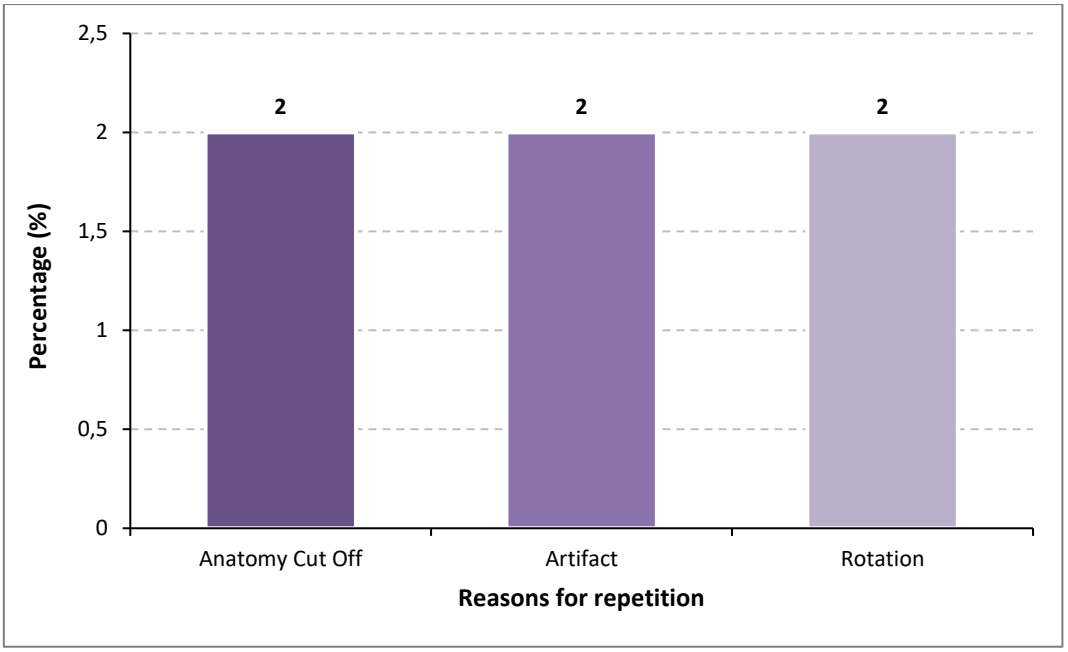



**Figure 4.53.** Reasons for repetition of X-rays (phase 4; n=45).

Table 4.24 shows that 16 (32%) X-rays obtained during the implementation phase produced an optimal image. The neonate's head and chin were facing up, with the arms abducted from the body. Neither thoracic nor pelvic rotation was visible on these images.



© Central University of Technology, Free State

**Table 4.24.** Optimal positioning technique for imaging protocols (phase 4).

| Arms abducted | Head up | Chin up | Rotation of the pelvis | Rotation of the thorax | n-value (%) |
|---|---|---|---|---|---|
| No | No | No | None | None | 1 (2) |
| No | Yes | No | None | None | 1 (2) |
| Yes | No | No | Minimal | Minimal | 1 (2) |
| Yes | No | No | n/a | None | 1 (2) |
| Yes | No | No | None | None | 1 (2) |
| Yes | No | Yes | Minimal | None | 1 (2) |
| Yes | No | Yes | None | Minimal | 1 (2) |
| Yes | No | Yes | None | None | 3 (6) |
| Yes | Yes | No | Minimal | None | 1 (2) |
| Yes | Yes | Yes | Minimal | Minimal | 9 (18) |
| Yes | Yes | Yes | Minimal | Moderate | 2 (4) |
| Yes | Yes | Yes | Minimal | None | 4 (8) |
| Yes | Yes | Yes | Moderate | Minimal | 3 (6) |
| Yes | Yes | Yes | Moderate | Moderate | 3 (6) |
| Yes | Yes | Yes | None | Minimal | 1 (2) |
| Yes | Yes | Yes | None | Moderate | 1 (2) |
| Yes | Yes | Yes | None | None | 16 (32) |

The findings of the fourth phase (implementation) were compared to the results from the second phase (observation). These findings are discussed in section 4.7, representing the next phase of the study (phase 5 – reflection).

## 4.7 PHASE 5: REFLECTION

During the reflection, the researcher compared the observational and implementation checklists completed in the second and fourth phase of the study, respectively. This comparison established if an improvement in positioning technique, exposure factors and image critique occurred after implementing the imaging protocol. In particular, differences between phases 2 and 4 regarding immobilisation techniques, rotation, lead marker and detector placement, main radiation beam direction, exposure factors (kVp and mAs) and changes in the exposure index were evaluated.

During phase 2, the most common immobilisation technique was the radiographers holding the patients during the X-ray exposure, which remained the case in phase 4. By comparing the head and chin position for the combined images (most X-rays performed during phase 4),



© Central University of Technology, Free State

the "head facing up" declined by 2%, while the "chin lifted" requirements increased by 10%. The participating radiographers complied with the positioning suggestions made by the proposed imaging protocol as supported by Lampignano and Kendrick (2021), Pedersen *et al.* (2018), Whitley *et al.* (2015) and Long *et al.* (2019). However, the most common immobilisation technique applied remains “rad assist” irrespective of the suggestions made by SAHPRA (2022: 17).

Rotation increased tremendously from phase 2 to phase 4. Rotation of the thorax increased from 6% to 42%, while pelvic rotation increased from 2% to 48%. For both the thorax and pelvis, the degree of rotation observed and honestly reported in phase 4, was mostly minimal to moderate, as presented in Figure 4.46.

The lead marker placement was reduced from 65% (phase 2) to 4% (phase 4). For detector placement during phase 2, tray placement was preferred, whereas placement under the mattress was selected by the radiographers during phase 4. This proved adherence to the imaging protocol. The placement of a lead marker in the primary radiation field is also a requirement of HPCSA (2020: 5) as it forms part of the scope of practice for radiographers in South Africa.

Moolman, Mulla and Mdletshe (2020: 120) concluded from their study that a majority of radiographers in South Africa do not understand the function of the exposure index (EI). EI is a mechanism providing feedback to the radiographer regarding their choice of exposure settings. Another article indicated that the EI can be used as a quality assurance tool for monitoring adequate equipment use and function. The authors also explained the importance and confusion of manufacturer-specified EI values as each machine’s EI differs and they proposed that future studies should investigate standardised EI and DI values (Mothiram *et al.,* 2014: 116).

Figure 4.54 presents the comparison of the exposure index captured during phase 4 and phase 2. The optimal EI of 50–200 for CXR was not exceeded in phase 4, which was the case during phase 2. In both phases, the minimum EI value remained inside the recommended EI range. Statistical analysis proved that there was a significant difference between phase 2 and phase 4 for CXR EI values (p=0.0374). The statistical values are included in Table 4.25.



© Central University of Technology, Free State

**Table 4.25.** Statistical comparison of the exposure index for chest X-rays performed during phases 2 and 4.

| Phase | n | Exposure index for chest X-rays | | | | |
|---|---|---|---|---|---|---|
| | | Median | 25th percentile | 75th percentile | Minimum | Maximum |
| Phase 2 | 109 | 268 | 192 | 341 | 78 | 642 |
| Phase 4 | 3 | 152 | 140 | 163 | 140 | 163 |

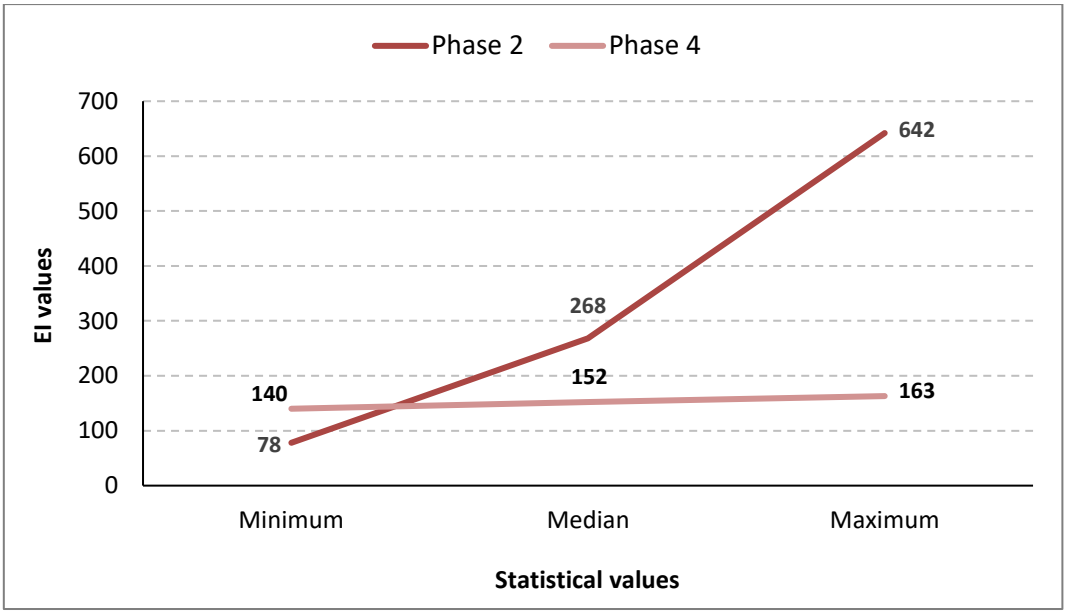



**Figure 4.54.** Comparison of the exposure index for chest X-rays in phase 2 (n=109) versus phase 4 (n=3). Recommended EI range: 50–200.

The optimal EI for abdominal X-rays of 125–500 was exceeded in phase 2, with a maximum EI value of 583. However, in phase 4, the maximum EI value remained well below upper limit at 382. In phase 2, the minimum EI value was below the recommended value. In phase four, the minimum value was inside the manufacturer's recommended EI range. These findings are presented in Figure 4.55. However, statistical analysis confirmed that the difference between the two phases was not significant (p=0.7254).



© Central University of Technology, Free State

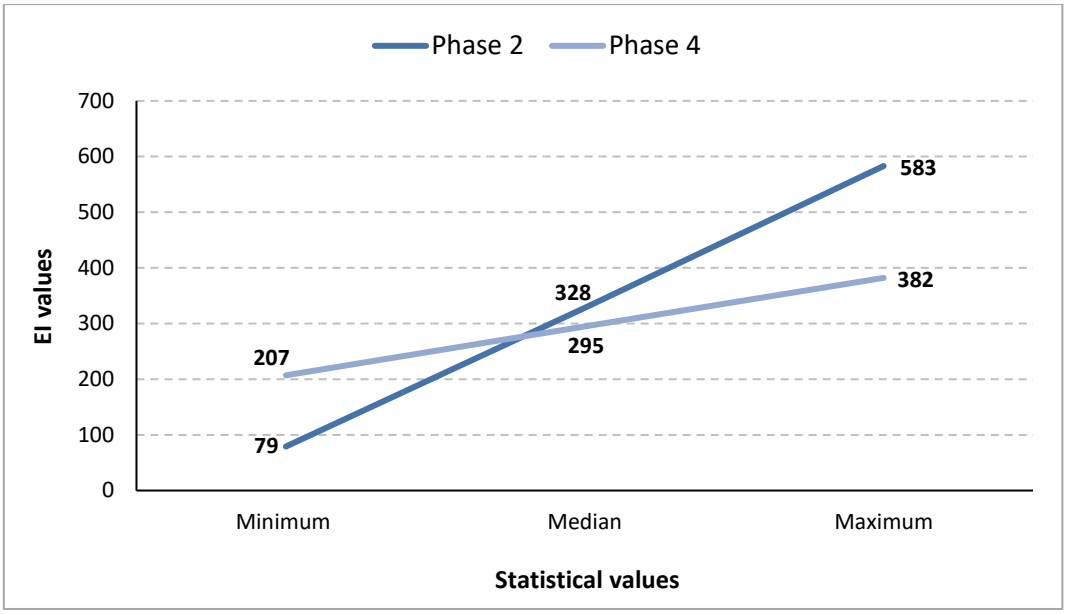



**Figure 4.55.** Comparison of the exposure index for abdominal X-rays in phase 2 (n=16) versus phase 4 (n=2). Recommended EI range: 125–500.

In Figure 4.56, the exposure index for combined CXR-AXR in phase 2 are compared with those of phase 4. The maximum EI value increased from 724 in phase 2 to 849 in phase 4. For both phases, the minimum EI value remained below the recommended value at 78 and 70, respectively. According to the statistical analysis, the p-value < 0.05, (p=0.0008) thus there was a significant difference between the EI values for combined images.

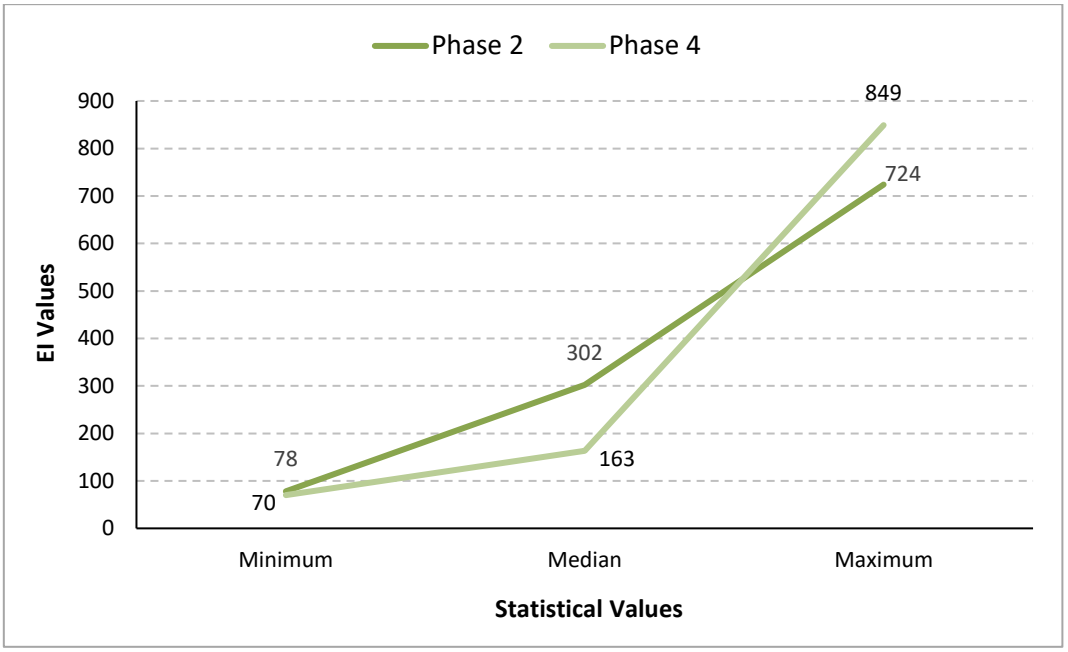



**Figure 4.56.** Comparison of the exposure index for combined chest and abdominal X-rays in phase 2 (n=33) versus phase 4 (n=45). Recommended EI range: 125–500.



© Central University of Technology, Free State

In phase 2, the most common centring point for CXR was the nipple line (n=71; 65%), while for abdominal X-rays and combined X-rays, it was the navel (n=10; 63% and n=21; 64%, respectively). The most common centring point used for CXR in phase 4 was the nipple line in all the images (n=3; 100%). The abdominal centring point was the navel (n=2; 100%). For combined CXR-AXR, the most common centring point used was also the navel (n=25; 56%). During phase 4 (implementation phase) while implementing the one-pager protocol, the radiographers applied the proposed centring points as proposed by literature in Chapter one and the experiments performed in Chapter 3.

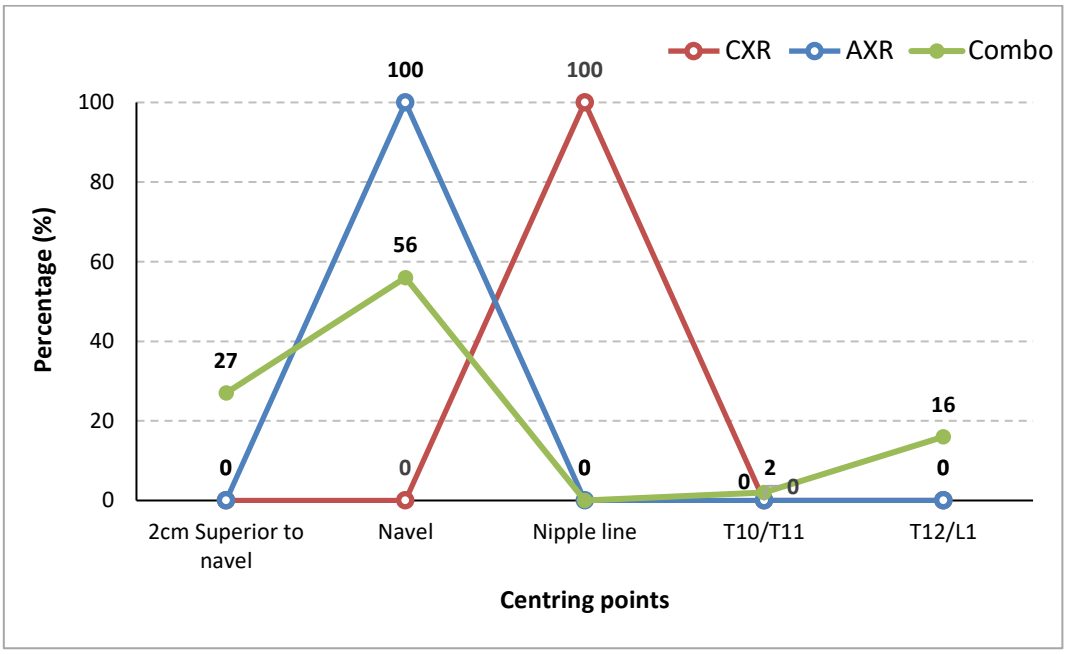



**Figure 4.57.** Centring points X-rays in phase 4 (chest X-rays [CXR] n=3; abdominal X-rays [AXR] n=2; combined chest and abdominal X-rays [Combo] n=45).

Pedersen *et al.* (2018: 262) states that collimation remains a crucial key factor in producing high quality radiographic images while keeping the radiation dose low. The authors indicated that tight transverse collimation makes a big difference in radiation dose by preventing irradiation of the upper arms. The authors indicated that the radiographers preferred larger craniocaudal collimation due to uncertainty of a specific centring point. The authors indicated that the specific centring point on a topographic landmark remains a gap in the literature, which is addressed by this study's collimation guidelines presented in Chapter 2, figure 2.11.

Table 4.26 summarises the findings of the comparison between phase 2 and phase 4 image evaluation regarding the inclusion and visibility of important anatomical structures. For phase 4, the results are mainly based on combined images representing the majority (n=45) of X-rays performed. Phase 2 results were calculated for 109 CXR, 16 AXR and 33 combined CXR-



© Central University of Technology, Free State

AXR images. Inclusion of the entire abdomen and the symphysis pubis increased from 24% to 94%.

**Table 4.26.** Comparison of image evaluation of phase 2 versus phase 4.

| PART 3: IMAGE EVALUATION | PHASE 2 | PHASE 4 |
|---|---|---|
| **CHEST X-RAYS** | **n=109** | **n=45** |
| **Criterion 1: anatomical structures included** | | |
| C7 superiorly | 100% | 98% |
| Bilateral costophrenic angles | 99% | 100% |
| Soft tissue laterally | 100% | 100% |
| ⅓ of the upper abdomen | 49% | 6% |
| Only up to level of gastric bubble | 16% | 0% |
| Mid-abdomen to IC | 12% | 0% |
| Entire abdomen including SP | 24% | 94% |
| **Criterion 2: anatomical structures visible** | | |
| Air-filled trachea | 100% | 100% |
| Carina | 100% | 98% |
| Lung markings | 100% | 100% |
| Hilar regions | 100% | 100% |
| Sharp heart border | 100% | 100% |
| Sharp costophrenic angles | 100% | 100% |
| Stomach bubble | 100% | 100% |
| **ABDOMINAL X-RAYS** | **n=16** | **n=45** |
| **Criterion 3: anatomical structures included** | | |
| Costophrenic angled superiorly | 100% | 100% |
| Symphysis pubis inferiorly | 100% | 100% |
| Soft tissue laterally | 100% | 100% |
| **Criterion 4: anatomical structures visible** | | |
| Stomach bubble | 100% | 100% |
| Gas-bowel pattern | 100% | 100% |

C7, 7$^{th}$ cervical vertebra; IC, iliac crest; SP, symphysis pubis.

Table 4.27 shows the post-processing techniques required. The results of phase 2 and phase 4 were compared to determine whether a significant difference in collimation size, exposure factors and rotation could be observed.



© Central University of Technology, Free State

**Table 4.27.** Comparison of post-processing required in phase 2 versus phase 4.

| Post-processing required | Phase 2 | Phase 4 |
|---|---|---|
| Collimation too big | 41% | 48% |
| Top border | – | 20% |
| Bottom border | – | 28% |
| Collimation too small (cut-off) | 2% | 2% |
| Overexposed (image too dark) | 9% | 4% |
| Underexposed (image to white) | 8% | 2% |
| Small rotational correction required (malalignment) | 14% | 28% |
| Electronic marker placement | 34% | 96% |

## 4.8 CONCLUSION

In this chapter, the results of phases 2 to 4 (observation, experiment and implementation) were summarised. All statistical analyses were presented and discussed in depth. Phase 2 and phase 4 findings were compared to determine whether implementing the standardised imaging protocol yielded a significant difference in the outcomes of the X-rays.

In Chapter 4, we saw the results of the second, third and fourths phases with a comparison between phase 2 (observational phase) and phase 4 (implementation phase). The results of arm immobilisation as well as the head and chin immobilisation were shown in this chapter. The most common immobilisation technique remained radiographers holding the neonate during image acquisition. The no rotation requirement of the thorax and pelvis were kept mainly with 58% and 50%, respectively. The lead marker placement was lower than in phase 2, with an absent physical lead marker in 96% of cases. The detector placement was most placed underneath the mattress (56%) and a straight main radiation beam was applied (98%). The exposure factor selection for each radiographic examination was displayed in Figures 4.50 and 4.51 respectively. Table 4.21 provides the results of the implementation of the one-pager protocol and Table 4.22 shows the adherence to the inclusion criteria of the important anatomical structures.

After presenting the results of the reflection phase, not all participants adhered to the proposed imaging protocol. The exposure index minimum increased from 78 during phase 2 to 140 during phase 4 while the maximum EI decreased from 642 to 163. Thus, during phase 4 the EI remained within the recommended range for chest X-rays. For the combined CXR-AXR, the EI increased from 724 to 849 which is above the recommended range and indicates overexposure of the images and leading to increased radiation dose to the neonates.



© Central University of Technology, Free State

Figure 4.57 shows the centring points for the different radiographic examinations, showing that most of the participants made use of the recommended centring points of the proposed imaging protocol.

In Chapter 5, the recommendations and limitations of the study, as well as possibilities for future research are discussed.



© Central University of Technology, Free State

# CHAPTER 5
## CONCLUSION, RECOMMENDATIONS, LIMITATIONS AND SIGNIFICANCE OF THE STUDY

### 5.1 INTRODUCTION

In this chapter, each objective, how they were met, the results obtained for each objective and research phase are discussed. Recommendations and limitations of the study are presented. Future research opportunities of a similar topic are proposed.

### 5.2 OVERVIEW OF THE STUDY

The main aim of this study was to design standardised imaging protocols for chest (CXR), abdominal (AXR) and combined chest and abdominal X-ray (CXR-AXR) images for neonatal patients in the neonatal intensive care unit (NICU). To achieve this aim, five objectives had to be achieved and each objective represented a phase of the study. The findings for each objective are discussed independently below.

**Objective 1** (Phase 1: Literature survey)

For the first objective, previously published imaging protocols were obtained to benchmark the observational checklist and the proposed baseline imaging protocols for the experimental phase for neonatal mobile CXR, AXR and combined CXR-AXR images. This objective was discussed in Chapter 2. Appendix M presents the literature on imaging protocols for the CXR, AXR and combined CXR-AXR imaging protocols. These literature-based imaging protocols were tested in the experimental phase. The literature survey presented the imaging protocols used during the third phase of the study. The survey presented in Chapter 3, Table 3.7, shows examples of the literature protocol for CXR, and Tables 3.10 and 3.12 indicate the protocol for AXR and combined CXR-AXR images, respectively. As seen from these tables, the literature available for these two types of imaging is lacking and requires more information.

**Objective 2** (Phase 2: Observations)

Observation of radiographers and nursing staff in their workspace was done during neonatal mobile CXR, AXR and combined image acquisition. All the imaging protocols used in the


© Central University of Technology, Free State

workspace were recorded. Appendix A shows the observational checklist used during phase 2 of the study to achieve the second objective.

The methods employed to meet this objective are discussed in Chapter 3 and the results of the objective in Chapter 4. During this phase, a total of 158 X-ray images were observed, which included 109 CXR, 16 AXR and 33 combined CXR-AXR images. During the observation, lead markers were used in 56% cases of image acquisition, while in61% of procedures, the detector was placed inside the detector tray. The source-to-image distance (SID) was set at 100 cm for 66% of the images, and 84% of the X-rays were performed with a straight main radiation beam. The results of the observation, along with the literature evaluated, allowed the researcher to create experimental protocols that were tested during phase 3 of the study. Phase 2 of the study produced 68 CXR, 45 AXR and 45 combined CXR-AXR imaging protocols that were tested during the experimental phase.

**Objective 3** (Phase 3: Experiment)

The estimated entrance skin dose for the different imaging protocols (recorded from the literature survey and observed in the workspace within the recommended exposure range) was compared to optimise the baseline imaging protocol. The experimental checklist is attached in Appendix C.

During this phase of the study, the researcher performed an experiment on a phantom neonate, testing the different imaging protocols while measuring the radiation dose produced for dose optimisation purposes. For each of the 68 CXR, 45 AXR and 45 combined CXR-AXR imaging protocols, each protocol was repeated three times to ensure accuracy with dose measurement.

For statistical analysis of the third phase, 56 CXR, 43 AXR and 41 combined CXR-AXR images were included in the analysis. Eighteen imaging protocols were excluded from the statistical analysis as they did not adhere to the required criteria. The experimental phase produced standardised imaging protocols implemented during the fourth phase. The CXR protocol is presented in Table 4.13 (Chapter 4). This protocol indicated that applying CXR exposure factors of 60 kVp and 0.8 mAs, at an SID of 100 cm and an OID of 0 cm with a straight main radiation beam, will provide an optimal EI, DI and ESD. The standardised imaging protocol for combined CXR-AXR images is presented in Table 4.15 (Chapter 4). This protocol indicated when radiographers apply exposure factors of 54 kVp and 1.8 mAs, at an



© Central University of Technology, Free State

SID of 100 cm and an OID of 2 cm with a straight main radiation beam, it will provide an optimal ESD. The experiment did not produce an optimal AXR imaging protocol.

**Objective 4** (Phase 4: Implementation)

The (standardised and optimised) baseline imaging protocols were implemented. To meet this objective in the fourth phase, participants first received training on performing the imaging and correct completion of the implementation checklist (Appendix B) through the PowerPoint presentation (Appendix P). The PowerPoint presentation was also used to explain the purpose and aim of the study to the participating radiographers, and to elaborate on what was expected of them. The training included the checklist completion steps and factors on the checklist. The participating radiographers were given the implementation checklists to complete during their daily routine images in the NICU. The standardised imaging protocol (one-pager) is presented as Appendix Q.

The radiographers did not entirely adhere to the protocol, as indicated in Chapter 4 (Table 4.23). The divergence from the optimal EI and DI could be attributed to the lack of applying the proposed exposure factors from the standardised imaging protocol, which is an important matter to be addressed by this specific department.

**Objective 5** (Phase 5: Reflection)

The effect that the implemented baseline imaging protocol had on the exposure index (for dose optimisation) and image critique were determined by comparing the results of phase 2 to that of phase 4.

The statistics from phase 2 were compared to that of phase 4 by the statistician. The findings are presented and discussed in Chapter 4. The exposure index (EI) was compared between these two phases. The DI and ESD were not measured during the second phase (observation phase). Consequently, an adequate comparison of these two factors could not be made between phases 2 and 4. Some of the positioning, technical and exposure factors were also compared between these two phases to determine validity and efficient use of the imaging protocol.

During phase 5 of the study, it was shown that the exposure index (EI) for CXR images was not exceeded during either of the phases compared, and the EI remained well inside the recommended range. For AXR images, the maximum EI did not exceed the manufacturer's



© Central University of Technology, Free State

recommendations. The maximum EI was exceeded in the second phase but not in phase 4, reflecting an improvement in the maximum EI value from phase 2 to phase 4. The comparison for combined CXR-AXR images showed that the minimum EI remained within the recommended EI range. In both phase 2 and phase 4, one of the values exceeded the manufacturer's recommended maximum EI. Thus, in neither phase 2 nor phase 4 the EI remained consistently inside the recommended range, and the images produced were still under- or overexposed.

## 5.3 RECOMMENDATIONS FOR THE APPLICATION OF A STANDARDISED PROTOCOL

A standardised protocol for the radiology department was proposed after the experimental phase was conducted to optimise the EI, DI and ESD. Although participating radiographers implemented the standardised imaging protocol for two weeks, certain recommendations are presented for best practice.

The radiographers complied with the positioning criteria, which improved from phase 2 to phase 4. However, most radiographers still applied their own technique with relation to immobilisation techniques and exposure factors.

Schaefer-Prokop, Neitzel, Venema, Uffmann and Prokop (2008: 1822) found that most radiographers favour overexposed over underexposed images during portable or paediatric radiography, to limit complaints or repeats related to exposure factors. This unnecessary increase in exposure factors leads to a phenomenon referred to as dose creep, which is the gradual increase of exposure parameters of certain X-ray examinations and ultimately the increase in radiation dose to the patient. The authors also emphasised that dose creep is very important when working with patients receiving multiple follow-up examinations, such as those admitted in intensive care units (ICU), and especially vulnerable patient groups, such as neonatal and paediatric patients (Schaefer-Prokop *et al*., 2008: 1822). Kim, Kim, Kang and Park (2019: 758) stated that dose creep is the unnecessary radiation exposure delivered to patients due to the negligence of the medical staff or even the lack of adequate experience. According to Choi, Cheon, Lee, Choi, Shin, Cho and Park (2020: 491), digital radiography (DR) systems have the potential to reduce the radiation dose received by patients and improve the performance of medical imaging. Thus, most neonatal units should convert from computed radiography systems to advanced technology, such as DR, to improve patient outcomes.



© Central University of Technology, Free State

Concerning immobilisation techniques, most radiographers held the neonate themselves instead of using immobilisation techniques such as sandbags, despite radiographers being taught not to hold the neonate themselves, speaking from experience. This is an important radiation protection factor that the department should focus on.

Lead marker placement decreased significantly to 4% in phase 4. The department accepts post-processing electronic markers for infection control purposes, especially with neonatal patients, as the markers were previously not cleaned sufficiently between patients. It is always recommended to place a physical lead marker to limit confusion during post-processing because of image orientation or possible congenital disorders. Titley and Cosson (2014: 43) also indicate that the presence of an anatomical lead marker in the primary radiation field is a medico-legal requirement. The department can implement rigorous infection control measures, especially for lead markers, to ensure their constant use and application. A study performed by Chung, Kumar, Oldfield, Phillips and Stratfold (2020: 12), stated that most radiographers lean toward electronic lead markers rather than placing a physical lead marker. This study highlighted the importance of physical lead markers, as it was performed in a paediatric setting where the radiograph obtained could be the child's first X-ray, and the placement of the physical lead marker is crucial for diagnostic purposes of possible congenital abnormalities. The study also identified several barriers to placing physical lead markers that should be taken into consideration when discussing the radiographers' hesitation to place the physical lead markers. Infection control was identified as a challenge when performing mobile X-rays, as the physical lead markers might contain microorganisms that could be transferred between patients. The authors further stated that radiographers have an option to place an electronic marker during post-processing, but this could be missed because of busy workloads and time constraints; thus, using a physical lead marker is still recommended as best practice (Chung *et al*., 2020: 12).

While the detector placement was recommended to be directly underneath the neonate, with compliance in only 12% of procedures, the detector was placed below the mattress in 56% of the X-rays. Singh and Pradham (2015: 79) evaluated neonatal chest imaging by comparing the image quality and dose for contact techniques versus under-tray techniques. They concluded that there was a small decrease in image sharpness and an increase in noise when placing the detector in the detector tray. These authors also proposed that the exposure factors should be altered between the two techniques due to the different placement of the detector and indicated that the dose received by the detector when placed in the tray will be lower than that of the detector placed underneath the neonate due to an air gap (Singh & Pradham, 2015: 79). As the participating radiographers mainly placed the detectors



© Central University of Technology, Free State

underneath the mattress, the difference in SID is not as great as when placed inside the detector. The radiographers also selected their own exposure factors; thus, it is difficult to know whether they adjusted the exposure factors due to patient size or because of detector placement.

In most of the procedures of the observational phase (phase 2), the anatomical structures required to be included were visible on the X-rays. The collimation was too big in approximately half of the images (48%), and 28% included the neonate's knees with the lower collimator, while 20% included the neonates' eyes with the top collimator. Collimation that is too big increases the radiation dose to the neonate significantly. The collimation applied reduces the volume of tissues irradiated; thus, decreasing the patient exposure and radiation dose (Stollfuss, Schneider & Kruger-Stollfuss, 2015: 119). This should be addressed in training. Stollfuss *et al*. (2015: 119) reported that the exposure of non-thoracic structures occurred frequently, and the complete or partial inclusion of the humeri was the most common finding in neonatal chest imaging due to incorrect collimation. In another study, Pedersen et al. (2018: 262) also acknowledged that careful collimation is an important factor in producing high-quality X-rays complying with the ALARA principle. This study also identified that the craniocaudal height of the collimation is difficult to establish for radiographers when they are uncertain of the anatomical landmarks in the thorax. Consequently, a gap in the literature was identified, as limited published literature is available to identify the surface anatomy of neonates (Pedersen *et al*., 2018: 262). A collimation diagram has been presented in Chapter 2 (Figure 2.11), where the researcher identified the craniocaudal and transverse collimation lines for collimation on neonatal CXR and AXR images using anatomical landmarks.

The proposed exposure factors for the combined CXR-AXR images were mostly ignored as the participating radiographers selected their own exposure factors. Therefore, the images remained underexposed compared to the exposure factors tested on the phantom. Only 7% of images had an optimal DI (cf. Table 4.21).

The participants who did not adhere to the protocol and still set their own exposure factors were still considered a crucial part of the study as each radiographer, patient and circumstance differ. Therefore no one can predict the different factors to be taken into consideration for each patient and each radiographer. Thus, one can provide the radiographers with a framework and they can build on an imaging protocol based on their experience and specific environment.

A recommendation from the study to implement standardised exposure factors is to adapt the exposure settings to requirements of the specific machine (make and model) used and apply



© Central University of Technology, Free State

the exposure factors as they would be set for an actual neonate patient instead of the phantom used during this study. This could be done by consulting experienced radiographers at the specific practice, or by reviewing previously acquired X-ray images and comparing the exposure settings. The exposure index for CXR remains 50–200, and 100% of the X-rays in the implementation phase were inside this recommended range. For the combined CXR-AXR images obtained, no participants selected the preferred kVp (54 kVp), but for 42% of the X-rays, a higher kVp value (55–56k kVp) was selected. Although1.80 mAs was the preferred setting of the protocol for the combined X-rays, no one selected the proposed value, with 51% of the exposures were performed at 2–2.50 mAs), which was notably higher than the desired setting. Bwanga and Bwalya (2021: 1168) stated there are several advantages of performing regular clinical audits. These advantages include improving patient care, upholding professional standards, promoting effective use of resources, enhancing job satisfaction and participating in educational activities.

Irsal (2021: 3) asserted that exposure factor parameters are influenced by several contributing aspects. The radiographers should keep in mind the neonate's age, the source-to-image distance (SID), the body habitus of the neonate, and the technique used for image acquisition. These factors, along with the selected exposure factors, all play a role in the radiation dose received by the neonate (Irsal, 2021: 3).

As a result, 89% of the AXR and combined CXR-AXR images were within the suggested EI range of 125–500. The EI is evaluated by radiographers to confirm the amount of radiation exposure, since there is a linear relationship between the EI value and the detector exposure (Cohen *et al.*, 2010: 593).

It was a matter of concern, however, that only 7% of the combined images reached the desired deviation index (DI) for the combined CXR-AXR procedures (DI=0). The DI is a simple numerical value to indicate the extent to which the EI value deviates from the intended and recommended EI range of the specific manufacturer for that exposure (Creeden & Curtis, 2020: 309). The finding that only 7% of combined images reached an optimal DI value during phase 4, indicated that the exposure factors applied during mobile examinations were not optimal and resulted in under- or overexposed images. Of the combined cases, 62% produced a DI value below zero, indicating underexposed images, while 36% of the combined X-rays were overexposed, with a DI value above zero. According to Moolman *et al.* (2020: 120) most radiographers in South Africa have a very poor understanding of the functionality of exposure index and how to incorporate it as a tool in reviewing a radiographic image.



© Central University of Technology, Free State

Bwanga (2020: 478) found that radiographers were reluctant to participate in continuous professional development (CPD) activities due to several factors. These factors included attitudinal, physical and structural barriers. Attitudinal barriers were further broken down into a lack of motivation and the feeling that some topics were irrelevant. Physical barriers included time constraints and limited learning resources, while structural barriers were a lack of knowledge, shortage of staff or lack of support (Bwanga, 2020: 477). All these factors are possible reasons for the poor implementation of the standardised imaging protocol during the fourth phase of the current study.

Another study (Su, Chen, Yeh, Chen, Tsai, Wu, Yang, Tey & Lin, 2023: 350) highlighted the unnecessary radiation exposure (URE) to neonatal patients in the NICU. The risk of radiation-induced damage to tissues and cells are much higher in neonates and paediatric patients than in adults at the same radiation dose. These authors also indicated that the application of the ALARA principle to reduce URE to neonates in very preterm neonates was unclear. They concluded that URE in neonates in the NICU was quite common and that training should be of high importance when requesting X-rays for these patients. Furthermore, improper positioning techniques and the lack of immobilisation were identified as some of the concerning factors leading to repeat X-rays, which increases the radiation dose received by the neonate. It was recommended that point-of-care ultrasound for lung disorders should be performed to reduce the radiation dose to the neonate. Another recommendation was proper training for all medical staff to adhere to the guidelines and follow standard protocols for diagnostic radiography (Su *et al*., 2023: 350). These findings confirm that the results of the current study can make a positive contribution to reduce URE and the radiation dose to neonatal patients by ensuring optimal image quality and a decrease in the repetition rate.

The barriers and enablers of implementing the protocol designed can be explored. The protocol can further be tested in other settings to evaluate the generalisability.

## 5.4 RECOMMENDATIONS FOR INFECTION CONTROL

In Table 3.8 (Chapter 3), the type of infection control measures applied by radiographers before and after interaction with the neonates were presented. It was found that in 36% of X-rays, radiographers applied no infection control before or after having contact with the patient. In 22% of procedures, radiographers washed their hands before the interaction, while they washed their hands before and after interaction with the neonates in only 18% of cases, Furthermore, radiographers only sanitised their hands for 13% of the procedures performed, instead of applying a complete and thorough hand-washing technique. The findings presented



© Central University of Technology, Free State

here could be used to the department's advantage as it identifies the shortcomings of the staff relating to infection control. Polin, Denson and Brady (2012: 1085) stated that health-care-associated infections have considerable health and economic consequences. The authors also concluded that these types of infections are important medical morbidity facing a very vulnerable population. The authors proposed that each healthcare provider should know their role in improving infection control and preventing health-care-associated infections as this remains a team effort (Polin *et al.,* 2012: 1091). The Free State Department of Health states in its directorate that hospital hygiene remains the responsibility of the management as well as all personnel, visitors and patients. They also indicated that a basic hand-washing technique is the cheapest, easiest and most effective way to reduce the risk of transmitting microorganisms (Free State Department of Health, 2008: 4).

## 5.5 VALIDITY AND RELIABILITY

Both the observational and implementation checklists were benchmarked and piloted on a smaller patient group before the primary study. This assured the reliability of the checklists and allowed sufficient time to correct any errors and make the necessary changes to ensure efficient use and the addition of relevant data. For the observational checklist, the researcher changed the layout to allow smooth and quick completion. No changes were made on the implementation checklist after the pilot study. The experimental checklist used during the third phase of the study was piloted on the same phantom and with the same mobile X-ray unit used in the primary study. This allowed the researcher to adapt the checklist as needed. No changes were made to the experimental checklist as the completion went smoothly and all relevant factors had already been included.

For each exposure made during the experimental phase (phase 3), the researcher kept all factors constant while changing only the one factor to be tested, known as the variable. The observational checklist during the second phase was completed with the same consistency as it was done by the researcher During the fourth phase consistency was attempted by training the participating radiographers to implement the protocol by means of providing a one pager and a neonatal imaging training presentation. Four radiographers completed the implementation checklists and used their experience and discretion when analysing images and image quality. This may have influenced the consistency of the checklist data slightly, but as image analysis forms part of the radiographers' scope of practice it remained that way during the implementation without interference from the researcher. It seemed as if radiographers were recording a true picture without hiding "non-compliant" aspects, for example 36% of cases minimal rotation was recorded and the selection of exposure factors.



© Central University of Technology, Free State

The recording of image analysis is a true picture of daily actions, and therefore a valid presentation of the usage of a protocol in this hospital.

## 5.6 CONTRIBUTION OF THE STUDY

The significance of this study lies in the standardised imaging protocol designed and created from the literature, observations made, and results obtained by putting the proposed protocols through several steps of experimentation. This imaging protocol can be adapted according to the specific needs of each department and hospital to motivate consistency when imaging neonatal patients in the NICU. The proposed imaging protocol will guide the user regarding several factors contributing to the acquired X-ray image such as the positioning, technical and exposure factors selected.

The imaging protocol can contribute to student radiographers' basic education and assist with implementation techniques when imaging neonatal patients to ensure an optimal image with diagnostic value. It may also allow junior radiographers to engage with neonatal patients with more confidence, as a basic framework is set out with this standardised imaging protocol, which could prevent errors or repeats due to a lack of experience.

The standardised imaging protocol compiled during this study can also be adapted to ensure consistency with any other X-ray examinations. It is not necessarily limited to neonatal X-rays.

By making use of this standardised imaging protocol, it could assist both junior and senior radiographers, as well as student radiographers, to obtain consistent X-ray images. This imaging protocol indicates the relevant anatomy to be included in the image. The implementation of the protocol intends the application of a consistent positioning technique with radiographer shift changes. Consequently, it could produce uniform image quality and image presentation regarding exposure and technical factors. For example, placing the detector in the same place (directly underneath the patient or in the detector tray), and consistently using the same source-to-image distance (SID), will reduce the magnification of anatomical structures.

The standardised imaging protocol can also serve as an encouragement for the radiographer to confidently image neonatal patients. Radiography students are taught to limit repeats on neonates, and by using this imaging protocol, restricting the number of repeats could be achieved by providing a framework for radiographers to deal with this specific patient group.



© Central University of Technology, Free State

A single protocol was compiled and presented as a one-pager to be implemented in any radiology department and can be adjusted to that department's distinctive needs and regulations. The CXR, AXR as well as the combined CXR-AXR imaging protocols are presented on a single page regarding positioning techniques, technical factors, and exposure factors. The one-pager also includes collimation guidelines with topical landmarks as a visual demonstration for the radiographer. This one-pager can easily be attached to a mobile X-ray machine and is a quick and easy read providing guidelines prior to image acquisition.

The exposure factors for an optimal ESD were deduced from the findings in the experimental phase. An optimal ESD was achieved by selecting 54 kVp and 1.80 mAs exposure factors when performing a combined CXR-AXR.

The implementation phase confirmed that radiographer-assisted immobilisation when performing the imaging reduced substantially from phase 2 to phase 4. For example, the position of the head facing upwards, as preferred, improved from 79% to 82% of the procedures, and the radiographer's assistance as an immobilisation technique reduced from 78% to 30% during image acquisition.

The protocol can be used periodically to observe best practice as was observed in this study. For example, lead marker use decreased from 65% to 4% during phase 4. The recommended source-to-image distance (SID) of 100 cm indicated in the imaging protocol reduced from 66% in phase 2 to 46% phase 4. Both these examples reflect practices of non-adherence.

Phase 1 (literature search) determined that optimal exposure factors include 55–58 kVp and 1.8–2.2 mAs. However, when performing the experiments (phase 3), it was determined that optimal exposure factors should be set at 57–60 kVp and 0.8 mAs. Furthermore, to obtain an optimal CXR image, the ESD should be less than 50 µGy and an SID of 100 cm should be applied.

## 5.7 LIMITATIONS OF THE STUDY

Numerous protocols were tested on the phantom during the experimental phase. However, disparities between the phantom and a real-life neonate could provide a differential absorbed radiation dose (ESD) due to tissue thickness and absorption factors. Consequently, exposure factors might differ slightly to reach an optimal exposure and deviation index.



© Central University of Technology, Free State

The implementation phase comprised mostly (90%) combined CXR-AXR examinations and very few CXR and AXR images. This limitation did not allow the researcher to make a comprehensive and accurate comparison between phase 2 and phase 4 for these specific X-ray examinations. Even though the experimental phase of the study provided a complete optimal standardised imaging protocol for CXR, it could not be implemented and reflected on as thoroughly to make valid conclusions.

None of the AXR protocols tested during the experimental phase provided an optimal DI, EI or ESD. Abdominal X-ray images were also the least performed examination during the observational and experimental phases. To reduce radiation dose and risk patient motion, future research could investigate the necessity of performing AXR images instead of obtaining a combined X-ray.

Another limitation of the study was that the researcher did not increase or decrease the exposure factors at random to find an optimal protocol for AXR and combined CXR-AXR. One of the objectives of the study was to test the preset protocols during phase 3 (experimental phase). This could be done during future studies to determine a precise protocol especially for abdominal radiographs.

In future, a higher number of only CXR examinations could be observed. However, in this hospital, mainly combined CXR-AXR imaging was requested by the physicians. The effectiveness of the collimation for the chest could not be evaluated in phase 4 and should be included in future studies.

Another important limitation of the study to note is the difference between a neonatal patient and the anthropomorphic phantom. The tissue thickness, patient size and absorption factors of the tissues are not the same, thus this could alter the exposure factors set. It is important to remember that the exposure factors should be adjusted according to patient size and habitual body type (Bontrager & Lampignano, 2014; Lampignano & Kendrick, 2021: 36).

## 5.8 RECOMMENDATIONS TO ADDRESS THE LIMITATIONS OF THE STUDY

Recommendations from the study include focusing on one examination type with fewer imaging protocols to test during the experimental phase, to evaluate more specific technical and exposure factors and combinations of different factors. Future research could also focus more on only mobile abdominal X-rays in the NICU, as limited data regarding these examinations were generated in this study. The barriers and enablers of implementing the



© Central University of Technology, Free State

protocol designed can be explored. The protocol can further be tested in other settings to evaluate the generalisability.

## 5.9 FEEDBACK TO THE RADIOLOGY DEPARTMENT REGARDING IN-SERVICE TRAINING

The researcher was privileged to have the opportunity to attempt implementation of a standardised protocol. During feedback to the department where the research was conducted, it would be important to acknowledge that most of the factors were implemented, and the subsequent improvements recorded. The department should also be informed about the areas where the best practice could be perfected.

The participating radiographers improved remarkably on the positioning techniques proposed by the standardised imaging protocol. However, it can be improved even more as these factors have a notable effect on image quality and diagnostic value of the image. Arm abduction (96%) and both the head (82%) and chin (88%) positions improved from phase 2 to phase 4.

During the implementation phase, radiation protection in terms of physical lead protection was lacking in most cases (99%), which could be improved with radiographer and nurse cooperation. Furthermore, collimation remained too big (48%) during image acquisition as implemented by the participating radiographers. This is another issue that the department could address to reduce radiation dose to the neonates and provide higher quality images.

For many of the X-ray examinations, the technical factors were not implemented as suggested by the standardised imaging protocol. The department could still apply the proposed recommendations but adjust the exposure factors until they reach optimal EI, DI and ESD. This could form part of an in-service training course for the department, and by doing this, they may adjust and personalise the imaging protocol for their specific needs.

In only 15% of cases, the identity of the patient was confirmed, and in 24%, the X-rays requested, and type of examination required were confirmed. This issue is another important factor the department has to address urgently to limit confusion and duplication of images. It will also ensure that the correct patient is X-rayed for the appropriate examination, and that X-rays are not performed incorrectly or unnecessarily.



© Central University of Technology, Free State

## 5.10 FINAL REMARKS

The research question was addressed in a positive sense, resulting in the establishment of image acquisition techniques and radiation protection measures to compile standardise neonatal CXR and AXR imaging protocols for alignment with dose optimisation principles. The standardised imaging protocol implemented in this study made a beneficial contribution when considering image uniformity and dose optimisation principles.

Comprehensive implementation of these protocols was challenging as every radiographer was trained differently and in a different era. Therefore, a new standardised imaging protocol can be to the advantage of all radiographers despite their training and background, as this protocol is based on has its foundation in current practice and modern technology. The researcher is optimistic that implementing this protocol and adhering to it, will reduce the radiation dose to neonatal patients when X-rays are required for diagnostic purposes.



© Central University of Technology, Free State

# BIBLIOGRAPHY


Al-Bar, M.A. & Chamsi-Pasha, H. 2015. *Contemporary Bioethics*. London: Springer.

Al-Murshedi, S.H., Hogg, P. & England, A. 2018. A comparative assessment of pathology visibility and radiation dose for routine neonatal chest radiography examinations in eight hospitals. *European Society of Radiology*, 1–7.

Alzen, G. & Benz-Bohm, G. 2011. Radiation protection in pediatric radiology. *Deutsches Ärzteblatt International*, 108(24):407–414.

Angrosino, M.V. 2007. *Naturalistic Observation*. 1st ed. London: Left Coast Press Inc.

Applegate, K. 2015. Image Gently: a campaign to promote radiation protection for children worldwide. *South African Journal of Radiology,* 19(2):a919.

Aramesh, M., Zanganeh, K.A., Dehdashtian, M., Malekian, A. & Fatahiasl, J. 2017. Evaluation of radiation dose received by premature neonates admitted to neonatal intensive care unit. *Clinical Medicine & Research*, 9(2):124–129.

Armpilia, C., Fife, I.A.J. & Croasdale, P.L. 2001. Radiation doses to neonates and issues of radiation protection in a special care baby unit. IAEA-CN-85-52, 539–543. Available at: https://inis.iaea.org/collection/NCLCollectionStore/_Public/32/039/32039928.pdf (accessed 24 July 2024).

Arthur, R. 2001. The neonatal chest X-ray. *Pediatric Respiratory Reviews*, 2(4):322–323.

Atherton, D.J., Gennery, A.R. & Cant, A.J. 2004. The neonate. In: Burns, T., Breathnach, S., Cox, N. & Griffiths, C. eds. *Rook's Textbook of Dermatology.* 7th ed. Vol. 1. Oxford: Blackwell Science Ltd., p. 14.1.

Avasthi, A., Ghosh, A., Sarkar, S. & Grover, S. 2013. Ethics in medical research: general principles with special reference to psychiatric research. *Indian Journal of Psychiatry*, 55(1):86–91.

Bahreyni Toossi, M.T. & Malekzadeh, M. 2012. Radiation dose to newborns in neonatal intensive care units. *Iranian Journal of Radiology*, 9(3):145–149.

Ball, J.L., Moore, A.D. & Turner, S. 2008. *Ball and Moore's Essential Physics for Radiographers.* 4th ed. Oxford: Blackwell Publishing.

Beauchamp, T.L. 2007. The 'four principles' approach to health care ethics. In: Ashcroft, R.E., Dawson, A., Draper, H. & McMillan, J.R., eds. *Principles of Health Care Ethics.* 2nd ed. Hoboken, NJ: John Wiley & Sons, p. 3–10.




© Central University of Technology, Free State

Bontrager, K.L. & Lampignano, J.P. 2014. *Textbook of Radiographic Positioning and Related Anatomy*. 8th ed. St. Louis, MO: Mosby Elsevier.

Bwanga, O. 2020. Barriers to continuing professional development (CPD) in radiography: a review of literature from Africa. *Health Professions Education*, 6(4):472–480.

Bwanga, O. & Bwalya, M. 2021. Clinical audit in diagnostic radiography. *British Journal of Medical & Health Sciences,* 3(10):1168–1172.

Choi, G., Cheon, J., Lee, S., Choi, Y.H., Shin, S.H., Cho, Y.J. & Park, S.W. 2020. Development of quality- controlled low-dose protocols for radiography in the neonatal ICU using a new mobile digital radiography system. *American Journal of Roentgenology*, 215(2):488–493.

Chowdhury, I.A. 2015. Issue of quality in qualitative research: an overview. *Innovative Issues and Approaches in Social Sciences*. 8(1):142–162.

Chung, L., Kumar, S., Oldfield, J., Phillips, M. & Stratfold, M. 2020. A clinical audit of anatomical side marker use in a pediatric medical imaging department: a quantitative and qualitative investigation. *PLoS One*, 15(11):e0242594.

Cohen, M.D., Cooper, M.L., Piersall, K. & Apgar, B.K. 2011. Quality assurance: using the exposure index and the deviation index to monitor radiation exposure for portable chest radiographs in neonates. *Pediatric Radiology*, 41(5):592–601.

Compagnone, G., Pagan, L. & Bergamini, C. 2005. Comparison of six phantoms for entrance skin dose evaluation in 11 standard X-ray examinations. *Journal of Applied Clinical Medical Physics*, 6(1):101–113.

Creeden, A. & Curtis, M. 2020. Optimising default radiographic exposure factors using deviation index. *Radiography (London)*, 26(4):308–313.

Crowe, S., Cresswell, K., Robertson, A., Huby, G., Avery, A. & Sheikh, A. 2011. The case study approach. *BMC Medical Research Methodology*, 11:100.

Décima, P., Stéphan-Blanchard, E., Pelletier, A., Ghyselen, L., Delanaud, S., Degrugilliers, L., Telliez, F., Bach, V. & Libert, J. 2012. Assessment of radiation temperature in a closed incubator. *European Journal of Applied Physiology*, 112(8):2957–2968.

Del Rosario Pérez M. 2015. Referral criteria and clinical decision support: radiological protection aspects for justification. *Annals of the ICRP*, 44(1 Suppl):276–287.



© Central University of Technology, Free State

Del Vecchio, A., Salerno, S., Barbagallo, M., Chirico, G., Campoleoni, M., Cannata, V., Genovese, E., Granata, C., Magistrelli, A. & Toma, P. 2020. Italian inter-society expert panel position on radiological exposure in neonatal intensive care units. *Italian Journal of Pediatrics*, 46(1):159.

DeMaio, D.N., Herrmann, T., Noble, L.B., Orth, D., Peterson, P., Young, J. & Odle, T.G. 2019. Best practices in digital radiography. *Radiologic Technology,* 91(2):198–201.

Don, S., MacDougall, R., Strauss, K., Moore, Q.T., Goske, M.J., Cohen, M., Herrmann, T., John, S.D., Noble, L., Morrison, G., Lehman, L. & Whiting, B.R. 2013. Image Gently campaign back to basics initiative: ten steps to help manage radiation dose in pediatric digital radiography. *American Journal of Roentgenology*, 200(5):431–436.

Ebdon-Jackson, S. & Friya, G. 2021. Improving justification of medical exposures using ionising radiation: considerations and approaches from the European Society of Radiology. *Insights into Imaging*, 12(1):2.

European Commission (EC). 1996. European guidelines on quality criteria for diagnostic radiographic images in paediatrics. EUR 161261 EN. Available at: https://op.europa.eu/en/publication-detail/-/publication/47eb62b0-698d-4166-bc34-cc3f8d07d2e3 (accessed 3 August 2024).

European Commission (EC). 2012. What are the health effects of exposure to ionizing radiation? Available at: https://ec.europa.eu/health/scientific_committees/opinions_layman/security-scanners/en/l-3/5-health-effect-radiation.htm (accessed 3 August 2024).

Faulkner, K., Barry, J.L. & Smalley, P. 1989. Radiation dose to neonates on a special care baby unit. *British Journal of Radiology*, 62(735):230–233.

Free State Department of Health. 2008. Infection prevention and control manual. Available at: https://www.health.fs.gov.za/wp-content/uploads/2011/07/Infection-prevention-and-control-Manual.pdf (accessed 24 November 2024).

Friedrich-Nel, H., van der Merwe, B. & Kotze, B. 2018. Neonatal chest image quality addressed through training to enhance radiographer awareness. *Health SA Gesondheid*. 23:1067.

Fox, N.S., Brennan, J.S. & Chasen, S.T. 2008. Clinical estimation of fetal weight and the Hawthorne effect. *European Journal of Obstetrics & Gynecology and Reproductive Biology*, 141(2):111–114.



© Central University of Technology, Free State

Govender, V., Ntholeng, T., Vawda, F. & Larson, C.O. 2013. The profile of indications for radiography in the neonatal intensive care unit at Universitas Academic Hospital, Bloemfontein. *South African Journal of Child Health*, 7(1):30–34.

Guba, E.G. 1981. Criteria for assessing the trustworthiness of naturalistic inquiries. *Educational Technology Research and Development*, 29(2):75–91.

Gunn, C., O'Brien, K., Fossa, K., Tonkopi, E., Lanca, L., Martins, C.T., Muller, H., Friedrich-Nel., H, Abdolell, M. & Johansen, S. 2019. A multi institutional comparison of imaging dose and technique protocols for neonatal chest radiography. *Radiography (London)*, 26(2):e66–e72.

Gupta, N. & Chawla, S. 2023. Reducing radiation dose in neonates: small efforts make big changes. *Indian Pediatrics*, 60(7):519–520.

Hanna, M., Shah, R., Marquez, L., Barzegar, R., Gordon, A. & Pammi, M. 2023. Infant isolation and cohorting for preventing or reducing transmission of healthcare-associated infections in neonatal units. *Cochrane Database of Systematic Reviews*, 6(6):CD012458.

Heale, R. & Twycross, A. 2015. Validity and reliability in quantitative studies. *Evidence-Based Nursing*, 18(3):66–67.

Health Professions Council of South Africa (HPCSA) 2020. Professional Board for Radiography and Clinical Technology: Scope of Practice: Diagnostic Radiography. Pretoria: HPCSA. Available at: https://www.hpcsa.co.za/Uploads/professional_boards/rct/guidelines/RCT_Scope_of_Practice_Diagnostic_Rad_22_May_2020_for%20Current_Scope.pdf (accessed 9 November 2024).

Huba, W. 2014. Kerma-area product in diagnostic radiology. *American Journal of Roentgenology*, 203(6):565–569.

International Atomic Energy Agency (IAEA) 2007. Dosimetry in diagnostic radiology: an international code of practice. Technical Reports Series No. 457. Vienna: IAEA. Available at: https://www.iaea.org/publications/7638/dosimetry-in-diagnostic-radiology-an-international-code-of-practice (accessed 6 August 2024).

International Atomic Energy Agency (IAEA). 2012. Radiation protection in paediatric radiology. Safety Reports Series No. 71. Vienna: IAEA. Available at: https://www-pub.iaea.org/mtcd/publications/pdf/pub1543_web.pdf (accessed 3 August 2014).



© Central University of Technology, Free State

International Commission on Radiological Protection (ICRP). 2007. The 2007 Recommendations of the International Commission on Radiological Protection. ICRP Publication 103. *Annals of the ICRP*, 37(2-4):1–339. Available at: https://journals.sagepub.com/doi/pdf/10.1177/ANIB_37_2-4 (accessed 3 August 2024).

Irsal, M. 2021. Exposure factor control with exposure index guide as optimizing efforts in chest Pa examination. *Journal of Physics: Conference Series*, 1842:012059.

Jain, S.N., Modi, T. & Varma, R.U. 2021. Decoding the neonatal chest radiograph: an insight into neonatal respiratory distress. *Indian Journal of Radiology and Imaging*, 30(4):482–492.

James, B. & Kelly, B. 2013. The abdominal radiograph. *Ulster Medical Journal*, 82(3):179–187.

Karami, V., Zabihzadeh, M., Isavand-Faraji, A. & Karampour, H. 2019. Radiological protection in the neonatal intensive care units (NICUs): a retrospective and observational audit at two teaching hospitals. *Journal of Pediatric and Neonatal Individualized Medicine*, 8(1):e080126.

Kartikeswar, G.A.P., Parikh, T.B., Pandya, D. & Pandit, A. 2019. Ionizing radiation exposure in NICU. *Indian Journal of Pediatrics*, 87(2):158–160.

Khalid, K., Hilman, H. & Kumar, D., 2012. Get along with quantitative research process. *International Journal of Research in Management*, 2(2):15–29.

Kim, K.T., Kim, K.B., Kang, S.S. & Park, J.K. 2019. The necessity of resetting the filter criteria for the minimization of dose creep in digital imaging systems. *Journal of the Korean Society of Radiology*, 13(5):757–763.

Kumar, R. 2011. *Research Methodology. A Step-by-Step Guide for Beginners*. 3rd ed. London: SAGE Publications Ltd.

Kyoto Kagaku. 2020. Newborn Whole Body Phantom “PBU-80”. Japan. Available at: https://www.kyotokagaku.com/en/products_data/ph-50b/ (accessed 13 November 2024).

Lampignano, J.P. & Kendrick, L.E. 2021. *Bontrager’s Textbook of Radiographic Positioning and Related Anatomy.* 10th ed. St. Louis, MO: Elsevier.

Lee, H. 2011. Plain abdominal radiography in infants and children. *Korean Journal Pediatric Gastroenterology*, 14(2):130–136.



© Central University of Technology, Free State

Lim, I. 2017. KUB – AP pediatric abdomen. Available at: https://www.radtechonduty.com/2017/05/kub-ap-pediatric-abdomen.html (accessed 3 August 2024).

Long, B.W., Rollins, J.H. & Smith, B.J. 2019. *Merrill's Atlas of Radiographic Positioning & Procedures.* 14th ed. St. Louis, MO: Elsevier.

Malone, J., Guleria, R., Craven, C., Horton, P., Jarvinen, H., Mayo, J., O'Reilly, G., Picano, E., Remedios, D., Le Heron, J., Rehani, M., Holmberg, O. & Czarwinski, R. 2012. Justification of diagnostic medical exposures: some practical issues. Report of an International Atomic Energy Agency Consultation. *British Journal of Radiology*, 85(1013):523–538.

Martire, F., Polito, C., Ciucci, D., Solfaroli Camillocci, E., Longo, M., Genovese, E., Cirillo, M., Tomà, P., Magistrelli, A. & Cannatà, V. 2023. Chest X-ray image quality assessment in a pediatric cardiac intensive care unit. *Radiation Physics and Chemistry*, 205:110740.

Maruyama, T. & Yamamoto, H. 2008. [Study of positioning techniques for radiography] [Article in Japanese]. *Nippon Hoshasen Gijutsu Gakkai Zasshi,* 64(1):25–34.

McQuillen Martensen, K. 2011. *Radiographic Image Analysis.* 3rd ed. St. Louis, MO: Elsevier.

McQuillen Martensen, K. 2015. *Radiographic Image Analysis*. 4th ed. St. Louis, MO: Elsevier.

Menashe, S.J., Iyer, R.S., Parisi, M.T., Otto, R.K., Weinberger, E. & Stanescu, A.L. 2017. Pediatric abdominal radiographs: common and less common errors. *American Journal of Roentgenology*, 209(2):417–429.

Moolman, N., Mulla, F. & Mdletshe, S. 2020. Radiographer knowledge and practice of paediatric radiation dose protocols in digital radiography in Gauteng. *Radiography*, 26(2):117–121.

Mothiram, U., Brennan, P.C., Lewis, S.J., Moran, B. & Robinson, J. 2014. Digital radiography exposure indices: a review. *Journal of Medical Radiation Sciences*, 61(2):112–118.

Murphy, A. & Bell, D.J. 2021. Entrance skin dose. *Radiopaedia*. Available at: https://radiopaedia.org/articles/entrance-skin-dose (accessed 3 August 2024).

Pathak, G., Kharol, D., Kharol, M. & Chaturvedi, D. 2022. Nurses awareness regarding prevention and control of nosocomial infection in NICU. *International Journal of Multidisciplinary Research*, 3(5):1042–1048.



© Central University of Technology, Free State

Pedersen, C.C.A., Hardy, M. & Blankholm, A.D. 2018. An evaluation of image acquisition techniques, radiographic practice and technical quality in neonatal chest radiography. *Journal of Medical Imaging and Radiation Sciences*, 49(3):257–264.

Peels, R. & Bouter, L. 2023. Replication and trustworthiness. *Accountability in Research*, 30(2):77–87.

Polin, R.A., Denson, S. & Brady, M.T. 2012. Strategies for prevention of health care–associated infections in the NICU. *American Academy of Pediatrics,* 129(4):1085–1093.

Potter, L. & Ward, D. 2024. Chest X-ray (CXR) interpretation. Geeky Medics. Available at: https://geekymedics.com/chest-X-ray-interpretation-a-methodical-approach/ (accessed 3 August 2024].

Quinn, B & Carroll, M. 2023. *Radiography in the Digital Age.* 4th ed. Illinois, USA: Charles C Thomas.

Rohmah, M., Saputri, N. & Bahari, J. 2020. Effectiveness of use of nesting on body weight, oxygen saturation stability, and breath frequency in prematures in NICU room Gambiran Hospital Kediri City. *STRADA Jurnal Ilmiah Kesehatan,* 9(1):119–128.

South African Health Products Regulatory Authority (SAHPRA). 2022. Guideline for code of practice for users of medical X-ray equipment. Available at: https://www.sahpra.org.za/document/guideline-for-code-of-practice-for-users-of-medical-xray-equipment/ (accessed 3 August 2024).

South African Health Products Regulatory Authority (SAHPRA). 2022. Guideline regarding protective clothing. Available at: https://www.sahpra.org.za/wp-content/uploads/2022/09/SAHPGL-RDN-XR-22_v1-Guideline-for-Protective-Clothing.pdf (accessed 24 November 2024).

Schaefer-Prokop, C., Neitzel, U., Venema, H.W., Uffmann, M. & Prokop, M. 2008. Digital chest radiography: an update on modern technology, dose containment and control of image quality. *European Radiology*, 18(9):1818–1830.

Schlaeppi, C., Minotti, C. & Bielicki, J.A. 2024. Infection control in the NICU: the roles of surveillance cultures. *The Pediatric Infectious Disease Journal,* 43(5):175–177.

Seibert, J.A. & Morin, R.L. 2011. The standardized exposure index for digital radiography: an opportunity for optimization of radiation dose to the pediatric population. *Pediatric Radiology*, 41(5):573–581.



© Central University of Technology, Free State

Shamsi, K., Monafred, A.S., Deevband, M.R., Mohsenzadeh, B., Ghorbani, M., Gorji, K.E. & Niksirat, F. 2020. Evaluaiton of effective dose and entrance skin dose in digital radiology, *Polish Journal of Medical Physics and Engineering*, 26(2):119–125.

Shenton, A.K. 2004. Strategies for ensuring trustworthiness in qualitative research projects. *Education for Information*, 22(2):63–75.

Siedlecki, S. 2020. Understanding descriptive research designs and methods. *Clinical Nurse Specialist*, 34(1):8–12.

Siemens Healthineers. 2014. Mobillett Mira Operator Manual March 2014. Erlangen, Germany: Siemens. Available at: https://www.bioclinicalservices.com.au/siemens/clinical/mobilett-mira-operator-manual-march-2014 (accessed 6 August 2024).

Sileyew, J. K. 2020. Research design and methodology. *Semantic Scholar*, Cyberspace. Available at: https://www.scirp.org/reference/referencespapers?referenceid=3043747 (accessed 24 July 2024).

Singh, V.H. & Pradhan, H. 2015. Neonatal chest radiography – comparing image quality and dose for contact-techniques vs. under-tray techniques. *Radiography Open,* 2(1):65–82.

Snyder, H. 2019. Literature review as a research methodology: an overview and guidelines. *Journal of Business Research*, 104:333–339.

Sprawls, P., Jr. 1995. *The Physical Principles of Medical Imaging*. 2nd ed. Madison, WI: Medical Physics Publishing.

Stanford Medicine Children's Health. 2020. The neonatal intensive care unit (NICU). Available at: https://www.stanfordchildrens.org/en/topic/default?id=the-neonatal-intensive-care-unit-nicu-90-P02389 (accessed 3 August 2024).

Stollfuss, J., Schneider, K. & Krüger-Stollfuss, I. 2015. A comparative study of collimation in bedside radiography for preterm infants in two teaching hospitals. *European Journal of Radiology Open*, 2, 118–122.

Su, Y., Chen, Y., Yeh, L., Chen, S., Tsai, Y., Wu, C., Yang, Y., Tey, S. & Lin, C. 2023. Unnecessary radiation exposure during diagnostic radiography in infants in a neonatal intensive care unit: a retrospective cohort study. *European Journal of Pediatrics*, 182(1):343–352.

Sukamolson, S. 2007. Fundamentals of quantitative research. Available at: https://www.researchgate.net/publication/242772176_Fundamentals_of_quantitative_research (accessed 24 July 2024).



© Central University of Technology, Free State

Sutoro, S.G., Irsal, M. & Cahya I. 2023. Implementation of deviation index to optimization principles on radiographic examination using digital radiography. *International Journal of Scientific Research in Science and Technology*, 10(6):57–64.

Swanson, R.A. & Holton, E.F. 2005. *Research in Organizations: Foundations and Methods in Inquiry*. Oakland, CA: Berrett-Koehler Publishers.

Sy, E., Samboju, V. & Mukhdomi, T. 2024. *X-ray Image Production Procedures*. Treasure Island, FL: StatPearls Publishing. Available at: https://www.ncbi.nlm.nih.gov/books/NBK564352/ (accessed 4 August 2024).

Taherdoost, H. 2021. Data collection methods and tools for research; a step-by-step guide to choose data collection technique for academic and business research projects. *International Journal of Academic Research in Management*, 10(1):10–38.

X-rayTitley, A.G. & Cosson, P. 2014. Radiographer use of anatomical side markers and the latent conditions affecting their use in practice. *Radiography*, 20(1):42–47.

Trotter, C. & Carey, B.E. 2000. Radiology basics: overview and concepts. *Neonatal Network*, 19(2):35–47. Available at: https://connect.springerpub.com/content/sgrnn/19/2/35 (accessed 3 August 2024).

Tugwell-Allsup, J. & England, A. 2020. Imaging neonates within an incubator - a survey to determine existing working practice. *Radiography (London)*, 26(1):e18–e23.

Tugwell-Allsup, J., Morris, R., Hibbs, R. & England, A., 2020. Optimising image quality and radiation dose for neonatal incubator imaging. *Radiography*, 26(4):e258–e263.

Unfors. 1997. Unfors Mult-O-Meter specifications. Hovås, Sweden: Unfors RaySafe AB. Available at: https://www.scribd.com/document/526881498/unfors-mult-o-meter-manual-1 (accessed 18 August 2024).

Whitley, A.S., Jefferson, G., Holmes, K., Sloane, C., Anderson, C. & Hoadley, G. 2015. *Clark's Positioning in Radiography.* 13th ed. London: CRC Press.

Wikimedia Commons. 2023. Normal neonatal chest X-ray. Available at: https://commons.m.wikimedia.org/wiki/File:Normal_neonatal_chest_X-ray.jpg (accessed 3 August 2024).

World Health Organization (WHO). 2020. Radiation. Available at: https://www.who.int/health-topics/radiation#tab=tab_2 (accessed 3 August 2024).

World Health Organization (WHO). 2023. Ionizing radiation and health effects. Available at: https://www.who.int/news-room/fact-sheets/detail/ionizing-radiation-and-health-effects (accessed 3 August 2024).



© Central University of Technology, Free State

World Health Organization (WHO). 2024. Newborn health. Available at: https://www.who.int/westernpacific/health-topics/newborn-health (accessed 3 August 2024).

Yoon, H. 2016. Interpretation of neonatal chest radiography. *Journal of the Korean Society of Radiology*, 74(5):279–290.

Yu, C. 2010. Radiation Safety in the Neonatal Intensive Care Unit: Too Little or Too Much Concern? *Pediatric Neonatology,* 51(6):311-319.



© Central University of Technology, Free State

## APPENDIX A
### OBSERVATIONAL CHECKLIST

**OBSERVATIONAL CHECKLIST**

| | |
|---|---|
| Checklist Number | 2 |
| Radiographer Number | 7 |
| Nurse Number | 4 |

| NEONATAL PATIENT INFO | | | |
|---|---|---|---|
| Gestational age | | | |
| Is the neonate intubated | Yes | | ~~No~~ |
| Type of examination | ~~CXR~~ | AXR | CXR + AXR |

| PART 1: RADIOGRAPHERS | | | |
|---|---|---|---|
| | YES | NO | COMMENT |
| **CRITERIA 1: POSITIONING FACTORS** | | | |
| Arms abducted from body | ✓ | | |
| Immobilisation technique | Rad Holding | | |
| Head facing up | ✓ | | |
| Immobilisation technique | | | |
| Chin lifted | ✓ | | |
| Immobilisation technique | | | |
| Rotation on pelvis | | | |
| Rotation of thorax | | | |
| **CRITERIA 2: TECHNICAL FACTORS** | | | |
| Lead marker placed? | | X | |
| Lead marker placement | On Pt | | On Detector |
| Placement of detector | ~~Inside tray~~ | | Directly under pt |
| Collimation | None | | Size: 24 X 25 |
| Artefacts removed? (i.e. teddy bears, sandbag, dummy clips etc.) | ✓ | | |
| SID (cm) in cm | ± 7cm | | |
| OID (cm) (distance from neonate to detector) | ± 100cm | | |
| Centering point | Sternal angle | | |
| Main beam direction (degrees of angulation) | Straight | | |
| Physical lead protection used (pt): (Elaborate) | – | | |
| Lead equivalence (Pb Eq) | 0.25Pb Eq | | 0.35Pb Eq |
| Detector | CR | | ~~DR~~ |
| Detector speed (Focus) | | | |
| X-Ray mobile machine make | Siemens ~~Mobilex 1~~ | | Siemens Mobilex 2 |
| Generator | 3 phase | | 3 phase |
| Filtration | Al | | Cu |



© Central University of Technology, Free State

| | | |
|---|---|---|
| Incubator brand | Dräger | |
| Mattress thickness (When applicable) | 2cm | |
| **CRITERIA 3: EXPOSURE FACTORS** | | |
| kVp value | 55 | |
| mAs value | 2 | |
| Exposure index | | |
| **CRITERIA 4: INFECTION CONTROL** | | |
| What infection control measures were followed? Elaborate below: | | |
| *Example given: detector was sanitised pre and post x-ray acquisition. Lead marker was sanitised and was not placed on the neonate* Hands washed | | |

**PART 2: NURSING STAFF**

| | YES | NO | COMMENT |
|---|---|---|---|
| **Is it preferred that the radiographer** | | | |
| Touch the neonate | ✓ | | |
| Place Pb protection directly on the pt | | ✓ | |
| Abduct the arms of the neonate | ✓ | | |
| Turn the head of the neonate | ✓ | | |
| Lift the chin of the neonate | ✓ | | |
| Move lines out of the FoV | | ✓ | |
| Place detector directly under them. | | | |
| Place the detector under the mattress | | | |
| Place the detector in the detector tray | | | |
| Comments radiographer/nurse interaction: | | | |
| Warned before exposure (exit room) | ✓ | | |
| Provided nurse shielding (in room) | | ✓ | |
| Extra: | | | |

**PART 3: IMAGE EVALUATION**

**CHEST X-RAY**



© Central University of Technology, Free State

| CRITERIA 1: ANATOMICAL STRUCTURES INCLUDED | | | |
|---|---|---|---|
| | YES | NO | COMMENT |
| C7 superiorly | ✓ | | |
| Bilateral costophrenic angles | ✓ | | |
| Soft tissue laterally | ✓ | | |
| ⅓ of the upper abdomen | ✓ | | |
| Only until level of gas bubble | | ✓ | |
| Mid-abdomen to IC | | ✓ | |
| Entire abdomen including SP | | ✓ | |
| **CRITERIA 2: ANATOMICAL STRUCTURES VISIBLE** | | | |
| Air-filled trachea | ✓ | | |
| Carina | ✓ | | |
| Lung markings | ✓ | | |
| Hilar regions | ✓ | | |
| Sharp heart border | ✓ | | |
| Sharp costophrenic angles | ✓ | | |
| Stomach bubble | ✓ | | |
| **ABDOMEN X-RAY** | | | |
| **CRITERIA 3: ANATOMICAL STRUCTURES INCLUDED** | | | |
| Costophrenic angled superiorly | | | |
| Symphysis pubis inferiorly | | | |
| Soft tissue laterally | | | |
| **CRITERIA 4: ANATOMICAL STRUCTURES VISIBLE** | | | |
| Stomach bubble | | | |
| Gas-bowel pattern | | | |

| PART 4: POST PROCESSING REQUIRED | |
|---|---|
| Collimation too big | ✓ |
| Collimation too small (cut-off) | |
| Overexposed (image too dark) | |
| Underexposed (image to white) | |
| Image requires small rotation (malalignment) | |
| Electronic marker placement | ✓ |



© Central University of Technology, Free State

# APPENDIX B

## EXPERIMENTAL CHECKLIST

To be completed during experiment (EI/DI on image), IAK from dosimeter. ESD calculated. EAK measured by dosimeter under phantom. AD calculated.

| Expnr | Collimation length (cm) | Collimation width (cm) | FOV (cm)² | SSD (cm) | Part thickness (cm) | OID (cm) | EI rep 1 | EI rep 2 | EI rep 3 | DI rep 1 | DI rep 2 | DI rep 3 | IAK rep 1 (µGy) | IAK rep 2 (µGy) | IAK rep 3 (µGy) | EAK rep 1 (µGy) | EAK rep 2 (µGy) | EAK rep 3 (µGy) | ExitSD rep 1 (µGy) | ExitSD rep 2 (µGy) | ExitSD rep 3 (µGy) |
|---|---|---|---|---|---|---|---|---|---|---|---|---|---|---|---|---|---|---|---|---|---|
| 16 | 9 | 12 | 108 | 84,5 | 5,5 | 0 | 969 | 972 | 973 | 6,0 | 6,0 | 6,0 | 107,8 | 107,8 | 107,4 | 4,32 | 4,349 | 4,359 | 18,1319 | 18,25362 | 18,29559 |
| 17 | 9 | 12 | 108 | 84,5 | 5,5 | 0 | 708 | 708 | 709 | 4,5 | 4,5 | 4,5 | 90,91 | 91,48 | 91,6 | 3,358 | 3,341 | 3,34 | 14,0942 | 14,02285 | 14,01865 |
| 18 | 9 | 12 | 108 | 84,5 | 5,5 | 0 | 554 | 553 | 553 | 3,5 | 3,5 | 3,5 | 79,6 | 78,46 | 79,83 | 2,743 | 2,729 | 2,716 | 11,51292 | 11,45416 | 11,3996 |
| 19 | 9 | 12 | 108 | 84,5 | 5,5 | 0 | 761 | 760 | 763 | 5,0 | 5,0 | 5,0 | 81,89 | 81,96 | 82,3 | 3,426 | 3,402 | 3,437 | 14,37961 | 14,27887 | 14,42578 |
| 20 | 9 | 12 | 108 | 84,5 | 5,5 | 0 | 654 | 655 | 655 | 4,0 | 4,0 | 4,0 | 70,65 | 70,81 | 70,99 | 2,977 | 2,974 | 3,006 | 12,49506 | 12,48247 | 12,61678 |
| 21 | 11 | 12 | 132 | 94,5 | 5,5 | 0 | 851 | 853 | 851 | 5,5 | 5,5 | 5,5 | 82,01 | 82,33 | 82,01 | 3,607 | 3,063 | 3,609 | 15,1393 | 12,85602 | 15,14769 |
| 22 | 9 | 12 | 108 | 74,5 | 5,5 | 0 | 1146 | 1146 | 1150 | 6,5 | 6,5 | 6,5 | 142,6 | 142,6 | 142,5 | 5,547 | 5,547 | 5,569 | 23,28187 | 23,28187 | 23,37421 |
| 23 | 10 | 13 | 130 | 84,5 | 5,5 | 0 | 1076 | 1076 | 1079 | 6,5 | 6,5 | 6,5 | 106,3 | 106,7 | 106,3 | 5,872 | 5,889 | 5,791 | 24,64596 | 24,71731 | 24,30599 |
| 24 | 10 | 14 | 140 | 84,5 | 5,5 | 0 | 1122 | 1118 | 1120 | 6,5 | 6,5 | 6,5 | 106,9 | 106,6 | 106,6 | 6,095 | 6,117 | 6,186 | 25,58193 | 25,67427 | 25,96388 |
| 25 | 10 | 12 | 120 | 84,5 | 5,5 | 0 | 1060 | 1060 | 1062 | 6,5 | 6,5 | 6,5 | 107,2 | 107,1 | 106,6 | 7,482 | 7,466 | 7,552 | 31,40345 | 31,3363 | 31,69725 |
| 26 | 10 | 13 | 130 | 84,5 | 5,5 | 0 | 1106 | 1107 | 1110 | 6,5 | 6,5 | 6,5 | 105,7 | 105,4 | 105 | 8,992 | 8,922 | 9,013 | 37,74122 | 37,44742 | 37,82936 |
| 27 | 10 | 12 | 120 | 84,5 | 5,5 | 0 | 1096 | 1097 | 1104 | 6,5 | 6,5 | 6,5 | 85,62 | 85,93 | 87,2 | 4,98 | 5,008 | 3,989 | 20,90206 | 21,01958 | 16,74263 |
| 28 | 10 | 16 | 160 | 84,5 | 5,5 | 0 | 1187 | 1188 | 1192 | 7,0 | 7,0 | 7,0 | 103,2 | 104,2 | 104,3 | 9,365 | 9,347 | 9,371 | 39,30678 | 39,23123 | 39,33196 |
| 29 | 9 | 11 | 99 | 75,5 | 5,5 | 9 | 853 | 859 | 857 | 5,5 | 5,5 | 5,5 | 128,7 | 127,9 | 127,9 | 4,851 | 4,832 | 4,843 | 20,36062 | 20,28087 | 20,32704 |
| 30 | 9 | 11 | 99 | 82,5 | 5,5 | 2 | 927 | 929 | 933 | 5,5 | 5,5 | 5,5 | 112,8 | 113,2 | 112 | 4,531 | 4,5 | 4,485 | 19,01751 | 18,8874 | 18,82444 |
| 31 | 11 | 17 | 187 | 72,5 | 5,5 | 2 | 523 | 525 | 524 | 3,0 | 3,0 | 3,0 | 73,08 | 72,89 | 73,17 | 2,317 | 2,335 | 2,306 | 9,724912 | 9,800462 | 9,678743 |
| 32 | 11 | 17 | 187 | 72,5 | 5,5 | 2 | 662 | 662 | 664 | 4,0 | 4,0 | 4,0 | 81,88 | 81,69 | 81,57 | 2,9 | 2,867 | 2,887 | 12,17188 | 12,03337 | 12,11732 |
| 33 | 11 | 17 | 187 | 72,5 | 5,5 | 2 | 966 | 971 | 967 | 6,0 | 6,0 | 6,0 | 99,26 | 99,73 | 99,47 | 3,863 | 3,795 | 3,844 | 16,21378 | 15,92837 | 16,13404 |
| 34 | 11 | 17 | 187 | 72,5 | 5,5 | 2 | 615 | 613 | 614 | 4,0 | 4,0 | 4,0 | 83,87 | 84,25 | 84,58 | 2,679 | 2,68 | 2,683 | 11,2443 | 11,2485 | 11,26109 |
| 35 | 11 | 17 | 187 | 72,5 | 5,5 | 2 | 815 | 816 | 808 | 5,0 | 5,0 | 5,0 | 110,5 | 110,5 | 111,9 | 3,522 | 3,559 | 3,427 | 14,78254 | 14,93783 | 14,3838 |
| 36 | 10 | 16 | 160 | 82,5 | 5,5 | 2 | 334 | 333 | 334 | 1,5 | 1,0 | 1,5 | 42,09 | 42,19 | 41,97 | 1,432 | 1,446 | 1,401 | 6,010039 | 6,069151 | 5,880277 |
| 37 | 9 | 17 | 153 | 82,5 | 5,5 | 2 | 413 | 414 | 417 | 2,0 | 2,0 | 2,0 | 52,48 | 52,37 | 53,03 | 1,702 | 1,705 | 1,705 | 7,143634 | 7,156226 | 7,156226 |
| 38 | 11 | 16 | 176 | 72,5 | 5,5 | 2 | 498 | 501 | 502 | 3,0 | 3,0 | 3,0 | 72,17 | 72,86 | 73,01 | 2,375 | 2,39 | 2,386 | 9,96835 | 10,03131 | 10,01452 |
| 39 | 11 | 15 | 165 | 72,5 | 5,5 | 2 | 468 | 476 | 479 | 2,5 | 3,0 | 3,0 | 71,84 | 72,76 | 72,57 | 2,288 | 2,318 | 2,384 | 9,603194 | 9,72911 | 10,00612 |
| 40 | 11 | 16 | 176 | 72,5 | 5,5 | 2 | 507 | 507 | 508 | 3,0 | 3,0 | 3,0 | 73,04 | 72,3 | 72,01 | 2,363 | 2,41 | 2,337 | 9,917984 | 10,11525 | 9,808856 |
| 41 | 11 | 15 | 165 | 72,5 | 5,5 | 2 | 486 | 490 | 490 | 3,0 | 3,0 | 3,0 | 72,17 | 72,43 | 72,54 | 2,298 | 2,359 | 2,321 | 9,645166 | 9,901195 | 9,741701 |
| 42 | 10 | 16 | 160 | 72,5 | 5,5 | 2 | 523 | 523 | 524 | 3,0 | 3,0 | 3,0 | 64,36 | 64,34 | 64,37 | 2,282 | 2,272 | 2,29 | 9,57801 | 9,536038 | 9,611588 |
| 43 | 12 | 16 | 192 | 72,5 | 5,5 | 2 | 451 | 451 | 452 | 2,5 | 2,5 | 2,5 | 73 | 72,68 | 73,17 | 2,454 | 2,479 | 2,49 | 10,29993 | 10,40486 | 10,45103 |
| 44 | 9 | 19 | 171 | 65,5 | 5,5 | 9 | 478 | 481 | 480 | 3,0 | 3,0 | 3,0 | 57,97 | 57,86 | 57,76 | 2,283 | 2,282 | 2,288 | 9,582208 | 9,57801 | 9,603194 |
| 45 | 10 | 15 | 150 | 74,5 | 5,5 | 0 | 442 | 441 | 441 | 2,5 | 2,5 | 2,5 | 70,38 | 70,16 | 69,79 | 2,305 | 2,321 | 2,312 | 9,674546 | 9,741701 | 9,703926 |



© Central University of Technology, Free State

**Radiographic image quality evaluation. Answer yes or no in relation to the thee images for the specific experiment:** **Important experimental set-up n**

| Exp nr | Include diaphragm and costophrenic angles | Include symphysis pubis | Include bilateral chest and abdominal walls | Air, soft tissue and fat distinguishable | Cortical outlines of bone visible | Outline of solid organs (liver, stomach) | Gas-bowel pattern visible | Exp nr | Variable tested |
|---|---|---|---|---|---|---|---|---|---|
| 16 | Y | Y | Y | Y | Y | Y | Y | 16 | None Protocol 2 baseline |
| 17 | Y | Y | Y | Y | Y | Y | Y | 17 | Protocol 1 Lower kVp |
| 18 | Y | Y | Y | Y | Y | Y | Y | 18 | Protocol 3 Lower kVp |
| 19 | Y | Y | Y | Y | Y | Y | Y | 19 | Protocol 1 Lower mAs |
| 20 | Y | Y | Y | Y | Y | Y | Y | 20 | Protocol 3 Lower mAs |
| 21 | Y | Y | Y | Y | Y | Y | Y | 21 | Protocol 1 SID |
| 22 | Y | Y | Y | Y | Y | Y | Y | 22 | Protocol 3 SID |
| 23 | Y | Y | Y | Y | Y | Y | Y | 23 | Protocol 1 Collimation U |
| 24 | Y | Y | Y | Y | Y | Y | Y | 24 | Protocol 3 Collimation U |
| 25 | Y | Y | Y | Y | Y | Y | Y | 25 | Protocol 1 Collimation L |
| 26 | Y | Y | Y | Y | Y | Y | Y | 26 | Protocol 3 Collimation L |
| 27 | Y | Y | Y | Y | Y | Y | Y | 27 | Protocol 1 Centering Point |
| 28 | Y | Y | Y | Y | Y | Y | Y | 28 | Protocol 3 Centering Point |
| 29 | Y | N | Y | Y | Y | Y | Y | 29 | Protocol 1 IR Placement |
| 30 | Y | Y | Y | Y | Y | Y | Y | 30 | Protocol 3 IR Placement |
| 31 | Y | Y | Y | Y | Y | Y | Y | 31 | None Protocol 3 baseline |
| 32 | Y | Y | Y | Y | Y | Y | Y | 32 | Protocol 1 Higher kVp |
| 33 | Y | Y | Y | Y | Y | Y | Y | 33 | Protocol 2 Higher kVp |
| 34 | Y | Y | Y | Y | Y | Y | Y | 34 | Protocol 1 Higher mAs |
| 35 | Y | Y | Y | Y | Y | Y | Y | 35 | Protocol 2 Higher mAs |
| 36 | Y | Y | Y | Y | Y | Y | Y | 36 | Protocol 1 SID |
| 37 | Y | Y | Y | Y | Y | Y | Y | 37 | Protocol 2 SID |
| 38 | Y | Y | Y | Y | Y | Y | Y | 38 | Protocol 1 Collimation U |
| 39 | Y | Y | Y | Y | Y | Y | Y | 39 | Protocol 2 Collimation U |
| 40 | Y | Y | Y | Y | Y | Y | Y | 40 | Protocol 1 Collimation L |
| 41 | Y | Y | Y | Y | Y | Y | Y | 41 | Protocol 2 Collimation L |
| 42 | Y | Y | Y | Y | Y | Y | Y | 42 | Protocol 1 Centering Point |
| 43 | Y | Y | Y | Y | Y | Y | Y | 43 | Protocol 2 Centering Point |



© Central University of Technology, Free State

## APPENDIX C

### IMPLEMENTATION CHECKLIST

**IMPLEMENTATION CRITERIA**

**Radiographer Number**..R2.....
**Patient ID**..[redacted].....
**Date**..22/11/23.....
**Exam Type**..CXR + AXR (M).....

# PICK THE ENDING

| POSITIONING FACTORS | | | |
|---|---|---|---|
| Arms abducted from body | Y | | |
| Immobilisation technique of above | Sandbags. | | |
| Head facing up | Y | | |
| Immobilisation technique of above | Sandbags. | | |
| Chin lifted | Y | | |
| Immobilisation technique of above | Sandbags. | | |
| No rotation on pelvis | None | Minimal ✓ | Moderate |
| No rotation of thorax | None | Minimal | Moderate ✓ |

| TECHNICAL FACTORS | | | |
|---|---|---|---|
| Lead marker placed | Yes | No ✓ | Placed but not visible |
| Detector placement | Under pt | Under mattress ✓ | In detector tray |
| Source to object distance (SOD) *Tube to mattress* | 109cm | | |
| Source to image distance (SID) *Tube to detector* | 111 cm. | | |
| Centering point | MSP + middle of Body. | | |
| Angulation of main beam | No | | |

| EXPOSURE FACTORS | |
|---|---|
| kVp value | 55 |
| mAs value | 2,5. |
| Exposure index | 234 |
| Deviation index | 1 |

Turn page over, please



© Central University of Technology, Free State

| CHEST X-RAY | | | |
|---|---|---|---|
| **ANATOMICAL STRUCTURES INCLUDED AND VISIBLE** | | | |
| | | Y | N |
| C7 superiorly | | ✓ | |
| Bilateral costophrenic angles | | ✓ | |
| Soft tissue laterally | | ✓ | |
| ⅓ of the upper abdomen | | ✓ | |
| Only until level of gas bubble | | ✓ | |
| Mid-abdomen to IC | | ✓ | |
| Entire abdomen including SP | | | |
| Air-filled trachea and visible lung markings | | ✓ | |
| Carina and hilar regions | | ✓ | |
| Sharp heart border and costophrenic angle | | | |
| **ABDOMEN X-RAY** | | | |
| **ANATOMICAL STRUCTURES INCLUDED AND VISIBLE** | | | |
| Costophrenic angled superiorly | | ✓ | |
| Symphysis pubis inferiorly | | ✓ | |
| Soft tissue laterally | | ✓ | |
| Stomach bubble | | ✓ | |
| Gas-bowel pattern | | ✓ | |
| **POST PROCESSING REQUIRED** | | | |
| | | Y | N |
| Collimation too big | | | ✓ |
| **Top border** | Chin ✓ | Eye level | Top of skull |
| **Bottom border** | Iliac crest | Symphysis pubis ✓ | Knees |
| Collimation too small (cut-off) | | | ✓ |
| Overexposed (image too dark) | | | ✓ |
| Underexposed (image to white) | | | ✓ |
| Image requires small rotation | | ✓ | |
| Electronic marker placement | | | ✓ |
| Any repeats | | | ✓ |
| Reason for repetition: | | | |



© Central University of Technology, Free State

## APPENDIX D
### PERMISSION FROM HOSPITAL MANAGER

**PERMISSION TO CONDUCT A RESEARCH PROJECT FROM [redacted] HOSPITAL MANAGER**

To the [redacted] Hospital manager

**STUDY TITLE:** A case study to standardise a chest and abdomen imaging protocol for neonates aligned with dose optimization principles.

Radiography is considered a crucial diagnostic method in the identification of pathologies in neonatal patients. Chest radiography was the leading examination performed on pediatric and neonatal patients. Normal routine x-ray imaging in the intensive care units is done with a portable x-ray unit to ensure accurate diagnosis, correct treatment and improved patient status.

This letter serves to request permission to observe the nursing staff in the neonatal intensive care unit which will contribute to the requirements for Master in Radiography (Diagnostics).

The aim of the study is to optimize the dose received by neonatal patients during chest and abdominal x-ray acquisition, by designing a protocol to assist the radiographers in setting adequate technical factors but keeping the image quality consistent and lowering the radiation dose.

The overall goal of the study is to design a standardised protocol for the imaging of the neonatal chest and abdomen, while keeping the dose as low as reasonably achievable. This protocol is to assist the radiographers in imaging the neonatal patients with regards to dose optimisation. The protocol will include different aspects such as positioning techniques, exposure factors and inclusion criteria of anatomy.

The research study's objectives are divided into different tools and phases. The first phase will state the current baseline protocol. It will be established by observing the nursing personnel in the neonatal intensive care unit as well as observation of the radiographers while performing mobile x-ray examinations. The next phase will commence at the Central University of Technology where the observed protocols will be experimented on a phantom. The protocols will then be simulated with the phantom and the mobile machine at the



© Central University of Technology, Free State

hospital. These images obtained will be presented to radiologists at the radiology department where a checklist will be provided to them to determine the diagnostic quality of the images.

An information document will be provided to all staff members involved in the observation or in the by completion of the radiologist checklist. Written consent will also be obtained prior to the observation process. Once consent is obtained the researcher will observe the routine mobile x-ray examinations done in the neonatal intensive care unit. The researcher will complete a checklist with each projection. The completed checklist will be used to determine the baseline protocol which will be executed on a phantom in the second phase of the project.

The protocol will be submitted to the Health Sciences Research Ethics Committee (HSREC) of the University of the Free State for ethical approval and clearance before proceeding with the study.

If you agree to allow permission, a signed copy of this document as well as the information document, which is a written summary of the research project, will be provided to you.

You may contact Ané at 076 146 2473 any time if you have questions or concerns about the research study. HSREC may be contacted on 051 401 7794 for any queries or concerns.

I [redacted], hereby grant permission to Ané Nel to conduct the research project at the named facility.

[redacted] 14/03/2022

Signature of hospital manager Date



© Central University of Technology, Free State

## APPENDIX E

### PERMISSION FROM RADIOLOGY DEPARTMENT

PERMISSION TO CONDUCT A RESEARCH PROJECT FROM THE HEAD OF THE RADIOLOGY DEPARTMENT: [redacted]

To the head of the radiology department at [redacted] Hospital

**STUDY TITLE:** Optimizing and Standardizing neonatal chest and abdomen imaging protocols

This letter serves to request permission to observe the radiographers in the neonatal intensive care unit for twelve weeks and to implement an optimized imaging protocol for four weeks which will contribute to the requirements for Master in Radiography (Diagnostics).
The research proposal will be submitted to the Health Sciences Research Ethics Committee (HSREC) of the University of the Free State for ethical approval and clearance before proceeding with the study.

The overall goal of the study is to standardize a protocol for the x-ray imaging of the neonatal chest and abdomen, thus minimizing the radiation dose. The aim of the study is to develop an imaging protocol to assist radiographers to produce diagnostic/ diagnosable x-ray images of the neonatal chest and abdomen while keeping the radiation dose as low as possible.

The radiographers and nursing staff will be observed in the neonatal intensive care unit to establish a baseline protocol for the imaging of chest and abdominal x-rays. I will accompany them during the routines from 6:00 every day to observe the process and to record the workflow on an observation checklist. I will be in the background and the checklist will be shared with the radiographers after the observation phase is completed These protocols will then be tested by taking x-rays of a phantom with the mobile machine whilst measuring dose with a dosimeter to ensure dose optimization. A final imaging protocol will be established. Our department will implement the optimal protocol for four weeks and the radiographers will then complete the reflection checklist to determine the effectiveness of the protocol.



© Central University of Technology, Free State

An information document will be provided to all staff members involved in the observation. Written consent will also be obtained prior to the observation process.

If you agree to allow permission, a signed copy of this document as well as the the research proposal will be provided to you.

You may contact Ané at 076 146 2473 any time if you have questions or concerns about the research study.

I [redacted], hereby grant permission to Ané Nel to conduct the research project at the named facility.

[redacted] 15/9/22.

Signature of head of radiology department Date



© Central University of Technology, Free State

## APPENDIX F

### PERMISSION FROM THE UNIT MANAGER: NEONATAL INTENSIVE CARE UNIT OF THE HOSPITAL

**PERMISSION TO CONDUCT A RESEARCH PROJECT FROM THE UNIT MANAGER OF THE NEONATAL INTENSIVE CARE UNIT.**

To the unit manager of the neonatal intensive care unit

**STUDY TITLE:** Optimizing and Standardizing neonatal chest and abdomen imaging protocols

Radiography is considered a crucial diagnostic method in the identification of pathologies in neonatal patients. Chest radiography was the leading examination performed on pediatric and neonatal patients. Normal routine x-ray imaging in the intensive care units is done with a portable x-ray unit to ensure accurate diagnosis, correct treatment and improved patient status.

This letter serves to request permission to observe the nursing staff in the neonatal intensive care unit which will contribute to the requirements for Master in Radiography (Diagnostics).

The protocol will be submitted to the Health Sciences Research Ethics Committee (HSREC) of the University of the Free State for ethical approval and clearance before proceeding with the study.

The overall goal of the study is to standardize a protocol for the x-ray imaging of the neonatal chest and abdomen, thus minimizing the radiation dose.

The aim of the study is to develop an imaging protocol to assist radiographers to produce diagnostic/ diagnosable x-ray images of the neonatal chest and abdomen while keeping the radiation dose as low as possible.

The research study's objectives are divided into different tools and phases. The first phase will state the current baseline protocol. It will be established by observing the nursing personnel in the neonatal intensive care unit as well as observation of the radiographers while performing mobile x-ray examinations.



© Central University of Technology, Free State

An information document will be provided to all staff members involved in the observation. Written consent will also be obtained prior to the observation process. Once consent is obtained the researcher will observe the routine mobile x-ray examinations done in the neonatal intensive care unit without interrupting routine workflow.

If you agree to allow permission, a signed copy of this document as well as the information document, which is a written summary of the research project, will be provided to you.

You may contact Ané at 076 146 2473 any time if you have questions or concerns about the research study. HSREC may be contacted on 051 401 7794 for any queries or concerns.

I [redacted], hereby grant permission to Ané Nel to conduct the research project at the named facility.

[redacted] 15/9/22

Signature of unit manager Date



© Central University of Technology, Free State

## APPENDIX G

## APPROVAL FROM THE HEALTH SCIENCES RESEARCH ETHICS COMMITTEE OF THE UNIVERSITY OF THE FREE STATE

UNIVERSITY OF THE FREE STATE
UNIVERSITEIT VAN DIE VRYSTAAT
YUNIVESITHI YA FREISTATA

UFS·UV
HEALTH SCIENCES
GESONDHEIDSWETENSKAPPE

**Health Sciences Research Ethics Committee**

23-Feb-2023

Dear **Mrs Ané Nel**

Ethics Clearance: **Optimizing and Standardizing neonatal chest and abdomen imaging protocols**
Principal Investigator: **Mrs Ané Nel**
Department: **CUT - Central University of Technology**
Submission Page

**APPLICATION APPROVED**

Please ensure that you read the whole document

With reference to your application for ethical clearance with the Faculty of Health Sciences, I am pleased to inform you on behalf of the Health Sciences Research Ethics Committee that you have been granted ethical clearance for your project.

Your ethical clearance number, to be used in all correspondence is:**UFS-HSD2022/1583/2803**

The ethical clearance number is valid for research conducted for one year from issuance. Should you require more time to complete this research, please apply for an extension.

We request that any changes that may take place during the course of your research project be submitted to the HSREC for approval to ensure we are kept up to date with your progress and any ethical implications that may arise. This includes any serious adverse events and/or termination of the study.

A progress report should be submitted within one year of approval, and annually for long term studies. A final report should be submitted at the completion of the study.

**Research conducted in any Department of Health facility:** Researchers are required to sign and return the HSREC approval letters to the provincial Department of Health where they applied. It is also a requirement for researchers to submit electronic copies of their final research findings, and/or make a presentation of their findings and recommendations at departmental research days when and where indicated.

The HSREC functions in compliance with, but not limited to, the following documents and guidelines: The SA National Health Act. No. 61 of 2003; Ethics in Health Research: Principles, Structures and Processes (2015); SA GCP(2020); Declaration of Helsinki; The Belmont Report; The US Office of Human Research Protections 45 CFR 461 (for non-exempt research with human participants conducted or supported by the US Department of Health and Human Services- (HHS), 21 CFR 50, 21 CFR 56; CIOMS; ICH-GCP-E6 Sections 1-4; International Council for Harmonisation (ICH) Harmonised Guideline, Integrated Addendum to ICH E6(R1), Guideline for Good Clinical Practice (GCP) E6(R2), 2016, SAHPRA Guidelines as well as Laws and Regulations with regard to the Control of Medicines, Constitution of the HSREC of the Faculty of Health Sciences.

The Principal Investigator (PI) bears final responsibility for the RIMS application. In the event of any misconduct or improper activities perpetuated by a third party, the PI will be held vicariously liable. The HSREC will bear no responsibility or liability for any actions of a PI and/or third party or breach of confidentiality caused by the PI and/or third party.

For any questions or concerns, please feel free to contact HSREC Administration: 051-4017794/5 or email EthicsFHS@ufs.ac.za.

Thank you for submitting this proposal for ethical clearance and we wish you every success with your research.

Yours Sincerely

Prof. A. Sherriff
Chairperson: Health Sciences Research Ethics Committee

**Health Sciences Research Ethics Committee**
**Office of the Dean: Health Sciences**
T: +27 (0)51 401 7795/7794 | E: ethicsfhs@ufs.ac.za
IRB 00011992; REC 230408-011; IORG 0010096; FWA 00027947
Block D, Dean's Division, Room D104 | P.O. Box/Posbus 339 (Internal Post Box G40) | Bloemfontein 9300 | South Africa
www.ufs.ac.za



© Central University of Technology, Free State

## APPENDIX H

### INFORMED CONSENT FOR PARTICIPATING RADIOGRAPHERS

**INFORMATION DOCUMENT FOR RADIOGRAPHERS**

**STUDY TITLE:** Optimising and Standardising neonatal chest and abdomen imaging protocols.

To whom it may concern

I, Ané Nel, am doing a research project to design an imaging protocol for chest and abdomen on neonatal patients. Qualified radiographers are hereby invited to participate in this research study.

Radiography is considered a crucial diagnostic method in the identification of pathologies in neonatal patients. Chest radiography is the leading examination performed on paediatric and neonatal patients. Normal routine X-ray imaging in the intensive care units is done with a portable X-ray unit to ensure accurate diagnosis, correct treatment and improved patient status.

The aim of the study is to optimise the dose received by neonatal patients during chest and abdominal X-ray acquisition, by designing a protocol to assist the radiographers in setting adequate technical factors but keeping the image quality consistent and lowering the radiation dose. The protocol will include different aspects such as positioning techniques, exposure factors and inclusion criteria of anatomy.

The radiographers and nursing staff will be observed while performing routine mobile X-rayradiographic examinations in the neonatal intensive care unit. I will accompany you to observe the process and to record your workflow on a checklist. In order not to influence your daily routine I will be in the background and the checklist will be shared with you after the observation phase is completed.
Your identification will not be disclosed, and your workflow will be confidential. All information will be kept confidential, and anonymity will be maintained. You will not be identifiable in the reporting of the data. For further information or any concerns of study-related nature, you may contact Ané at 076 146 2473.

The research received ethics approval from the Health Sciences Research Ethics Committee (HSREC) of the University of the Free State. You may contact HSREC on 051 401 7794 for any queries or concerns regarding the study.



© Central University of Technology, Free State

**CONSENT TO PARTICIPATE IN RESEARCH STUDY FOR RADIOGRAPHERS AND TO USE THE INFORMATION GATHERED**

CONSENT TO PARTICIPATE IN RESEARCH STUDY FOR RADIOGRAPHERS AND TO USE THE INFORMATION GATHERED

**STUDY TITLE:** Optimizing and Standardizing neonatal chest and abdomen imaging protocols.

You have been asked to participate in a research study. Participation is voluntary and refusal to participate will involve no penalty or loss of benefits to which the participant is otherwise entitled. The participant may discontinue participation at any time without penalty or loss of benefits to which the participant is otherwise entitled; No remuneration will be given for participation, nor will it cost the participant anything to participate in the study; Confidentiality will be maintained throughout the study and no personal information will be included in publication.

Efforts will be made to keep personal information confidential although absolute confidentiality cannot be assured. Personal information may be disclosed when required by law.

You may contact Ané at 076 146 2473 any time if you have questions or concerns about the research project.

The research study, including the above information has been verbally described to me. I understand what my involvement in the study means and I voluntarily agree to participate. I understand what is required of me and I voluntarily provide consent.

Signature of researcher — Date: 2 May 2023

[redacted] — Signature of radiographer — Date: 02 · 05 · 2023



© Central University of Technology, Free State

## APPENDIX I

### INFORMED CONSENT FOR PARTICIPATING NURSES

## INFORMATION DOCUMENT FOR NURSES

**STUDY TITLE:** Optimising and Standardising neonatal chest and abdomen imaging protocols.

To whom it may concern

I, Ané Nel, am doing a research project to design an imaging protocol for chest and abdomen on neonatal patients. Registered nurses are hereby invited to participate in this research study. Radiography is considered a crucial diagnostic method in the identification of pathologies in neonatal patients. Chest radiography was the leading examination performed on paediatric and neonatal patients. Normal routine radiographic X-ray imaging in the intensive care units is done with a portable X-ray unit to ensure accurate diagnosis, correct treatment and improved patient status.

The aim of the study is to optimise the dose received by neonatal patients during chest and abdominal radiographic X-ray acquisition, by designing a protocol to assist the radiographers in setting adequate technical factors but keeping the image quality consistent and lowering the radiation dose.

The radiographers and nursing staff will be observed while performing mobile radiographic X-ray examinations in the neonatal intensive care unit. I will accompany the radiographer to observe the process and to record the workflow on a checklist. In order not to influence your daily routine I will be in the background and the checklist will be shared with you after the observation phase is completed.

All information will be kept confidential, and anonymity will be maintained. For further information or any concerns of study-related nature, you may contact Ané at 076 146 2473.

The research protocol received ethical approval from the Health Sciences Research Ethics Committee (HSREC) of the University of the Free State You may contact HSREC on 051 401 7794 for any queries or concerns regarding the study.



© Central University of Technology, Free State

**CONSENT TO PARTICIPATE IN RESEARCH FOR NURSES AND TO USE THE INFORMATION GATHERED**

**CONSENT TO PARTICIPATE IN RESEARCH FOR NURSES AND TO USE THE INFORMATION GATHERED**

**STUDY TITLE:** Optimizing and Standardizing neonatal chest and abdomen imaging protocols.

You have been asked to participate in a research study. Participation is voluntary and refusal to participate will involve no penalty or loss of benefits to which the participant is otherwise entitled; The participant may discontinue participation at any time without penalty or loss of benefits to which the participant is otherwise entitled; No remuneration will be given for participation nor will it cost the participant anything to participate in the study; Confidentiality will be maintained throughout the study and no personal information will be included.

Organizations that may inspect or copy your research records for quality assurance purposes and data analysis include groups such as the Ethics Committee for Medical Research and the Medicines Control Council.

You may contact Ané at 076 146 2473 any time if you have questions or concerns about the research project.

The research study, including the above information has been verbally described to me. I understand what my involvement in the study means and I voluntarily agree to participate. I understand what is required of me and I voluntarily provide consent.

Signature of researcher — Date: 17 May 2023

Signature of nurse — Date: 17/5/2023



© Central University of Technology, Free State

## APPENDIX J

### INFORMED CONSENT FROM PARENTS OR GUARDIANS OF NEONATAL PATIENTS

**INFORMATION AND CONSENT DOCUMENT FOR A PARENT OR GUARDIAN OF NEONATAL PATIENTS**

**STUDY TITLE:** Optimizing and Standardizing neonatal chest and abdomen imaging protocols.

Dear Mrs./Mr. [redacted].....

**INTRODUCTION**

I, Ané Nel, invite your child to participate in my research study. I want to observe how the radiographers take the x-rays that the doctor requests as a routine every day. This document will help you decide if your child may participate, and it will explain the entire process. If you have any questions that remain unanswered by this document, please do not hesitate to me.

**PURPOSE OF THE STUDY**

The aim of the study is to develop an imaging protocol to assist radiographers to produce diagnostic/ diagnosable x-ray images of the neonatal chest and abdomen while keeping the radiation dose as low as possible.

**EXPLANATION OF THE PROCEDURE**

The researcher will observe the radiographers and nursing staff in the neonatal intensive care unit while taking x-rays of your child. The researcher will then record this information on a checklist.

**POSSIBLE RISKS INVOLVED**

No risks are involved in participating in this study. No additional images will be taken, only x-rays requested by the pediatrician.

**POSSIBLE BENEFITS OF THIS STUDY**



© Central University of Technology, Free State

Your child may not benefit from this study directly, however the results of this study will allow radiographers in future to limit radiation exposure to babies and to minimize repeat x-rays, which benefits the patient group in the future.

## YOUR CHILD'S RIGHTS AS A PARTICIPANT?

Your child's participation in this study is entirely voluntary. You can refuse participation or stop your child's participation at any time during the study without providing any reason. Your child's lack of participation or withdrawal from the study will not affect his/her treatment or access to x-rays.

## ETHIS APPROVAL

The study received ethical approval from the Health Sciences Research Ethics Committee (HSREC) of the University of the Free State.

You may contact HSREC on 051 401 7794 for any queries or concerns regarding the study.

## INFORMATION AND CONTACT PERSON

The contact person for the study is Ané Nel. If you have any questions regarding the study, please contact her at the following number 076 146 2473. Alternatively, you may contact my supervisors at telephone number 083 272 8647 (Dr Belinda van der Merwe) or 083 270 4663 (Mrs Beatrix van der Linde).

## COMPENSATION

Neither you nor your child will be paid to participate in this research study. There are also no costs involved for your child's participation in this study.

## CONFIDENTIALITY

All information about your child will be kept strictly confidential. Research articles and reports in scientific journals will not include any information regarding you or your child.



© Central University of Technology, Free State

## CONSENT TO PARTICIPATE IN THIS STUDY

- I confirm that the person requesting my consent for my child's participation in this research study has explained the nature of the study, the possible risks and benefits of the study.
- I have received, read and understood the information provided about the study.
- I have had time to ask questions and I have no objections for my child's participation in this study.
- I am aware that the information obtained in the study will be anonymously processed and kept confidential.
- I understand that my child will not be penalized in any way should I decide to discontinue his/her participation in the study and that withdrawal from the study will not affect my child's healthcare.
- My child's participation is voluntary.

[redacted]

Parent/ Legal Guardian's name

[redacted] 30 May 2023

Parent/ Legal Guardian's signature Date

**Mrs. A Nel**

Researcher's name

**January 2023**

Researcher's signature Date



© Central University of Technology, Free State

**INFORMATION AND CONSENT DOCUMENT FOR A PARENT OR GUARDIAN OF NEONATAL PATIENTS – AFRIKAANS**

**STUDIE TITEL:** Optimalisering en Standarisering van neonatale borskas en abdomen beelding protokol.

Geagte Mev./Mnr. ……..

**INLEIDING**

Ek, Ané Nel, nooi n baba om deel te neem aan n navorsingstudie. Ek gaan observeer hoe radiografiste x-strale neem wat die pediaters en relevante dokters aanvra vir daaglikse roetine opvolg op u baba. Hierdie dokument sal u help besluit of u wil toestemming gee dat u baba mag deelneem aan hierdie navorsingstudie. Hierdie inligtinsdokument sal ook al die nodige inligting oor die hele proses bevat en verduidelik u baba se rol in die studie. Indien u enige vrae oor die het wat onbeantwoord bly aan die einde van die dokument, moet asseblief nie huiwer om my te kontak nie.

**DOEL VAN DIE STUDIE**

Die doel van die studie is om the bepaal wat die beste en veiligste manier is om x-strale van babas te neem en om beskerming teen radiasie in ag te neem.

**VERDUIDELIKING VAN DIE NAVORSINGSPROSES**

Die navorser gaan die radiografiste en verpleegsusters observeer in die neonatale intensiewe eenheid terwyl x-strale op u baba geneem word. Die navorser gaan dan al die relevante inligting aanteken op n kontrolelys.

**MOONTLIKE RISIKO'S BETROKKE**

Geen risiko's is verbonde deur deelname aan die studie. Geen addisionele beelde gaan geneem word op u baba nie, slegs die x-strale wat aangevra word deur die pediater.

**MOONTLIKE VOORDELE VAN DIE STUDIE**

U baba gaan nie direk voordeel trek uit die navorsingstudie, maar die resultate van die studie gaan radiografiste in die toekoms toelaat om radiasie te verminder op babas en herhaalde x-strale te verminder wat hierdie spesifieke pasiënt groep baat in die toekoms.

**U BABA SE REGTE AS DEELNEMER VAN DIE STUDIE**

U baba se deelname is vrywlliglik. U mag deelname weier en kan u baba enige tyd tydens die studie onttrek sonder enige verduideliking of rede. U baba se onttrekking uit die studie of gebrek aan deelname sal nie hul mediese sorg of toegang tot x-strale beïnvloed nie.

**ETIESE GOEDKEURING**

Hierdie navorsingstudie het etiese goedkeuring ontvang van die Etiekkomitee van die Fakulteit van Gesondheidswetenskappe, Universiteit van die Vrystaat (UV).

U kan die etiekkomitee kontak by 051 401 7794 vir enige navrae of bekommernisse wat verband hou met die studie.

**INLIGTING EN KONTAK PERSOON**

U kan my, Ané Nel, kontak by 076 146 2473. Alternatiewelik kan u my studieleiers kontak by 083 272 8647 (Dr B van der Merwe) of by 083 270 4663 (Mev B van der Linde).

**VERGOEDING**

Geen ouer, voog of deelnemende baba ontvang enige vergoeding om aan die bogenoemde studie deel te neem nie. Daar is ook geen koste verbonde vir deelname aan die studie.

**VERTROULIKHEID**

Alle inligting rakende u baba sal streng konfidensieël gehou word. Geen navorsingsartikels of wetenskaplike joernale sal enige vertroulike inligting van u baba bevat nie.



© Central University of Technology, Free State

**TOESTEMMING VIR DEELNAME AAN DIE NAVORSINGSTUDIE**

- Ek bevestig dat die persoon wat my toestemming verkry vir my baba se deelname aan die studie, die proses van die studie, die doel van die studie asook die moontlike risiko's en voordele van die studie aan my verduidelik het.
- Ek het inligting rakende die studie ontvang, die inligting gelees en verstaan.
- Ek is tyd gegun om vrae te vra en ek het geen beswaar teen my baba se deelname aan die studie.
- Ek is bewus dat die inligting wat verkry word van die studie konfidensieël gehou gaan word.
- Ek verstaan dat my baba nie gepenaliseer gaan word sou ek besluit om hom/haar the onttrek van die studie en dat onttrekking uit die studie nie my baba se mediese sorg sal affekteer nie.
- My baba se deelname is vrywillig.

Ouer/ Wettige Voog Voorletters en Van

Ouer/ Wettige Voog Handtekening Datum

**Mev. A Nel**

Navorser Voorletters en Van



**Januarie 2023**

Navorser Handtekening Datum



© Central University of Technology, Free State

**INFORMATION AND CONSENT DOCUMENT FOR A PARENT OR GUARDIAN OF NEONATAL PATIENTS – SESOTHO**

Ratehang Mme/ Ntate …….

**SELELEKELA**

Ke, Ane Nel, ke u mema ngoana hore u kenye letsoho thutong ea ka ea lipatlisiso. Ke batla ho sheba hore na litsebi tsa radiograph li nka X-ray joang seo ngaka e se kopang e le tloaelo letsatsi le leng le le leng. Tokomane ena e tla u thusa ho etsa qeto haeba lesea la hao le ka nka karolo mme e tla hlalosa tshebetso yohle. Haeba u na le lipotso tse setseng li sa arajoa ke tokomane ena, ke kopa o seke oa qeaqea ho ikopanya le nna.

**SEPHEO SA THUTO**

Sepheo sa thuto ke ho tseba tsela e molemohali ea ho nka litšoantšo tsa X-ray tsa masea ha a ntse a li sireletsa khahlanong le X-ray.

**TLHALOSO YA MOKGWA**

Mofuputsi o tla sheba di-radiographer le basebeletsi ba booki ba setsing sa tlhokomelo e matla ya neonatala ha ba ntse ba nka di X-ray tsa lesea la hao. Jwale mofuputsi o tla ngola tlhahisoleseding ena lethathameng la tlhahlobo.

**DIKOTSI TSE KA BANG TENG**

Ha ho na dikotsi tse amehang ho keneng ha dipatlisisong tsena. Ha ho ditshwantsho tse ding tse tla nkuwa, ke di-X-ray feela tse kopilweng ke ngaka ya bana.

**MELEMO E KA BANG TENG THUTONG ENA**

Ngwana wa hao a kanna a se ke a rua molemo thutong ena ka kotloloho, leha ho le jwalo, diphetho tsa phuputso ena di tla dumella ditsebi tsa radiography nakong e tlang ho fokotsa ho pepeswa mahlasedi ho masea le ho fokotsa ho pheta-pheta di X-rays, e leng se thusang sehlopha sa bakudi nakong e tlang.

**DITOKELO TSA LESEA LA HAO JWALO KA MOTHO KA SEBELE?**

Ho nka karolo ha ngwana wa hao thutong ena ke boithaopo ka ho felletseng. O ka hana ho nka karolo kapa wa emisa ho nka karolo ha lesea la hao ka nako efe kapa efe nakong ya phuputso ntle le ho fana ka lebaka lefe kapa lefe. Ho se be le seabo kapa ho ikgula ha lesea la hao phuputsong ho ke ke ha ama phekolo ya hae kapa monyetla wa hae wa ho fumana di X-ray.

**TUMELO YA MATSHWAO**

Thuto ena e fumane tumello ya boitshwaro ho tswa ho komiti ya boitshwaro ba saense ya bophelo bo botle (Health Sciences Research Ethics Committee- HSREC) ya Unibesithi ya Free State.

O ka ikopanya le HSREC ho 051 401 7794 bakeng sa dipotso kapa dingongoreho dife kapa dife mabapi le phuputso ena.



© Central University of Technology, Free State

**TSEBISO LE MOTHO**

Ikopanye le nna, Ané Nel, nomorong e latelang 076 146 2473. Ho seng jwalo, o ka ikopanya le baokamedi ba ka, ka nomoro ya mohala 083 272 8647 (Ngaka Belinda van der Merwe) kapa 083 270 4663 (Mof Beatrix van der Linde).

**MATSHEDISO**

Ha ho wena kapa lesea la hao le tla lefuwa ho nka karolo phuputsong ena. Hape ha ho na ditshenyehelo tse amehang bakeng sa ho nka karolo ha ngwana wa hao phuputsong ena.

**LEKUNUTU**

Dintlha tsohle tse mabapi le lesea la hao di tla bolokwa e le lekunutu. Dingodilweng tsa dipatlisiso le ditlaleho dikoranteng tsa saense di ke ke tsa kenyelletsa tlhahisoleseding efe kapa efe mabapi le wena kapa lesea la hao.

Lebitso la motswadi/ mohlokomedi wa semolao Letsatsi

Mosaeno wa motswadi/ mohlokomedi wa molao Letsatsi

**Mev. A Nel**

Lebitso la mofuputsi

**Pherekgong 2023**

Mosaeno wa mofuputsi Letsatsi



© Central University of Technology, Free State

## APPENDIX K
### CALIBRATION CERTIFICATE

nmisa
National Metrology Institute of South Africa

# Certificate of Calibration

[redacted]

www.nmisa.org

| | |
|---|---|
| **Calibration of:** | RF Unfors Multi-O-Meter for Air Kerma Measurements |
| **Manufacturer:** | RaySafe |
| **Model number:** | 587L |
| **Serial number:** | 164717 |
| **Calibrated for:** | CENTRAL UNIVERSITY OF TECHNOLOGY - FREE STATE<br>[redacted]<br>9301 |
| **Calibration procedure:** | RD-DRD-0001 |
| **Period of calibration:** | 26 October – 01 November 2021 |

## 1 PROCEDURE

### 1.1 Set-Up Procedure

1.1.1 The instrument was calibrated free in air in X-rays produced with constant potential generator against a relevant standard, using the substitution method. The detector was positioned in the radiation beam with its long axis perpendicular to the axis of the beam.

1.1.2 The X-ray beam was aligned at the centre of reference markings on the front surface of the detector and the distance from the focal spot to the reference plane of measurement was 1000 mm. The reference plane of the measurement is defined at the depth of 5.5 mm below the front surface of the detector.

### 1.2 Preliminary Settings

1.2.1 The measurements were carried out using default setting.

1.2.2 No correction for environmental conditions was applied.

[redacted]

| Metrologist (Technical Signatory) | Metrologist | |
|---|---|---|
| Date of Issue<br>**22 November 2021** | **Page 1 of 3** | Certificate Number<br>**NMISA-DOS-2021-0648** |

*Your measure of excellence*

TQM 5095 28



© Central University of Technology, Free State

### 1.3 Traceability

1.3.1 The results of the measurements are traceable to the relevant national measurement standard for air kerma.

## 2 RESULTS

2.1 The results of measurements are shown in the table 1 below. The radiation beam qualities at which the measurements were performed are given in columns 1, 2, and 3 respectively.

2.2 The corresponding calibration factor (CF) is given in column 6.

**Table 1:** Measured air kerma for reference standard and the unit under test (UUT)

| Radiation Quality | Energy (kV) | First HVL mm Al | Ref Air Kerma (mGy) | UUT Air Kerma (mGy) | CF |
|---|---|---|---|---|---|
| RQA-2 | 40 | 2,28 | 1,338 | 1,321 | 1,013 |
| RQA-3 | 50 | 3,82 | 1,315 | 1,329 | 0,989 |
| RQA-4 | 60 | 5,43 | 1,302 | 1,305 | 0,998 |
| RQA-5* | 70 | 6,84 | 1,292 | 1,293 | 0,999 |
| RQA-6 | 80 | 8,22 | 1,328 | 1,313 | 1,012 |
| RQA-7 | 90 | 9,27 | 1,329 | 1,312 | 1,013 |
| RQA-8 | 100 | 10,28 | 1,335 | 1,330 | 1,004 |
| RQA-9 | 120 | 11,71 | 1,371 | 1,361 | 1,007 |
| RQA-10 | 150 | 13,31 | 1,409 | 1,325 | 1,063 |

**Reference radiation quality according to TRS 457*
Inherent Filtration of 1 mm Be

2.3 The uncertainty in the air kerma is estimated not to exceed ± 3 %.

[redacted]



© Central University of Technology, Free State

CALIBRATION OF UNFORS MULT-O-METER
**Serial number: 164717, Model: 587L**

## 3 REMARKS

3.1 The reported uncertainties of measurement were calculated and expressed in accordance with the BIPM, IEC, ISO, IUPAP, OIML document entitled "A Guide to the Expression of Uncertainty in Measurement" (International Organisation for Standardisation, Geneva, Switzerland).

3.2 The reported expanded uncertainty of measurement is stated as the standard uncertainty of measurement multiplied by a coverage factor of k = 2, which for a normal distribution approximates a level of confidence of 95,45%.

3.3 Certain of the NMISA certificates are consistent with the capabilities that are included in appendix C of the MRA (Mutual Recognition Arrangement) drawn up by the CIPM. Under the MRA, all participating institutes recognise the validity of each other's calibration and measurement certificates for the quantities and ranges and measurement uncertainties specified in Appendix C. For details see http://www.bipm.org.

3.4 The calibrations were carried out at an ambient temperature of 19,5 °C ± 0,2 °C, an ambient pressure of 86,7 kPa ± 0,4 kPa and a relative humidity of 62,9 %rh ± 15 %rh.

---------- *end of certificate* ----------

[redacted]

| Metrologist (Technical Signatory) | Metrologist [redacted] | |
|---|---|---|
| Date of issue<br>**22 November 2021** | **Page 3 of 3** | Certificate Number<br>**NMISA-DOS-2021-0648** |

TQM-5095-28



© Central University of Technology, Free State

## APPENDIX L

### QUALITY CONTROL OF MOBILE X-RAY MACHINE (PHASE 3)

**III.1.1. General Tests (Daily) – X – (Indicators, mechanical and other safety checks)**

**III.1.1. General Tests (Daily) – 38-(Radiation warning light)** Must work when beam is activated

ROOM: Mira 2

| mm/yy: July 23 | 1 | 2 | 3 | 4 | 5 | 6 | 7 | 8 | 9 | 10 | 11 | 12 | 13 | 14 | 15 | 16 | 17 | 18 | 19 | 20 | 21 | 22 | 23 | 24 | 25 | 26 | 27 | 28 | 29 | 30 | 31 |
|---|---|---|---|---|---|---|---|---|---|---|---|---|---|---|---|---|---|---|---|---|---|---|---|---|---|---|---|---|---|---|---|
| Test 1: Indicators, mechanical and other safety checks & warm-up | SS | ✓ | ✓ | ✓ | ✓ | ✓ | ✓ | SS | ✓ | ✓ | ✓ | ✓ | ✓ | ✓ | SS | ✓ | ✓ | ✓ | ✓ | ✓ | ✓ | SS | ✓ | ✓ | ✓ | ✓ | ✓ | ✓ | SS | S | |
| Test 38: Radiation warning light at entrance AC&E | | | | | | | | | | | | N/A | | | | | | | | | | | | | | | | | | | |

| mm/yy: Aug 23 | 1 | 2 | 3 | 4 | 5 | 6 | 7 | 8 | 9 | 10 | 11 | 12 | 13 | 14 | 15 | 16 | 17 | 18 | 19 | 20 | 21 | 22 | 23 | 24 | 25 | 26 | 27 | 28 | 29 | 30 | 31 |
|---|---|---|---|---|---|---|---|---|---|---|---|---|---|---|---|---|---|---|---|---|---|---|---|---|---|---|---|---|---|---|---|
| Test 1: Indicators, mechanical and other safety checks & warm-up | ✓ | ✓ | ✓ | ✓ | SS | ✓ | ✓ | ✓ | H | ✓ | ✓ | SS | S | ✓ | ✓ | ✓ | ✓ | ✓ | SS | ✓ | ✓ | ✓ | ✓ | ✓ | ✓ | SS | ✓ | ✓ | ✓ | ✓ | ✓ |
| Test 38: Radiation warning light at entrance AC&E | | | | | | | | | | | | N/A | | | | | | | | | | | | | | | | | | | |

| mm/yy: Sept 23 | 1 | 2 | 3 | 4 | 5 | 6 | 7 | 8 | 9 | 10 | 11 | 12 | 13 | 14 | 15 | 16 | 17 | 18 | 19 | 20 | 21 | 22 | 23 | 24 | 25 | 26 | 27 | 28 | 29 | 30 | 31 |
|---|---|---|---|---|---|---|---|---|---|---|---|---|---|---|---|---|---|---|---|---|---|---|---|---|---|---|---|---|---|---|---|
| Test 1: Indicators, mechanical and other safety checks & warm-up | ✓ | SS | ✓ | ✓ | ✓ | ✓ | ✓ | ✓ | SS | SS | ✓ | ✓ | ✓ | ✓ | ✓ | SS | SS | ✓ | ✓ | ✓ | ✓ | ✓ | SS | S | ✓ | ✓ | ✓ | ✓ | SS | S | S |
| Test 38: Radiation warning light at entrance AC&E | | | | | | | | | | | | | | | N/A | | | | | | | | | | | | | | | | |

Notes:



© Central University of Technology, Free State

## III.1.1. General Tests (6 monthly) – 3 – (Appropriate technique chart displayed at X-ray unit)

**ROOM:** Mobiel 2

| | | 1st 6 months Date: 23/5/2023 | | 2nd 6 months Date: _____ | |
|---|---|---|---|---|---|
| | | X or ✓ | Cor | X or ✓ | Cor |
| **3. Appropriate technique chart displayed at X-ray unit** | See each room | ✓ | | | |



© Central University of Technology, Free State

Central University of Technology, Free State

## III.1.2. X-ray Tubes and Generators – Tests 4 to 8

ROOM: Mobile 2

| Deviation must be □ ±1 cm @1m -image-distance (SID) With a SID of 115cm the deviation must be less than 1.15cm | | 1st 3 months Date: 13/8/2022 | | 2nd 3 months Date: 16/11/2022 | | 3rd 3months Date: 24/2/23 | | 4th 3 months Date: 31/5/2023 | |
|---|---|---|---|---|---|---|---|---|---|
| | Test on NX 2 Yes/No ? | X or ✓ | Cor | X or ✓ | Cor | X or ✓ | Cor | X or ✓ | Cor |
| 4. Alignment of centre of the X-ray field and the centre of the bucky | No | N/A | | N/A | | N/A | | N/A | |
| 5. The X-ray field dimensions in the plane of the image receptor must correspond with those indicated by the beam-limiting device. | No | ✓ | | ✓ | | ✓ | | ✓ | |
| 6. Congruence between the x-ray field and light field | No | ✓ | | ✓ | | ✓ | | ✓ | |
| 7. X-ray light-beam centering | No | ✓ | | ✓ | | ✓ | | ✓ | |
| 8. Alignment and collimation to film changer/bucky | No | N/A | | N/A | | N/A | | N/A | |

**Notes:** e.g. If a correction must be made by a technician – then a job card must be filed. Fill in the date at Cor when the correction was made and file the jobcard.



© Central University of Technology, Free State

Central University of Technology, Free State

## III.1.10. – Test 36 - Repeat and Reject Analysis

**Machine or Room** Module 2

| | 1st Analysis | 2nd Analysis | 3rd Analysis | 4rd Analysis |
|---|---|---|---|---|
| **Every 3 months**<br>**Repeat and reject analysis** - Digital: Must use software supplied by vendor<br>May not increase with more than **2%** from the previous determined rate and<br>**Total rate should not exceed 10%** | 13/8/2022<br>**Date**<br>13% wastage<br>91% posible | 16/ /2022<br>**Date**<br>14% wastage<br>90% posisioning | 24/2/2023<br>**Date**<br>14% wastage<br>Posible 9[illegible]% | 31/5/2023<br>**Date**<br>16 wastage<br>71% posisie is |

**Notes:** Write here the where the most rejections are e.g. – what is the rejection rate for positioning?:

How does the rejection rate compare with the other machines:?



© Central University of Technology, Free State

Central University of Technology, Free State

# APPENDIX M

## LITERATURE IMAGING PROTOCOLS

### Chest protocols (N=109)

| Protocol (medium) | 1 | Observation statistic to support | |
|---|---|---|---|
| kVp | 55 | mean (p-value = 0,446293) | *SD = 2* |
| mAs | 2 | mean (p-value = 0,0384) | *SD = 0.2* |
| SID | 100 | 66% | *n-vallue = 105* |
| Collimation upper margin (edge of margin placed on) | Upper shoulder margin (C7) | 100% | *n-value = 109* |
| Collimation lower margin (edge of margin placed on) | Lower costal margin | 63% | *n-value = 69* |
| Collimation on sides (edge of margin placed next to) | Soft tissue margin | 100% | *n-value = 109* |
| Centring | Nipple line | 66% | *n-value = 73* |
| Main radiation beam angulation (angle the neonatal bed until) | Straight | 76% | *n-value = 83* |
| IR placement | Incubator IR tray | 61% | *n-value = 66* |

| Protocol (small) | 2 | Observation statistic to support | |
|---|---|---|---|
| kVp | 57 | 55kVp (mean) + SD of 2kVp | |
| mAs | 2.2 | 2mAs (mean) + SD of 0.2mAs | |
| SID | 90 | 22% | *n-value = 34* |
| Collimation upper margin (edge of margin placed on) | Thyroid cartilage | Literature | |
| Collimation lower margin (edge of margin placed on) | Xiphoid process | 22% | *n-value = 23* |
| Collimation on sides (edge of margin placed next to) | Soft tissue margin | 100% | *n-value = 109* |
| Centring | Sternal angle | 15% | *n-value = 16* |
| Main radiation beam angulation (angle the neonatal bed until) | 5° bed angulation (paralell to sternum) | 24% | *n-value = 26* |
| IR placement | Under patient | 39% | *n-value = 43* |

| Protocol (large) | 3 | Observation statistic to support | |
|---|---|---|---|
| kVp | 52 | 55kVp (mean) - SD of 2kVp and machine cannot give 53kVp | |
| mAs | 1.8 | 2mAs (mean) - SD of 0.2mAs | |
| SID | 80 | 12% | *n-value = 19* |
| Collimation upper margin (edge of margin placed on) | Lip line | Literature | |
| Collimation lower margin (edge of margin placed on) | Navel | 15% | *n-value = 16* |
| Collimation on sides (edge of margin placed next to) | Soft tissue margin | 100% | *n-value = 109* |
| Centring | Lower costal margin | 17% | *n-value = 18* |
| Main radiation beam angulation (angle the neonatal bed until) | Straight | 76% | *n-value = 83* |
| IR placement | Under mattress | 100% | *n-value = 8* |

| Protocol | 4 | Reference(s) to support |
|---|---|---|
| kVp (60) | 50-65 | del Vecchio, Bontrager and Lampignano, Gunn |
| mAs (0.8) | 0.5-3 | del Vecchio, Bontrager and Lampignano, Gunn |
| SID | 100 | del Vecchio, Pederson |
| Collimation upper margin (edge of margin placed on) | Mentum | del Vecchio |
| Collimation lower margin (edge of margin placed on) | Below nipples | del Vecchio |
| Collimation on sides (edge of margin placed next to) | Soft tissue margin | del Vecchio |
| Centring | Nipple line | Bontrager and Lampignano |
| Main radiation beam angulation (angle the neonatal bed until) | 5°-10° Caudal | ISRRT |
| IR placement | Under mattress | BvdLinde se thesis, Tugwell-Allsup |



© Central University of Technology, Free State

Central University of Technology, Free State

## Abdomen protocols (N=16)

| Protocol (medium) | 1 | Observation statistic to support | |
|---|---|---|---|
| kVp | 57 | mean (p-value = 1,48183) | *SD = 3* |
| mAs | 2.6 | mean (p-value = 0,214445) | *SD = 0.4* |
| SID | 100 | 66% | *n-vallue = 105* |
| Collimation upper margin (edge of margin placed on) | Axilla (Diaphragm) | 100% | *n-value = 16* |
| Collimation lower margin (edge of margin placed on) | Symphysis pubis | 100% | *n-value = 16* |
| Collimation on sides( edge of margin placed next to) | Soft tissue margin | 100% | *n-value = 16* |
| Centring | Navel | 63% | *n-value = 10* |
| Main radiation beam angulation (angle the neonatal bed until) | Straight | 100% | *n-value = 16* |
| IR placement | Incubator IR tray | 56% | *n-value = 9* |

| Protocol (small) | 2 | Observation statistic to support | |
|---|---|---|---|
| kVp | 60 | 57kVp (mean) + SD of 3kVp | |
| mAs | 3 (or 3.2) | 2.6mAs (mean) + SD of 0.4mAs | |
| SID | 90 | 22% | *n-value = 34* |
| Collimation upper margin (edge of margin placed on) | Nipple line | Literature | |
| Collimation lower margin (edge of margin placed on) | Greater trochanter | Literature | |
| Collimation on sides( edge of margin placed next to) | Soft tissue margin | 100% | *n-value = 16* |
| Centring | Lower costal margin | 25% | *n-value = 4* |
| Main radiation beam angulation (angle the neonatal bed until) | Straight | 100% | *n-value = 16* |
| IR placement | Under patient | 44% | *n-value = 7* |

| Protocol (large) | 3 | Observation statistic to support | |
|---|---|---|---|
| kVp | 54 | 57kVp (mean) - SD of 3kVp | |
| mAs | 2.2 | 2.6mAs (mean) - SD of 0.4mAs | |
| SID | 80 | 12% | *n-value = 19* |
| Collimation upper margin (edge of margin placed on) | Clavicle | Literature | |
| Collimation lower margin (edge of margin placed on) | Diaper edge | Literature | |
| Collimation on sides( edge of margin placed next to) | Soft tissue margin | 100% | *n-value = 16* |
| Centring | 2.5cm superior to navel | 12% | *n-value = 2* |
| Main radiation beam angulation (angle the neonatal bed until) | Straight | 100% | *n-value = 16* |
| IR placement | Under mattress | 100% | *n-value = 8* |

| Protocol | 4 | Reference(s) to support |
|---|---|---|
| kVp | None found | |
| mAs | None found | |
| SID | 100cm | del Vecchio, Bontrager and Lampignano |
| Collimation upper margin (edge of margin placed on) | Top of diapraghm | del Vecchio, Menashe |
| Collimation lower margin (edge of margin placed on) | Symphysis pubis | del Vecchio, Menashe |
| Collimation on sides( edge of margin placed next to) | Lateral abdominal walls | del Vecchio |
| Centring | 2.5cm above navel | Bontrager and Lampignano |
| Main radiation beam angulation (angle the neonatal bed until) | Straight | Bontrager and Lampignano |
| IR placement | Under pt | Tugwell-Allsup, Bontrager and Lampignano |

© Central University of Technology, Free State

Central University of Technology, Free State

## Chest abdomen combination protocols

| Protocol (medium) | 1 | Observation statistic to support | |
|---|---|---|---|
| kVp | 57 | mean (p-value = 1,20403) | *SD = 3* |
| mAs | 2.3 | mean (p-value = 0,15843) | *SD = 0.4* |
| SID | 100 | 66% | *n-vallue = 105* |
| Collimation upper margin (edge of margin placed on) | Upper shoulder margin (C7) | 100% | *n-value = 33* |
| Collimation lower margin (edge of margin placed on) | Symphysis pubis | 100% | *n-value = 33* |
| Collimation on sides( edge of margin placed next to) | Soft tissue margin | 100% | *n-value = 33* |
| Centring | Navel | 64% | *n-value = 21* |
| Main radiation beam angulation (angle the neonatal bed until) | Straight | 100% | *n-value = 33* |
| IR placement | Incubator IR tray | 64% | *n-value = 21* |

| Protocol (small) | 2 | Observation statistic to support | |
|---|---|---|---|
| kVp | 60 | 57kVp (mean) + SD of 3kVp | |
| mAs | 2.7 | 2.3mAs (mean) + SD of 0.4mAs | |
| SID | 90 | 22% | *n-value = 34* |
| Collimation upper margin (edge of margin placed on) | Thyroid cartilage | Literature | |
| Collimation lower margin (edge of margin placed on) | Greater trochanter | Literature | |
| Collimation on sides( edge of margin placed next to) | Soft tissue margin | 100% | *n-value = 33* |
| Centring | Lower costal margin | 33% | *n-value = 11* |
| Main radiation beam angulation (angle the neonatal bed until) | Straight | 100% | *n-value = 33* |
| IR placement | Under patient | 36% | *n-value = 12* |

| Protocol (large) | 3 | Observation statistic to support | |
|---|---|---|---|
| kVp | 54 | 57kVp (mean) - SD of 3kVp | |
| mAs | 1.9 | 2.3mAs (mean) - SD of 0.4mAs | |
| SID | 80 | 12% | *n-value = 19* |
| Collimation upper margin (edge of margin placed on) | Lip line | Literature | |
| Collimation lower margin (edge of margin placed on) | Diaper edge | Literature | |
| Collimation on sides( edge of margin placed next to) | Soft tissue margin | 100% | *n-value = 33* |
| Centring | 4cm superior to navel | 3% | *n-value = 1* |
| Main radiation beam angulation (angle the neonatal bed until) | Straight | 100% | *n-value = 33* |
| IR placement | Under mattress | 100% | *n-value = 8* |

| Protocol | 4 | Reference(s) to support |
|---|---|---|
| kVp | None found | |
| mAs | None found | |
| SID | 100cm | del Vecchio |
| Collimation upper margin (edge of margin placed on) | None found | |
| Collimation lower margin (edge of margin placed on) | None found | |
| Collimation on sides( edge of margin placed next to) | Lateral chest and abdominal walls | del Vecchio |
| Centring | None found | |
| Main radiation beam angulation (angle the neonatal bed until) | Straight | Bontrager and Lampignano |
| IR placement | Under pt | Tugwell-Allsup |



© Central University of Technology, Free State

## APPENDIX N

### PERMISSION FROM THE HEAD RADIOGRAPHER TO IMPLEMENT THE IMAGING PROTOCOL

**PERMSSION FROM HEAD RADIOGRAPHER FOR THE IMPLEMENTATION OF IMAGING PROTOCOL**

To the head radiographer

**Study title: Standardizing and optimizing of neonatal chest and abdomen imaging protocols.**

The radiographers and nursing staff will be observed in the neonatal intensive care unit to establish a baseline protocol for the imaging of chest and abdominal x-rays. These protocols will then be tested by taking x-rays of a phantom with the mobile machine whilst measuring dose with a dosimeter to ensure dose optimization. A final imaging protocol will be established and implemented in the radiology department for four weeks to ensure usefulness and of the imaging protocol.

Your permission is requested to implement the final imaging protocol in the radiology department for four weeks to determine accuracy and improvement of the x-ray images and provide guidance for the radiographers.

I [redacted], hereby grant permission to Ané Nel to implement the imaging protocol in the radiology department for said period.

Si [redacted] 20 November '23

Date



© Central University of Technology, Free State

## APPENDIX O

### PERMISSION FROM A BLOEMFONTEIN HOSPITAL FOR THE IMPLEMENTATION PILOT STUDY

**PERMSSION FROM HEAD RADIOGRAPHER TO PERFORM PILOT STUDY AT [redacted] HOSPITAL**

To whom it may concern

**Study title: Standardising and optimising of neonatal chest and abdomen imaging protocols.**

The radiographers and nursing staff will be observed in the neonatal intensive care unit to establish a viable and valid protocol for the imaging of chest and abdominal x-rays. This imaging protocol will be used during a study for the degree Master in Radiography for Ané Nel.

Your permission is requested to perform the pilot study for the imaging protocol in the radiology department and neonatal intensive care unit to ensure accuracy and improvement of the x-ray imaging protocol to be used during the primary study.

I [redacted], hereby grant permission to Ané Nel to test the observational checklist in the radiology department and neonatal intensive care unit.

[redacted] 28/2/2023

Signature of Radiographer Date

[redacted] 1/03/2023

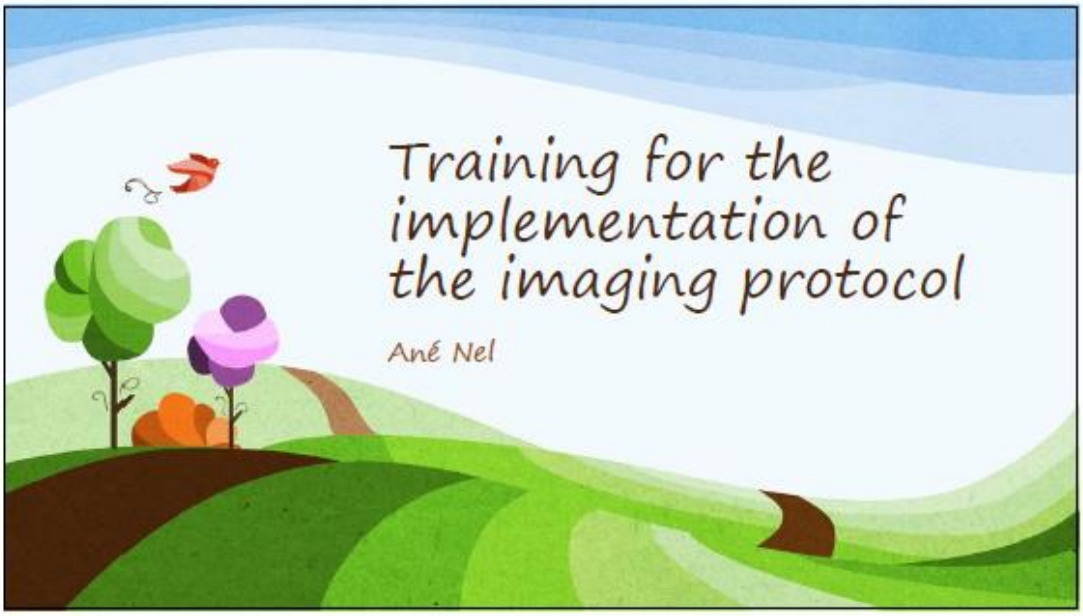
Signature of Radiologist Date



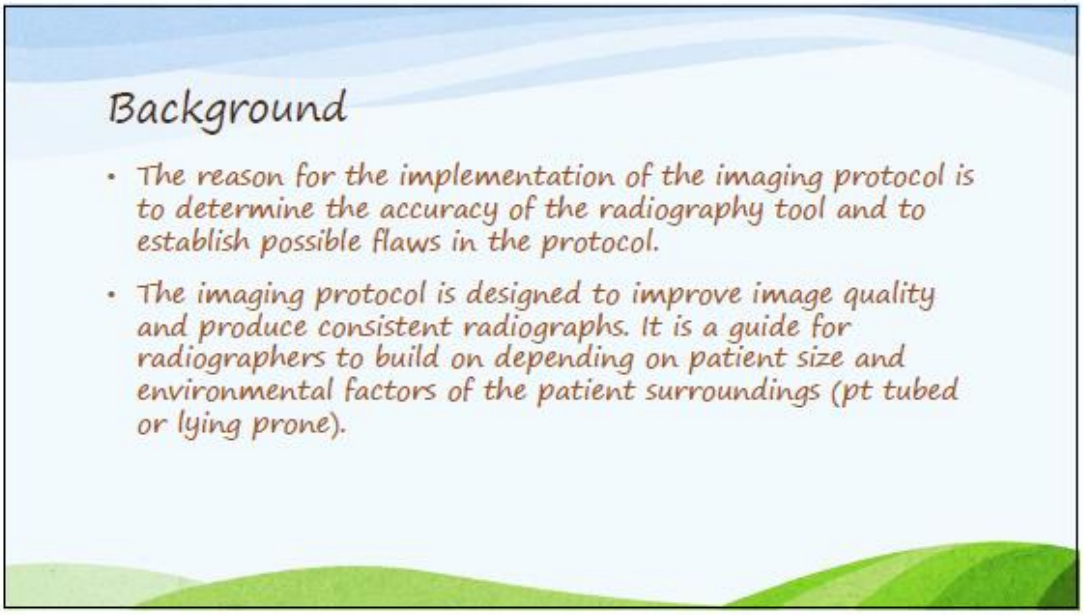
© Central University of Technology, Free State

## APPENDIX P

### POWERPOINT PRESENTATION FOR PRE-IMPLEMENTATION TRAINING




1




2



© Central University of Technology, Free State

## Pick The Ending

- Pick the ending refers to the three sections forming part of the final x-ray image. the three sections include the positioning factors, the technical factors and the exposure factors.
- The positioning factors include positioning and immobilization of the patient while the technical factors include the set up of the machine with the SID, OID and marker and detector placement. The exposure factors include the kVp and mAs values as well as the exposure and deviation index respectively.

3

## Examples

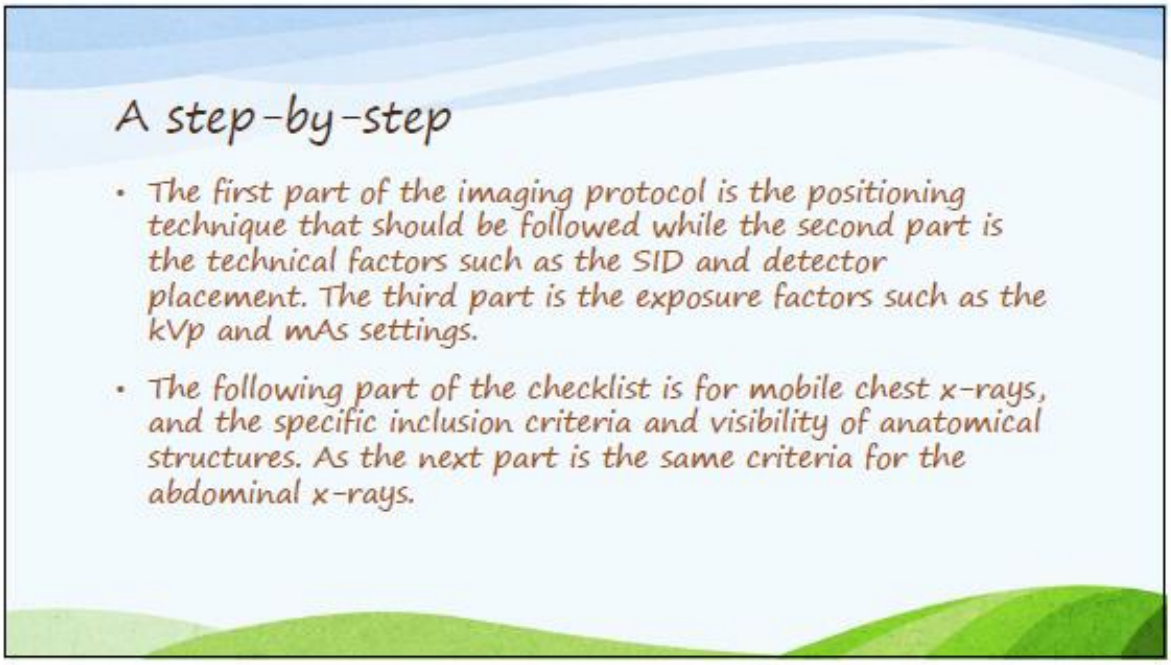
- Included is an example of the checklist to be completed for the technical and exposure factors.

| TECHNICAL FACTORS | | | |
|---|---|---|---|
| Lead marker placed | Yes | No | Placed but not visible |
| Detector placement | Under pt | Under mattress | In detector tray |
| Source to object distance (SOD)<br>Tube to ~~room~~mattress where? | | | |
| Source to image distance (SID)<br>Tube to detector mattress | | | |
| Centering point | | | |
| Angulation of main beam | | | |
| **EXPOSURE FACTORS** | | | |
| kVp value | | | |
| mAs value | | | |
| Exposure index | | | |
| Deviation index | | | |

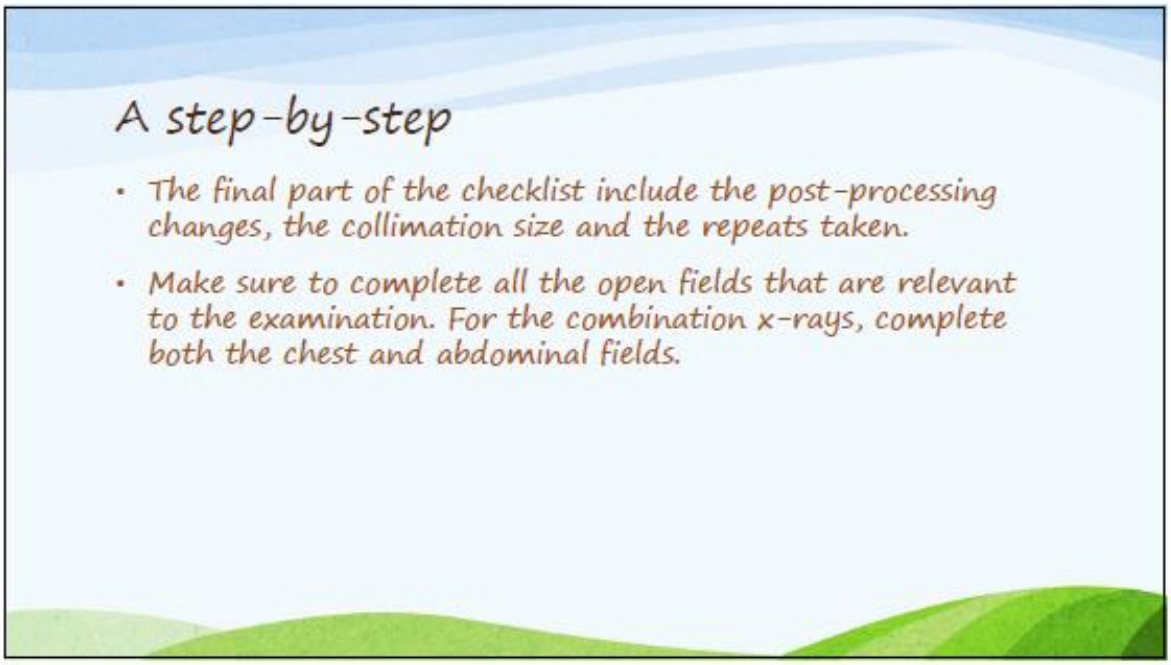
4



© Central University of Technology, Free State




5




6



© Central University of Technology, Free State

## The picture

- With the imaging protocol you will find a small picture of a baby, this is a guide on collimation for the specific examination.
- All the lines are placed on a topographic landmark for easy access. The lines represent the upper and lower borders of the collimation, and by doing this the included anatomical structures will form part automatically.

7

## How to...

- After each patient, complete an implementation checklist by selecting "Yes" or "No" for the relevant setting or criteria.
- It is important to complete all the open fields and if any repeats were done, provide a reason for the repetition.
- At the start of the checklist, complete the space for radiographer and patient identification with the date of completion for the researcher to easily find the images on PACS.

8

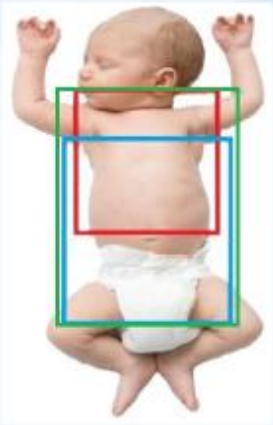


© Central University of Technology, Free State

## After the mobile

- When you are done with the checklist place it in the box placed in the radiographer's tearoom for the researcher to collect at the end.

9



## Demonstration

The RED box indicate the collimation borders for the chest x-ray. The superior border should be on the lip line and the inferior border on the navel.

The BLUE box indicate the collimation borders for the abdominal x-ray. The superior border should be on the nipple line and the inferior border on the mid-femur.

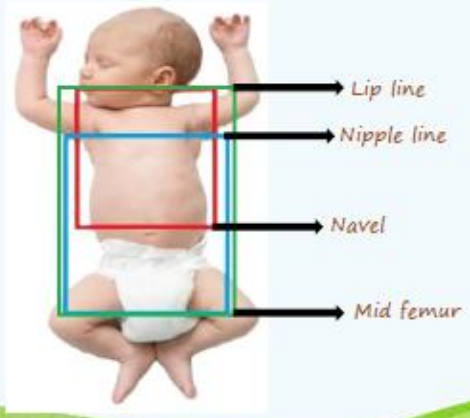
The GREEN box indicate the collimation borders for the combination x-ray. The superior border should be on the lip line and the inferior border on the mid-femur.

10



© Central University of Technology, Free State

## Collimation borders




11

## Important

- Please note that there is no correct answer. All answers should be as the mobile was performed to ensure validity and accuracy.
- Thank you for your participation during this final step of my research journey.

12

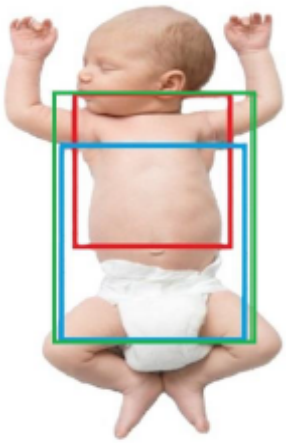


© Central University of Technology, Free State

## APPENDIX Q
### STANDARDISED IMAGING PROTOCOL

# PICK THE ENDING

| POSITIONING FACTORS | | | |
|---|---|---|---|
| Arms abducted from body | | | |
| Head facing up | | | |
| Chin lifted | | | |
| No rotation on pelvis | | | |
| No rotation of thorax | | | |
| **TECHNICAL FACTORS** | | | |
| Lead marker placed | | | |
| Detector placement | Underneath patient if possible | | |
| Source to object distance (SOD)<br>*Tube to mattress* | 98cm (depending on mattress thickness) | | |
| Source to image distance (SID)<br>*Tube to detector* | 100cm | | |
| Centering point | Nipple line | Navel | Navel |
| Angulation of main beam | Straight beam | | |
| **EXPOSURE FACTORS** | | | |
| **Exam type:** | **CXR** | **AXR** | **Combo** |
| kVp value | 57 or 60kVp | 54kVp | 54kVp |
| mAs value | 0.80mAs | 1.80mAs | 1.80mAs |
| Exposure index | Optimal EI: 50 - 200 | Optimal EI: 125 - 500 | |
| Deviation index | Optimal DI: 0 | | |



RED – Chest X-ray
BLUE – Abdomen X-ray
GREEN – Combo X-ray



© Central University of Technology, Free State

## APPENDIX R

### SAFEASSIGN SIMILARITY INDEX SUMMARY

Optimising and standardising neonatal chest and abdomen imaging protocols

ORIGINALITY REPORT

| 9% | 6% | 3% | 4% |
|---|---|---|---|
| SIMILARITY INDEX | INTERNET SOURCES | PUBLICATIONS | STUDENT PAPERS |



© Central University of Technology, Free State

## APPENDIX S
### LETTER FROM THE STATISTICIAN

Maryn Viljoen
Statistics Consulting Services

082 823 5731
maryn.viljoen1@gmail.com

Protocol & research methodology consultation | Ethical consultation | Database construction & capturing of data
Analysing data using statistical software packages (SAS Version 9.2) | Statistics consultation services to analyse and interpret data
Conveys results with statistical tables & figures where needed

**The Chairperson: Health Sciences Research Ethics Committee (HSREC)**
For Attention: Mrs. M.G.E. Marais
Block D, Room 104
Francois Retief Building
Faculty of Health Sciences
University of the Free State

25 July 2022

**Title:** "Optimizing and standardizing neonatal chest and abdomen imaging protocols

**Researcher:** Ané Nel (Ackermann)
Master in Radiography (Diagnostic)
Department of Clinical Sciences
Faculty of Health and Environmental Sciences
Central University of Technology, Free State
Bloemfontein

I have seen and read through this protocol. I gave input and recommendations and will be the biostatistician responsible for the analysis of the data.

Maryn Viljoen
M.Sc. Risk Analysis (UFS)
maryn.viljoen1@gmail.com
082 82 35 731



© Central University of Technology, Free State

## APPENDIX T
### LETTER FROM THE LANGUAGE EDITOR

**TO WHOM IT MAY CONCERN**

I hereby declare that regarding the following document:

**Author:** Ané Nel
**Title:** Optimising and standardising neonatal chest and abdomen imaging protocols

1. I have performed the language editing (grammar, vocabulary and syntax).
2. I assisted the author with the technical preparation of the thesis, including the layout and formatting.
3. I verified the accuracy of the citations in the bibliography.
4. Where applicable, I obtained and verified the most recent active uniform resource locator (URL) for internet-based references.

**Important notice:** The verification of the accuracy of citations in the list of references (authors and title of the article, journal name, date, volume, issue and page numbers, and DOI, if applicable; or similar information and the URL for internet references; or textbooks used as references) does not include authentication of the content that was cited from the reference. The editor cannot be held accountable for any changes made to the text, including language, formatting and layout, or any addition or deletion of text performed by the author after the document has been returned by the editor. The application or rejection of queries, comments and recommendations made during the editing process remains the responsibility of the author and is decided based on the author's discretion. It is the author's obligation to adhere to the similarity index requirements and policies of the CUT. The author is responsible to review the final document prior to submission for assessment and cannot hold the editor accountable for any errors occurring in the document.



_____

**DR. DALEEN STRUWIG**
BSc, BSc (Hons), MMedSc, PhD

Address: 16 Harrismith Street, Dan Pienaar, Bloemfontein
Telephone: +27 82 562 8461
Email address: daleenstruwig@gmail.com

**Date:** 18 August 2024



© Central University of Technology, Free State